

**Benjamin B. de Glanville**

Thesis submission for Doctor of Philosophy in Immunology

**Activation and Regulation of  
the Innate Immune System in  
Response to *Ureaplasma*  
Infection**

**Supervised by Prof. Kathy Triantafilou  
and Dr. Martha Triantafilou**

Submitted September 2014



## **DECLARATION**

This work has not previously been accepted in substance for any degree and is not concurrently submitted in candidature for any degree.

Signed ..... Date .....

## **STATEMENT 1**

This thesis is being submitted in partial fulfillment of the requirements for the degree of Doctor of Philosophy

Signed ..... Date .....

## **STATEMENT 2**

This thesis is the result of my own independent work/investigation, except where otherwise stated.  
Other sources are acknowledged by explicit references.

Signed ..... Date .....

## **STATEMENT 3**

I hereby give consent for my thesis, if accepted, to be available for photocopying and for inter-library loan, and for the title and summary to be made available to outside organisations.

Signed ..... Date .....

## **STATEMENT 4: PREVIOUSLY APPROVED BAR ON ACCESS**

I hereby give consent for my thesis, if accepted, to be available for photocopying and for inter-library loans **after expiry of a bar on access previously approved by the Graduate Development Committee.**

Signed ..... Date .....

## Acknowledgements

I would like to take this opportunity to express my immense gratitude to my supervisor, tutor and mentors Prof. Kathy Triantafilou and Dr. Martha Triantafilou for their invaluable guidance and support throughout this project. Furthermore I would like to thank them both for their constant and incredible support over the years, and to acknowledge the fact that I would not be where I am today if it were not for them.

I would like to thank Ali F. Aboklaish, O. Brad Spiller and Saim Kotecha for their help in *Ureaplasma* culturing techniques.

I thank my friend and laboratory colleague Robin Olden for putting up with me during the project.

Finally, I'd like to thank the support of my parents and sister for all their love and support and keeping me sane over the past few years.

## **Publications**

**The results and findings of chapter 5 were peer reviewed and published in the immunology journal PlosOne in 2001.** Triantafilou M, de Glanville B, Aboklaish AF, Spiller OB, Kotecha S, Triantafilou K. Synergic activation of toll-like receptor (TLR) 2/6 and 9 in response to *Ureaplasma parvum* & *urealyticum* in human amniotic epithelial cells. *PLoS ONE*. 2013;8(4):e61199.

## **Contributions**

This thesis is the result of my own independent work/investigation. I have designed most of the experiments and have carried out all the experimental work. Other sources are acknowledged by explicit references.



# Summary

The bacteria *Ureaplasma* has long been associated with a wide range of adverse health implications, including preterm birth, preterm premature rupture of the membrane and lung disorders, such as bronchopulmonary dysplasia in neonatal infants, but still, little is known about the pathogenic properties of *Ureaplasma* and possible direct association with adverse health complications. Estimated prevalence of *Ureaplasma* colonisation in sexually active adults is between 40 – 80%, therefore further understanding of its pathogenic properties and its ability to initiate an immune response is crucial.

Specifically selected human cell-lines were examined *in vitro* to determine whether an innate immune response could be activated by *Ureaplasma* infection. If inflammatory immune responses were detected in human cell-lines, pathogenic properties of *Ureaplasma* would be confirmed, and its role in pregnancy and neonatal complications could be supported.

Using a range of techniques, activation of immune response pathways were examined, as too were the production of detrimental pro-inflammatory cytokines that would strengthen the suggested associations of *Ureaplasma* infection with the above-mentioned complications.

Myeloid-derived leukocytic monocytes, human bronchial epithelial cells and human amniotic epithelial cells were examined, as these would be the most relevant cell lines to determine if *Ureaplasma* could induce preterm birth, preterm premature rupture of the membrane and bronchopulmonary dysplasia. All cell lines studied showed immune response and inflammatory cytokine production after stimulation with *Ureaplasma*. This supports that *Ureaplasma* is capable of causing tissue damage in neonatal respiratory tracts that may lead to bronchopulmonary dysplasia and damage to the amniotic and chorion membranes that may lead to preterm premature rupture of the membrane.

*Ureaplasma* was detected at the cell surface of human amniotic epithelial cells (HAECs) by TLR2 and TLR2/6 heterodimers. Results suggest that *Ureaplasma* multiple banded antigen (MBA) is the strong ligand for TLR2 and TLR6 and stimulation of HAECs with MBA alone caused an immune response. TLR9 was responsible for the detection of internalised *Ureaplasma*, which is also able to initiate an immune response and inflammatory cytokine production.

*Ureaplasma* stimulation results in the production of the inflammatory cytokines TNF- $\alpha$ , IL-8 IL-6 via the NF- $\kappa$ B signaling pathway.

Production of the potent inflammatory cytokine IL-1 $\beta$  was also observed, which would suggest the formation of inflammasome complexes. NLRs were investigated to find which NLR inflammasome were activated. It was shown that genetically knocking down NLRP7 significantly reduced the amount of IL-1 $\beta$  that was produced after *Ureaplasma* stimulation, suggesting that NLRP7 inflammsones are activated by *Ureaplasma*. Reduction in IL-1 $\beta$  was also observed, but to a lesser extent, when NLRP3 was knocked down.

We decided to investigate the role of NLRP7 further and found a novel immune pathway, where NH<sub>3</sub> causes activation and formation of the NRLP7 inflammasone. NH<sub>3</sub> is produced as a bi-product of urease activity, which an essential process for *Ureaplasma*. The addition of a potent urease inhibitor to HAECs being stimulated with *Ureaplasma* significantly reduced the production of IL-1 $\beta$ , strongly supporting that NH<sub>3</sub> plays a significant role in the detection of *Ureaplasma* infection and is responsible for causing the tissue damage that contributes to preterm premature rupture of the membrane leading to preterm birth.

This investigation strongly supports that *Ureaplasma* is responsible for causing preterm birth and health complications in neonates, and that more robust treatment and monitoring of *Ureaplasma* is required, especially in pregnant women. These undertakings will hopefully reduce the rates of preterm birth and the associated health implications, in addition to reducing rates of bronchopulmonary dysplasia in neonates.

<b>Chapter 1:</b>	<b>1</b>
<b>Introduction</b>	<b>1</b>
<b>Abbreviations:</b>	<b>2</b>
<b>1.1: Introduction into <i>Ureaplasma</i>:</b>	<b>6</b>
<b>1.1: Introduction into <i>Ureaplasma</i>:</b>	<b>6</b>
1.1.2: <i>U. urealyticum</i> and <i>U. parvum</i> : what is the difference?	7
1.1.3: Epidemiology of <i>Ureaplasma</i> :	8
1.1.4: Proposed pathogenic and virulence factors of <i>Ureaplasma</i> spp:	8
1.1.4.1: Multiple Banded Antigen (MBA):	9
1.1.4.2: Other <i>Ureaplasma</i> antigenic properties:	9
1.1.5: Implications associated with <i>Ureaplasma</i> :	11
<b>1.2: Preterm birth:</b>	<b>12</b>
1.2.1: Preterm premature membrane rupture (pPROM):	13
1.2.2: Preterm birth associated and contributing factors:	14
<b>1.3: <i>Ureaplasma</i> spp. detection methods and associated problems:</b>	<b>14</b>
1.3.1: Possible reason for inconsistency between the rate of people presenting with <i>Ureaplasma</i> colonisation and the rate of adverse effect experienced:	15
<b>1.4: Association between <i>Ureaplasma</i> spp. and PTB/pPROM:</b>	<b>16</b>
1.4.1: Brochopulmonary dysplasia and associations with <i>Ureaplasma</i> spp. infections:	17
1.4.2: Immune response pathways linking <i>Ureaplasma</i> spp. infection to BPD:	19
1.4.3: <i>Ureaplasma</i> spp. related BPD treatment:	19
<b>1.5: The immune system:</b>	<b>21</b>
1.5.1 History of Toll-like receptors (TLRs):	23
1.5.2: Toll-like receptor family:	25
1.5.2.1: TLR2, TLR2/1 and TLR2/6:	28
1.5.2.2: TLR4:	29
1.5.2.3: TLR9:	30
1.5.2.4: TLR7:	31
<b>1.6: TLR signaling pathways:</b>	<b>31</b>
1.6.1: MyD88-dependent signaling pathway:	31
1.6.2: TRIF-dependent signaling pathway:	33
<b>1.7: TLR accessory molecules:</b>	<b>35</b>
1.7.1: CD36:	36
1.7.2: CD14:	36
<b>1.8: TLR adverse effects to PRR response:</b>	<b>37</b>
<b>1.9: NLR proteins:</b>	<b>38</b>
1.9.1: Brief introduction into NLR proteins:	38
1.9.2: NLR family tree:	40

1.9.3: NLR structure: .....	41
1.9.4: Functions of NLR: .....	41
1.9.5: Non-inflammasome NLRs: .....	42
1.9.5.1: NOD1 and NOD2: .....	43
1.9.5.2: NLRC5 and CIITA: .....	46
<b>1.10: The Inflammasome: .....</b>	<b>48</b>
1.10.1: Inflammasome component proteins: .....	49
1.10.2: Caspase-1 and other member of the caspase family: .....	50
1.10.3: Inflammasome activated cytokines IL-1 $\beta$ and IL-18: .....	53
1.10.4: NLRP1 inflammasome: .....	54
1.10.5: NLRP3 inflammasome: .....	55
1.10.6: NLRP7: .....	60
1.10.7: NLRP12: .....	61
<b>1.11: Aims of this study: .....</b>	<b>63</b>
<b>Chapter 2: .....</b>	<b>67</b>
<b>Materials and Methods .....</b>	<b>67</b>
<b>2.1: Antibodies: .....</b>	<b>68</b>
<b>2.2: Tissue Culturing: .....</b>	<b>69</b>
2.2.1: Semi-adherent cell lines: .....	70
2.2.2: Adherent cell lines: .....	71
2.2.2.1: Bronchial Epithelial cell line: .....	71
2.2.2.2: Human Embryonic Kidney cell line: .....	72
2.2.2.3: Human primary amniotic epithelial cells: .....	73
<b>2.3: <i>Ureaplasma</i>: .....</b>	<b>73</b>
2.3.1: <i>Ureaplasma</i> cultures: .....	73
2.3.2: Harvesting <i>Ureaplasma</i> : .....	74
2.3.3: Recombinant Multiple Banded Antigen: .....	74
<b>2.4: Cell concentration calculation: .....</b>	<b>74</b>
<b>2.5: Cryogenic cell storage: .....</b>	<b>75</b>
2.5.1: .....	75
2.5.2: Cryogenic preservation of cells: .....	76
2.5.2.1: Semi-adherent cell line cryogenic preservation: .....	76
2.5.2.2: Cryogenic preservation of cell lines: .....	76
<b>2.6: Cell stimulation with <i>Ureaplasma</i> spp.: .....</b>	<b>77</b>
<b>2.7: Indirect Immunofluorescence and Flow Cytometry to measure PRR: .....</b>	<b>77</b>
<b>2.8: Fluorescence Activated Cell Sorter (FACS): .....</b>	<b>79</b>
2.9.1: Protein and cytokine measurement: .....	82
2.9.2.1: SDS-PAGE: .....	83
2.9.2.2: SDS-PAGE protocol: .....	85
2.9.3: Western Blot: .....	86

<b>2.10: Cytokine Bead Array (CBA):</b>	<b>89</b>
2.10.1: BD CBA protocol:	90
<b>2.11: Transfection and gene silencing:</b>	<b>91</b>
2.11.1: psiRNA:	92
2.11.2: Agarose gel electrophoresis:	95
2.11.3: Lipofectamine transfection:	96
2.11.4: RNA interference:	96
<b>2.12: Confocal Microscopy:</b>	<b>97</b>
2.12.1: Cell labelling for Confocal microscopy:	98
2.12.2: Confocal imaging of NLRP7-ASC and mitochondrial interaction:	99
2.12.3: Confocal pH sensitivity:	99
<b>2.13: Förster Resonance Energy Transfer (FRET):</b>	<b>99</b>
2.13.1: Cell labelling for FRET:	101
<b>2.14: Profos EndoTrap® endotoxin extraction:</b>	<b>102</b>
<b>2.15: Optimisation of drug concentration for inflammasome inhibitors:</b>	<b>104</b>
<b>2.16: Determination of ammonia concentration:</b>	<b>104</b>
<b>2.17: Bacteria viability detection using flow cytometry:</b>	<b>104</b>
<b>2.18: Determination of pH</b>	<b>105</b>
<b>2.19: Statistical analysis:</b>	<b>105</b>
<b>Chapter 3:</b>	<b>106</b>
<b><i>Ureaplasma</i>-induced innate immune responses in human monocytes</b>	<b>106</b>
<b>3.1: Introduction:</b>	<b>107</b>
<b>3.2: Results:</b>	<b>109</b>
3.2.1: TLR expression levels in mono-mac 6 monocytes in response to yeast in the culture medium of <i>Ureaplasma</i> :	109
3.2.2: Investigating mono-mac 6 innate immune responses and pathways activated in response to <i>Ureaplasma</i> stimulation:	114
3.2.3: <i>Ureaplasma</i> serovar-induced innate immune responses in MM6 cells using yeast positive and yeast negative <i>Ureaplasma</i> culturing medium:	117
3.2.4: TLR expression in mono-mac 6 in response to stimulation by specific <i>Ureaplasma</i> serovars:	119
3.2.5: Determining which PRRs are involved in the innate immune sensing of <i>Ureaplasma</i> using HEK-293 transfected cells:	121
3.2.6: The expression regulation of NLRs in <i>Ureaplasma</i> -activated immune response in mono-mac 6 cells:	124
3.2.7: <i>Ureaplasma</i> serovar-induced innate immune responses in mono-mac 6 monocytes via NLRs:	126
<b>3.3: Conclusion:</b>	<b>128</b>
<b>Chapter 4:</b>	<b>130</b>

<b><i>Ureaplasma</i>-activated immune response in bronchial epithelial cells</b>	<b>130</b>
<b>4.1: Introduction:</b>	<b>131</b>
<b>4.2: Results:</b>	<b>133</b>
4.2.1: Pathogen recognition receptor expression in response to <i>Ureaplasma</i> serovars 2, 3 and 14 in human bronchial epithelial cells:	133
4.2.2: <i>Ureaplasma</i> -induced cytokine production in bronchial epithelial cells:	134
4.2.3: IL-1 $\beta$ production in bronchial epithelial cells in response to <i>Ureaplasma</i> occurs via NLRP3 and NLRP7 inflammasome activation:	138
<b>4.3: Conclusion:</b>	<b>141</b>
<b>Chapter 5:</b>	<b>143</b>
<b><i>U. parvum</i> SV3, SV14 and <i>U. urealyticum</i> SV2 activation of human amniotic epithelial cells</b>	<b>143</b>
<b>5.1: Introduction:</b>	<b>144</b>
<b>5.2: Results:</b>	<b>145</b>
5.2.1: <i>Ureaplasma</i> -activation of human amniotic epithelial cells:	145
5.2.2: TLR expression on human amniotic epithelial cells:	146
5.2.3: TLR2/6, TLR4 and TLR9-dependent cytokine secretion in response to <i>Ureaplasma</i> serovars:	148
5.2.4: Inhibition of <i>Ureaplasma</i> -induced activation of human amniotic epithelial cells by silencing TLR2, TLR6 and TLR9:	151
5.2.5: TLR2 heterotypic association in response to <i>Ureaplasma</i> :	153
5.2.6: TLR and GM-1 ganglioside FRET measurements before and after <i>Ureaplasma</i> stimulation:	155
5.2.7: <i>Ureaplasma</i> internalization recruits MyD88 in endosomes:	158
<b>5.3: Conclusion:</b>	<b>159</b>
<b>Chapter 6:</b>	<b>161</b>
<b>Investigation into NLRs in <i>Ureaplasma</i>-activated immune response in human amniotic epithelial cells</b>	<b>161</b>
<b>6.1: Introduction:</b>	<b>162</b>
<b>6.2: Results:</b>	<b>164</b>
6.2.1: <i>Ureaplasma</i> infection induces inflammasome activation:	164
6.2.2: The NLRP7 and NLRP3 inflammasome are triggered in response to <i>Ureaplasma</i> infection:	167
6.2.3: Effects of inhibitors on <i>Ureaplasma</i> -induced inflammasome activation:	170
6.2.4: NH <sub>3</sub> triggers NLRP7 inflammasome activation:	172
6.2.5: pH alkalization in response to <i>Ureaplasma</i> infection is sensed by NLRP7:	174
6.2.6: Localisation of NLRP7 in alkalinized mitochondria in response to <i>Ureaplasma</i> infection:	177
<b>6.3: Conclusion:</b>	<b>178</b>
<b>Chapter 7:</b>	<b>181</b>

<b>Discussions .....</b>	<b>181</b>
7.1: <i>Ureaplasma</i> activated immune response in mono-mac 6 monocytes: .....	182
7.2: <i>Ureaplasma</i> -activated immune response in bronchial epithelial cells: .....	184
7.3: <i>Ureaplasma</i> -induced immune response via TLR- activated immune response in human amniotic epithelial cells: .....	186
7.4: NLRP7 inflammasome role in the immune activation of human amniotic epithelial cells after stimulation with <i>Ureaplasma</i> : .....	190
7.5: Overall conclusions: .....	193

## **Chapter 1:**

# **Introduction**



## Abbreviations:

AF	Amniotic Fluid
AIM	Absent in melanoma-1
AP-1	Activator protein-1
APC	Antigen presenting cell
ASC	Apoptosis-associate speck-like protein
ATP	Adenosine triphosphate
BAPTA	(1,2-bis(o-aminophenoxy)ethane-N,N,N',N'-tetraacetic acid)
BCECF	2,7-bis(carboxyethyl)-5-(6)-carboxyfluorescein
Bcl-2	B-cell lymphoma 2
BIR	Baculovirus Inhibitor of Apoptosis Domain
BLP	Bacterial lipoprotein
BPD	Bronchopulmonary dysplasia
BSA	Bovine serum albumin
BSS	Bacterial secretion system
Ca <sup>2+</sup>	Calcium
CARD	Caspase Activation and Recruitment Domains
CBA	Cytokine bead assay
CLD	Chronic lung disease
CO(HN <sub>2</sub> ) <sub>2</sub>	Urea
CO <sub>2</sub>	Carbon
COX-2	Cyclooxygenase-2
CpG	Cytosine-phosphate-guanine
CREB	cAMP response element-binding protein
DAMP	Damage associated molecular pattern
DAP	Diaminopimelic acid
DC	Dendritic cell
DD	Death domain
DED	Death effector domain
DMEM	Dulbecco's Modified Eagle's medium
DMSO	Dimethyl sulphoxide
DPI	Diphenyleneiodonium
dsDNA	Double stranded DNA
<i>E.coli</i>	<i>Escherichia coli</i>
ECL	Enhanced chemoluminescence
EDTA	Ethylenediaminetetraacetic acid
ELISA	Enzyme linked immunosorbent assay
ER	Endoplasmic reticulum
ERK	Extracellular signal-regulated kinase
FACS	Fluorescence-activated cell sorter
FCS	Fetal calf serum
FIGO	International Federation of Gynecology and Obstetrics
FITC	Fluorescein isothiocyanate
FL	Fluorescent light

FRET	Förster Resonance Energy Transfer
FSC	Forward scattered
GFP	Green fluorescent protein
GI	Gastrointestinal
GPI	Glycosylphosphatidylinositol
H <sub>2</sub> O <sub>2</sub>	Hydrogen peroxide
HAEC	Human amniotic epithelial cell
HEK	Human embryonic kidney
HRP	Horseradish peroxidase
Hsp	Heatshock protein
iE-DAP	D-glutamyl-meso-diaminopimelic acid
IFN	Interferon
IgA	Immunoglobulin A
IL	Interleukin
IL-1R	Interleukin-1-receptor
IPS-1	Interferon- $\beta$ promoter stimulator 1
IRF	Interferon regulatory factor
IUI	Intrauterine infection
I $\kappa$ B	Inhibitor of kappa-B
JNK	c-Jun N-terminal kinase
K <sup>+</sup>	Potassium
KD	Knock-down
LBP	Lipid binding domain
LPS	Lipopolysaccharide
LRR	Leucine-rich domain
LTA	Lipoteichoic acid
MAPK	Mitogen-activated protein kinase
MBA	Multiple banded antigen
MDA	Malondialdehyde
MDP	Muramyl dipeptide
MEM	Minimum essential medium
MM6	Monomac-6
MMP-9	Matrix metalloproteinase 9
mRNA	Messenger RNA
MSU	Monosodium urate
MW	Molecular weight
Na <sub>2</sub> HPO <sub>4</sub>	Sodium phosphate dibasic
NaAc	Sodium Acetate
NADPH	Nicotinamide adenine dinucleotide phosphate
NaN <sub>3</sub>	Sodium Azide
NaOH	Sodium hydroxide
NBD	Nucleotide binding domain
NCM	Nitrocellulose membrane
NF- $\kappa$ B	Nuclear factor kappa-light-chain-enhancer of activated B cells
NH <sub>3</sub>	Ammonia
NH <sup>4+</sup>	Ammonium
NK	Natural killer

NLR	Nod-like receptor
NLRP	Nod-like receptor PRYIN domain containing
NO	Nitric oxide
NOD	Nucleotide-binding oligomerisation domain receptor
OMV	Outer membrane vesicles
OPI	Oxaloacetate pyruvate insulin
P-I $\kappa$ B	Phospho-inhibitor of kappa-B
PAMP	Pathogen-associated molecular pattern
PBS	Phosphate buffer saline
PCR	Polymerase chain reaction
PFT	Pore forming toxins
PGE	Prostaglandin E
PGF2	Prostaglandin F2
PGN	Peptidoglycan
PI	Propidium iodide
PK	Pharmokinectic
PL	Phospholipase
PMT	Photomultiplier tube
Poly I:C	Polyinosinic-polycytidylic acid
pPROM	Preterm premature rupture of the membrane
PRR	Pattern recognition receptor
PTB	Preterm birth
PTL	Preterm labour
PYD	Pyrin domain
RLR	Rig-like receptor
ROS	Reactive oxygen species
rpm	Revolutions per minute
rRNA	Ribosomal RNA
SD	Standard deviation
SDS-PAGE	Sodium dodecyl sulphate gel electrophoresis
SEAP	Secreted embryonic alkaline phosphates
SEM	Scanning electron microscopy
shRNA	Small hairpin RNA
siRNA	Small interfering RNA
SSC	Side scattered
ssRNA	Single stranded RNA
STET	Saline/Tris/EDTA/Triton
SV	Serovar
TC	Tissue culture
TGF	Transforming growth factor
TIR	Toll/interleukin receptor
TLR	Toll-like receptor
TNF	Tumour necrosis factor
TO	Triazole orange
<i>U. parvum</i> (UP)	<i>Ureaplasma parvum</i>
<i>U. urealyticum</i> (UU)	<i>Ureaplasma urealyticum</i>
<i>Ureaplasma</i> spp.	<i>Ureaplasma</i> (multiple) species
UV	Ultraviolet

V	Voltage
WHO	World Health Organization
WT	Wild-type
y-	Yeast negative
y <sup>+</sup>	Yeast positive

## **1.1: Introduction into *Ureaplasma*:**

### **1.1: Introduction into *Ureaplasma*:**

*Ureaplasma* was first isolated in 1954 as a potential pathogenic cause of non-gonococcal urethritis. Reports of possible associations between the newly identified bacteria and adverse pregnancy outcomes and complications in the neonates, in particular low infant birth weight were also suggested<sup>1</sup>.

The genus of bacteria, *Ureaplasma* belong to the class Mollicutes, a class of bacteria that is defined by a lack of a true cell wall, due to an absence and inability to synthesise a cell wall structural component, peptidoglycan<sup>2</sup>. The inability to produce peptidoglycan is unique in the bacterial kingdom and creates many differences in biological features and processes<sup>1</sup>.

*Ureaplasma* possess one of the smallest recorded genomes to date, as a consequence, the number of their biosynthetic processes is extremely limited. *Ureaplasma* is restricted in its generation of ATP, to the hydrolysis of urea (substrate), by the action of the enzyme urease<sup>3</sup>; a property that is entirely unique to all known bacteria<sup>4</sup>. Urease hydrolyses urea into ammonia (NH<sub>3</sub>) and carbon dioxide (CO<sub>2</sub>) and ATP<sup>5</sup>. *Ureaplasmas* dependence on urea as a sole energy source generally restricts *Ureaplasmas* growth to the genitourinary (in adults) and respiratory tracts (in newborn infants), though *Ureaplasma* has been found to colonise other compartments of the body<sup>6</sup>. Further limitations are imposed on *Ureaplasma* due to its small genome, and require that it must adhere to mucosal cells of its host to enable sufficient urea uptake; this dependence on adherence to host cells accounts for *Ureaplasma* to sometimes be referred to as a parasitic organism.

Genetic analyses of *Ureaplasma* identified 2 species (biovars), 1) *Ureaplasma urealyticum* (*U. urealyticum*) and 2) *Ureaplasma parvum* (*U. parvum*)<sup>7</sup>. Further investigations have identified 14 subspecies (serovars) with the 2 biovars; serovars (SV), SV 2, 4, 5, 7-13 belong to *U. urealyticum* and SV 1, 3, 6 and 14 belong to *U. parvum*<sup>6,8</sup>.

Until recent advances in culturing techniques, *Ureaplasma* proved difficult to culture *in vitro*, preventing in depth investigation into the biological and pathogenic properties of *Ureaplasma*, however these properties are rapidly being further understood by studies carried out in recent years<sup>9</sup>.

### **1.1.2: *U. urealyticum* and *U. parvum*: what is the difference?**

As previously stated there are 14 known and classified serovars of *Ureaplasma* that have been segmented to 2 biovars, *U. urealyticum* (biovar 2) and *U. parvum* (biovar 1). Genome size, sequencing of 16S rRNA gene and differences in intergenic region spacing of 16S-23S rRNA, urease gene subunits variations, enzyme polymorphisms and target sequences of 5' ends of the multiple-banded antigen (MBA) gene are all used to differentiate each bacterium into its relevant biovar and serovar<sup>5,10,11</sup>.

The most striking difference between the 2 biovars is the genome size and in differentiating serovars, 5' end of MBA gene sequence is specific to each serovar<sup>10,11</sup>.

A significant number of papers and studies published on the issues and implications of *Ureaplasma* disregard specifying not only *Ureaplasma* to biovar type, but also to the specific serovar being investigated, and simply use the names *Ureaplasma urealyticum* or *Ureaplasma spp.*, as reported by Sung 2013, and as a result, serovar specific pathogenic activity is unclear<sup>5</sup>.

### *1.1.3: Epidemiology of Ureaplasma:*

Accurate values of the prevalence and rates of infection of *Ureaplasma* prove to be a difficult task to achieve in both the general population and within specific/target groups of people. This is mainly due to a large number of studies on the subject, with many studies using differing methods of accumulating data, obtaining information from different bodily compartments, demographic sources and cause for investigation, (during pregnancy, general public investigation, etc.). The most commonly stated prevalence of *U. urealyticum* in the lower genital tract flora of pregnant women is 40-80%<sup>12</sup>, though one study suggested an incidence range of 35-90%<sup>13</sup>. *U. urealyticum* incidence in sexually inactive women was reported to be up to 40%<sup>8</sup>. Association of *Ureaplasma* and infertility has been reported to be as high as 78% of infertile men testing positive for *Ureaplasma* colonisation, where as only 19% of fertile men investigated were shown to have *Ureaplasma* colonisation<sup>8,14,15</sup>.

### *1.1.4: Proposed pathogenic and virulence factors of Ureaplasma spp:*

Several possible pathogenic properties and virulence factors of *Ureaplasma spp.* have been suggested over the years, predominantly: multiple banded antigen (MBA), ureaplasma immunoglobulin A (IgA) protease, ammonia (NH<sub>3</sub>), phospholipase (PL) A1, A2 and C and the production of hydrogen peroxide (H<sub>2</sub>O<sub>2</sub>)<sup>16-18</sup>. There have been many studies into the pathogenic properties of *Ureaplasma spp.* many with conflicting results and conclusions. Older studies suggested the roles of the above-mentioned possible factors, but were disputed by later studies. These disputes were often based on the inability to identify and locate the genes coding for the suspected proteins and structures. Further investigation and understanding of *Ureaplasma spp.*

genetic sequence and gene coding has once again opened the door to the possible pathogenic roles of PLA1, PLA2, PLC and IgA protease.

#### ***1.1.4.1: Multiple Banded Antigen (MBA):***

MBA has been implicated as a major ureaplasma molecule and has been implicated in possible immune evasion mechanisms. MBA is a *Ureaplasma* cell surface exposed lipoprotein capable of size and phase variation and has been studied *in vitro* and *in vivo* to determine its role as an antigen<sup>19-21</sup>. Further studies have compared MBA antigen properties to whole cell *Ureaplasma* bacterial infection, to investigate immune pathway activation and signalling induced by MBA and *Ureaplasma*<sup>22</sup>.

Genetic sequencing of MBAs in each *Ureaplasma* serovar were extensively investigated by Paralanov et al, and several interesting features of MBAs were proposed. MBA studies suggest that *Ureaplasma spp.* have an ability to vary MBA variable domains by each serovar and may initiate differing innate immune responses when detected by the innate immune system<sup>10,23</sup>. The ability to adjust the MBA variable domain may therefore be an immune evasion mechanism of the bacterium, once it has been detected by the host immune system<sup>10</sup>.

#### ***1.1.4.2: Other Ureaplasma antigenic properties:***

IgA protease is an established pathogenic component in other bacteria, especially those that colonise mucosal tissues. IgA protease is believed to cleave host IgA, which enables them to evade immune recognition and therefore preventing immune responses in the mucosal tissue. *Ureaplasma spp.* IgA protease activity has been detected in *Ureaplasma spp.* infections; however, a gene coding for IgA protease has not been identified in *Ureaplasma spp.* to date. *Ureaplasma spp.* genome does not appear to contain genetic coding sequences for proteins that have similar functions and roles in other bacteria. *Ureaplasma spp.* IgA protease appears to be novel and



share no homology with IgA genes in any other bacterial genomes. Gene BLASTing was unable to find orthologues (homologous gene sequences) in any other recorded genome<sup>24</sup>. There are still several coding genes in *Ureaplasma spp.* genome whose function remains unknown, and it is more than possible that within these functionally unidentified genes, the IgA protease coding is contained.

IgA protease's pathogenic properties lie in its ability to evade detection in the mucosal tissue of the cervix and uterus, enabling not only colonisation to remain undetected but also enabling *Ureaplasma spp.* to ascend from the lower genital tract to the (normally) sterile upper genital track<sup>24</sup>.

Similarly PLA1, PLA2 and PLC coding gene sequences have not yet been identified in *Ureaplasma spp.* genome, suggesting that these genes are encoded in the genes of the known gene sequences that have an unknown function.

The activity of *Ureaplasma* urease metabolises urea ( $\text{CO}(\text{NH}_2)_2$ ) into  $\text{NH}_3$  and  $\text{CO}_2$  with the production of ATP, which is the main energy source for *Ureaplasma*.  $\text{NH}_3$  may act as a damage associated molecular pattern (DAMP), and could possibly activate the immune response. A model was set up to test the detrimental effect of *Ureaplasma*-produced  $\text{NH}_3$  on mice, and found that indeed  $\text{NH}_3$  was not only detrimental but also highly lethal to mice<sup>25</sup>. After administering an intraperitoneal dose of 100 $\mu\text{g}$  whole *Ureaplasma*, 100% of the four control mice died after 5 minutes. However, by administering a urease inhibitor (flurofamidine) 2 hours prior to the lethal dose of whole *Ureaplasma*, survival rate of four test mice was 100%. This study strongly supports that  $\text{NH}_3$  produced by *Ureaplasma* urease acts as a DAMP and is likely to be a strong candidate for initiating an immune response.

However there has been little further investigation into  $\text{NH}_3$  as a *Ureaplasma* pathogenic factor since this study.

### *1.1.5: Implications associated with Ureaplasma:*

Since its initial identification as the potential pathogen in causing non-gonococcal urethritis, *Ureaplasma* has been attributed as the possible cause of a plethora of adverse conditions. Most notably in the literature is the range and extent of studies into the role that (if any) *Ureaplasma* plays in pregnancy complications, adverse outcomes during labour and severe implications for newborns, especially neonate. Increasingly in the literature is the growing interest in *Ureaplasma* as a cause of female and especially male infertility<sup>26,27</sup>. *Ureaplasma spp.* have also been implicated urogenital infections, the formation of kidney stones, renal abscesses, meningitis and arthritis<sup>28,29,8</sup>. Accumulating epidemiologic and experimental data suggests that intrauterine *Ureaplasma* infection is strongly associated with, bronchopulmonary dysplasia (BPD) in neonates, intra-amniotic infection (IAI), and preterm premature rupture of the membrane (pPROM) leading to preterm birth (PTB)<sup>13,30</sup>.

This study concentrates solely on adverse pregnancy outcomes and neonatal complications as a result of *Ureaplasma* initiating an inflammatory response via the innate immune system. Maternal *Ureaplasma* associated complications include, postpartum endometritis, bacterial vaginosis and salpingitis, and death through complications during labour. Complications associated with *Ureaplasma* infections carry a significantly higher rate of morbidity and mortality in the neonate than in the mother. *Ureaplasma spp.* has been thought to be the cause of stillbirths and miscarriages and is strongly implicated throughout the literature in its involvement in exacerbating and maybe even inducing premature labour/preterm birth (PTL/PTB)<sup>1</sup>. Rates of neonatal morbidity and mortality have an inverse relationship to the gestation period, where full term births occur around the completion of week 40, and

the near zero rate of survival of infants born  $\leq 20$  weeks are after conception. As a result of its implication to PTB, *Ureaplasma spp.* could be considered the direct cause of complications common to PTB for example neurological, developmental disorders and necrotising enterocolitis<sup>6,31</sup>. Other direct complications and disorders associated with *Ureaplasma spp.* are bronchopulmonary dysplasia (BPD), pneumonias, cerebral white matter lesions invasive diseases, bacteraemia and rarely sepsis, central nervous system invasion (meningitis), cerebral palsy, intraventricular hemorrhage and hydrocephalus and septic arthritis and osteomyelitis<sup>2,8,32-35</sup>. While the mechanisms linking *Ureaplasma* to these adverse reaction is unclear, a likely cause is the inappropriate induction of inflammatory immune responses, likely to be triggered by the innate immune system upon detection of the bacteria<sup>36,37</sup>.

## 1.2: Preterm birth:

### Time map of prenatal development last from menstruation to birth:

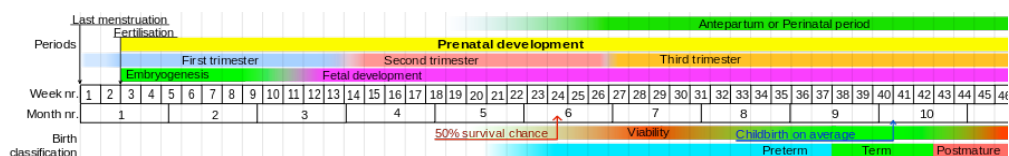


Figure 1.2: Schematic time map of developmental stages, trimesters, preterm, term and post-mature gestation periods in accordance with weeks and months ([URL:http://en.wikipedia.org/wiki/Preterm\\_birth](http://en.wikipedia.org/wiki/Preterm_birth) (14/06/14)).

The World Health Organization (WHO) and the International Federation of Gynecology and Obstetrics (FIGO) define preterm birth also known as preterm labour (PTL) to be when a baby is born before the completion of 37 weeks of gestation. WHO estimates that around 15 million babies born each year globally are preterm, at a rate of between 5-18%, and the rate continues to be rising, (WHO 11/06/14). However the gestation cutoff period for PTB varies by location<sup>38</sup>. Rates in

the USA are recorded to be between 12-13%, in Europe and other developed countries the rate is slightly lower at around 5-9%, whilst figures of 25% have been reported in developing countries<sup>39,40</sup>. Discrepancies in defining PTB is a constant problem when trying to accurately determine rates of PTB, for example a gestation period of 36 weeks and 6 days should (according to WHO and FIGO) be defined as preterm, but many clinicians and midwives will round up 36 weeks and 6 days to 37 weeks, erroneously classing the birth as a full term birth<sup>41</sup>. A study by Balchin et al. of 17 London hospitals found that rounding up was still commonly practiced and accounted for up 10.1% of PTB misclassification<sup>42</sup>.

Prenatal mortality rates are recorded to be as high as 75%, and account for over 50% of long term morbidity<sup>43</sup>.

PTB can be subdivided by period of gestation: near term (34-36 weeks) 60-70%, moderate prematurity (32-33 weeks) 20%, severe prematurity (28-31 weeks) 15% and extreme prematurity (<28 weeks) 5%<sup>38</sup>.

Records taken from North West Thames database (1988-2000 inclusive) of 517,381 births that required transfer to special care baby unit, where as follows: 90% for those born before 33 completed weeks of gestation, but this number fell steadily to below 5% by 39 weeks (83% at 34 completed weeks, 58% at 35 weeks, 31% at 36 weeks, 14% at 37 weeks and 7% at 38 weeks)<sup>41</sup>.

### ***1.2.1: Preterm premature membrane rupture (pPROM):***

pPROM is defined as rupture of the fetal (amniotic sac and chorion) membrane with leakage of amniotic fluid 1 hour or more before the initial onset of uterine contractions. pPROM occurs in about 25-30% of PTB<sup>38</sup>, and complicates around 4-7% of all births and it directly correlated to short gestation periods and high

association with perinatal morbidity and mortality rates<sup>46</sup>. Risk factors associated with pPROM increase significantly with the time between rupture of the membrane and the actual onset of labour.

### ***1.2.2: Preterm birth associated and contributing factors:***

PTB carries with it potential risk factors for both mother and infant and has been attributed to a wide range of causes: maternal age, number of sexual partners, multiple births (twins, triplets, etc), emotional stress in mother, maternal hormone variations, trauma, length of cervix, racial and socioeconomic factors, number of previous pregnancies, predisposition to PTB variation in vaginal microbial flora, intrauterine infection and many more<sup>38,40,41,44</sup>.

The three precursors of PTB are medical intervention (medically induced or caesarian section), spontaneous preterm labour, with intact membrane, and preterm premature rupture of the membrane (pPROM), irrespective of caesarian or vaginal delivery<sup>45</sup>.

### **1.3: *Ureaplasma spp.* detection methods and associated problems:**

Detection of *Ureaplasma spp.* was initially limited to bacterial culturing of samples, progressing to antibody specific detection and more recently PCR. Detection of *Ureaplasma spp.* through culturing methods have led to inaccuracies in *Ureaplasma spp.* epidemiological rates in older studies, as it is known to be a difficult organism to culture and proved to produce high rates of false-negative results. Furthermore, bacterial culturing gives qualitative but not quantitative results and cannot differentiate between different serovars. Antibody detection methods produced more accurate results, but the method is an arduous and time-consuming one and was

therefore not a common way of detecting *Ureaplasma spp.* in samples. With the development and advances in PCR, highly accurate qualitative, quantitative and serovar specific measurements and detection is possible. An example of culturing inaccuracy was shown by a 91% false-negative detection rate when compared to PCR based methods<sup>46</sup>. In addition, quantitative PCR measurements showed that *Ureaplasma spp.* load impacts *Ureaplasma spp.* associated complications. The quantitative load of *Ureaplasma spp.* load found by PCR, directly implicated the outcome of infection, due to increased IL-6 levels in amniotic fluid (AF) with increased *Ureaplasma spp.* load<sup>46</sup>.

*1.3.1: Possible reason for inconsistency between the rate of people presenting with Ureaplasma colonisation and the rate of adverse effect experienced:*

MBA has been identified as a possible pathogenic structure that can trigger an immune response. MBA has been shown an ability to vary its MBA phase and size, which could result in MBA of varying pathogenicity not only in different serovars, but also in different colonies of the same serovar. The variation of MBA phase could be a deliberate immune evasion technique employed by *Ureaplasma* to reduce the likelihood of all bacteria in a colony to be detected and killed by the host immune system. The immune evasion technique could explain why the rate of *Ureaplasma* colonisation and adverse health outcome may vary.

Another possible explanation is that not all human immune systems detect *Ureaplasma* and thus mount no immune/inflammatory response to it. The immune response to *Ureaplasma* is likely to be the cause of the detrimental health effects

caused by *Ureaplasma*, therefore only people with immune systems that detect its presence will experience health complications.

*Ureaplasma* may be able to colonise a host at levels that the body does not react to for long periods of time. Thus people would present with *Ureaplasma* colonisation without the presentation of any symptoms.

#### **1.4: Association between *Ureaplasma* spp. and PTB/pPROM:**

The statistics of *Ureaplasma* spp. infection with newborn implications varies greatly throughout the literature. However the general consensus is that there is a general and direct increase in infant morbidity and mortality with a greater period of uterine infection during gestation.

In a Belgian study of approximately 2000 women, 4.9% experienced PTB and of whom 53.6% tested positive for *Ureaplasma* spp<sup>47</sup>. In a study of 150 women with pPROM, 96% tested *Ureaplasma* spp. positive, whilst 32% of women who tested positive did not experience membrane rupture<sup>46</sup>. In a Czech study of 225 women with pPROM showed 68% *Ureaplasma* spp. cervical colonization, while only 17% of *Ureaplasma* spp. negative women experienced pPROM<sup>48</sup>.

Neonates with gestation periods of <33 weeks showed 35% *Ureaplasma* spp. colonization from tracheal or nasopharyngeal aspirates/specimens taken within 1 week after birth<sup>49</sup>.

From *Ureaplasma* spp. colonized women, De Francesco *et al.* found *Ureaplasma parvum* serovars 3 and 14 to colonise 86% of symptomatic women<sup>50</sup>. In a study by Kong *et al.*, of 263 vaginal swabs tested, 228 (87%) presented with *Ureaplasma parvum* colonisation, and 50 (19%) presented with *Ureaplasma urealyticum*, suggesting a higher prevalence of *U. parvum* than *U. urealyticum*<sup>51</sup>.

Hilton *et al.* showed highly significant association between *Ureaplasma spp.* colonization and late term abortion and early PTB<sup>52</sup>.

A proposed theory for the role of Toll like receptors (TLRs) in pPROM leading to PTB is that TLRs would detect *Ureaplasma* PAMPs and initiate an immune response. TLRs activation would lead to production of inflammatory cytokine such as TNF- $\alpha$ , IL-6 via the NF- $\kappa$ B signaling pathway, which in turn would lead to IL-1 $\beta$  production via NLR inflammasome formation. The effects of the inflammatory cytokines could damage the cells of the amniotic membrane, causing its rupture, leading to premature birth.

#### *1.4.1: Brochopulmonary dysplasia and associations with Ureaplasma spp. infections:*

Viscardi *et al.* (2009) propose a new and more accurate definition of BPD characterized by more uniform inflation, decreased number but larger sized alveoli that occurs via prolonged (less fulminant) inflammation<sup>18</sup>.

The unique defining feature of BPD that distinguishes it from other lung disorders is a major arrest in the development of the alveolar and microvascular system, thought to be associated with robust inflammatory response during the saccular stage of lung development. Unlike other neonatal lung disorders BPD is not associated with fibrosis, airway injury or emphysema<sup>53</sup>. BPD mortality is due to poor vascular networking through the lungs, which in turn impacts later development<sup>53</sup>. Neonate that present with BPD often require intensive care for the first few week after birth, with incubation in high oxygen environments, as the oxygen uptake efficiency of



defective lungs is poor. In addition antibiotic and corticosteroid anti-inflammatory treatment are administered.

A study by Jobe *et al.* gives the rate of BPD association with *Ureaplasma spp.* to be 43%, compared to 19% in the control group, and a study by Kallapur *et al.* stated a risk factor of BPD 1.6 (C.I. 1.1. - 2.3) in association with *Ureaplasma spp.* infection at 36 weeks and 2.8 (C.I. 2.3 – 3.5) at 2 weeks compared to uncolonized control groups<sup>17,53</sup>. Viscardi *et al.* show figures of 30% of neonates with a gestation period of  $\leq 28$  weeks presented with BPD, whilst several animal models of intrauterine infection with solely *Ureaplasma spp.* have shown direct association with increased pro-inflammatory cytokine abundance, furthermore that this increase can be a direct cause of BPD<sup>18</sup>. It must be taken into consideration that many animal models may not produce results that are relevant to humans as their immune response has been shown to differ from the human immune response, for example in mouse and sheep studies, however Rhesus macaque model studies have been shown to be accurate models as their immune response is very similar to human responses. *Ureaplasma spp.* Intrauterine infection (IUI) causes invasion of the chorion and amniotic fluid by inflammatory cells, which create an inflammatory response cascade that can potentially lead to premature birth and pPROM. The production of pro-inflammatory cytokines, TNF- $\alpha$ , IL-1 $\beta$ , IL-6, IL-8, prostaglandins PGE2 and PGF2- $\alpha$ , and MMP-9, in addition to the production of prostaglandins and COX-2 by placental infection can lead to uterine contractions, cervical dilation and effacement, and membrane rupture, ultimately initiating PTB and pPROM<sup>54</sup>. Placental trophoblast cells initiate MAPK, ERK1 and ERK2 pathways via TLR2, 4 and 6 pathways. Further support that *Ureaplasma spp.* infection is the cause for this cascade comes from studies where the use of heat killed *Ureaplasma parvum* 1 and 8 failed to initiate the same immune

cascade. Histopathology specimens of BPD tissue after IUI in Rhesus models showed increased infection period correlated to increased neutrophil and macrophage influx, epithelial necrosis, type II cell proliferation, with increased collagen deposition and thickening of alveoli walls<sup>55</sup>. These changes are also observed in human BPD tissue that presented with moderate to severe fibrosis, increased myofibroblasts, disordered elastin accumulation and elevated numbers of TNF- $\alpha$  and TGF- $\beta$ -1 immunoreactive cells, when compared to lung tissue sample from infants that died from other lung associated disorders. Tracheal aspirates from infants with BPD showed increased NF- $\kappa$ B, VEGF, inducible nitric oxide synthase (iNOS), soluble and cell associated ICAM-1 activation. These *Ureaplasma spp.* associated inflammation responses cause hyperoxia, volutrauma, barotrauma insults and increased risk of perinatal pulmonary infections<sup>3,46</sup>.

#### ***1.4.2: Immune response pathways linking Ureaplasma spp. infection to BPD:***

The major cytokine that is associated with intra-amniotic *Ureaplasma spp.* infection is IL-6, although TNF- $\alpha$ , IL-1- $\beta$ , IL-8 and several other cytokines have been reported as possible causes. These cytokines create a pro-inflammatory response in the lung epithelial tissue, causing fibrosis and inhibition of adequate tissue development<sup>54</sup>.

#### ***1.4.3: Ureaplasma spp. related BPD treatment:***

It is unknown if the eradicate of *Ureaplasma spp.* colonisation with antibiotics of the respiratory tracts of neonates will prevent or significantly treat *Ureaplasma spp.* mediated lung injuries. It is likely that infants presenting with BPD have already sustained the causal damage to their lungs, and that use of antibiotic treatment

cannot reverse the damage. Erythromycin is currently the antibiotic of choice when treating neonates with *Ureaplasma* infections, but has been shown ineffective in the treatment/prevention of BPD (likely due to reason explained above)<sup>56</sup>. Erythromycin has also been shown to be unable to fully eradicate *Ureaplasma* colonisation from the respiratory tract of infected neonates<sup>56,57</sup>.

*In vitro* studies have shown that newer 14-member macrolides and 15-member azalides show improved pharmacokinetic (PK) activity, when compared to erythromycin, with the additional benefit of possible anti-inflammatory properties, which may reduce the risk of further damage to lung tissue caused by sustained innate immune inflammatory responses<sup>58,59</sup>. Two such antibiotics are azithromycin and clindamycin, however their dosage and safety in neonates is still in debate, with azithromycin being associated with cardiac disorders and death in neonates<sup>60-63</sup>. Viscardi *et al.* have shown that azithromycin can be administered at safe doses with the complete eradication of *Ureaplasma* from the respiratory tract, but the test sample size was too small for conclusive results<sup>62</sup>. Further investigations into the effectiveness of azithromycin and clindamycin over erythromycin are required.

In a study of 5377 pregnant patients, treatment with clindamycin at 25-37 weeks of gestation, a significant reduction in the rate of preterm labour in women infected with *Ureaplasma* colonisation was observed<sup>64</sup>. Equally important, a significant reduction in neonatal complication was also observed, suggesting that treatment with clindamycin during pregnancy could substantially reduce rates of PTB and associated risk factors. It is important to state however, that this study could not conclude whether *Ureaplasma spp.* infection itself was the cause of PTB or respiratory disorders, as clindamycin is not specific to *Ureaplasma spp.* Kallapur *et al.* (2013) also ran randomized trials of erythromycin, against amoxicillin plus

clavulanic acid and a placebo, and found that only erythromycin decreased the rate of mortality, BPD and other (potentially) *Ureaplasma spp.* associated implications<sup>17</sup>. This is of significance as amoxicillin is a broad spectrum antibiotic that is ineffective against *Ureaplasma spp.* as it contains no cell wall (specifically PGN).

#### Fetal compartment development during gestation:

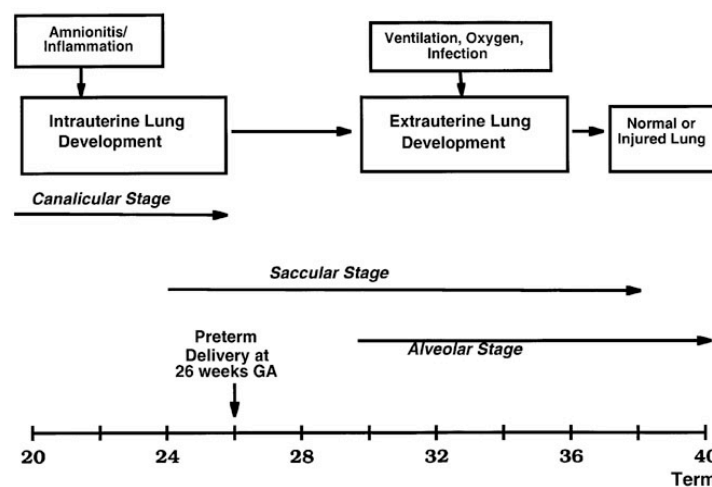


Figure 1.4.3: Lung development must continue for survival of the very low birth weight infant after preterm delivery at 26 weeks. Antenatal infection/inflammation associated with chorioamnionitis can modulate lung development, as can postnatal causes of inflammation such as mechanical ventilation, supplemental oxygen, or infection. The stages of lung development are modified from Burri<sup>65</sup>.

### **1.5: The immune system:**

The world presents a diverse and constant variety of potentially damaging and life threatening pathogens, toxins and other harmful particles that if unchecked and protected against, would make life extremely difficult. Since life began, the evolutionary struggle to survive required development in even the most primitive life forms to defend themselves against such hazardous threats. All living organisms have, at some level, mechanisms for minimizing and repairing damage caused by potential threats. Higher organisms have developed highly specialized and effective

methods of defending themselves against antigenic agents such as bacteria, fungi, parasites and viruses, in addition to other hazardous sources like UV and endogenous metabolic stresses. In vertebrates a two-part immune system has been developed, consisting of the innate immune system and the acquired immune system. For decades nearly all of medical research revolved around furthering the understanding of the acquired immune system, as it was thought this system would hold the keys to overcoming pathogen induced disorders. In contrast, over the previous 20 years or so, interest has increasingly turned to the innate immune system in preventing and treating disorders caused by pathogenic and antigenic sources.

The acquired immune system is a highly specific and highly evolved system of targeting and combating pathogens via unique molecular patterns present in/on the antigen. B and T-cells (antibody producing and killer/helper respectively) are presented with these unique pathogen associated molecular patterns (PAMPs) via innate immune, antigen-presenting cells, after which antibodies and other specialized anti-antigenic molecules are produced to eradicate infected cells and pathogens. Though the acquired immune system is incredibly effective at fighting off infections, there is an initial 3-4 day lag between infection by the antigen/pathogen and the complete activation of the B and T-cells, as this time is required for recognition and antigen presenting to these immune cells by innate immune system cells.

In humans, we have many ways of preventing the infiltration of the body proper by both antigens and pathogens. These include physical barriers such as the skin, antimicrobial secretions, such as mucosal secretions and tears, and mechanical mechanisms, such as cilia in the lung, nasal hairs, vomiting, and clotting of blood after injury. In addition and almost paradoxically, humans have a symbiotic relationship with a variety of microbes, mainly in the gastrointestinal tract that also

provide a defense against pathogenic non-commensal microbes. All of these structures and mechanisms form part of the innate immune system, which as the name implies is an immune system that is present and functioning from not only the time of birth, but even during the gestation period. The innate immune system also comprises a complex and diverse range of germ-line cells that encode specialized receptors that recognise and interact with antigens, via pattern recognition receptors (PRR) that target highly conserved structures belonging to a plethora of antigens. These PRRs are found on all myeloid (innate immune) cell-lines, such as monocytes, which differentiate into macrophages and dendritic cells, as well as certain epithelial cells. PRR expression in epithelial cells can be explained by the nature of their position in the body, which is mostly at points of possible antigen interaction, such as the lungs and gastrointestinal tract. The myeloid cell-lines constantly circulate the body in the blood stream, migrate through tissues and localize at junctions in the body where antigen detection is optimal, such as in the lymphatic system. PRRs belong to three functionally similar but structurally and behaviorally different groups. These are the Toll-like receptors (TLRs), RIG-1-like receptors (RLRs) and NOD-like receptors (NLRs) and they work both individually and cooperatively with each other to bring about the most effective and efficient response to the antigen that is encountered.

#### ***1.5.1 History of Toll-like receptors (TLRs):***

Anderson *et al.* first identified a protein in *Drosophila* in 1985 that was suggested to be important in the dorsal-ventral polarity during *Drosophila*'s developmental process and named it Toll<sup>66,67</sup>. Little did they know that this protein would not

control the developmental process in *Drosophila* but would eventually prove to be key proteins in the innate immune recognition.

Prior to the discovery of the TLRs, the innate immune system was thought to be a non-specific response to infection. How inflammation was triggered or how the microbial pathogens were sensed was unknown.

Charles Janeway was the first to hypothesise that the innate immune system was highly complex and specific in his paper written for the Cold Spring Harbor Symposia in 1989. Janeway *et al.* (1989) proposed the innate immune system must have molecules encoded in the germline that would be able to recognize signatures of motifs from pathogens. He named the molecules, PRRs and the motifs that they would recognize PAMPs<sup>68</sup>.

Janeway's hypothesis was proven right almost ten years later, when *Drosophila* that did not express the Toll protein was found to be highly susceptible to the fungi *Aspergillus fumigates*. *Drosophila* that did not express this PRR were highly susceptible to fungal infections that eventually led to their death after 2-3 days of infection<sup>69</sup>. The rate of mortality in Toll deficient *Drosophila* was 100%, in comparison to ~10% mortality rate in wild-type and uninfected Toll deficient groups. This demonstrated the importance of Toll protein in *Drosophila* immune defense against this pathogen and linked for the first time the Toll protein with innate immunity.

Genetic homology was found between the *Drosophila* Toll proteins and proteins found in humans<sup>70</sup>. These proteins shared the PRR characteristic observed in the Toll protein and were shown to be similar to the human orthologue gene that was named the hToll. Five further Toll homologues were discovered in humans by Rock *et al.*,

naming them Toll-like receptors, with the initial hToll protein being named TLR4, and the others, TLR1, 2, 3 and 5<sup>71</sup>.

#### ***1.5.2: Toll-like receptor family:***

To date there have been 10 human TLRs identified, each is activated by a specific individual or group of ligands. The cellular distribution of TLRs varies, some are located in the cellular membrane able to bind to extracellular PAMPs, and others are located in intracellular compartments, incorporated in structures such as the endoplasmic reticulum and endosomes, and recognise intracellular PAMPs, such as pathogenic nucleic acids and viral capsid proteins.

TLRs are Type 1 transmembrane proteins that share a similar architecture, with three key constituent domains, a LRR ectodomain, single transmembrane domain and an intracellular Toll-interleukin-1 receptor (TIR) domain. An LRR typically contain 24-29 amino acids, in a conserved sequence of an “LxxLxLxxNxL” motif in addition to a variable region. The LRR domain is formed of approximately 19-24 consecutive LRRs that create a coiled solenoid like structure. The leucine amino acids orientate inwards and form hydrophobic interactions in the LRR domain core. The hydrophobic interactions in addition to the asparatines side chain in the LRR motif form a stable horseshoe like structure<sup>72</sup>. Cysteine rich regions at the C-terminal end of the LRR domain form the strong binding TLR transmembrane domain. Upon interaction with a ligand, TLRs dimerise in a hetero- or homodimerisation fashion, via the C-terminal region of the ectodomain. This dimerisation causes conformational changes in the two dimerised proteins, bringing together the TLR TIR domains, with additional adaptor molecules, that initiate downstream immune response pathways. X-ray crystallography of the heterodimerisation of TLR1/2



shown that the TIR domains were brought close enough to form the heterodimer that brought about the theorized signal transduction and initiation of the intracellular signaling cascade<sup>73</sup>.

TLR signaling cascades ultimately lead to the activation of transcription factors nuclear factor kappa-light-chain-enhancer of activated B-cells (NF-κB), mitogen-activated protein kinases (MAPK) and interferon regulatory factor (IRF) genes<sup>74</sup>.

### TLR ligands and their origins:

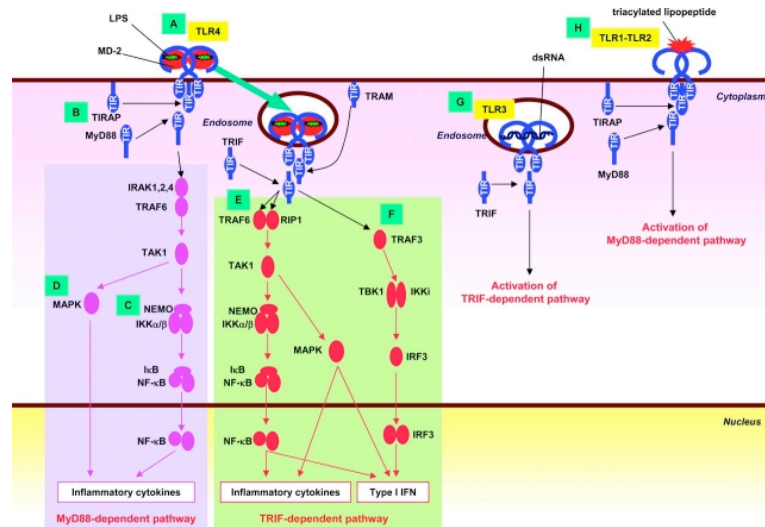
Table 1   <b>Toll-like receptors and their ligands</b>			
Receptor	Ligand	Origin of ligand	References
TLR1	Triacyl lipopeptides	Bacteria and mycobacteria	112
	Soluble factors	<i>Neisseria meningitidis</i>	113
TLR2	Lipoprotein/lipopeptides	Various pathogens	114
	Peptidoglycan	Gram-positive bacteria	115,116
	Lipoteichoic acid	Gram-positive bacteria	116
	Lipoarabinomannan	Mycobacteria	117
	Phenol-soluble modulin	<i>Staphylococcus epidermidis</i>	118
	Glycoinositolphospholipids	<i>Trypanosoma cruzi</i>	119
	Glycolipids	<i>Treponema maltophilum</i>	120
	Porins	<i>Neisseria</i>	121
	Atypical lipopolysaccharide	<i>Leptospira interrogans</i>	122
	Atypical lipopolysaccharide	<i>Porphyromonas gingivalis</i>	123
	Zymosan	Fungi	124
	Heat-shock protein 70*	Host	125
TLR3	Double-stranded RNA	Viruses	52
TLR4	Lipopolysaccharide	Gram-negative bacteria	9
	Taxol	Plants	126
	Fusion protein	Respiratory syncytial virus	127
	Envelope protein	Mouse mammary-tumour virus	128
	Heat-shock protein 60*	<i>Chlamydia pneumoniae</i>	129,130
	Heat-shock protein 70*	Host	131
	Type III repeat extra domain A of fibronectin*	Host	132
	Oligosaccharides of hyaluronic acid*	Host	133
	Polysaccharide fragments of heparan sulphate*	Host	134
	Fibrinogen*	Host	135
TLR5	Flagellin	Bacteria	136
TLR6	Diacyl lipopeptides	<i>Mycoplasma</i>	137
	Lipoteichoic acid	Gram-positive bacteria	116
	Zymosan	Fungi	138
TLR7	Imidazoquinoline	Synthetic compounds	139
	Loxoribine	Synthetic compounds	12
	Bropiramine	Synthetic compounds	12
	Single-stranded RNA	Viruses	140,141
TLR8	Imidazoquinoline	Synthetic compounds	142
	Single-stranded RNA	Viruses	140
TLR9	CpG-containing DNA	Bacteria and viruses	143
TLR10	N.D.	N.D.	–
TLR11	N.D.	Uropathogenic bacteria	144

\*It is possible that these ligand preparations, particularly those of endogenous origin, were contaminated with lipopolysaccharide and/or other potent microbial components, so more-precise analysis is required to conclude that TLRs recognize these endogenous ligands. N.D., not determined; TLR, Toll-like receptor.

Table 1.5.2: Table of the TLRs, their ligands and the origins of the ligands<sup>75</sup>

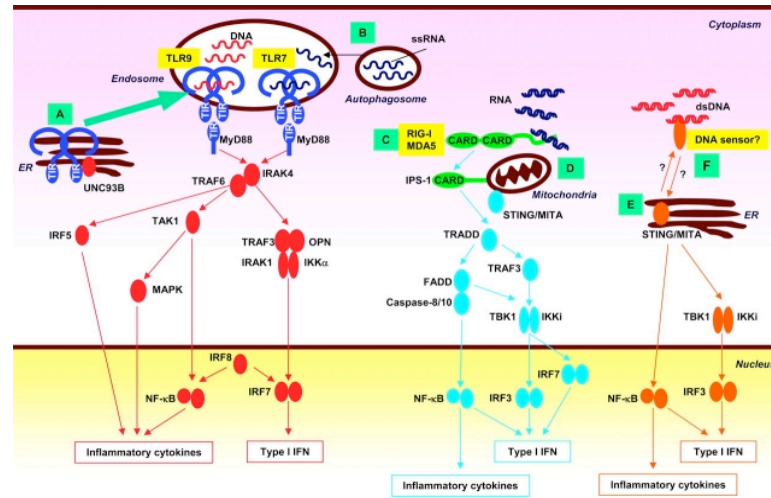
Table 1.5.2 lists the 10 human TLRs (1-9 and 11) and the ligands that activate them. TLRs detect a broad spectrum of PAMPs and DAMPs, and the initiate specific and efficient immune responses to the specific ligand.

#### TLR-activation of immune response signaling pathways:



**Figure 1.5.2.1:** Signaling pathways triggered by TLR3, TLR4 and TLR1–TLR2. (A) The TLR4–MD-2 complex engages with LPS on the cell surface via LBP and CD14 (data not shown) and then recruits a TIR domain-containing adapter complex including TIRAP and MyD88. The TLR4–MD-2–LPS complex is subsequently trafficked to the endosome, where it recruits TRAM and TRIF adapters. (B) TIRAP–MyD88 recruits IRAK family members and TRAF6 to activate TAK1. (C) The TAK1 complex activates the IKK complex composed of IKKα, IKKβ and NEMO (IKKγ), which catalyze phosphorylation of IκB proteins. Phosphorylated IκB proteins are degraded, allowing NF-κB to translocate to the nucleus. (D) TAK1 simultaneously activates the MAPK pathway. The activation of NF-κB and MAPK results in induction of inflammatory cytokine genes (MyD88- dependent pathway). TRAM–TRIF recruits (E) TRAF6 and RIP-1 for activation of TAK1 as well as (F) TRAF3 for activation of TBK1–IKKε that phosphorylates and activates IRF3. Whereas NF-κB and MAPK regulate expression of inflammatory cytokine genes in both pathways, IRF3 regulates expression of type I IFN in the TRIF-dependent pathway only. (G) TLR3 resides in the endosome and recognizes dsRNA. It recruits TRIF to activate the TRIF-dependent pathway. (H) TLR1–TLR2 recognizes bacterial triacylated lipopeptide and recruits TIRAP and MyD88 at the plasma membrane to activate the MyD88-dependent pathway (<sup>76</sup>).

### Intracellular TLR-activated immune response signaling pathways:



**Figure 1.5.2.2:** Recognition of viral nucleic acids by TLRs, RLRs and the cytosolic DNA sensor. (A) In pDCs, TLR7 and TLR9 reside in the ER and interact with UNC93B and are trafficked to the endosome to recognize viral ssRNA and DNA, respectively. These TLRs recruit MyD88, IRAK4 and TRAF6, which in turn activates TAK1, IRF5 and TRAF3. TAK1 mediates activation of NF- $\kappa$ B and MAPK, which leads to the induction of inflammatory cytokine genes. IRF5 also mediates inflammatory cytokine expression. TRAF3 activates IRAK1 and IKK $\alpha$ , which catalyze the phosphorylation of IRF7 and induce type I IFN genes. OPN is involved in the activation of IRF7. IRF8 facilitates NF- $\kappa$ B and IRF7 activation. (B) In addition, pDCs exhibit constitutive autophagy induction, which deliver viral RNA to the endosome or lysosome, where TLR7 is expressed. (C) In cDCs, macrophages and fibroblast cells, viral RNA species are preferentially recognized by RLRs. RIG-I and MDA5 recruit the adapter IPS-1 via CARDs. IPS-1 is localized to mitochondria, and recruits TRADD, which then forms a complex with FADD, caspase-8 and caspase-10 to activate NF- $\kappa$ B. TRADD also recruits TRAF3 to activate the TBK1–IKK $\epsilon$ –IRF3 axis. FADD is also implicated in IRF3 activation. STING (also known as MITA) localizes to (D) mitochondria or (E) ER; in mitochondria, STING (MITA) interacts with IPS-1 and RIG-I and activates NF- $\kappa$ B and IRF3. (F) Cytosolic dsDNA is thought to be sensed by an as-yet-undefined host DNA sensor. In the ER, STING (MITA) plays an essential role in the responses to dsDNA. DsDNA activates NF- $\kappa$ B and IRF3 via the IKK complex (data not shown) and TBK1–IKK $\epsilon$ , respectively.<sup>76</sup>

#### **1.5.2.1: TLR2, TLR2/1 and TLR2/6:**

TLR2 is a cellular membrane localized receptor that forms a TLR2 homodimer, as well as forming heterodimers with TLR1 and TLR6 (TLR2/1 and TLR2/6 respectively). In addition to TLR1 and TLR6, TLR2 has been shown to associate with non-TLR proteins, Dectin-1, CD14 and CD36<sup>77</sup>.

TLR2 homo- and heterodimers suggested ligands include: lipoteichoic acid (LTA) from Gram-positive bacteria (*Staphylococcus aureus* and *Streptococcus pneumonia*), PGNs (*S. aureus*), bacterial lipoproteins (BLPs), bacterial lipopeptides,

lipoarabinomannans (*Mycobacteria spp.*), zymosan, phenol soluble modules, glycolipids, in addition to many more<sup>75</sup>.

As a homodimer TLR2 has been reported to recognize bacterial PGN, lipoprotein, LTA, porins, viral hemagglutinin, glycoproteins and possibly LPS due to association of increased CD14<sup>78,79</sup>.

TLR2/1 heterodimer is activated by bacterial triacylated lipopeptides and TLR2/6 has been reports to be activated by bacterial diacylated lipopeptides and LTA<sup>78,80</sup>.

Most BLPs are triacylated at their N-terminal cysteine residues, however myoplasmal macrophage-activated lipopeptide-2 kD (MALP-2) has a diacylated structure at its N-terminal cysteine residue. TLR2/6

The diversity of TLR2 ligands is greatly increased by its ability to form heterodimers with TLR1 and TLR6, each of which has highly specific target structures, where the specificity between TLR2/1 and TLR2/6 can be separated by molecular differences of a single additional acyl group on an entire lipopeptide<sup>81,82</sup>. In 2007 Jin *et al.* showed the crystal structure of TLR2/1 heterodimer binding to the bacterial triacylated lipopeptide Pam<sub>3</sub>C5K<sub>4</sub><sup>73</sup>.

Triantafilou *et al.* (2006) showed that TLR2/1 and TLR2/6 heterodimers existed in the cellular membrane prior to ligand recognition, however heterotypic associations between TLR2 and CD36 are ligand-induced. Upon activation by their respective ligands, all TLR2 complexes are trafficked to the Golgi apparatus via association with lipid rafts, where immune response pathways are initiated<sup>83</sup>.

#### **1.5.2.2: TLR4:**

TLR4 is responsible for the recognition of a diverse range of PAMPs, most notably LPS, but also other bacterial, viral, fungal mannans and zymosam PAMPs, in

addition to the parasitic PAMP glycoinositolphospholipids belonging to *Trypanosoma*. TLR4 has been reported to recognise endogenous DAMPs such as Hsp60 and Hsp70<sup>84,85</sup>.

TLR4 binding of LPS requires a number of additional association and chaperone proteins, namely LPS-binding protein (LBP), CD14 and MD-2, although it is thought the TLR4 signaling also requires Hsp70, CD11b/CD18, CD36 and CXCR4<sup>85,86</sup>. LBP directly binds to LPS where it is then transferred to a CD14 adaptor molecule, and it is the CD14 adaptor molecule that facilitates the transfer of LPS to the TLR4 signaling complex. TLR4 associates and binds with MD-2 through their TIR domains, then forms a TLR4-MD-2/TLR4-MD-2 homodimer complex upon stimulation<sup>87</sup>. The TLR4-MD-2 homodimer is thought to require CD14, cellular membrane anchored protein glycosylphosphatidylinositol (GPI) and LBP (cytosolic protein), in facilitating in the transfer of the LPS to the homodimer<sup>88</sup>.

#### ***1.5.2.3: TLR9:***

Unlike TLR1, 2, 4 and TLR6, TLR9 is an intracellular PRR that is found in the ER membrane in its unstimulated form. Upon recognition of its ligands, TLR9 translocates to the endolysosome via Golgi trafficking pathways that require Unc93B, Gp96, High-mobility group box-1 (HMGB-1) protein and the chaperone proteins PRAT4A and GRP94<sup>86,89</sup>. Once activated, TLR9 homodimerises initiating MyD88-dependent signaling pathways, leading to upregulation of pro-inflammatory cytokine gene transcription in the nucleus. TLR9 was initially thought to detect and respond to CpG DNA that is more abundant in non-mammalian organisms, however mammalian DNA still consists of CpG DNA<sup>90,91</sup>. Non-mammalian DNA is only four times more abundant in CpG DNA, which would create the potential danger of “self” DNA recognition by TLR9 by accident. It has instead been proposed that

TLR9 recognises the 2' deoxyribose phosphate backbone of DNA present in endocytosed PAMP containing vesicles that triggers the immune response, rather than the direct detection of specific CpG DNA sequences. This activation pathway would defend against unwanted “self” DNA recognition. CpG motif consists of two 5' purine residues and two 3' pyrimidine residues flanking an unmethylated dinucleotide CpG molecule. In addition to CpG DNA, TLR9 has been suggested to recognise the hydrophobic heme polymer produced during the malaria parasite infection and degradation of hemoglobin, as well as hemozoin and viral DNA.

#### ***1.5.2.4: TLR7:***

TLR7 is an intracellular PRR localized at endosome and is known to detect single stranded RNA (ssRNA), which is produced by certain viruses, and activates MyD88-dependent immune signaling cascades<sup>92</sup>. Bacteria do not possess ssRNA, and viruses do not produce CpG DNA or RNA, thus TLR7 is a PRR specific to detecting viral PAMPs. For this reason TLR7 is used in the current study as a negative control PRR to compare PRR expression induced by *Ureaplasma* (bacteria).

### **1.6: TLR signaling pathways:**

#### ***1.6.1: MyD88-dependent signaling pathway:***

All TLRs dimerize upon recognition of their ligands, as previously mentioned in either a hetero- or homodimeric association. All TLRs, with the exception of TLR3 recruit the master adaptor protein MyD88 for MyD88-dependent signaling pathways. MyD88 signals downstream via a number of pathways all of which require a number of additional associated adaptor proteins. MyD88 recruits interleukin-1 receptor-

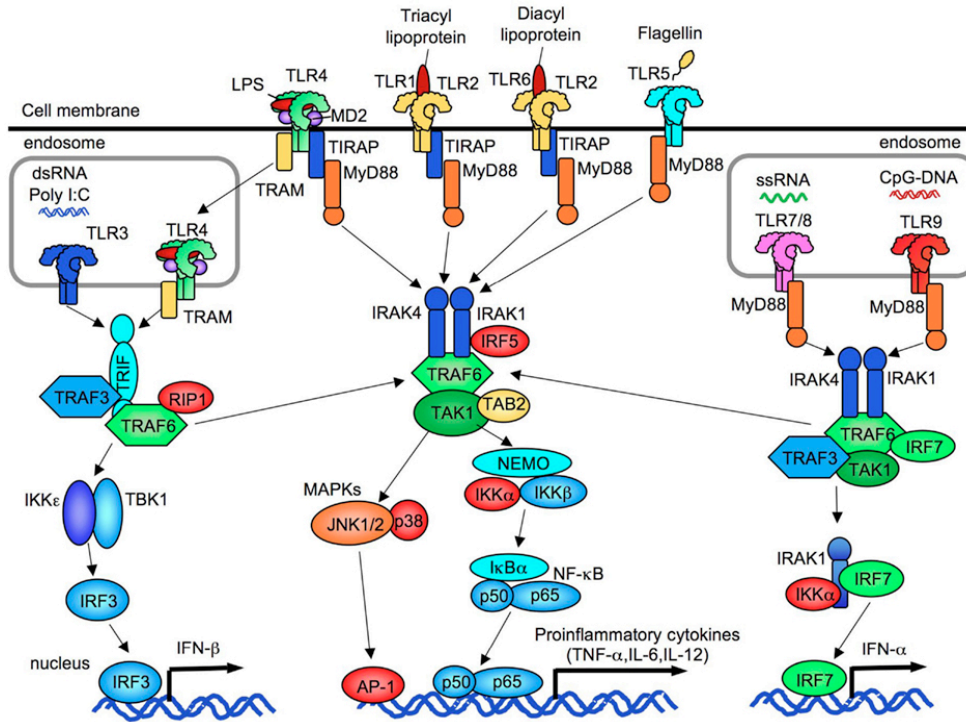
associated kinase 4 (IRAK4) via the interaction of the N-terminal death domain (DD) on MyD88 and the IRAK4 DD, in a DD-DD complex. TLR2/1, TLR2, TLR2/6, TLR4 and TLR5 MyD88-IRAK4 complexes recruit and phosphorylate IRAK1 and IRAK2. IRAK1 binds and phosphorylates tumour-necrosis-factor receptor-associated factor 6 (TRAF6), activating it. TRAF6 (an E3 polyubiquitin ligase) forms polyubiquitin linked Lys63 chains on itself with the association of Ubc13 and Uev1A<sup>84,93</sup>. This active TRAF6 dissociates from IRAK1 and allows binding with transforming-growth factor- $\beta$ -activated kinase (TAK1) via the Lys63 polyubiquitin chains and novel zinc finger-type ubiquitin-binding domain on TAK1. TAK1 and TRAF6 form proteins the protein complex of TRAF6, TAK1, TAK1-binding protein 2 and 3 (TAB2 and TAB3 respectively). This complete TAK1 complex then initiates the upregulation of pro-inflammatory cytokine genes via two separate pathways, AP-1 and NF- $\kappa$ B.

The AP-1 pathway is initiated by TAK1 complex phosphorylating IKK- $\beta$  subunit of I $\kappa$ B-kinase (IKK). IKK is a complex made comprising IKK- $\alpha$ , IKK- $\beta$  and IKK- $\gamma$ . Phosphorylated IKK- $\beta$  activates IKK, causing degradation of p105, activating MAP3K8, which in turn activates MKK1 and MKK2 (MKKs)<sup>88</sup>. MKKs activate extracellular signal related kinases (ERK1 and ERK2) and Jun kinases (JNKs). In addition TAK1 activates MAPKs, which also activate JNKs, as well as p38 and CREB. Together ERKs, JNKs, p38 and CREB bring about AP-1 upregulation of proinflammatory cytokines transcription.

Additionally the Lys63 polyubiquitin chains bind to the ubiquitin-binding domain of NF- $\kappa$ B essential modulator (NEMO), which in addition with IKK- $\alpha$  and IKK- $\beta$  cause polyubiquitination of I $\kappa$ B. I $\kappa$ B is the inhibitory protein of NF- $\kappa$ B, and is responsible in keeping NF- $\kappa$ B in an inactive state<sup>93</sup>. Proteosomal degradation of

ubiquitinated I $\kappa$ B releases NF- $\kappa$ B from its inactive state, allowing it to translocate to the nucleus where it upregulates pro-inflammatory cytokine gene transcription.

#### TLR-activation of MyD88-dependent signaling cascade:



**Figure 1.6.1:** The overview of TLR signaling. TLR1, TLR2, TLR4, TLR5, and TLR6 are expressed on cell membrane. TLR3, TLR7/8, and TLR9 are expressed in endosome. All TLRs, except for TLR3, activate MyD88-dependent pathway to induce NF- $\kappa$ B and p38/JNK activation. TLR2 and TLR4 signaling require TIRAP and MyD88. TLR3 requires IRIF to activate TBK1/IKK $\epsilon$ . Subsequent to TLR4 internalization, TLR4 signaling activates TRAM/TRIF-dependent pathway. TLR3/4-dependent TRIF-dependent signaling induces IRF3 activation and IFN- $\beta$  production. TLR7/8 and TLR9 induce IFN- $\alpha$  production through IRF7<sup>94</sup>.

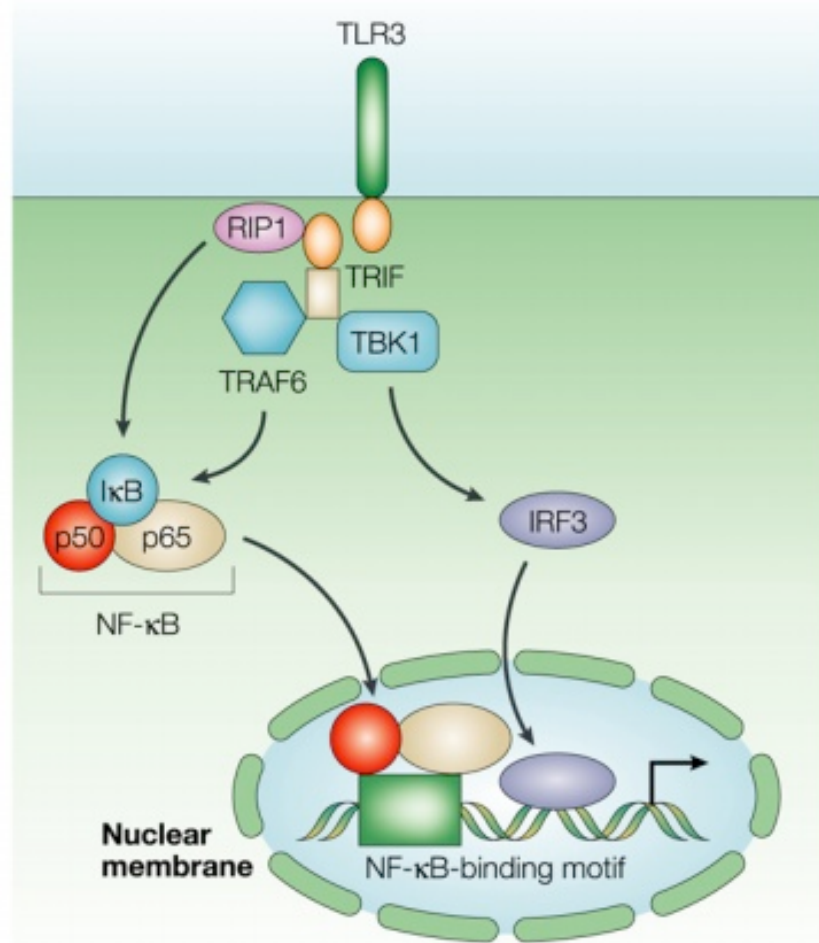
#### **1.6.2: TRIF-dependent signaling pathway:**

TRIF-dependent signaling pathway is primarily initiated by binding of TLR3 activation, but TLR4 activation can also signal via through this pathway. TLR3 recruit TRIF through its TIR domain upon dimerisation, but TLR4 requires the association of TRAM to recruit TRIF and activate TRIF-dependent signaling pathways. TRIF activates IKK complex that consists IKK-epsilon and TRAF-



associated NF- $\kappa$ B activator (TANK)-binding kinase-1 (TBK-1) via TRAF3 activity<sup>75</sup>. IKK phosphorylates IRF3 and IRF7 causing dimerisation and activation, leading to translocation to the nucleus, and with CREB binding protein, assembles on the IFN- $\beta$  enhancer, initiating IFN- $\beta$  pro-inflammatory immune response<sup>75</sup>.

TRIF-dependent signaling pathway:



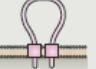

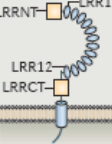
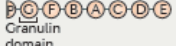
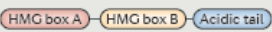


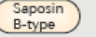



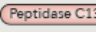


Nature Reviews | Immunology

**Figure 1.6.2:** TRIF-dependent induction of IFN- $\beta$ . The amino-terminal region of TRIF (Toll/interleukin-1-receptor (TIR)-domain-containing adaptor protein inducing interferon (IFN)- $\beta$ ) interacts with both TRAF6 (tumour-necrosis-factor-receptor-associated factor 6) and TBK1 (TRAF-family-member-associated nuclear factor- $\kappa$ B (NF- $\kappa$ B) activator (TANK)-binding kinase 1). TRIF-dependent activation of TBK1 leads to the phosphorylation of IRF3 (IFN-regulatory factor 3), and TRAF6 mediates NF- $\kappa$ B activation. RIP1 (receptor-interacting protein 1) mediates the NF- $\kappa$ B activation that is induced through the carboxy-terminal region of TRIF. Activation of both NF- $\kappa$ B and IRF3 contributes to the activation of the IFN- $\beta$  gene. I $\kappa$ B, inhibitor of NF- $\kappa$ B; TLR, Toll-like receptor<sup>75</sup>.

## 1.7: TLR accessory molecules:

TLR accessory molecule table:

Name	Protein domain structure	Localization	Interacting TLR	Interacting ligand	Refs
<b>Mediators of ligand delivery and/or recognition</b>					
LBP		Secreted	None demonstrated	LPS	12
MD2		Plasma membrane	TLR4	LPS	19–21
CD36		Plasma membrane, Golgi	TLR2, TLR4, TLR6	FSL1, LTA, oxLDL, amyloid- $\beta$ fibrils	23,26, 99–101
CD14		Secreted, plasma membrane (GPI-linked), endolysosomes	TLR2, TLR3, TLR4, TLR7, TLR8, TLR9	LPS, peptidoglycan, Pam <sub>2</sub> CSK <sub>4</sub> , polyI:C, CpG DNA	14,23,29–31, 102,103
TRIL		Plasma membrane, early endosomes	TLR3, TLR4	LPS	41,42
Progranulin		Secreted, endolysosomes	TLR9	CpG-A, CpG-B, CpG-C and inhibitory ODNs	45
HMGB1		Nucleus, cytoplasm, can be secreted following TLR ligation	TLR9, possibly TLR3 and TLR7	CpG-A ODNs, CpG-B ODNs, DNA, RNA	48,49,53
LL37		Early endosomes	Possibly TLR7 and TLR9	Mammalian DNA, mammalian RNA	54,57
<b>Chaperones</b>					
GRP94		ER	TLR1, TLR2, TLR4, TLR9	None demonstrated	58,60,62,64
PRAT4A		ER	TLR1, TLR2, TLR4, TLR9	None demonstrated	64–67
<b>Molecules that facilitate the trafficking of endosomal TLRs</b>					
UNC93B1		ER, endolysosomes	TLR3, TLR7, TLR8, TLR9, TLR13	None demonstrated	68,70,71
AP3		TGN, endolysosomes, LROs	TLR9	None demonstrated	75
<b>TLR-processing enzymes</b>					
Cathepsins		Endosomes, lysosomes	TLR9, possibly TLR3 and TLR7	None demonstrated	79,80,84
AEP		Endosomes, lysosomes	TLR9, possibly TLR3 and TLR7	None demonstrated	83,84

**Figure 1.7:** AEP, asparagine endopeptidase; AP3, adaptor protein 3; BPI1, BPI/LBP/CETP N-terminal domain; BPI2, BPI/LBP/CETP C-terminal domain; ER, endoplasmic reticulum; FSL1, *S*-(2,3-bisphalmitoyloxypropyl)-CGDPKHSPKSF; GPI, glycosylphosphatidylinositol; GRP94, glucose-regulated protein of 94 kDa; HMGB1, high-mobility group box 1 protein; LBP, LPS-binding protein; LPS, lipopolysaccharide; LRO, lysosome-related organelle; LRR, leucine-rich repeat; LRRCT, LRR C-terminal domain; LRRNT, LRR N-terminal domain; LTA, lipoteichoic acid; ML, MD2-related lipid-recognition domain; ODN, oligodeoxynucleotide; oxLDL, oxidized low-density lipoprotein; polyI:C, polyinosinic-polycytidylic acid; PRAT4A, protein associated with TLR4 A; TGN, *trans*-Golgi network; TLR, Toll-like receptor; TRIL, TLR4 interactor with leucine-rich repeats; UNC93B1, uncoordinated 93 homolog B1. Table of TLR accessory molecules<sup>86</sup>.

### ***1.7.1: CD36:***

CD36 is a double membrane spanning glycoprotein, which is a member of the class B family of scavenger receptors that is located in lipid rafts<sup>95</sup>. TLR2/6 detection of diacylglycerides is thought to require the recruitment of CD36 to the TLR2/6 heterodimer in lipid rafts, enabling MyD88-dependent signaling pathways<sup>96</sup>. CD36 is thought to augment the TLR2/6 immune response and the inhibition of CD36 association with TLR4/6 blocks NF- $\kappa$ B pathway activation in response to oxidised low-density lipoproteins<sup>83</sup>.

### ***1.7.2: CD14:***

CD14 is both a blood soluble leucine rich repeat glycoprotein and a glycosylphosphatidylinositol (GPI)-anchored myeloid cell membrane protein. It is associated with a number of TLR immune pathways and is thought to directly bind to microbial molecules, such as LPS, peptidoglycan, Pam<sub>3</sub>CSK<sub>4</sub>, poly I:C and CpG DNA<sup>97-100</sup>. CD14 associates with TLR4 as it chaperones LPS from LBP to TLR4-MD2 complex, which enables activation of TLR4 MyD88-mediated signaling cascade<sup>101-104</sup>. CD14-mediated TNF production to response of TLR2/6 has been shown via activation of ligands, such as Pam<sub>3</sub>CSK<sub>4</sub>, MALP2 and LTA<sup>98,105,106</sup>.

### **1.8: TLR adverse effects to PRR response:**

TLR4 is to date the most studied of the TLRs as it is activated by LPS and has been strongly linked to the adverse effects of the innate immune response during sepsis induced by Gram-negative bacteria. Sepsis is the systemic inflammatory response that affects millions of people every year and carries with it high mortality and morbidity rates<sup>107</sup>. Huge quantities of money are spent worldwide in the treatment of sepsis and even with modern medical advances and antibiotic treatments; sepsis remains one of the higher causes of death in the USA and the modern world. Complications during sepsis occur due to an overreaction of the innate immune response, producing excessive levels of pro-inflammatory cytokines that lead to over vasodilation of the microcirculatory system, causing extreme hypotension, reduced tissue perfusion pressure, hypoxia, acidosis and toxemia. Unless treated rapidly, prognosis remains very poor<sup>107</sup>. Modern therapies involving TLR4 inhibitors during early stages of LPS induced sepsis have shown great potential in future treatments in recent trials<sup>108</sup>.

## **1.9: NLR proteins:**

### *1.9.1: Brief introduction into NLR proteins:*

As previously described, the innate immune system possesses several PRR receptors that are categorized into three specific family groups: the previously described TLR family, NLR or RLR families. Like all families of PRRs, NLR proteins are shown to recognise and interact with highly specific molecular sequences via highly conserved LRR domain, (which is present in all PRRs), though similar to TLRs the exact mechanism of interaction is as yet not fully understood. Nucleotide-binding oligomerization domain (NOD)-like receptors (NLRs) share a tripartite structural architecture: 1) a central nucleotide binding domain (NBD), 2) C-terminal LRR domain and 3) N-terminal domain that contains one of a number of immune pathway activating proteins<sup>109</sup>.

NLRs are characterized into sub-families, based upon the function and structure of the N-terminal domain, which include N-terminal CARD, BIR, Pyrin, acidic trans-activation and X domains (the function of which remains unknown),<sup>74</sup>. The typical and best-studied NLR N-terminal domains are the Caspase Activation and Recruitment Domains (CARDs), Baculovirus Inhibitor of Apoptosis Domain (BIR) and the Pyrin domains (PYDs), though there are (to date) 23 NLR family members each with a specific role in PAMP, DAMP, homeostasis and apoptotic detection and interaction<sup>110</sup>.

Unlike TLRs, NLRs are only found in the cellular cytosol, acting as intracellular PRRs that reside and detect pathogenic or other antigenic material that has invaded the cell. It was initially thought that NLRs could only detect PAMPs after they had invaded and entered the host cell, however recent studies have shown that NLRs

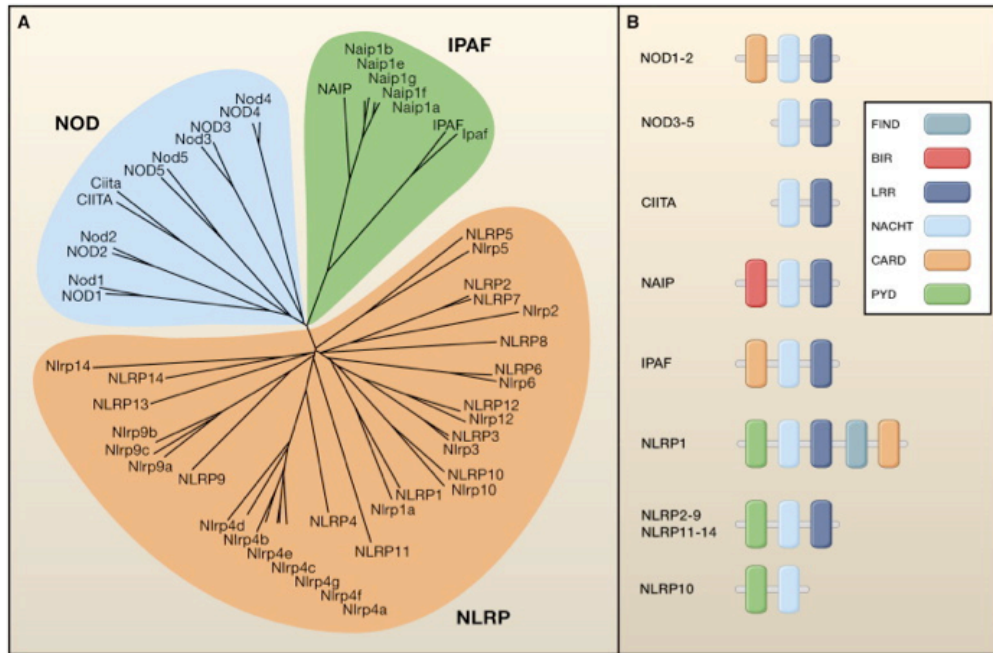
detect and initiate immune responses from extracellular pathogens via a number of possible antigen internalization mechanisms. These proposed mechanisms include bacterial secretion system (BSS), outer membrane vesicles (OMVs), pore forming toxins (PFTs), endocytosis and autophagy<sup>109</sup>.

Activation of NLR receptors can initiate several immune response pathways via a diverse, but still not fully understood, number of mechanisms. Several NLRs such as NOD1 and NOD2 can activate NF- $\kappa$ B, MAPK and TRAF3 pathways, while certain NLRP and NLRP-like proteins once activated, assemble high-molecular weight catalytic protein scaffold platforms, called inflammasomes. The regulation of the inflammasome is very tightly regulated by several mechanisms and the requirement of a number of signal-dependent activation and transcriptional-dependent safeguards. The inflammasome is an extremely potent immune response system, regulating pro-inflammatory cytokines that, if are not tightly controlled, can have highly detrimental effects on the host organism. An example of is the regulation of type 1 Interleukin family pro-form pro-inflammatory cytokines, which are kept in an inactive state until caspase-1 activity, via the inflammasome, cleaves the inhibitory subunit from the pro-form, creating active (mature) pro-inflammatory cytokines<sup>110-112</sup>. Lupter *et al.* categorized NLR into four groups<sup>113</sup>:

- 1) Inflammasome activating
- 2) NF- $\kappa$ B and MAPK activators
- 3) Inflammatory signal inhibitors
- 4) Transactivators of MHC expression

### 1.9.2: NLR family tree:

Phylogenetic map of the human and mouse NLR family members:



**Figure 1.9.2:** (A) Phylogenetic relationships between NACHT domains of each human (uppercase) and mouse (lowercase) NLR (NOD-like receptor) protein show 3 distinct subfamilies within the NLRs: the NOD, NLRP, and IPAF subfamilies.

(B) Domain structures for human NLRs reveal commonalities within the subfamilies. Domains are classified according to the NCBI domain annotation tool for the longest human protein product, with the exception of the FIIND domain that was identified independently of NCBI (Tschopp et al., 2003). It should be noted that CIITA is often annotated as harboring a CARD domain, because a splice variant expressed in dendritic cells contains a domain with homology to CARD domains (Nickerson et al., 2001); however, the translated transcript variant is not classified as containing a classical CARD domain by typical approaches (NCBI conserved domains, Simple Modular Architecture Research Tool [SMART]). Likewise, these domain prediction approaches do not classify NOD3 and NOD4 as CARD-containing and experimental evidence for a CARD domain function has yet to be reported. Domains: BIR, baculoviral inhibition of apoptosis protein repeat domain; CARD, caspase recruitment domain; FIIND, domain with function to find; LRR, leucine-rich repeat; NACHT, nucleotide-binding and oligomerization domain; PYD, pyrin domain<sup>111,114</sup>.

### ***1.9.3: NLR structure:***

Similar to the structural architecture of TLRs, NLRs consist of three constituent domains: the C-terminal LRR, NBD (nucleotide binding domain) (also known as a NACHT domain) and an N-terminal effector domain. The LRR share PAMP and DAMP detection similarities with those of TLRs, and like in TLRs the exact mechanism of ligand recognition is still not fully understood. The NBD or NACHT [NAIP (neuronal apoptotic inhibitory protein), CIITA (MHC class II transcription activator), HET-E (incompatibility locus protein from *Podospora anserine*) and TP1 (telomerase-associated protein)] domain possesses the dNTPase activity that binds nucleotides, (primarily ATP), undergoing self-oligomerizational conformational changes to form a signal receptive state<sup>115</sup>. The NACHT domain is the only structural domain that consistent throughout the NLR family<sup>111</sup>.

The sub-categorization defining structure is the N-terminal effector domain, as it is this domain that dictates the protein-protein interactions, downstream signaling, and therefore the end immune response. Effector domains include; CARD, PYD, N-terminal AD (activation domain) and BIR<sup>109,116</sup>.

### ***1.9.4: Functions of NLR:***

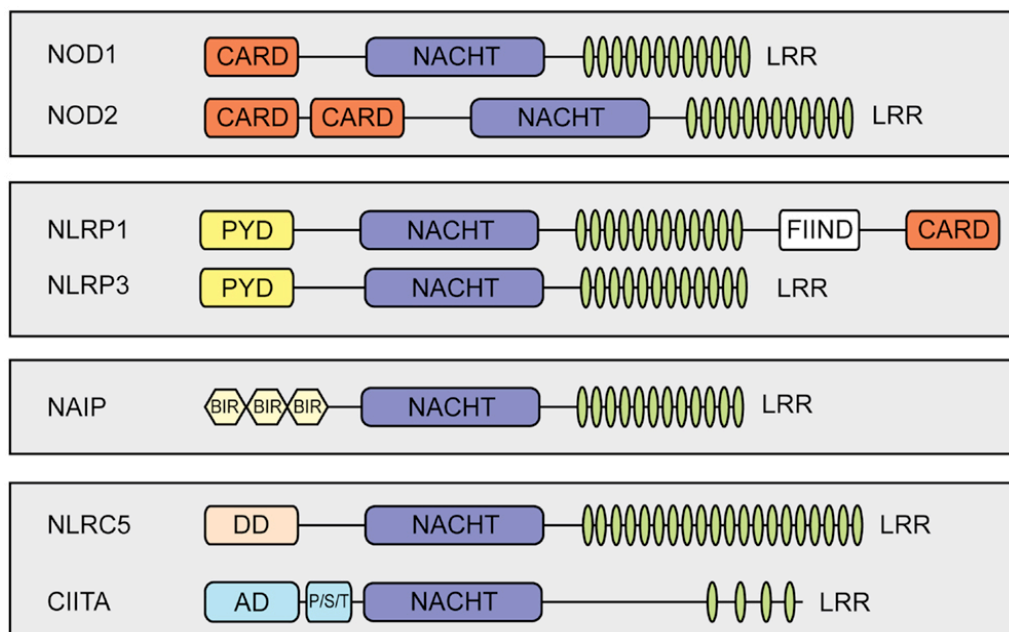
NLRs fall into one of two categories, non-inflammasome NLRs, and inflammasome NLRs. The phylogenetics of all of the NLR is highly conserved, and as mentioned above it is the N-terminal domain, possibly in addition to other as of yet unknown accessory proteins that gives each NLR its immune response properties. Even more interestingly, all NLRs, especially NLRP3 has been shown to not only upregulate the inflammatory immune response, but under certain conditions, has been shown to downregulate immune responses, and does this via several mechanisms and



signaling pathway interactions. NLRP3, NLRP6, NLRP7, NLRP12 and NLRX1 are the most documented of the NLRs for their ability to both up- and down-regulate inflammatory response<sup>113</sup>.

NLRs CIITA and NLRC5 are as of yet the only NLRs identified that initiate transcription within the nucleus and possess other functional roles within the nucleus upon activation<sup>117,118</sup>.

#### Schematic representation of members of the mammalian NLR-family:



**Figure 1.9.4:** NLRs share a tripartite domain architecture and can be subdivided based on the identity of their N-terminal effector domain which links to different cellular signaling pathways. All NLRs contain a central nucleotide-binding domain (NACHT) that mediates oligomerization. In addition, most NLRs contain putative ligand-sensing leucine-rich repeats (LRRs) and a variable N-terminal effector domain. The effector domain can be a pyrin domain (PYD), a caspase recruiting domain (CARD), or a baculovirus inhibitor of apoptosis repeat (BIR). Additional abbreviations: FIIND, function to find; DD, death-domain different from a typical CARD and PYD; AD, activation domain; P/S/T, proline/serine/threonine-rich protein domain<sup>117</sup>.

#### **1.9.5: Non-inflammasome NLRs:**

As mentioned above, most non-inflammasome NLRs act via NF- $\kappa$ B, MAPK, and TRAF3 pathways, initiating pro-inflammatory cytokine upregulation responses to those seen in TLRs. They appear to be an integral part of the human innate immune

system as there are many immune disorders attributed to the mutation or deficiency of such receptors, one of the most common cited examples is and NOD2 deficiency is strongly associated with Crohn's disease.

#### ***1.9.5.1: NOD1 and NOD2:***

NOD1 and NOD2 were the first identified members of the NLR family and their activation is initiated by interaction with bacterial PGN structural proteins iE-DAP and MDP. These highly conserved bacterial structures must enter the cellular cytoplasm of the host immune and/or epithelial cells to interact with these intracellular PRRs. After activation by their specific ligands, NOD1 and NOD2 initiate JNK, p38 MAPK and NF- $\kappa$ B pathways to upregulate cytokine and chemokine gene expression (IL-1 $\beta$ , IL-6, TNF- $\alpha$  and IL-8; CCL5 and CXCL5 respectively) <sup>119</sup>. NOD1 and NOD2 can initiate their immune response pathways independently of TLR activation. NOD2 is highly expressed in tissues where TLR expression is lower, for example in the gastrointestinal tract, where it is thought that high TLR expression would produce undesired immune responses to commensal GI tract microbial flora<sup>120</sup>.

A recent review describes the possible role of extracellular bacterial component injection into cellular cytosol via type-3 or type-4 secretion systems (T3SS and T4SS respectively). T3SS also known as the "injectisome" shares structural architecture with bacterial flagellar apparatus and is a well conserved bacterial component. T4SS is a bacterial macromolecular machine that is believed to be associated with bacterial DNA conjugation apparatus, via which bacterial DNA enters the cellular cytoplasm<sup>110</sup>.

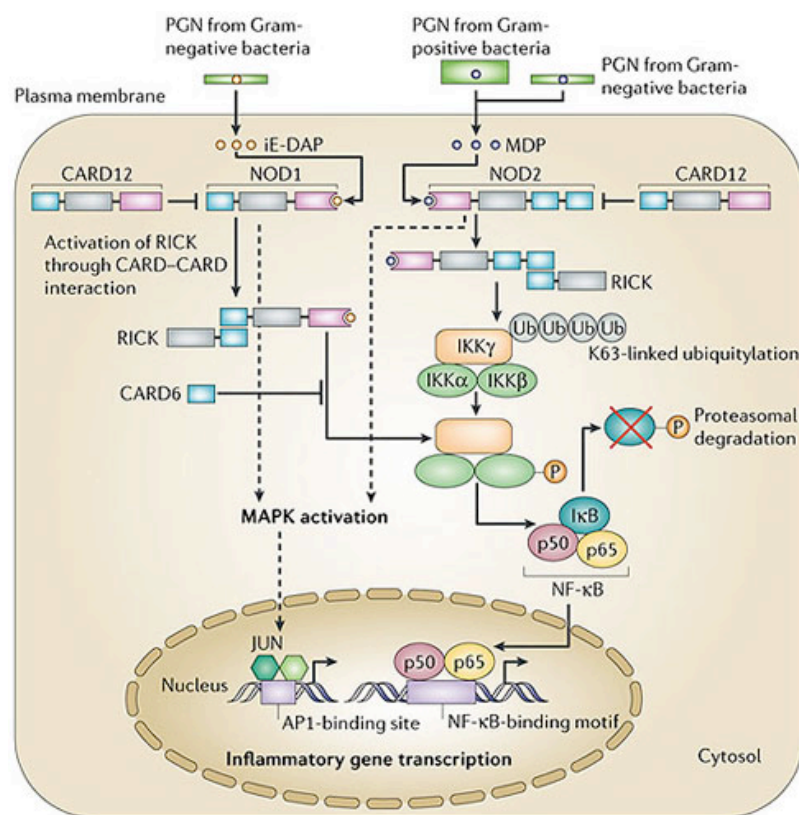
Endocytosis of bacterial NOD1 and NOD2 ligands are proposed to occur via different mechanisms in different cell-lines; in epithelial cells a clathrin-mediated endocytosis internalization mechanism is thought to be involved, whereas in immune cells, internalization is thought to occur through phagocytosis. In either case, a family of transport protein has been proposed in transporting the ligands from the internalized vesicles to NOD1 and NOD2. SLC15 transporter protein A1 (SLC15A1, also known as PetT1) is associated with the transporting of ligands to NOD2, and SLC15A4 (PHT1) and SLC15A2 (PetT2) are associated with trafficking to NOD1 receptors<sup>121</sup>. Interestingly NOD1- or NOD2-deficient mice showed to have decreased phagocytotic ability in mouse models<sup>122,123</sup>.

NOD1 detects *meso*-diaminopimelic acid (DAP)-containing PGN, which are predominantly found in Gram-negative bacteria<sup>124-126</sup>. NOD1 is most sensitive to Tri<sub>DAP</sub> (L-Ala-D-Glu-*meso*-DAP)- and Tetra<sub>DAP</sub> (L-Ala-D-Glu-*meso*-DAP-D-Ala)-containing structures respectively, but is also sensitive to, but to a lesser degree, iE-DAP ( $\gamma$ -D-Glu-*meso*-DAP). NOD2 detects the largest PGN motif found in most Gram-negative and Gram-positive bacteria, MDP (muramyl dipeptide; MurNAc-L-Ala-D-isoGln)<sup>116,124,127</sup>.

NOD1 and NOD2 recruit RIP2 (receptor-interacting protein 2) also known as RICK [Rip-like interacting CLARP (caspase-like apoptosis-regulatory protein) kinase], upon interaction with their respective ligands. RIP2 interacts with IKK complex, activating NF- $\kappa$ B-activating pathways, such as TLR-, IL-1- and TNF-mediated signaling cascades<sup>116</sup>. Stimulation of TLRs with NOD1 and NOD2, work synergistically to produce the optimum response to a given PAMP, cooperatively increasing sensitivity to PAMPs whilst reducing the threshold stimulation for NOD1 and NOD2<sup>128</sup>. NOD1 and NOD2 signaling pathways are very similar to those of

MyD88-dependent TLR pathways, with the additional associations with CARD6 and possibly SGT1 (suppressor of G2 allele of Skp1), which is a Hsp90 co-chaperone<sup>116</sup>. CARD9 is also reported to be necessary for NOD2 signaling<sup>76</sup>.

### Signaling pathways of NOD1 and NOD2:

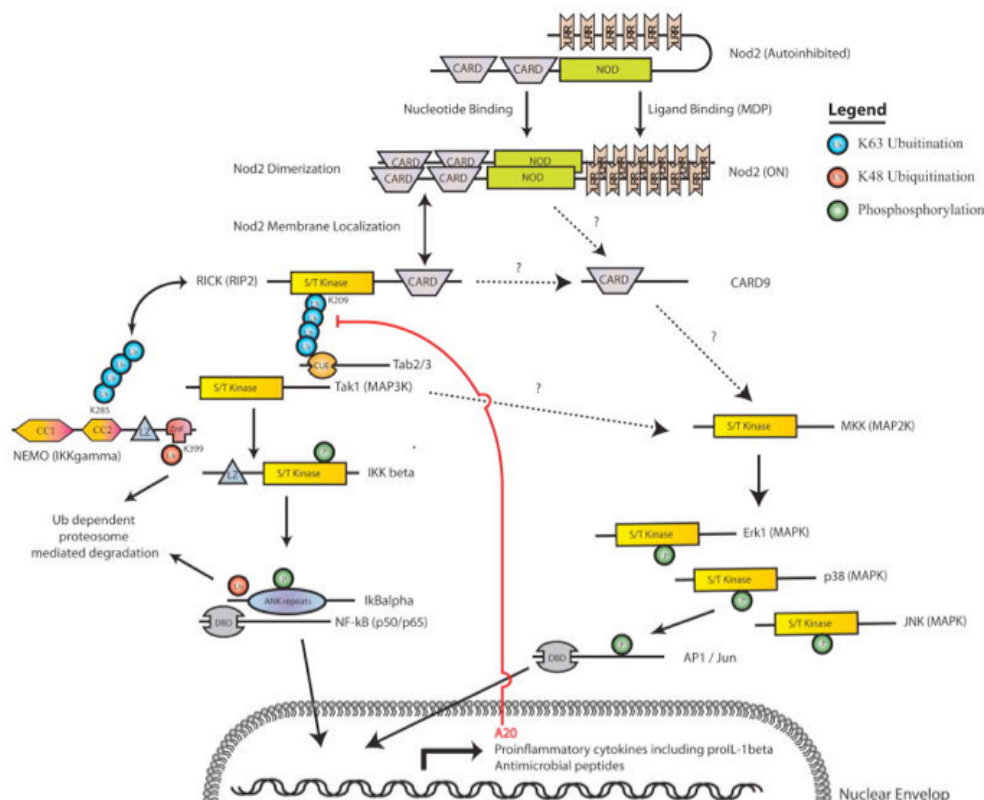


Copyright © 2005 Nature Publishing Group  
Nature Reviews | Immunology

**Figure 1.9.5.1.1:** Recognition of muramyl dipeptide (MDP) and  $\gamma$ -D-glutamyl-meso-diaminopimelic acid (iE-DAP) through leucine-rich repeat (LRR) domains activates the NOD (nucleotide-binding oligomerization domain) proteins NOD2 and NOD1, respectively, which then recruit receptor-interacting serine/threonine kinase (RICK) through caspase-recruitment domain (CARD)-CARD interactions. In the case of NOD2, activation of RICK leads to K63 (Lys63)-linked polyubiquitylation of IKK- $\gamma$ , the scaffold of the inhibitor of NF- $\kappa$ B (I $\kappa$ B)-kinase complex (the IKK complex), which also consists of IKK- $\alpha$  and IKK- $\beta$ . This is followed by the phosphorylation of IKK- $\beta$ , as well as the phosphorylation of I $\kappa$ B and the release of nuclear factor- $\kappa$ B (NF- $\kappa$ B) for translocation to the nucleus. In the case of NOD1, ubiquitylation of IKK- $\gamma$  by RICK has not been studied, and the mechanism of NF- $\kappa$ B activation is not clear. CARD12 negatively regulates RICK-mediated NF- $\kappa$ B activation by both NOD1 and NOD2, whereas CARD6 negatively regulates only RICK-mediated NF- $\kappa$ B activation by NOD1 (for further details, see the main text).

In addition to NF- $\kappa$ B activation, NOD1 and NOD2 signalling gives rise to the activation of mitogen-activated protein kinases (MAPKs) such as JUN amino-terminal kinase (JNK), extracellular-signal-regulated kinase (ERK) and p38MAPK by as-yet-unknown mechanisms (denoted by dashed arrows). AP1, activator protein 1; PGN, peptidoglycan<sup>129</sup>.

Schematic representation of the Nod2 signaling pathway:



**Figure 1.9.5.1.2:** The NLR Nod2 recognizes bacterial PGN fragments such as MDP and activates NF- $\kappa$ B and MAPK signaling via the indicated proteins leading to the transcriptional upregulation of a variety of proinflammatory cytokines and antimicrobial peptides. Negative feedback regulation occurs upon induction of the deubiquitinase A20. The posttranslational regulation of various components of the pathway is indicated by green circles (phosphorylation) and red or blue circles (ubiquitination). In the case of RICK, K63-mediated polyubiquitination at K209 is essential for recruitment of Tak1. For NEMO, K48-mediated ubiquitination at residue K399 targets it for proteasome-dependent degradation. K63-linked polyubiquitination at amino acid K285 is important for complex formation with RICK<sup>130</sup>.

#### 1.9.5.2: NLRC5 and CIITA:

NLRC5 [CITA (class I transactivator)] is one of the latest NLR's functions to be investigated and documented. NLRC5 has been shown to have high structural similarity to CIITA, which is a NOD subfamily NLR responsible for the tight regulation of MHC class II gene expression. NLRC5 has been shown to tightly regulate the expression of MHC class I genes, and both CIITA and NLRC5 regulate their respective gene

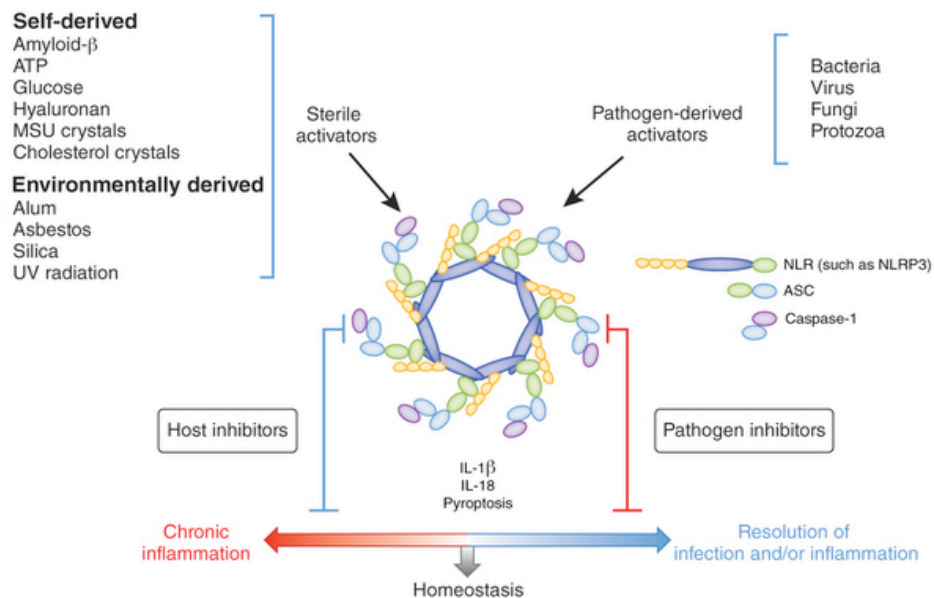
expression in association with interactions with other MHC promoter-bound factors. MHC class I and II molecules are an essential part of the bodies immune defense, as they are the mechanism by which PAMPs, detected by the innate immune antigen presenting cells (APCs), are presented to the B- and T- immune cells of the acquired immune system<sup>118</sup>. In this study though, NLRC5 is being investigated as recent studies have shown that it can negatively regulate TLR4 signaling and has also been suggested to be an activator and component of inflammasome protein complexes, and therefore impact NF- $\kappa$ B expression via interactions with IKK- $\alpha$ , as well as IL-1 $\beta$  and IL-18, via caspase-1 modulation<sup>131,132</sup>.

### 1.10: The Inflammasome:

In addition to the recent advances and discoveries in the role of TLRs in the innate immune response, studies in the last decade have revealed the presence and function of a previously unknown immune mechanism that maybe hugely influential and integral to the host's response to PAMPs and DAMPs.

The proposed mechanism of action of this area of the innate immune system involves the assembly of a multi-subunit proteolytic complex that converts inactive pro-inflammatory cytokines into active forms.

#### Schematic of the NLRP3 inflammasome:



**Figure 1.10:** Illustration of the multi-subunit complex, formed (in this diagram) of the homo-dimerisation of NLRP3 subunits, in addition to ASC and caspase-1 proteins, to form a proteolytic complex that converts inactive pro-IL-1 $\beta$  and pro-IL-18 into their active forms<sup>133</sup>.

### *1.10.1: Inflammasome component proteins:*

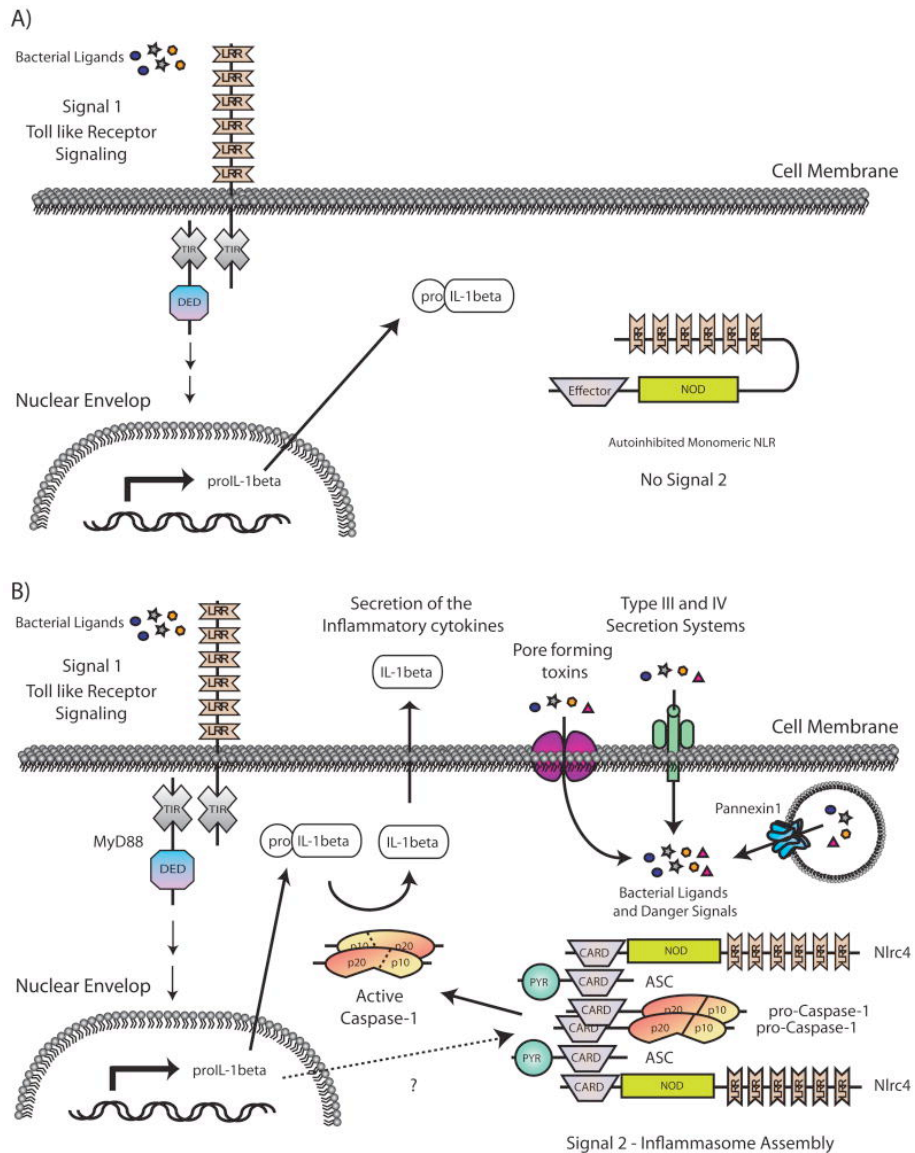
The inflammasome has only been known about for several years now, but the importance of its role in the innate immune response has created great interest and rapid advances in furthering our knowledge in the literature. As of yet, four types of inflammasome have been investigated and identified, though more are sure to be uncovered shortly. Each identified inflammasomes name is based upon its constituent NLR and/or PYHIN ((PYRIN and HIN-200) proteins, namely, NLRP1, NLRP3, NLRC4 and AIM2. In addition to the NLR, and PYHIN each inflammasome contains additional proteins and has a specific stimuli and downstream signaling pathway. The adapter-apoptosis- associated speck-like protein containing a CARD (ASC) protein, links the NLR to the caspase-1 protein and appears to be present in all forms of inflammasome yet identified. NLRP3 inflammasome also contains CARDINAL proteins in its structure<sup>76,121</sup>.

The NLR and PYHIN proteins detect endogenous and exogenous PAMPs and DAMPs, and undergo heteromerization and homomerization and with the addition of the associated proteins assemble to form a recruitment scaffold for procaspase-1. Each inflammasomes structure is specific to the stimuli PAMP or DAMP detected<sup>134</sup>. Homophilic CARD-CARD and PYD-PYD interactions between NLRs, PYHIN, ASC, and procaspase-1 proteins are proposed to be the binding mechanism in inflammasome assembly<sup>109</sup>.



### 1.10.2: Caspase-1 and other member of the caspase family:

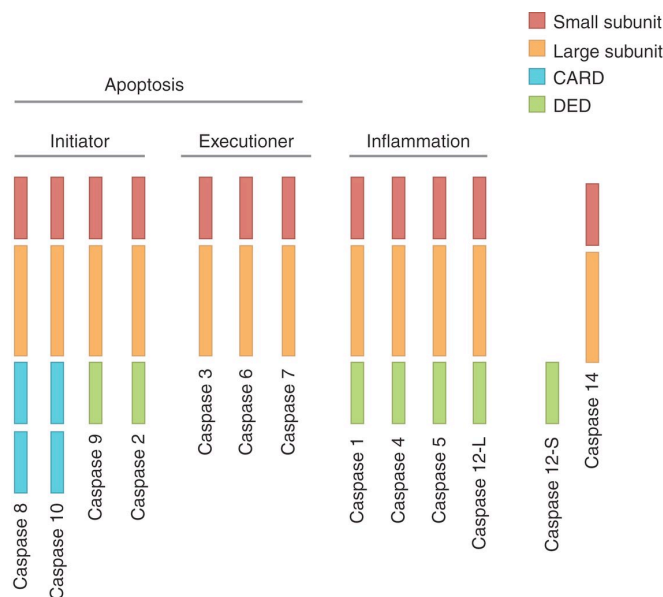
The two-step model for the induction and maturation of the pro-inflammatory cytokine IL-1 $\beta$  during the innate immune response:



**Figure: 1.10.2:** (A) In the absence of NLR signals, TLR signaling (Signal 1) leads to the upregulation of pro-IL-1 $\beta$  transcription. (B) In response to a variety of intracellular signals (Signal 2) such as bacterial ligands and endogenous danger signals, NLRs are released from their auto-inhibited monomeric conformation leading to the assembly of a function inflammasome capable of activating the cysteine protease caspase-1. Active caspase-1 catalyzes the proteolytic processing of pro-IL-1 $\beta$  (and IL-18 not shown) into active cytokines that are then released from the cell<sup>130</sup>.

Caspase-1 is a cysteine protease that plays the primary direct role in activating the pro-inflammatory cytokines IL-1 $\beta$  and IL-18 from their immature pro-forms into active mature forms of the cytokines. Caspase-1 belongs to a family of endoproteases that hydrolyse peptide bonds, in a specific sequence orientation of cysteine-aspartic acid residue sequences. Caspases generally fall into two categories, apoptotic-mediating pathway caspases, such as caspase-3, 6, 7, 8 and 9; and inflammasome associated caspases-1, 4, 5 and 12; whilst the roles of caspase-2, 10 and 14 remain yet unknown. Inactive pro-caspase-1 zymogens are activated by the macromolecular complexes (NLRP1 and NLRP3 inflammasomes) via recruitment and association with the inflammasome CARD domains<sup>135</sup>.

#### Domain structures of human caspases:



**Figure: 1.10.2.1:** Caspases are initially produced as inactive monomeric procaspases that require dimerization and often cleavage for activation. Assembly into dimers is facilitated by various adapter proteins that bind to specific regions in the prodomain of the procaspase. The exact mechanism of assembly depends on the specific adapter involved. Different caspases have different protein–protein interaction domains in their prodomains, allowing them to complex with different adapters. For example, caspase-1, -2, -4, -5, and -9 contain a caspase recruitment domain (CARD), whereas caspase-8 and -10 have a death effector domain (DED)<sup>136</sup>.

## Summary of caspase-deficient mouse phenotypes

Caspase	Mouse mutant phenotype	Function derived from deficient phenotype	References
Caspase-1	Develop normally; have no defects in apoptosis	Are more susceptible to virus infection (Thomas et al. 2009); show enhanced tumor formation (Hu et al. 2010); have reduced apoptosis in several models such as neuronal cell death, myocardial infarct, and heart failure (Frantz et al. 2003; Arai et al. 2006; Merkle et al. 2007); caspase-1-deficient mice are protected against cisplatin-induced apoptosis and acute tubular necrosis (Faubel et al. 2004)	Kuida et al. 1995; Li et al. 1995; Thomas et al. 2009; Hu et al. 2010
Caspase-2	Develop normally and are fertile; have only minor apoptotic defects in some cell types; MEFs show resistance to killing by HS and specific drugs	Caspase-2 has been proposed to be involved in different proapoptotic pathways, but the data from the gene-deficient mice do not support the majority of the in vitro results	Bergeron et al. 1998; O'Reilly et al. 2002; Tu et al. 2006
Caspase-3	Mice die perinatally in mixed background; some can survive to adulthood; show brain hyperplasia	Essential for neuronal cell death; caspase-3 is an essential component in some apoptosis pathways, dependent on the stimulus and cell type; essential for the regulation of B-cell homeostasis	Kuida et al. 1996; Woo et al. 1998, 2003
Caspase-6	Develop normally	No apoptotic defects	Unpublished (see Zheng et al. 1999)
Caspase-7	Develop normally	No apoptotic defects	Lakhani et al. 2006
Caspase-8	Embryonic lethal; defects in heart muscle development	Cells from caspase-8-deficient mice are resistant to death-receptor-induced apoptosis; inactivating mutation in humans shows immunodeficiency; tissue-specific deletion of caspase-8 revealed functions in T-cell homeostasis, in the generation of myeloid and lymphoid cells and the differentiation into macrophages, and in skin inflammation and wound healing; suppresses RIPK3-dependent necrosis	Juo et al. 1998; Varfolomeev et al. 1998; Chun et al. 2002; Salmena et al. 2003; Kang et al. 2004; Beisner et al. 2005; Kovalenko et al. 2009; Lee et al. 2009a; Li et al. 2010; Kaiser et al. 2011; Oberst et al. 2011; Zhang et al. 2011
Caspase-9	Perinatal lethal, but not 100% penetrant	Brain hyperplasia caused by decreased apoptosis and excess neurons; cells from caspase-9-deficient mice show resistance to apoptosis induced by a variety of cytotoxic drugs and irradiation	Hakem et al. 1998; Kuida et al. 1998
Caspase-10	No mouse homolog	Human inactivating mutations are associated with ALPS II	Wang et al. 1999
Caspase-11	Develop normally and are fertile	Mutant mice are resistant to endotoxic shock induced by LPS; IL-1 production after LPS stimulation is blocked; is necessary for caspase-1 activation; regulates cell migration in lymphocytes	Wang et al. 1998; Li et al. 2007
Caspase-12	Develop normally	Mice are resistant to ER stress-induced apoptosis, but their cells undergo apoptosis in response to other death stimuli; thus, caspase-12 mediates an ER-specific apoptosis pathway; show an enhanced bacterial clearance and are more resistant to sepsis	Nakagawa et al. 2000; Saleh et al. 2006
Caspase-14	Develop normally and are fertile; their long-term survival was indistinguishable from that of wild-type mice	Mice show increased sensitivity to UVB irradiation; caspase-14-deficient epidermal cells show no defect in apoptosis; caspase-14 is responsible for the correct processing of (pro)filaggrin during cornification	Denecker et al. 2007

**Table 1.10.2.2:** MEF, mouse embryonic fibroblast; HS heat shock; ALPS, autoimmune lymphoproliferative syndrome; LPS, lipopolysaccharide; ER, endoplasmic reticulum; RIPK3, receptor-interacting serine/threonine-protein kinase 3<sup>135</sup>.

### ***1.10.3: Inflammasome activated cytokines IL-1 $\beta$ and IL-18:***

IL-1 $\beta$  and IL-18 are potent pro-inflammatory cytokines that belong to the Interleukin 1 (IL-1) family of inflammatory and innate immune mediator molecules. Unlike other members of the IL-1 family, IL-1 $\beta$  and IL-18 are present in the cellular cytosol, in an inactive pro-form. Activation of these inactive cytokines requires cysteine protease action of caspase-1<sup>137</sup>. The mechanisms by which IL-1 $\beta$  and IL-18 are controlled are tightly regulated requiring a two-step process for activation to be achieved. The initial step requires synthesis of pro-forms of IL-1 $\beta$  and IL-18 mRNA in response to TLR and RLR activation, whilst the second step requires NLR-mediated activity of the inflammasome via caspase-1, although other proteases have been shown to active IL-1 $\beta$  in certain circumstances<sup>138</sup>. IL-1 $\beta$  and IL-18 secretion and bioactivity require the posttranslational catalytic activity of the inflammasome. Regulation of caspase-1 itself is also highly regulated as it too is present in the cytosol as the inactive pro-form pro-caspase-1 and requires inflammasome activity to cleave the inactive form into active caspase-1<sup>137</sup>. The tight regulation of these IL-1 cytokines indicates the potency of their active forms, and the potentially detrimental effect that ineffective regulation can cause. The process of IL-1 $\beta$  and IL-18 induced pyroptosis is a strong support for the theory of such rigorous regulatory system. IL-18 has been reported in several studies to promote IFN- $\gamma$  production by T-cells and NK cells, which induces NO production by macrophages in an antimicrobial function. IL-18 has also been shown to promote the secretion of pro-inflammatory cytokines TNF- $\alpha$ , IL-1 $\beta$ , IL-8, which increase neutrophil proliferation and migration to the area of IL-18 secretion<sup>139,140</sup>.

IL-1 $\beta$  is described to be one of the most powerful cytokines in its downstream actions, which affects virtually all of the bodies organs and causes extremely strong

and rapid recruitment of neutrophils to the site of infection, via the production and secretion of cytokines and chemokines<sup>140</sup>.

Pyroptosis is a process of cell death that differs from the normal cell death pathways of necrosis and apoptosis. Caspase-1-dependent DNA fragmentation and pore formation of the cellular membrane cause cell death through lysis<sup>112</sup>. Pyroptosis occurs in myeloid cell lines upon intracellular infection by pathogenic molecules that although not being well understood, appears to increase with increased inflammasome activation, suggesting possible links between pyroptosis and an overwhelmed autophagy system and cytosolic caspase-1 suppression mechanism<sup>111</sup>.

#### ***1.10.4: NLRP1 inflammasome:***

NLRP1 NLR was the first inflammasome NLR identified by Martinon *et al.* in 2002, and though being structurally different to the NLRP3 inflammasome, also interacts with caspase-1 cleaving the inactive pro-forms of IL-1 $\beta$  and IL-18 into their active pro-inflammatory cytokine forms<sup>141</sup>. Unlike the NLRP3 inflammasome, the NLRP1 C-terminal domain-caspase-1 association does not require ASC as the C-terminal domain contains an extended, incorporated CARD. Though the NLRP1 inflammasome does not require ASC to bind pro-caspase-1, the inclusion of ASC augments the inflammasome activity<sup>111,142</sup>.

Studies have shown NLRP1 is expressed in a variety of cell types, including monocytes, granulocytes, DC, T and B cells<sup>111</sup>. In addition to the C-terminal CARD, NLRP1 contains a FIIND motif that makes it unique to other NLR family members<sup>130</sup>. Binding of MDP to NLRP1 activates a two-step mechanism of activation, with conformational changes induced by MDP-NLRP1 interaction, which then allows NTP binding and self-oligomerization<sup>142</sup>. Anti-apoptotic proteins Bcl-2

and Bcl-X(L) bind to NLRP1 in resting cells and suppress its ability to activate caspase-1<sup>112,143</sup>. It has been suggested in recent studies HSU et al. that for full response to MDP via NLRP1, interaction with NOD2 is required. NOD2 upregulates pro-IL-1 $\beta$  expression via NF- $\kappa$ B-dependent manner and regulates caspase-1 activation by MDP by direct interaction with NLRP1<sup>144</sup>.

#### ***1.10.5: NLRP3 inflammasome:***

To date the NLRP3 inflammasome is the most studied and well documented of the NLR inflammasomes. Like all NLR inflammasomes, NLRP3 has been shown to positively and negatively regulate the innate immune response to PAMP and DAMP stimuli. The ligands associated with activating NLRP3 are extremely broad, ranging from a variety of DAMPs, PAMPs and environmental ligands. PAMP associated ligands include whole pathogen exposure, viral material, bacterial components, pore forming toxins, such as nigericin and maitotoxin, which is a potent marine toxin, PAMP induced ATP and K<sup>+</sup> fluctuations<sup>111,145</sup>. It is currently thought that activation of NLRP3 inflammasome complex formation requires a two-step signaling process. Step-one requires the upregulation of specific cytokine gene transcription, via immune pathways such as MyD88-dependent cascades activated by TLR- NOD1- or NOD2-activation pathways, which upregulates pro-IL-1 $\beta$  and pro-IL-18 expression. The mechanisms for step-two of inflammasome formation is yet unknown, but with such a wide range of ligands that activate NLRP3 inflammasome formation, it is likely that the second-step occurs through more than just one stimuli. Four such stimuli have been proposed in the literature; 1) potassium efflux<sup>146</sup>, 2) generation of reactive oxygen species (ROS)<sup>147</sup>, 3)lysosomal disruption and most recently<sup>148,149</sup>, 4) Ca<sup>2+</sup> influx<sup>150-152</sup>.

NLRP3 has been shown to activate in response to host derived ligands such as amyloid- $\beta$ , uric acid levels and monosodium urate (MSU) crystals, and DAMPs such as reactive oxygen species (ROS) released by damaged or stressed cells, these include elevated extracellular ATP levels, hyaluronan and NADPH oxidase released from aggravated endosomes<sup>148,149,153,154</sup>. Environmental stimuli of NLRP3 inflammasomes include UVB irradiation, silica and asbestos<sup>111,147,150</sup>.

The major stimulatory factor for activating NLRP3 appears to be via ROS signaling or interactions. Though the mechanisms remain unclear there are many studies support the role of  $K^+$  efflux as an inflammasome assembly requirement<sup>155,156</sup>.  $K^+$  flux has been attributed to lysosomal destabilization and can result in release of proteases from endosomes, cause NLRP3 activation<sup>113</sup>. A study showed  $K^+$  efflux alone does not appear to cause direct NLRP3 signaling activation as ATP is required to activate pro-caspase-1 into its active form<sup>157</sup>. The addition of association/adaptor molecules required for NLRP3 regulation is highly likely, for example the requirement of Cathepsin B for NLRP3 regulation in a study<sup>149</sup>. The activation of the inflammasome assembly must therefore rely on a network of signals and is dependent on the interaction of a number of different pathways. This is supported by the fact that NLRP3 has such a multitude ligands, yet the LRR remains the same.

As mentioned above ATP and  $K^+$  imbalance often cause this signal, but other signals such as  $Ca^{2+}$  and pH imbalances have also been shown to cause NLRP3 inflammasome assembly<sup>146,152,158,159</sup>.

As an example of bacterial PAMP-induced NLRP3 inflammasome assembly, TLR ligands LPS, PGN or LTA, increase NF- $\kappa$ B expression as well as NLRP3 expression. Due to bacterial presence and damage to cells and cellular components, which leads to increased extracellular ATP levels, will initiate NLRP3

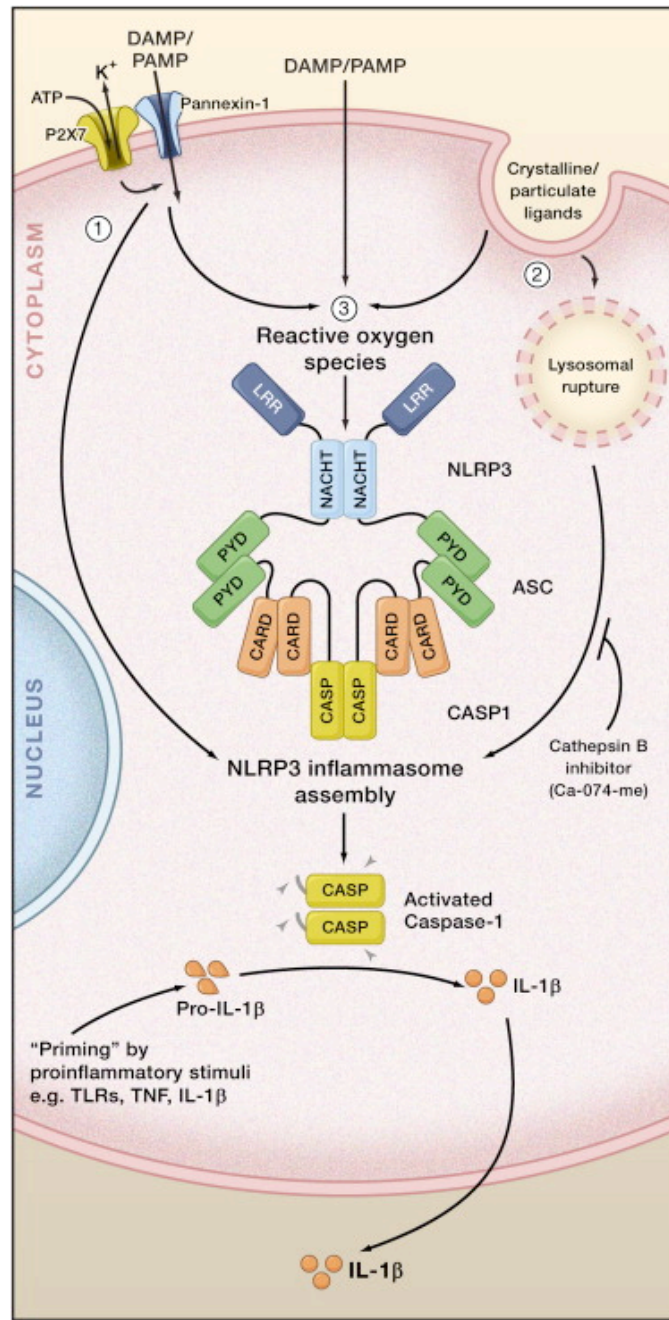
inflammasome assembly and activation<sup>113</sup>. ATP is released by pathogens, necrotic damaged cells and TLR ligand-stimulated monocytes, causes activation of the purinergic P2X7 ATP-gated ion channel, triggering efflux of K<sup>+</sup> ions, which in turn recruits pannexin-1 hemichannel proteins activating NLRP3 via the pannexin-1 mediated PAMP delivery mechanism into the cellular cytoplasm, though no direct PAMP-NLRP3 interaction has been observed<sup>76,146,158,159</sup>.

The NLRP3 gene lacks a CARD and thus can only recruit pro-caspase-1 in the presence of ASC<sup>115</sup>. The NLRP3 inflammasome consists of a scaffold complex of NLRP3, ASC and pro-caspase-1, which when recruited to the NLRP3-ASC complex, forms a pro-caspase-1 cluster, via the proteolytic activity of ASCs CARD domain. Caspase-1 then auto-cleaves its inhibitory subunits and forms the active p10/p20 caspase-1 tetramer<sup>160</sup>.

The NLRP3 LRR is thought to mediate an auto-inhibitory state that keeps the NLR inactive prior to stimulation, by association with SGT1 and Hsp90 chaperone proteins<sup>161</sup>.

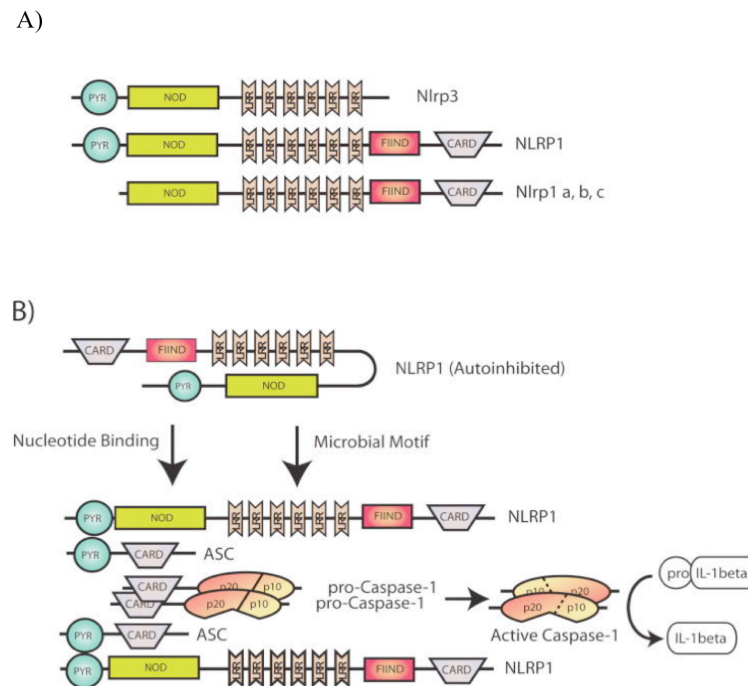


### NLRP3 inflammasome activation:



**Figure 1.10.5.1:** Three major models for NLRP3 inflammasome activation are favored in the field, which may not be exclusive: (1) The NLRP3 agonist, ATP, triggers P2X7-dependent pore formation by the pannexin-1 hemichannel, allowing extracellular NLRP3 agonists to enter the cytosol and directly engage NLRP3. (2) Crystalline or particulate NLRP3 agonists are engulfed, and their physical characteristics lead to lysosomal rupture. The NLRP3 inflammasome senses lysosomal content in the cytoplasm, for example, via cathepsin-B-dependent processing of a direct NLRP3 ligand. (3) All danger-associated molecular patterns (DAMPs) and pathogen-associated molecular patterns (PAMPs), including ATP and particulate/crystalline activators, trigger the generation of reactive oxygen species (ROS). A ROS-dependent pathway triggers NLRP3 inflammasome complex formation. Caspase-1 clustering induces autoactivation and caspase-1-dependent maturation and secretion of proinflammatory cytokines, such as interleukin-1 $\beta$  (IL-1 $\beta$ ) and IL-18,<sup>111</sup>

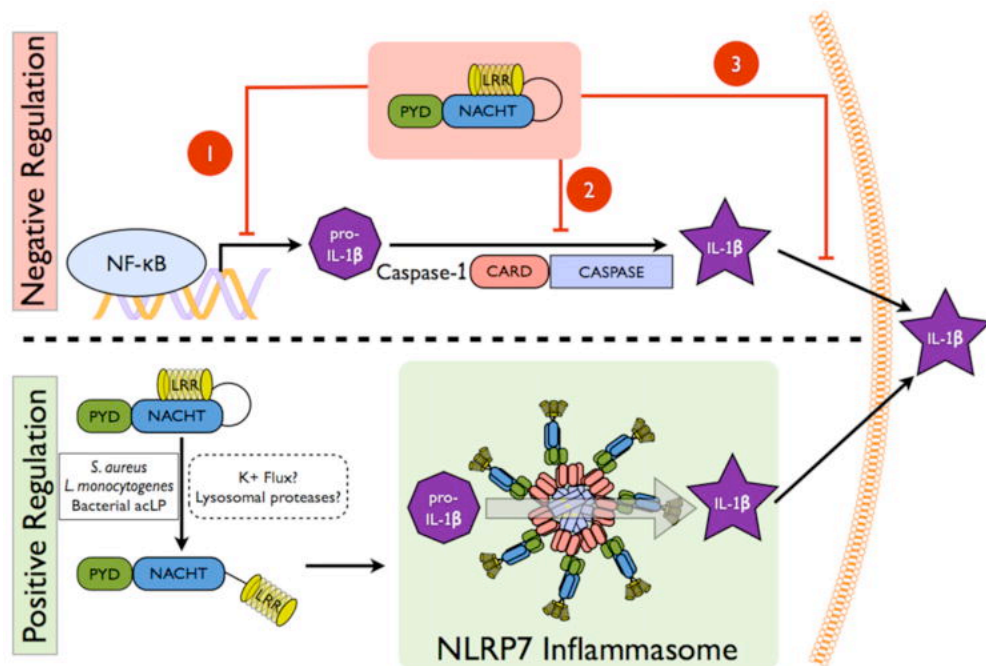
Schematic representation of the multi-domain architectures of various NLRs and their assembly into a functional inflammasome:



**Figure 1.10.5.2:** Apaf-1 is a multi-domain scaffolding protein critical for the assembly of the apoptosome (not shown), a multi-protein complex critical for mediating apoptotic cell death. Subsequently, several NLR proteins were identified as Apaf-1-related molecules based on similar domain architectures (A). In response to various intracellular stimuli including microbial moieties and endogenous products released by dying cells, NLRs are released from their auto-inhibited monomeric conformation and act as molecular scaffolds to assemble multi-protein complexes known as inflammasomes. Assembly of the inflammasome leads to caspase-1 activation and proteolytic processing of pro-inflammatory cytokines such as IL-1 $\beta$  (B). In this review we focus on three of the best characterized inflammasomes: Ipaf1, Nalp3, and Nalp1 (adapted from Franchi *et al.* 2009,<sup>130</sup>).

#### 1.10.6: NLRP7:

##### Mechanisms of NLRP7 function in inflammation and host defence:



**Figure 1.10.6:** The top panel depicts the proposed mechanisms by which NLRP7 inhibits IL-1 $\beta$  release. 1) NLRP7 inhibits NF- $\kappa$ B activation by an unknown mechanism, which may involve FAF1, which prevents transcription of pro-IL-1 $\beta$ . 2) NLRP7 directly interacts with pro-Caspase-1 and pro-IL-1 $\beta$ , which might prevent their activation or recruitment into inflammasomes. 3) NLRP7 localizes to the Golgi and was predicted to affect trafficking of mature IL-1 $\beta$  containing vesicles necessary for release. The bottom panel depicts NLRP7 inflammasome formation in response to sensing bacterial acylated lipoproteins (acLP) <sup>162</sup>.

Recent investigations into NLRP7 have shown to that it can both positively and negatively regulate innate immune responses via interactions with several inflammasome-associated proteins that regulate the activity of NLRP3 and therefore effect the expression and activity of NF- $\kappa$ B, IL-1 $\beta$  and IL-18<sup>162</sup>. Though the exact mechanisms of both positive and negative regulation of NLRP3 by NLRP7 are yet unknown, it is thought that the direct interaction between proteins such as pro-caspase-1, pro-IL-1 $\beta$ , ASC and Fas associated factor 1 (FAF1) are the cause of regulations. Negative inhibition of NLRP3 by NLRP7 causes inhibition of NLRP3

and caspase-1-mediated NF- $\kappa$ B activation, the inhibitory interaction is thought to be via specific interaction with NLRP3 as there is no inhibition of IL-1 $\beta$  transcription as NF- $\kappa$ B was not itself effected<sup>163</sup>.

Increased immune response activity by NLRP7 is brought about by the formation of a NLRP7, ASC and pro-caspase-1 complex called the NLRP7 inflammasome. NLRP7 inflammasome association and formation activates caspase-1 activity and in turn activates the pro-IL-1 $\beta$  cytokine, <sup>164</sup>. These studies and finding would suggest that NLRP7 acts as both an inflammasome and a non-inflammasome NLR.

NLRP7 gene mutations have recently been implicated in recurrent miscarriages in a study by Murdoch et al<sup>165</sup>. In addition NLRP7 has been shown to regulate inflammatory activation in response to bacterial acylated lipoproteins (FSL-1) and triacylated Pam<sub>3</sub>CSK<sub>4</sub><sup>164</sup>. The mechanisms of how NLRP7 regulates immune response and developmental functions are still unclear.

#### *1.10.7: NLRP12:*

NLRP12 has been shown to negatively regulate NF- $\kappa$ B signaling, via the possible mechanism of interacting and inhibiting with the NF- $\kappa$ B pathway proteins, NF- $\kappa$ B inducing kinase (NIK), IRAK4 and/or TRAF3. NLRP12 is thought to phosphorylate (inhibit) IRAK1 and cause degradation of NIK, though the mechanism by which this is done remains unclear <sup>166,167</sup>. Another proposed mechanism for NF- $\kappa$ B regulations is through the increased ATP levels, which would suggest a negative feedback mechanism, as ATP elevations initiate inflammatory responses, thus keeping said response in a regulated system<sup>113,168</sup>.

Schematic illustrating NLRP12 attenuation of NF- $\kappa$ B signalling:

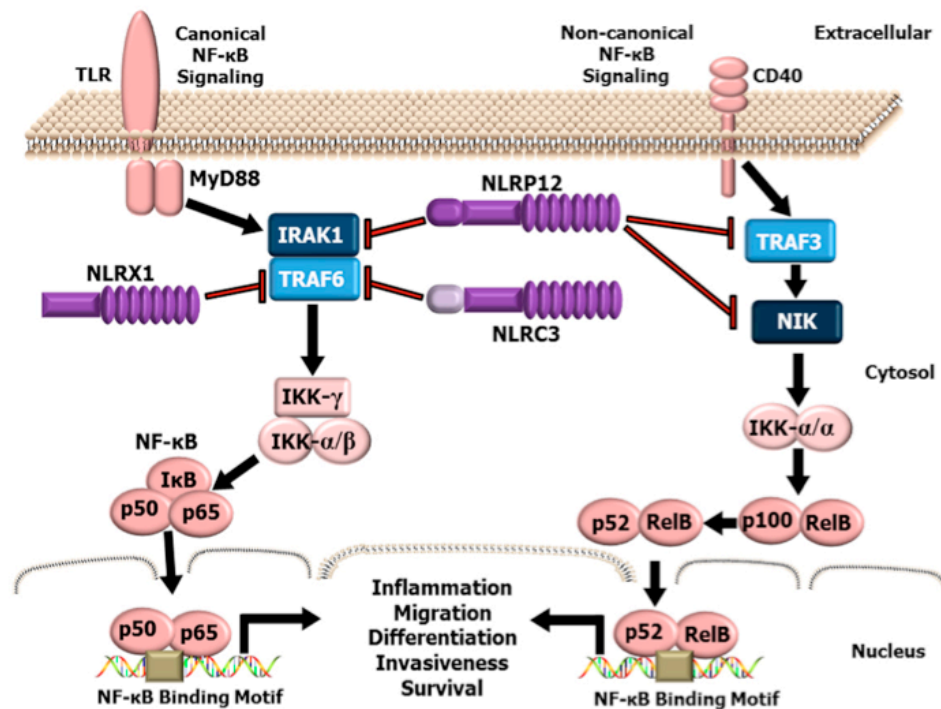


Figure 1.10.7: NF- $\kappa$ B is a master regulator of gene transcription and contributes to several hallmarks of cancer. NLRX1, NLRP12, and NLRC3 negatively regulate NF- $\kappa$ B signaling at multiple levels. NLRX1 interacts with and inhibits TRAF6 and the IKK complex resulting in the attenuation of NF- $\kappa$ B signaling following TLR stimulation. Likewise, NLRC3 was also shown to interact with TRAF6 and attenuate NF- $\kappa$ B signaling through a similar mechanism. NLRP12, has been shown to attenuate both the canonical NF- $\kappa$ B signaling pathway through modulating the phosphorylation of IRAK-1 and the non-canonical NF- $\kappa$ B pathway through interactions with TRAF3 and NIK<sup>169</sup>.

### 1.11: Aims of this study:

As previously stated, *Ureaplasma spp.* do not possess a cell wall, nor are they able to synthesize cell wall components, such as peptidoglycans (PGNs) (MDPs or iE-DAPs), LTA or LPS, nor do they express flagella, or many other highly conserved bacterial pathogen-associated molecular patterns (PAMPs) that the innate immune system primarily detects.

The mechanisms by which *Ureaplasmas* cause such diseases remain unclear, but it is believed that inappropriate induction of inflammatory responses is involved, most likely triggered by the innate immune system<sup>36,37</sup>. It is believed that the innate immune response to these bacteria can lead to the activation of pattern recognition receptors (PRRs), production and release of pro-inflammatory mediators leading to the complications associated with preterm and term infants. Increased levels of pro-inflammatory mediators such as interleukin-6 (IL-6), tumour-necrosis-factor (TNF- $\alpha$ ), IL-1 $\beta$  and IL-8 have been shown in amniotic fluid infected with *Ureaplasma*, supporting this hypothesis<sup>170</sup>. The question that remains is, which PRRs are involved since this is a wall-less bacterium?

Very little is known about the innate immune recognition of *Ureaplasma*. There is a single study that implicates TLR1, TLR2 and TLR6 in *Ureaplasma parvum* innate-immune recognition, but this study was performed with *U. parvum* serovar 3 (SV3), which was cultured in broths enriched with yeast, thus results obtained for the activation of certain TLRs might be attributed to the contaminating yeast components<sup>171</sup>.

The aim of this study is to elucidate the molecular mechanisms behind the innate immune recognition of *Ureaplasma*. In doing so, we will initially elucidate whether

the traditional ways of culturing *Ureaplasma* in yeast-enriched media provide yeast contaminants that activate the innate immune system and invalidate the studies. The involvement of both TLRs and NLRs will be investigated, using *Ureaplasma* that has been grown in a yeast-free environment.

TLR1, 2, 4, 6, and 9 are to be investigated in their role (if any) in response to *Ureaplasma spp.* stimulation, as all have potential (either from the literature or known cellular components) to initiate TLR-dependent immune responses. NLRs, such as NOD1, NOD2, NLRP1, NLRP3, NLRP7 and NLRP12 will be investigated for their role in immune response to *Ureaplasma spp.*, as they have a plethora of PAMP and DAMP ligands, that will further our understanding of the innate immune response (if any) to *Ureaplasma spp.* ligands, which are likely to be unlike those possessed by other bacteria, on account of its genetic and over all divergence from other known bacteria.

TLR1, 2, 4, 6, and 9 are to be investigated in their role (if any) in response to *Ureaplasma spp.* stimulation, as all have potential (either from the literature or known cellular components) to initiate TLR-dependent immune responses. NLRs, such as NOD1, NOD2, NLRP1, NLRP3, NLRP7 and NLRP12 will be investigated for their role in immune response to *Ureaplasma spp.*, as they have a plethora of PAMP and DAMP ligands, that will further our understanding of the innate immune response (if any) to *Ureaplasma spp.* ligands, which are likely to be unlike those possessed by other bacteria, on account of its genetic and over all divergence from other known bacteria.

Given the strong association between *Ureaplasma* colonization and preterm birth (PTB) and bronchopulmonary dysplasia in neonatal infants, I hypothesize that there is likely to be some factor of *Ureaplasma* that does contribute to the PTB.

Furthermore, I find it likely that *Ureaplasma*, once detected in the body, is likely to initiate an immune response, with the production of inflammatory cytokines that will be capable of damaging surrounding tissues, thus *Ureaplasma* will be able to cause premature preterm rupture of the membrane (pPROM) leading to PTB, and BPD is respiratory tracts that possess *Ureaplasma* colonisations.

#### Aims

- To find the pattern recognition receptor(s) responsible for detecting *Ureaplasma* serovars.
- To identify immune response pathways activated by the detection of *Ureaplasma* in different cell lines.
- Determine if genetically knocking down certain PRRs has an affect on the immune response, thus strengthening the findings of which PRRs are associated with *Ureaplasma* detection.
- Investigate the cytokines produced in the immune response to *Ureaplasma*, which will enable us to determine the possible detrimental affects that *Ureaplasma* colonization may have on pregnant women and in preterm infants.
- Determine whether regulating immune response pathways can reduce the adverse affects of *Ureaplasma* in colonized individuals.

Through this study, we may be able to determine finally if *Ureaplasma* is pathogenic and if it does have the potential to cause the adverse outcomes that it has so long been associated. If *Ureaplasma* does possess the pathogenic properties required to initiate an immune response, we will be in a better position to decide whether *Ureaplasma* infections require more robust detection and treatment methods than are



in place today. The ultimate goal of this investigation would be to reduce the rate of PTB and in turn, reduce the rates of neonatal complications

## **Chapter 2:**

# **Materials and Methods**

## 2.1:Antibodies:

Primary Antibodies	Species	Company/origin
TLR1	Mouse	Santa Cruz Biotechnology Inc.
TLR2	Goat	Santa Cruz Biotechnology Inc.
TLR4	Goat	Santa Cruz Biotechnology Inc.
TLR6	Goat	Santa Cruz Biotechnology Inc.
TLR7	Mouse	Santa Cruz Biotechnology Inc.
TLR9	Goat	Santa Cruz Biotechnology Inc.
NOD1	Goat	Santa Cruz Biotechnology Inc.
NOD2	Mouse	Santa Cruz Biotechnology Inc.
NLRP1	Mouse	Santa Cruz Biotechnology Inc.
NLRP3	Rabbit	Santa Cruz Biotechnology Inc.
NLRP7	Goat	Santa Cruz Biotechnology Inc.
NLRP12	Goat	Santa Cruz Biotechnology Inc.
NLRC5	Rabbit	Santa Cruz Biotechnology Inc.
Streptavidin	Rabbit	BioRad
GM-1 gangliocide	Goat	Donated by Prof K. Triantafilou
Phospho-IkB- $\alpha$	Rabbit	New England BioLabs
Caspase-1 (P10)	Rabbit	Santa Cruz Biotechnology Inc.
ASC	Mouse	Santa Cruz Biotechnology Inc.

Secondary Antibodies	Label	Company
Rabbit anti mouse	FITC	Dako cytometry
Rabbit anti goat	FITC	Dako cytometry
Swine anti rabbit	FITC	Dako cytometry
Rabbit anti mouse	Cy 3	GE
Rabbit anti goat	Cy 3	Jackson ImmunoResearch Laboratories
Rabbit anti goat	Cy 5	Jackson ImmunoResearch Laboratories
Goat anti rabbit	HRP	Dako cytometry
MyD88 (Direct)	FITC	Donated by Prof K. Triantafilou
Mitotracker (Direct)	Alexa 546	Life Technologies
Anti TLR9 (Direct)	TRITC	Life Technologies
Rabbit anti goat	Alexa 488	Life Technologies
Goat anti mouse	Alexa 546	Life Technologies
Anti TLR9 (Direct)	TRITC	Life Technologies
TOPRO	Alexa 633	Life Technologies

Table 1.1 List of the primary and secondary antibodies used during this investigation.

## 2.2: Tissue Culturing:

Throughout these entire investigations the highest care and attention was used to produce a sterile growth environment for culturing tissue, whilst at the same time providing optimal growth conditions. By creating sterile, optimal growth conditions, contamination from foreign bodies and from stress factors poor growth conditions, can be kept to a minimum.

Cells were cultured using incubators at of 37°C in a humidified 5% CO<sub>2</sub> environment.

Experiments were carried out in Microflow Advanced Biosafety Class II laminar flow hoods, sterilised prior to and after every use, using 1% Virkon solution.

### Microflow Advanced Biosafety Class II laminar flow hood



Figure 2.2.1: Microflow Advanced Biosafety Class II laminar flow hood. Provides a sterile environment for tissue culturing, stimulation and investigations. (<http://www.astec-microflow.com/Microflow/index.htm>)

### *2.2.1: Semi-adherent cell lines:*

Mono-mac 6 (MM6) cells were obtained from the German Tissue Culture Collection (DSMZ). MM6 cells are a human monocytic cell line. MM6 are a semi-adherent cell line, cultured in 24-well ( $1.9\text{cm}^2$ ) plates (Nunc). Each well is cultured in 2ml 10% FCS, 0.006% OPI, RPMI growth medium.

Propagating MM6 cell line requires gentle aspiration of 1.5ml of the old growth medium from each well of the 24-well plate, making sure not to aspirate cells from the bottom of each well. The cells are re-suspended in 1.5ml of fresh medium pipetted into each well and then agitated by pipetting up and down. 1ml of the re-suspended cells was transferred into a new well, and all wells were made up to 2ml by the addition of another 1ml of fresh medium to all wells. The 24-well plate was then returned to the incubator and left to propagate.

#### Nunc 24-well culture plate



Figure 2.2.1.1: Nunc 24-well flask used for the culturing of semi adherent cells lines, each well with 2ml volume and lid to cover the 24-well plate (<http://www.capitolscientific.com/Nunc-174899-UpCell-24-Well-x-1mL-MultiDish-Cell-Culture-Dish-With-Lid-And-Airvent-Temperature-Res>)

### ***2.2.2: Adherent cell lines:***

#### ***2.2.2.1: Bronchial Epithelial cell line:***

Bronchial Epithelial Cells (BEAS-2B) were obtained from the American Type Culture Collection [ATCC]). BEAS cells were cultured in 25cm<sup>2</sup> filter topped flasks (Nunc), in 4ml Dulbecco's Modified Eagle's Medium (1mg/l glucose), Gluta-Max, supplemented with 10% fetal calf serum (FSC), 1% non-essential amino acids (Invitrogen, UK).

Propagating (splitting) adherent cells was performed when cell confluency was 70-90%. When at this confluency, all medium was aspirated from the flask; 1ml phosphate buffer saline (PBS) or medium was added to the flask and then aspirated, to remove any dead cells or cell debris. 2ml of trypsin (proteolytic enzyme (Sigma)) was pipetted into the flask to lift the adherent cells from the base of the flask. Once the cells started to lift, the flask was agitated until all cells were suspended. 2ml of fresh medium was added to the flask to inactivate the trypsin, leaving 4ml of suspended cells. One third of the suspension was transferred to a new flask, twice, making three equal flasks. 5ml medium was added to each flask, which was then laid flat and agitated to distribute the cells throughout the flask. Flasks were then returned to the incubator to propagate.

### Nunc 25cm<sup>2</sup> filter topped flask



Figure 2.2.2.1.1: Nunc 25cm<sup>2</sup> filter topped flask used for culturing adherent cell lines, such as BES cells, allowing sterile airflow and gas exchange through the filter top, (<http://www.fishersci.com/ecom/servlet/itemdetail?catnum=12565351&storeId=10652#>)

### Bronchial epithelial cells (BEAS-2B)

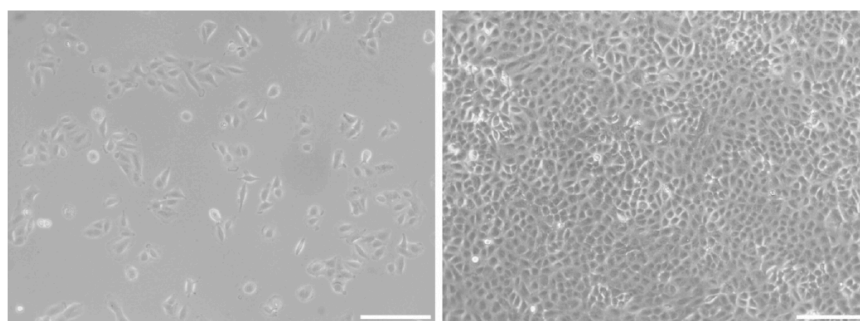


Figure 2.2.2.1.2: Left image shows BEAS-2B cells at low confluence, right image shows BEAS-2B cells at high confluence in 75cm<sup>2</sup> Nunc flask. Scale bar (bottom right of each image) 100µm. (<http://reinnervate.com/using-alvetex/protocols/lung-carcinoma-a549-cell-line-on-alvetex-scaffold-in-well-insert-plate-formats/>)

### **2.2.2.2: Human Embryonic Kidney cell line:**

Human Embryonic Kidney (HEK) 293 (ECACC) were cultured in 25cm<sup>2</sup> filter topped flasks (Nunc), using Dulbecco's Modified Eagle's Medium (1mg/l glucose), Gluta-Max, supplemented with 10% FSC, 1% non-essential amino acids (Invitrogen UK).

HEK 293 TLR2, TLR2/6 and TLR4 transfected cells (provided by Professor D. Golenbock, University of Massachusetts Medical School, Worcester, USA), were

cultured with the addition of 0.5 units/ml penicillin, 0.5 units/ml streptomycin 400µg/ml G418 and 10µg/ml ciprofloxacin.

HEK 293 TLR7 and TLR9 transfected cell lines (Invitrogen USA), were cultured with the addition of 10µg/ml blasticidin.

#### **2.2.2.3: Human primary amniotic epithelial cells:**

Primary human amniotic epithelial cells were purchased from TCS Cells Works (Buckingham, UK). Human amniotic epithelial cells are isolated from human amniotic membranes. Each isolate undergoes extensive testing for the presence of specific amniotic epithelial cell markers.

### **2.3: *Ureaplasma*:**

#### **2.3.1: *Ureaplasma* cultures:**

*Ureaplasma urealyticum* serovar SV2 (Cook strain) was obtained from American Type Culture Collection (ATCC) and SV4 was obtained from Health Protection Agency Centre for Infections (Colingdale, UK).

*Ureaplasma parvum* serovars SV1 and SV6 were obtained from Health Protection Agency Centre for Infections (Colingdale, UK) and SV3 (HPA5) and SV14 (HPA32) colonies were taken from stocks of clinical isolates, shown to be susceptible to bactericidal serum activity.

During preliminary protocols each *Ureaplasma* serovar was grown and cultured in two separate types of *Ureaplasma* selective medium (Mycoplasma Experience, Surrey, UK), 1) *Ureaplasma* selective culturing medium with the addition of yeast and 2) *Ureaplasma* selective culturing medium yeast free medium. These two



*Ureaplasma* culturing mediums were used to propagate the bacteria, in order to investigate whether the addition of yeast to the culturing medium produced different immune responses after *Ureaplasma* stimulations.

#### *2.3.2: Harvesting Ureaplasma:*

To produce pellets of each *Ureaplasma* strain, 20ml of bacterial suspension were centrifuged at 12,000 rpm for 20 minutes. The pellets were washed and re-suspended in 500ml of PBS, centrifuged again (as above), creating a washed pellet. This washing was carried out a total of 3 times. A bacterial number of between  $1 \times 10^7$  and  $1 \times 10^8$  were used for stimulations throughout the investigations and the cell concentration determined by absorbance,  $A_{600} \times 0.1 = 10^8$  bacteria/ml.

#### *2.3.3: Recombinant Multiple Banded Antigen:*

Recombinant multiple banded antigen (MBA) was obtained from Genway Biotech Inc (San Diego, USA), and to passed through Profos Endotraps® blue 10 columns (Hyglos, Germany), to ensure that all MBA samples were not contaminated with LPS. The recombinant MBA obtained was derived from *Ureaplasma parvum* 3.

### **2.4: Cell concentration calculation:**

It was essential throughout the investigation to have as an accurate cellular concentration as possible, in order to preserve consistency and significance of the results collected. Through the method of Hemacytometry, an average concentration of cells in a suspension could be calculated. Counting exact numbers of cells in a sample suspension would have been impossible, so a mean average was calculated using Specialized Neubauer Hemacytometer. A large grid area, made up of  $0.1 \text{mm}^2$

squares, allows the number of cells within a known surface area to be counted, using light microscopy. By placing a quartz cover slide exactly 0.1mm above the floor of the hemacytometer chamber, the cellular concentration of 1µl (0.1mm<sup>3</sup>) of cell suspension can be calculated, (cells/µl). A number of central squares and squares from each corner of the chamber are selected at random, the cells in each square counted, then combined to produce a random mean average of cellular concentration in a sample solution.

$$\text{Conc. (cells/ml)} = (\text{Total cells counted} / \text{Number of squares counted}) \times 10$$

#### Hemocytometer and cell counting grid:

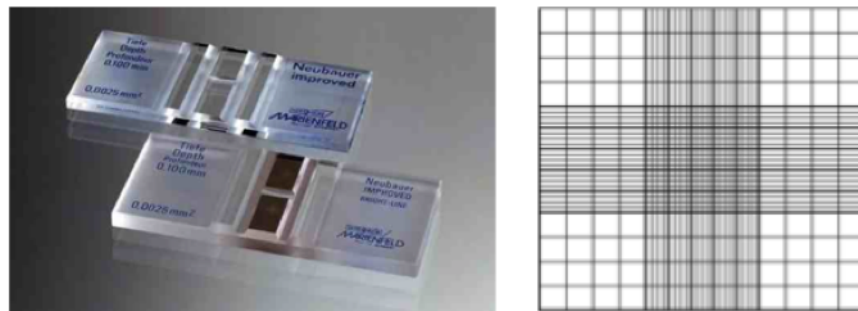


Figure 2.4.1: Hemocytometer slides (left) are used for calculating (approximate) cell concentration under magnification using a light microscope. Number of cells (n) is calculated by counting the number of cells present in the grid system (right) using the equation above. (left <http://www.bestinshowdaily.com/blog/the-informed-breeder-semen-collection-and-packaging-for-chilled-semen-shipment/>) (right – <http://hemocytometer.wordpress.com/2013/04/04/hemocytometer-protocol/>)

## **2.5: Cryogenic cell storage:**

### **2.5.1:**

Corresponding cryotubes were removed from liquid nitrogen storage, stored on ice and taken to TC room. For each cryotube, 9ml of appropriate growth medium was added into a 15ml Falcon tube,. The content of the cryotube was then defrosted quickly by the addition of 1ml of medium to the tube. The cells were centrifuged at

12,000 rpm for 10 minutes. Falcon tubes were then removed and the supernatant was aspirated off, leaving a pellet of cells, which was then re-suspended in the appropriate volume of fresh growth medium and transferred to its culture container, for example, 24-well plate (Nunc) or 25cm<sup>2</sup> flask (Nunc). It was then placed in a humidified incubator at 37°C and 5% CO<sub>2</sub> to propagate.

#### *2.5.2: Cryogenic preservation of cells:*

To preserve cell culture for long periods of time, without having to consistently culture them, a process of cryogenic storage was used. By storing the cells at extremely low temperatures (-196°C) in liquid nitrogen, cell cultures would remain dormant and genetically unchanged for time periods of years.

##### *2.5.2.1: Semi-adherent cell line cryogenic preservation:*

Non-adherent cells cultured in Nunc 24-well plates were pipetted up (with culture medium) and transferred into a 15ml Falcon tube and centrifuged at 12,000rpm for 5 minutes. The supernatant was aspirated off, leaving a cell pellet. The pellet was re-suspended in 1.5ml freezing medium for every two wells of cultured cells. Suspension was then quickly transferred to a cryotube (Nunc), and placed in -80°C for 24 hours. Speed of transfer was important, as DMSO is toxic to cells. Cryotubes were placed in liquid nitrogen, in labelled containers.

##### *2.5.2.2: Cryogenic preservation of cell lines:*

Adherent cell lines were trypsinised in order to generate a cell suspension.

Cells were suspended in 10ml of their specific growth mediums in 15ml Falcon tubes (Nunc). The tubes were then centrifuged at 12,000rpm for 5 minutes. The

medium was aspirated off and the pellet re-suspended in 1500µl (1.5 ml) of freezing medium specific to each cell line (see table below). Suspension was then quickly transferred to a cryotube (Nunc), and placed in -80°C for 24 hours. Speed of transfer was important, as DMSO is toxic to cells. Cryotubes were then placed in liquid nitrogen, in labelled containers.

## **2.6: Cell stimulation with *Ureaplasma* spp.:**

In order to investigate PRR expression before and after *Ureaplasma* infection, cells were either stimulated with *Ureaplasma* serovars ( $1 \times 10^8$  bacteria/ml to  $1 \times 10^7$  cells/ml) for 1h or not, prior to fixation with 4% paraformaldehyde. The cells were subsequently washed and permeabilised using PBS/0.02%BSA/0.02% Saponin. After permeabilisation, the cells were incubated with antibodies against different PRRs and the appropriate secondary antibodies conjugated to FITC. The cells were washed twice in PBS/0.02% BSA/0.02% Saponin and resuspended in 500 µl of PBS. Fluorescence was detected using a FACSCalibur counting 10,000 cells not gated.

## **2.7: Indirect Immunofluorescence and Flow Cytometry to measure PRR:**

Indirect Immunofluorescence and Flow Cytometry are techniques that produce accurate quantitative data that can be used to detect and measure the expression levels of specific target molecules. In this investigation Indirect Immunofluorescence and Flow Cytometry were used to target and measure expression levels of PRR's, (TLR2, 4, 6, 7 and 9, NOD1 and 2, NALP1, 3, 7 and 9 and NLRC5), in selected cell lines after stimulation with *Ureaplasma* or MBA. By comparing expression levels of

selected PRRs in cells stimulated and unstimulated samples (with the relative antigen), an impression of the immune response to an antigen and can be established. This technique utilises the specific binding properties of antibodies (immunoglobulins), to selectively bind to target proteins sequences and enabled detection through fluorescent light emission produced by a conjugated fluorescent marker sequence in an antibodies structure. Exciting electrons (with energy from a laser) in the fluorophore activate the fluorescent emission with a laser, which is then measured quantitatively (by fluorescence intensity) by Flow Cytometer.

In this investigation Indirect Immunofluorescence was the method of molecular expression level detection used, as opposed to an alternative technique called Direct Immunofluorescence. Direct Immunofluorescence utilises a single fluorescently conjugated antibody to bind a specific target structure. Indirect Immunofluorescence uses to separate, corresponding antibodies to target a specific target structure. Firstly a primary antibody (1°) is used to bind to the target structure, and then a secondary (2°) antibody binds to a structure specific to the primary antibody. The 2° antibody contains the conjugated fluorescent sequence, which is the measured upon activation. Indirect Immunofluorescence is a more accurate method of measuring protein expression levels.

### Direct and Indirect Immunofluorescence binding:

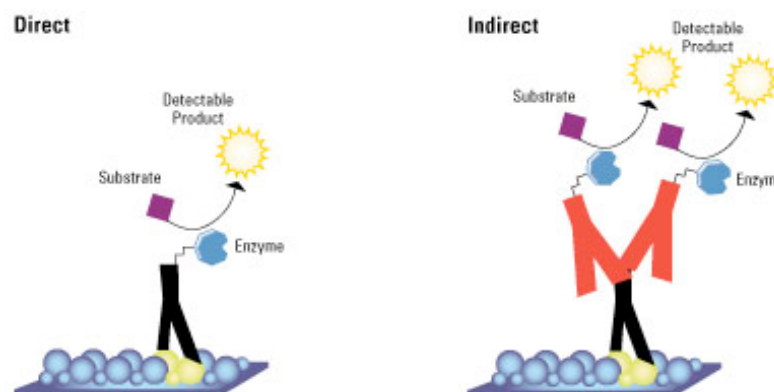


Figure 2.7.1: Direct immunofluorescence (left) shown by direct binding of antibody to antigen and fluorescent emission upon activation of the fluorophore. Indirect Immunofluorescence utilises the binding of a specific (primary) antibody to the target molecule, then the addition of a second antibody with specific binding affinity to the primary antibody. The secondary antibody has a conjugated fluorophore that emits fluorescence when activated.

(<http://www.piercenet.com/method/secondary-antibodies-as-probes>)

### **2.8: Fluorescence Activated Cell Sorter (FACS):**

FACS is a machine used to measure the fluorescent intensity emitted by FITC-conjugated antibodies bound to target proteins in a sample. Other fluorophores conjugated antibodies; emitting different wavelengths of light (photons) can be used at the same time, by selectively detecting photons at wavelengths specific to each fluorophore, multiple proteins to be investigated in a single sample. FITC is activated by E at a wavelength of 495nm and emits E at a wavelength of 519nm, (yellow/green colour).

FACS analyses 10,000 cells per sample, by passing them individually through a flow tube in single file. As the cells flow through the tube, they pass through a laser beam that provides the E required for FITC activation as well as enabling a structural and morphological image of each cell to be calculated. The laser beam is split into 3 detectable types, Forward Scattered (FSC), Sideway Scattered (SSC) and

Fluorescent light (FL), where FL and SSC are detected at  $90^\circ$  and FSC at  $20^\circ$  from the initial direction of the laser beam. The FSC and SSC combined produce structural and morphological information that distinguishes between live or dead cell, cell or bead size or type, which when combined with FL, produces a detailed location and abundance of the structures being investigated within the cells.

FACS illustration:

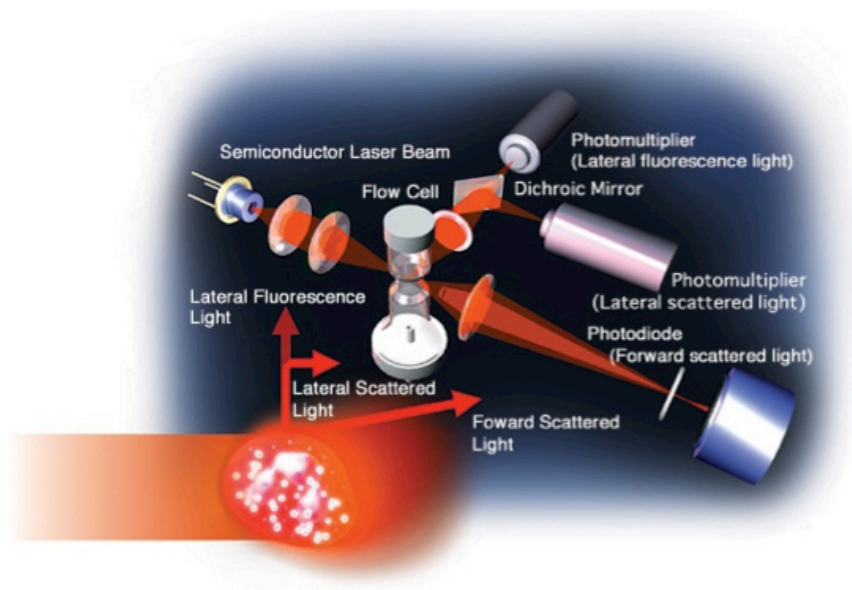


Figure 2.8.1: FACS optics system illustrating the arrangement of filters and detectors at the different angles, ( $90^\circ$  for SSC and at  $20^\circ$  for FSC) ([www.nci.cu.edu.eg/images/flow.jpg](http://www.nci.cu.edu.eg/images/flow.jpg)).

A process called hydrodynamic focusing achieves the single file arrangement of cells through the flow tube. Sample cells from an inner core are propelled through the flow tube at high velocity sheath fluid from a surrounding outer core.

### FACS hydrodynamic fluidics system:

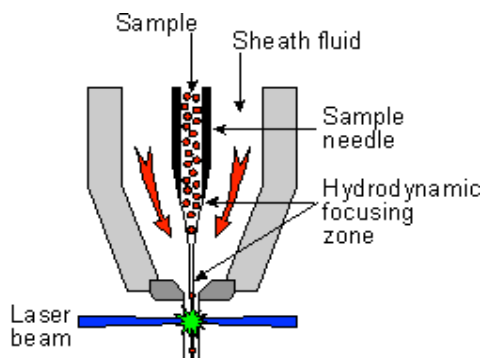


Figure 2.8.2: Hydrodynamic fluidics system of FACS, enables focusing of a sample by injecting sample (inner core) suspension into the higher velocity sheath fluid (outer core), causing a single file arrangement of cells as the suspension passes through the FACS (<http://olomouc.ueb.cas.cz/book/export/html/18>).

The information in the form of photons of different wavelengths is detected by the PMT, which converts the photons wavelength ( $1/E$ ) into electrical charge and therefore voltage (V) that is proportional to the E emitted from the sample. BD CellQuest software was used to process the recorded data by selecting specific detection and analysis parameters.

As the PRRs in being investigated are distributed throughout the cell, with some on the cell surface and others located internally in the cells, pores in the cells membrane must be made to enable antibodies to enter the cell and bind to their target PRRs. To form the pores in the cell membranes, saponin used in a buffer solution if x1 PBS/0.02% NaN<sub>3</sub> saponin/0.02%, where the NaN<sub>3</sub> (sodium azide) kills any organisms present or introduced to samples.



### ***2.9.1: Protein and cytokine measurement:***

To determine and measure the presence of specific protein in a sample, Western Blotting was performed with the use of Enhanced Chemoluminescence (ECL). Western Blotting uses antibodies conjugated to a chemoluminescent molecule, in this case horseradish peroxidase (HRP), which emits light when it interacts with the ECL reagent Amersham. The light emission, like in fluorescent tags, occurs when energy from the reaction excites electrons in the HRP, from their ground state to an excited state, and upon returning to their previous ground state, release energy in the wavelength of light photons. Using X-ray film, the light emitted can be detected and recorded. By tagging all the protein being investigated, a quantitative measurement of protein abundance can be obtained. Western Blotting requires several initial procedures, namely: either Discontinuous SDS-PAGE (sodium dodecyl sulphate gel electrophoresis), Western Blotting, blocking the nitrocellulose membrane (NCM), washing, incubation in primary antibody, washing, incubation in secondary antibody, washing and finally imaging and development of X-ray film, using ECL.

### Western Blot illustration:

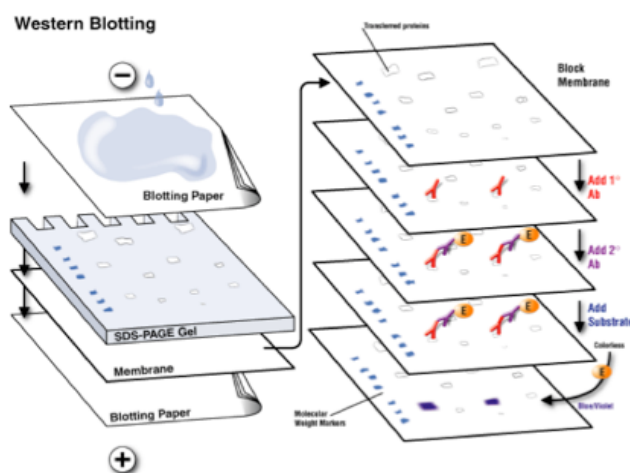


Figure 2.9.1 Western Blotting – the transfer of proteins from SDS-PAGE (polyacrylamide) gel to a NCM. Presence and quantity of protein on NCM detected using primary and secondary antibodies, with a conjugated chemiluminescent molecule emitting photons after activation with substrate (HRP) (<http://www.komabiotech.co.kr/www/techniques/immunodection/wbProtocol.html>).

#### **2.9.2.1: SDS-PAGE:**

Discontinuous SDS-PAGE is a process by which proteins are separated by electrophoresis according to their molecular weight. SDS (Sodium Dodecyl Sulphate) is an anionic detergent that reduces proteins to their primary structures, essentially a single strand of amino acids. It does this by both interfering with the proteins structural hydrogen bonds, non-disulphide covalent bonds (bridges) and Van der Waals interactions, which form secondary, tertiary and quaternary structures. SDS also binds to the proteins amino acids, creating an overall negative charge that is proportional to the proteins molecular weight/number of amino acids. Using an electric current passed through a porous gel, the proteins separate, travelling at different speeds toward the positive terminal. The rate at which the proteins move is determined by their size, where smaller proteins will move faster

through the gels pores, experiencing less resistance than larger proteins. When run in a linear fashion, the proteins within a sample will form bands (lines) down the gel.

Varying the concentration of Acrylamide/Bis in the gels mixture, (where increased Acrylamide/Bis concentrations produce a matrix with a smaller pore size), can control the size of the pores in the gel matrix. The size of the pores is an important factor when trying to separate proteins, as proteins with a smaller molecular weight may “run off” the gel if the matrix is too large, conversely, if larger proteins are being investigated a larger matrix allows sufficient movement to be achieved, enabling differentiation between two larger proteins of a similar molecular weight.

The proteins bands in the gel are then transferred to a nitrocellulose membrane. Nitrocellulose has a high affinity for the negatively charged polypeptide chains, fixing the proteins securely to the membrane.

To determine and measure the amount of protein in a sample, monoclonal antibodies were used in a similar way to those that were used in Indirect Immunofluorescence. Binding of a primary antibody to a specific amino acids target sequence, and the additional binding of a secondary antibody (to the primary) containing a conjugated chemoluminescent molecule, enabled the presence of target protein to be detected and measured. An example was the use of anti-phospho-I $\kappa$ B (primary antibody) produced from a mouse (used to detect NF- $\kappa$ B), would bind to any I $\kappa$ B protein present in the sample. A secondary IgG is used that targets the mouse *Fc* region of the primary IgG, for example, goat anti-mouse IgG (produced by a goat host), which binds to the primary IgG. The secondary IgG is conjugated to an HRP chemoluminescent molecule, which emits light that is detected by X-ray film, producing darkening of the film. The light expose is proportional to the abundance of the target protein. To help identify the proteins present in the samples, a molecular

weight (MW) marker is used in each gel. The marker contains proteins of known MW, which produce a ladder effect on the ECL film, so the distance travelled by the sample proteins can be compared to the known MW markers, otherwise the distance travelled would be an arbitrary value. Biotinylated SDS-PAGE Standards Broad Range (BioRad) was the MW marker used, with Streptavidin-HRP conjugate as its fluorescent activating catalyst.

#### SDS-PAGE apparatus and illustration:

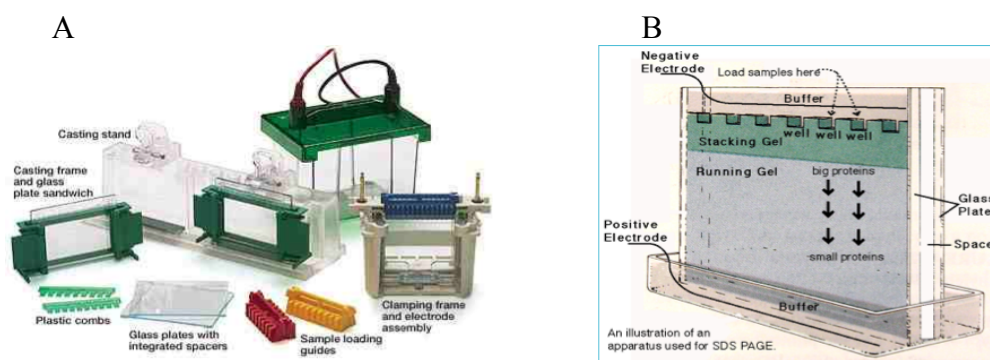


Figure 2.9.1.1.1: (A) Apparatus used in casting SDS-PAGE gel and electrophoresis ([http://www.oswego.edu/academics/colleges\\_and\\_departments/departments/interdisciplinary/maspec.html](http://www.oswego.edu/academics/colleges_and_departments/departments/interdisciplinary/maspec.html)). (B) Electrophoresis of amino acid chains through polyacrylamide gel during SDS-PAGE, where the distance travelled is proportional to the size of the proteins amino acid sequence (protein size) ([http://en.wikipedia.org/wiki/Polyacrylamide\\_gel\\_electrophoresis](http://en.wikipedia.org/wiki/Polyacrylamide_gel_electrophoresis))

#### **2.9.2.2: SDS-PAGE protocol:**

Resolving gel was then poured into the cassettes to a designated level, on top of which a few drops of propan-2-ol were added to ensure a level surface of the gel. The gel was then left to set for approx. 45 minutes. Propan-2-ol was removed from cassettes and washed away with  $\text{dH}_2\text{O}$ , which was also entirely removed. Cassettes were filled with stacking gel and well combs were placed in the top of the cassettes, whilst ensuring no bubbles were present. Gel was then left to set.

Samples were defrosted and 40µl of each sample was pipetted into an assigned and labelled eppendorf. 1µl/20µl MW marker/reducing buffer (per gel) was pipetted into a separate labelled eppendorf. Eppendorf caps were placed on each eppendorf to ensure lids did not pop open, and placed in a boiling water bath for 5 minutes. Running buffer was poured into the cassette chamber until level is above that of the wells in the gel. Using a loading column, each sample and MW marker was pipetted into its respective well trying to avoid any overflow of the sample outside its well. The gels were run at 200V for 45 minutes or until dye neared the bottom of the gel.

#### Preparation of protein sample for SDS-PAGE:

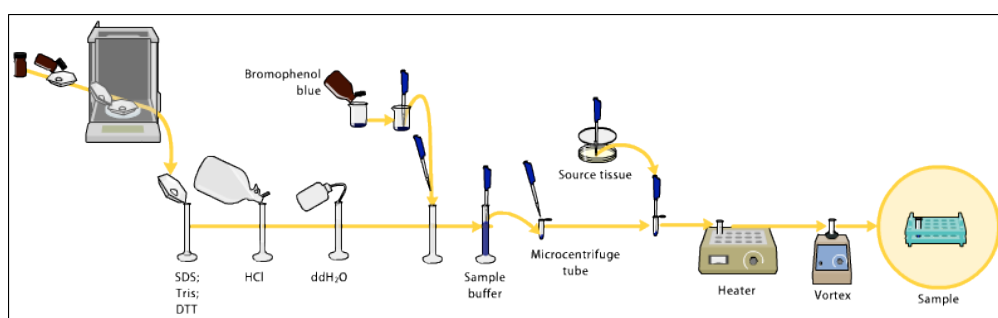


Figure 2.9.2.2.1: Sample preparation for SDS-PAGE using x2 SDS-PAGE reducing buffer ([https://ww2.chemistry.gatech.edu/~lw26/bCourse\\_Information/4581/techniques/gel\\_elect/page\\_protein.html](https://ww2.chemistry.gatech.edu/~lw26/bCourse_Information/4581/techniques/gel_elect/page_protein.html))

#### **2.9.3: Western Blot:**

BioRad Transblot plastic support placed in a tray filled with transfer buffer. Gel was carefully removed from the cassette, avoiding tearing by lubricating with transfer buffer. Gel was incubated for 10 minutes in transfer buffer tray. NCM was cut to a size just larger than that of the gel, as well as 4 pieces of filter paper and porous pad. All were soaked in transfer buffer, and then layered in order onto the black side of the support. First 2 pieces of porous pad, then 2 pieces or filter paper, then the gel, then NCM, then 2 pieces of filter paper, 2 porous pads, and then the support wash

closed. Supports were placed in Transblot apparatus, with black sides back to back. Ice cooling unit was inserted and the tank was filled with transfer buffer. 220mA were run for 1 hour.

### Western Blot apparatus:

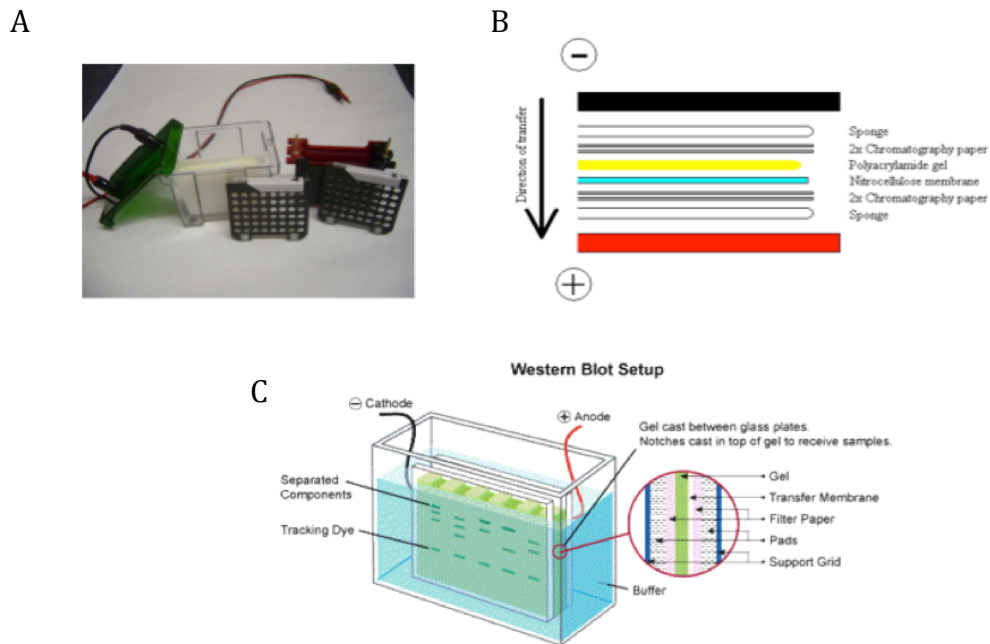


Figure 2.9.3.1: BioRad Transblot apparatus (A) contains 2 NCM supports that are submerged in transfer buffer whilst current is passed through the system to transfer protein from the polyacrylamide gel to the NCM (B). Western Blot overview (C) with transfer of protein from polyacrylamide gel onto NCM in the direction of cathode to anode.  
([http://www.leinco.com/general\\_wb](http://www.leinco.com/general_wb))

Supports were disassembled and the NCM was incubated in 4% blocking agent for hour on a rocking table. NCM was then rinsed twice with PBS-TWEEN (PBS-T) and washed in PBS-T for 30 minutes on a rocking table, and repeated with fresh PBS-T. NCM was then incubated overnight at 4°C in 8ml (per membrane) of primary (1°) antibody solution, ensuring that the whole membrane was submerged in solution. The membrane was placed on the rocking table for 20 minutes, then removed and rinsed twice with PBS-T and 1° antibody solution was collected and

frozen for future use. NCM was washed in PBS-T for 30 minutes on rocking table, repeated 3 times with fresh PBS-T. NCM was incubated in 8ml (per membrane) secondary (2°) antibody and streptavidin-HRP solution for 45-60 minutes on the rocking table, rinsed twice with PBS-T, and washed in PBS-T for 30 minutes on rocking table, and repeated 5 times. ECL was performed in the dark room, where NCM was incubated for 1 min in 1:1 ECL reagent A:B. NCM was wrapped in saran wrap, removing any air bubbles or creases in the saran wrap. In the dark, ECL film was placed over the NCM in an exposure cassette for a period of time (approx. 30 seconds), film was then removed and developed in developing reagent, washed in water and fixed in fixing reagent. If the film was unsatisfactory, the procedure was repeated, altering the exposure time to obtain a desired film.

#### ECL illustration:

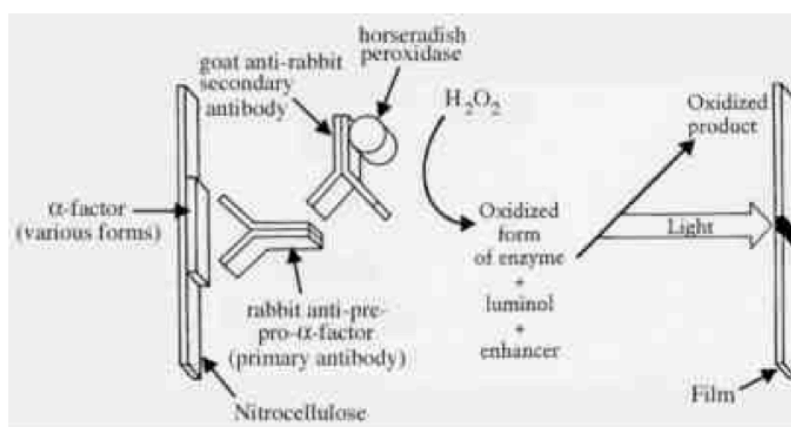


Figure 2.9.3.2: Schematic of ECL process in the Western blotting, shows the secondary antibody containing the conjugated chemoluminescent molecule emitting light upon activation with the enzyme horseradish peroxidase (HRP).  
([http://openwetware.org/wiki/BISC220/S13:\\_Mod\\_2\\_Lab\\_7](http://openwetware.org/wiki/BISC220/S13:_Mod_2_Lab_7)).

### **2.10: Cytokine Bead Array (CBA):**

BD™ CBA was a method used to assay multiple analytes in a single assay sample. Beads coated in Immunofluorescent capture antibodies bind to target cytokines (antigens) in sample solutions. 6 different beads types of equal concentration in bead mixture solution, each coated in specific capture antibodies were used bind 6 different cytokines in sample suspensions: IL-8, IL-1 $\beta$ , IL-6, IL-10, TNF and IL-12p70. After binding of the cytokine to its capture protein, the addition of Phycoerythrin (PE)-conjugated detection antibody (PE-CDA) was added to the sample/bead mixture and incubated to produce a sandwich complex of cytokine specific bead – target cytokine – PE-CDA. After 3 hours incubation period, mixtures were centrifuged, and the pellet was washed in wash buffer (BD Biosciences). Flow cytometry in combination with BD CBA Analysis Software, produced graphical and tabular formatted data of the sample suspensions. Cytokine concentration in the sample produced as pg/ml. BD CBA was a favourable method of cytokine assaying over ELISA assaying as the number of cytokines being measured in each sample was greater, requiring less sample solution volume and saves time, without losing accuracy in data collected.



### CBA schematic representation of immunoassay sandwich:

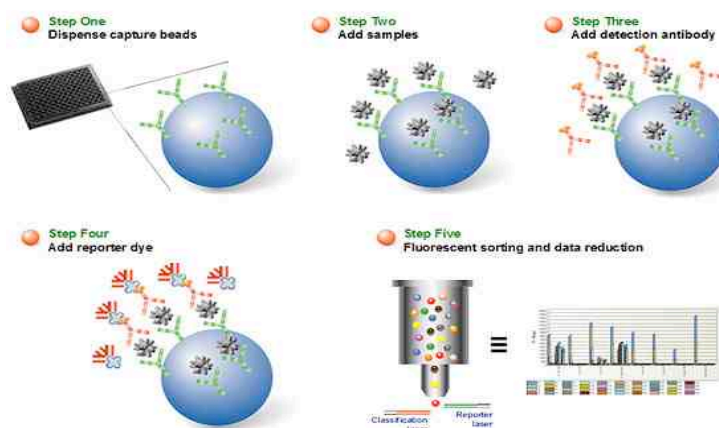


Figure 2.10.1. Illustration of cytokine specific bead – target cytokine – PE-CDA sandwich and assay workflow through FACS (<http://www.bio-rad.com/en-uk/applications-technologies/bio-plex-multiplex-immunoassays>)

#### **2.10.1: BD CBA protocol:**

BD™ CBA was a method used to assay multiple analytes in a single assay sample. Beads coated in Immunofluorescent capture antibodies bind to target cytokines (antigens) in sample solutions. 6 different beads types of equal concentration in bead mixture solution, each coated in specific capture antibodies were used bind 6 different cytokines in sample suspensions: IL-8, IL-1 $\beta$ , IL-6, IL-10, TNF and IL-12p70. After binding of the cytokine to its capture protein, the addition of Phycoerythrin (PE)-conjugated detection antibody (PE-CDA) was added to the sample/bead mixture and incubated to produce a sandwich complex of cytokine specific bead – target cytokine – PE-CDA. After 3 hours incubation period, mixtures were centrifuged, and the pellet was washed in wash buffer (BD Biosciences). Flow cytometry in combination with BD CBA Analysis Software, produced graphical and tabular formatted data of the sample suspensions. Cytokine concentration in the

sample produced as pg/ml. BD CBA was a favourable method of cytokine assaying over ELISA assaying as the number of cytokines being measured in each sample was greater, requiring less sample solution volume and saves time, without losing accuracy in data collected.

### **2.11: Transfection and gene silencing:**

Transfection is a technique used to insert desired foreign genetic material into a target cell that does not use a viral vector. Transfection is a hugely useful method of examining and enabling insight into the internal workings of a cell. It has a wide range of applications by identifying the role and function of specific genes. Lipofectamine 2000 (Invitrogen, Paisley, UK) was used to transfect siRNA into target cells via the process of lipofection. siRNA is encapsulated by lipid vesicles (liposomes) that merge with the target cell membrane, allowing internalisation of siRNA into target cell cytoplasm, where it can be transcribed.

By targeting and silencing/reducing the expression of specific genes, the function of that gene can be identified and further understood. In this investigation by silencing specific PRRs, we hoped to further our understanding of the role of each chosen PRR in the initial innate immune response after coming into contact with certain *Ureaplasma* serovars.

Small inhibitory RNA (siRNA) binds specifically to its complementary DNA target during transcription, in this case PRR genes. By binding to the target gene, transcription of that gene is inhibited, causing down regulation and lowered expression of the target protein.

By comparing WT cell reaction to stimulation with *Ureaplasma* with genetic knock down (KD) cells, the function and downstream signalling response can be examined.

### ***2.11.1: psiRNA:***

The plasmids belong to a family of expression vectors that can transcribe foreign genetic material in target human cells. Human 7SK RNA polymerase III promoter genetic sequence is encoded in the plasmid, which enables transcription to the plasmid by the target cell. 7SK promoter generates large amounts of shRNA, which increases plasmid DNA uptake into target cells genome. The plasmid contains a specific antibiotic resistance gene that enables specific isolation of the desired bacterial hosts (the bacteria that have incorporated the plasmid), at the same time preventing contamination of foreign bacteria. The plasmids encodes the essential specific RNA genetic sequence that targets and binds the target gene mRNA in the transfected cell, whilst the cell is undergoing mitosis. Once the siRNA binds to its complimentary target mRNA sequence, the target gene transcription is inhibited, causing down regulation of the encoded product of the gene.

### Gene silencing via transfection:

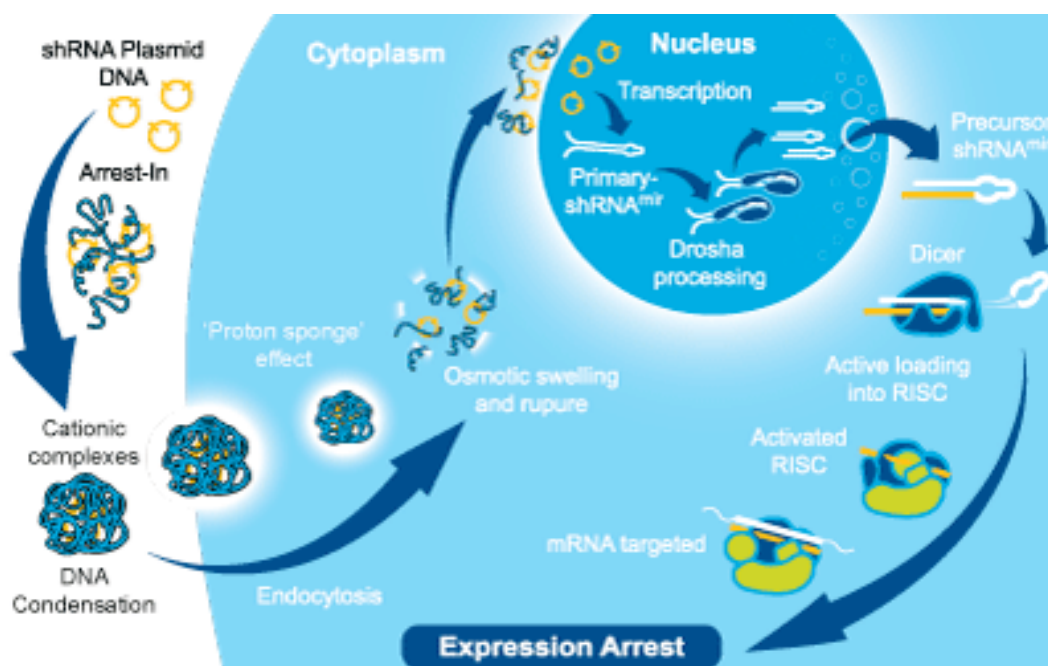


Figure 2.10.1: siRNA incorporation into bacterial plasmid, which is then transfected into the target cell, where the siRNA is transcribed in the nucleus, specifically binding to, and silencing the target gene ([http://www.bioxys.com/i\\_openbio/arrest-in\\_transfection\\_reagent.htm](http://www.bioxys.com/i_openbio/arrest-in_transfection_reagent.htm))

To increase volume of siRNA plasmids to a quantity that is adequate for experiments in this investigation, the siRNA plasmids were grown in competent bacteria; in this case *E.coli* was used.

Ampicillin resistant *E.coli* cultures containing siRNA plasmids were cultured on Agar plates containing ampicillin to prevent contamination from unwanted bacteria. 4 sterile universal tubes were prepared in a sterile hood, into which 20ml Luria broth was pipetted into each tube. 20 $\mu$ l (0.1g/ml) Ampicillin was pipetted into each tube. The *E.coli* containing the specific siRNA plasmid was introduced to the tubes using sterile toothpicks, which were left in the tubes and then incubated in a shaking incubator at 37°C for overnight, until the solution was cloudy with bacterial culture. The toothpicks were removed from the tubes under sterile conditions and the universal tubes were centrifuged at 2500rpm for 20 minutes to form a pellet of *E.coli*

at the base of each tube. The supernatant from each tube was removed and the pellet was resuspended in 400µl STET (sucrose, triton, EDTA, Tris-HCL and dH<sub>2</sub>O, at a pH 8) and transferred to individual eppendorfs, which were then vortexed to ensure complete suspension of the pellet. 10µl (50mg/ml) lysozyme was pipetted into each tube and boiled in a water bath for 60 seconds then immediately placed on ice for 5 minutes, after which the tubes were centrifuged at 13,000rpm for 30 minutes. The pellet formed was removed using a sterile toothpick and disposed of appropriately, and to the remaining solution 5µl (20µg/ml) RNase A was added to each eppendorf and incubated in a heat block for 30 mins at 42°C. An equal volume (400µl) phenol/chloroform isoamyl alcohol to STET was added in a fume cupboard, and then vortexed. Phenol is a hazardous chemical, so extra care was taken whilst handling. After centrifuging for 15 minutes at 13,000rpm, the eppendorfs were returned to the fume cupboard and the upper fractions of the two-layered mixture were carefully pipetted into a new sterile eppendorfs, making sure not to transfer any of the lower fraction, which is discarded appropriately. To each eppendorf 400µl chloroform/isoamyl alcohol was added, and again centrifuged for 15 minutes at 13,000rpm. The upper fractions were again transferred to a new sterile eppendorfs in the fume cupboard and the lower fraction was discarded appropriately. 1/20 volume 2M NaAc (20ml) and 2.5 volume (1ml) ethanol were pipetted into the eppendorfs and then stored at -80°C over night. The eppendorfs were then centrifuged for 20 minutes at 13,000rpm and the upper fraction was aspirated off, and then repeated (but only centrifuged for 1 min) to remove as much supernatant as possible. 80µl of dH<sub>2</sub>O was pipetted into each of the eppendorfs and the DNA pellet was re-suspended and stored at -20°C.

### 2.11.2: Agarose gel electrophoresis:

1g agarose was added to 100ml (x1) ELFO buffer solution in a conical flask and microwaved (agitated every 20-30 seconds) until the agarose had completely dissolved. The solution was allowed to cool slightly; 10 $\mu$ l (10 $\mu$ l/100ml) Gelred was added. The mixture was poured into a container containing well combs and allowed to set. 500ml ELFO buffer solution was added to the electrophoresis apparatus basin, into which the agarose gel was carefully placed. For each siRNA sample being tested, 7 $\mu$ l ELFO buffer was added to an eppendorf with 15 $\mu$ l of siRNA suspension. Vortex each eppendorf and pipette the content into assigned well in the agarose gel. In addition a marker ladder should be prepared (5 $\mu$ l marker solution and 10 $\mu$ l loading dye and pipetted into assigned well. The gel was run at 100V (samples move from black pole to red pole) until the dye reaches the designated distance on the gel. Transfer gel to UV transilluminator to image the results.

### Agarose gel electrophoresis:

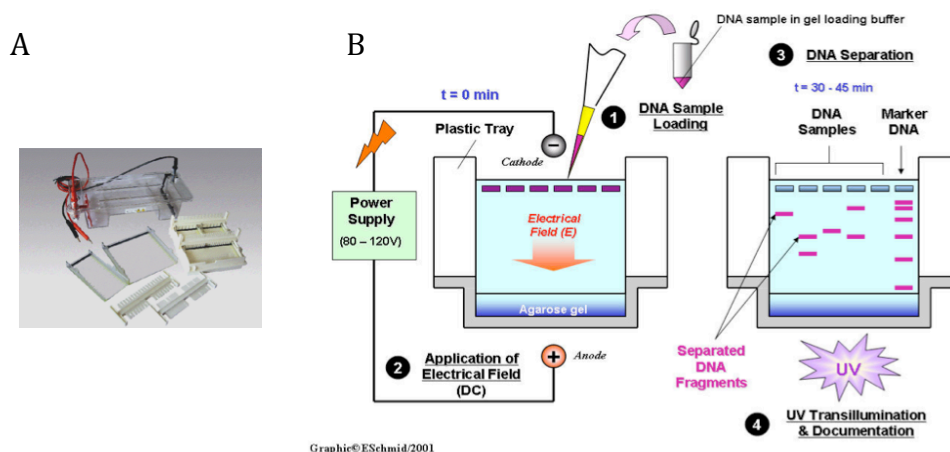


Figure 2.11.2: BioRad agarose gel electrophoresis apparatus (A) (<http://www.assay-protocol.com/molecular-biology/electrophoresis/agarose-gel-electrophoresis>). (B) Agarose gel electrophoresis, illustrating loading of DNA samples into sample wells, and direction of movement of DNA through the agarose gel, the distance travelled by the DNA is proportional to the size of the DNA fragments. UV Transillumination enables imaging and measurement of the DNA bands in the agarose gel (<http://classroom.sdmesa.edu/eschmid/Lab12%20-%20Biol210.htm>)

### ***2.11.3: Lipofectamine transfection:***

Done in duplicate for each PRR being investigated and carried out in sterile TC lab.

A 25cm<sup>2</sup> (Nunc) flask of BEAS-2B cells or human amniotic epithelial cells at a confluence of 70%, with even cellular distribution were selected and used for transfection.

10µl siRNA containing suspension was pipetted into an eppendorf tube in addition to 40µl Optimem medium. At the same time into separate eppendorf tubes 5µl lipofectamine and 45µl Optimem medium were added and both were incubated for 5 minutes. The content of both eppendorfs were combined into 1 eppendorf tube and agitated to ensure thorough mixing and incubated for a further 20 minutes. During this time period the medium from the cells was aspirated, washed with 1ml of Optimem, which was then aspirated off. Another 1ml Optimem is pipetted into the flask making sure the medium was spread evenly over the base of the flask. After the 20 minutes incubation period, the entire (100µl) siRNA/lipofectamine mixture is pipetted into the flask, agitating to ensure even distribution of the mixture in the flask and then incubated at 37°C 5% CO<sub>2</sub> overnight (maximum 24 hrs). The Optimem was aspirated from the flask, washed with 1ml DMEM and aspirated. 5ml selection medium (DMEM and ampicillin (1µl/ml)) was added to the flask and incubated (same conditions as above) overnight. The flask was then propagated as previously described, with the exception of using selection medium instead of standard DMEM growth medium.

### ***2.11.4: RNA interference:***

RNA interference was used in order to silence the TLR1, TLR2, TLR4, TLR6, TLR7 and TLR9, NOD1, NOD2, NLRP1, NLRP3, NLRP7, NLRP12 and NLRC5 genes.

psiRNA clones were obtained from InvivoGen (San Diego, USA). Human primary amniotic epithelial cells, BEAS or MM6 cells ( $1 \times 10^5$ ) were seeded in six well plates and transfected with 0.5  $\mu$ g of psiRNA using Lipofectamine 2000 (Invitrogen, Paisley, UK). After 48h the level of silencing was determined and cells were used for activation assays.

To determine if RNA interference (genetic KD) had been achieved, the transfected cell lines (not antigen stimulated) expression level of KD PRR were compared with PRR expression level of unstimulated WT cells using western blotting and flow cytometry to detect GFP in silenced (KD) cells.

If PRR KD was achieved, the cell lines were stimulated with *Ureaplasma* in the methods as described above.

## **2.12: Confocal Microscopy:**

Confocal Microscopy is a powerful method of visualising interactions and locations of target molecules in a cell. It has many advantages over Scanning Electron Microscopy (SEM) and other high-resolution microscopy methods, namely: cells can be alive during examination (*in vivo* studying); multiple (immunofluorescent) fluorophores target and bind to multiple corresponding specific molecular sequences; measurements can be recorded at low fluorescent intensities and third dimensional images can be formed. By imaging cells *in vivo*, a more accurate investigation into cellular processes is possible. For example, cell trafficking, co-localisation of molecules; protein productions/expression levels can be monitored over a time period within the same cell/cellular area.

By exposing a whole sample to light (from a laser), information in the form of light emission at specific wavelengths was detected throughout the sample. However in



this state the information in the emitted light is useless. By focusing and isolating specific paths of light and excluding out of focus or interfering light beams, a high resolution, accurate image can be detected and recorded. This light isolation is achieved using an adjustable pinhole aperture device and a pair of motorised mirrors. The mirrors allowed for light beams to scan through sample, imaging the same area through different angles, which can be combined to form a 3-D image. The emitted light is detected by a photomultiplier tube (PMT), which can enhance weak light signals, making low abundant targets detectable. The emitted light is filtered by wavelength to image individual target structures (fluorophores).

In this investigation human amniotic epithelial cells were stimulated with either MBA or *Ureaplasma urealyticum* for a number of time periods; then different PRRs and signalling molecules were targeted for imaging using indirect immunofluorescent technique, as explained above.

#### ***2.12.1: Cell labelling for Confocal microscopy:***

Human amniotic epithelial cells on microchamber culture slides (Lab-tek, Gibco), were stimulated with *Ureaplasma* or MBA (1 µg/ml) for different time points, and were subsequently rinsed twice in PBS/0.02% BSA, prior to fixation with 4% formaldehyde for 15 min. The cells were fixed in order to prevent potential re-organisation of the proteins during the course of the experiment. Cells were permeabilised using PBS/0.02% BSA/0.02% Saponin and labelled with antibodies against the PRRs of interest followed by incubation with the appropriate fluorescently labelled secondary antibody. Cells were imaged on a Carl Zeiss, Inc. LSM510 META confocal microscope (with an Axiovert 200 fluorescent microscope) using a 1.4 NA 63x Zeiss objective.

### ***2.12.2: Confocal imaging of NLRP7-ASC and mitochondrial interaction:***

For NLRP7-mitochondrial association NLRP7 was stained using rabbit anti-NLRP7 Fab conjugated to Alexa 488, mitochondria were stained with mitotracker and ASC was stained using an anti-goat-ACS Fab conjugated to Alexa 633.

### ***2.12.3: Confocal pH sensitivity:***

Confocal microscopy was used during pH-sensitivity experiments using pH-sensitive, fluorescent, cytoplasmic dye 2,7-bis(carboxyethyl)-5(6)-carboxyfluorescein (BCECF) for human amniotic epithelial cell (HAEC) culture staining. HAEC samples were stimulated in *Ureaplasma* SV2 in culture incubated both with and without the presence of acetohydroxamic acid, a urease inhibitor (250uM). Cell samples were loaded with 5umol/L BCECF-AM at 37°C for 1-hour, then fixed and the BCECF was excited with 488nm laser line.

Quantification of degree of co-localisation was established using Costes' approach; Pearson's correlation coefficient and P-values were calculated using MBF ImageJ with JACoP (Just Another Colocaliation Plugin).

### **2.13: Förster Resonance Energy Transfer (FRET):**

FRET is a method used to measure and quantify cellular molecular dynamic interactions, such as protein-protein interaction in cells. Donor fluorophore conjugated antibody emits energy at a specific wavelength that excites an (corresponding) acceptor fluorophore conjugated antibody, with specific binding to the second target protein. The acceptor emits energy of known wavelength, which is specifically detected and measured using confocal microscopy.

## FRET:

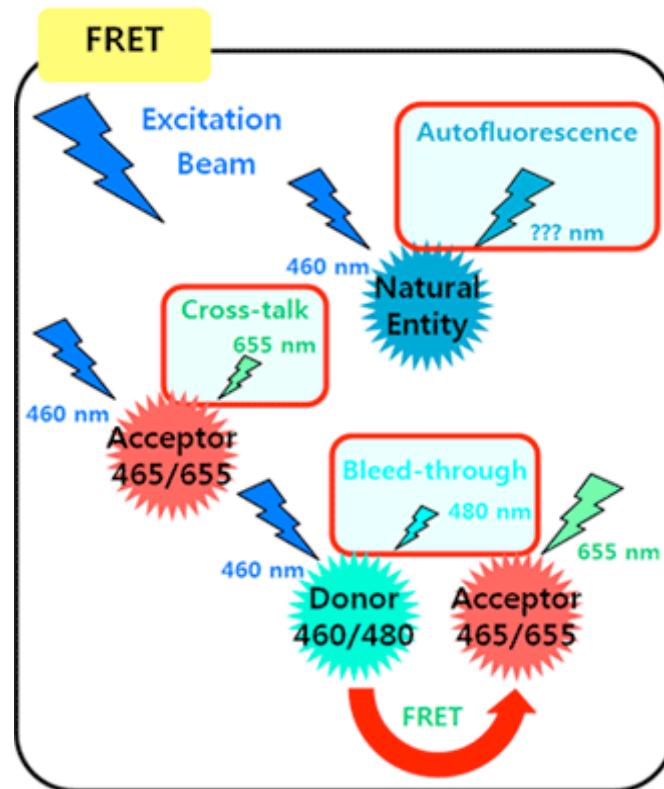


Figure 2.13.1: Energy (at a specific wavelength) is absorbed by the donor fluorophore, causing emission of light at a wavelength specific to the donor fluorophore. Using a second (acceptor) fluorophore that emits photons upon activation from photon energy emitted from donor fluorophore, protein-protein interaction can be observed and measured. Targeting 2 proteins whose interactions want to be investigated with specific corresponding acceptor and donor fluorophore conjugated antibodies; measurements of interaction can be measured. If there is no protein-protein interaction, only donor fluorophore emitted photons are detected. If there is interaction between the 2 proteins, photons emitted from acceptor fluorophores will be detected.

FRET enables protein-protein interaction to be measured through donor-acceptor fluorophore emission variations. Donor fluorophore photon emission only indicates no protein-protein interaction. Detection of photons emitted at a wavelength specific to acceptor fluorophores indicates protein-protein interaction, at an interaction activity that is inversely proportional to the power of 6. Distances of  $<10\text{nm}$  between the 2 conjugated antibodies are required, and enables protein-protein interaction

measurements on scale that is unachievable by other methods. In this investigation the donor fluorophore Cy3 and the acceptor fluorophore Cy5 conjugated antibodies with binding specificity to different immune response molecules and receptors, revealing PRR-PAMP activation, PRR-lipid raft molecule and PRR-PRR interaction, allowing imaging of initial immune activation to specific pathogens and the immune response that proceed it.

#### ***2.13.1: Cell labelling for FRET:***

Human amniotic epithelial cells were labelled with 100 ml of a mixture of donor-conjugated antibody Cy3 and acceptor conjugated antibody Cy5. The cells were either; not stimulated, or stimulated with *Ureaplasma parvum*, *urealyticum* or MBA for 1h, and were rinsed twice in PBS/0.02% BSA, prior to fixation with 4% formaldehyde for 15 min. The cells were fixed in order to prevent potential re-organisation of the proteins during the course of the experiment

Cells were imaged on a Carl Zeiss, Inc. LSM510 META confocal microscope (with an Axiovert 200 fluorescent microscope) using a 1.4 NA 63x Zeiss objective. The images were analysed using LSM 2.5 image analysis software (Carl Zeiss, Inc.). Cy3 and Cy5 were detected using the appropriate filter sets. Using typical exposure times for image acquisition (less than 5 s), no fluorescence was observed from a Cy3-labelled specimen using the Cy5 filters, nor was Cy5 fluorescence detected using the Cy3 filter sets.

### Energy transfer during FRET:

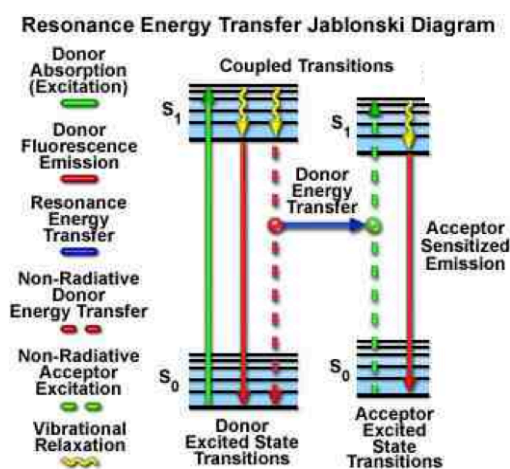


Figure 2.13.1: Energy transfer, electron excitation and photon emission with in fluorophores during FRET (<http://micro.magnet.fsu.edu/primer/techniques/fluorescence/fret/fretintro.html>)

### **2.14: Profos EndoTrap® endotoxin extraction:**

*Ureaplasma spp.* recombinant MBA was obtained from Genway Biotech Inc. (San Diego, USA). Contamination of samples by bacterial endotoxins is not an uncommon event, even when working in environments. Bacterial endotoxin initiates a very strong innate immune response when it is recognised by the PRRs and even the smallest of quantities would completely compromise the validity of any data obtained from any experiment where the toxin was present. For this reason Profos EndoTrap® equipment is used in a process that ensures any endotoxin present in any sample will be selectively removed after passing through EndoTraps (according to the protocols in appendix).

Profos EndoTrap® blue 10 assay is an extremely effective way of purifying and removing bacterial endotoxin from aqueous sample solutions. EndoTraps are pre-packed columns that contain agarose beads that are covalently bonded to endotoxin blue ligands. These ligands have extremely high binding affinity and specificity to

endotoxin and a very low non-specific binding affinity to other protein structures. By passing aqueous sample solutions through these EndoTraps, in an ultra-filtration method using EndoTraps and centrifugation, endotoxin free solutions (identified by assaying) are produced and can be used for investigations of specific proteins in the confidence that the samples will be free of endotoxin.

#### Endotoxin Profos EndoTrap®:

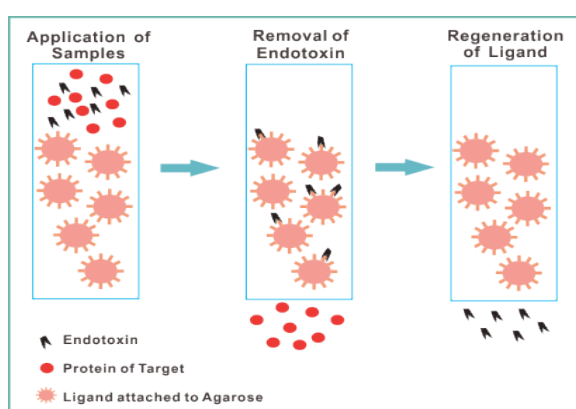


Figure 2.14.1: Removal of bacterial endotoxin for sample solutions by high affinity ligands covalently bound to agarose beads in gel matrix ([http://www.youzre.com/\\_d275835832.htm](http://www.youzre.com/_d275835832.htm))

#### EndoTrap kit:



Figure 2.14.2: Profos EndoTrap® blue 10 (Hyglos) kit. Bacterial endotoxin is removed from aqueous solution by ligand specific affinity chromatography (<http://www.hyglos.de/en/products-services/products/endotoxin-removal/endotrapp-blue.html>)

### **2.15: Optimisation of drug concentration for inflammasome inhibitors:**

HAECs were seeded onto 6-well plates and incubated overnight. The cells were then stimulated with *Ureaplasma* serovars in culturing medium containing appropriate concentrations of each drug for a time period of 1-hour (Cathepsin B inhibitor (CA-074) 100 $\mu$ M, BAPTA 10 $\mu$ M, Benzamil 50 $\mu$ M and DPI 10 $\mu$ M). All inhibitors were dialysed against 20mM Phosphate buffer prior to their use *in vitro* experiments. Cell-free supernatant was collected after 12-hours after stimulation and then analysed for IL-1 $\beta$  by CBA bead array (Becton Dickinson). The viability of cells was determined by using 0.2% trypan blue and examining cells under a microscope.

### **2.16: Determination of ammonia concentration:**

The concentration of ammonia in the culture supernatants was determined by the indophenol reaction, according to the modified methods originally reported by Okuda et al, using an Ammonia-Test-Wako kit (Wako Pure Chemical Industries)<sup>172</sup>. Briefly the supernatant was added to phenol and sodium nitroprusside and subsequently was mixed with a solution consisting of NaOH, Na<sub>2</sub>HPO<sub>4</sub> 12H<sub>2</sub>O and antiformin. The mixture was incubated for 20 min at 37C and the absorbance was measured on a spectrophotometer at 630 nm.

### **2.17: Bacteria viability detection using flow cytometry:**

In order to determine bacterial viability in the presence and absence of urease inhibitor flow cytometry was employed. Bacterial suspensions in the presence of absence of urease inhibitor were labelled with propidium iodide 48  $\mu$ M (PI) and 420nM triazole orange (TO) for 5 min at room temperature. PI only stains bacteria

with compromised membranes (dead bacteria), whereas TO is a permeant dye that enters live and dead cells. A combination of these dyes provides a rapid and reliable method in order to determine bacterial viability (Becton Dickinson Application Note – Microbial flow cytometry). An unstained bacterial suspension was used as a control. Samples were analysed using a FACSCalibur (Becton Dickinson, Oxford, UK). FL1 vs FL3 dot plots were used to discriminate between live and dead bacteria and to determine their percentage.

### **2.18: Determination of pH**

The pH of the medium was measured by using a pH meter. In order to determine the effect of alkalization in inflammasome activation, amniotic epithelial cells were treated with 4 mM of  $\text{NH}_3$ ,  $\text{NH}_4^+$  or NaOH solution for 6 hours. The supernatant was collected and the level of cytokines was determined using the cytometric bead array kit.

### **2.19: Statistical analysis:**

The results shown in all graphs are mean averages of data, showing the standard deviation and where applicable, showing paired t-tests to demonstrate significance.

The statistical significance is indicated by, \* =  $p < 0.05$ , \*\* =  $p < 0.01$  and \*\*\* =  $p < 0.005$ .



## **Chapter 3:**

# ***Ureaplasma*-induced innate immune responses in human monocytes**

### 3.1: Introduction:

*Ureaplasma* has been shown in many studies to constitute the commensal bacterial flora of the urogenital tract of a significant proportion of the human population. Although the estimated prevalence of *Ureaplasma* colonization in the population varies greatly, there is significant enough information in the literature to associate its presence with the activation of the human immune response. The majority of studies investigating the association with *Ureaplasma* colonization with immune response activation come from a top down, retrospective approach, where the presence of *Ureaplasma* is investigated after the presentation of adverse immune responses. The other major method of investigating this association, is information collected from study groups, mainly from pregnant women, collecting samples to establish who in these study groups present with *Ureaplasma* colonization, and then comparing adverse immune reactions between the control groups (do not present with *Ureaplasma*) and the sample groups, who test positive to *Ureaplasma* colonization. These methods of determining *Ureaplasma*-induced immune activation produce results of limited reliability and can be open to scrutiny and supposition. Studies on the pathogenic properties of *Ureaplasma* and its effect to the immune response have been carried out *in vivo* in animal models, however problems in data reliability arise again due to the animal models used in the studies, for it has been shown that the immune response observed in most animal models differ significantly from those observed in humans. The most reliable animal models found are studies carried out in Rhesus macaque monkeys, which have strengthened the association of *Ureaplasma spp.* infections with immune response and pathogenic properties of the bacteria. There have been very few *in vitro* studies of *Ureaplasma spp.* infections of

human cell-lines in order to determine a ‘ground up’ immune response to the bacteria.

Mono-mac 6 (MM6) cells were chosen for this investigation, as they are the most abundant white blood cell in the body, and they are able to migrate to any non-immunoprivileged site. Therefore they are likely to be the first immune cell to come into contact with *Ureaplasma*, once it has colonised in the body. MM6 cells are known to possess all the PRRs that we are investigating in this chapter, in addition to utilising all the immune pathways being investigated.

In this chapter we will mainly investigate the cytokines TNF- $\alpha$  and IL-1 $\beta$  as these two inflammatory cytokines are of interest in the systemic immune response. As previously mentioned MM6 cells are the most abundant white blood cell and infiltrate all accessible compartments of the body. Both TNF- $\alpha$  and IL-1 $\beta$  are potent inflammatory cytokines and are good indicators of immune response throughout the body. By measuring the levels of these cytokines will confirm if these immune signalling pathways produce the NF- $\kappa$ B and inflammasome pathways are activated as TNF- $\alpha$  and IL-1 $\beta$  respectively. An increase in TNF- $\alpha$  and IL-1 $\beta$  after stimulation with *Ureaplasma spp.* would strongly support an immune response in any tissue or compartment that *Ureaplasma* was detected in by MM6 cells.

Previously published papers on the human PRR immune response to *Ureaplasma spp.* infections have used growth culture mediums that contain additional growth medium components, such as yeast extracts, which could produce erroneous or inaccurate results since they are PAMPs themselves and can trigger an innate immune response<sup>171</sup>. In the current study, we set out to determine the molecular mechanisms behind the innate immune response to *Ureaplasma*. In order to achieve this, we wanted to make sure that the growth medium used did not provide extra

PAMPs that would interfere with our findings, therefore we originally set out to compare different growth mediums on samples of immune cells *in vitro* and measured the effects on PRR expression, activation of immune signaling pathways and pro-inflammatory cytokine levels, in response to each growth culture medium. The *Ureaplasma* selective culture medium, obtained from Mycoplasma Experience (Surrey, UK), was the basic medium, to which yeast was added, to form the yeast positive growth culture medium. To produce yeast negative culture medium the basic *Ureaplasma* selective culture medium had ovine (swine) growth serum added to it. By comparing the results of immune activation between these two culture mediums we could decide the most appropriate growth culture medium to use in order to perform investigations that would give us the most reliable results; specific to *Ureaplasma* derived PAMPs and not to contaminants from the culture medium. After culturing *Ureaplasma* serovars 2, 3 and 14 in the ovine and yeast supplemented *Ureaplasma* selective culture medium, there was no significantly measurable difference between bacterial cell yields or propagation rates. As a result, the *Ureaplasma* could be cultured and prepared for experimenting on the same time line.

### **3.2: Results:**

#### **3.2.1: TLR expression levels in mono-mac 6 monocytes in response to yeast in the culture medium of *Ureaplasma***

The addition of yeast, a known PAMP, to the culture medium could potentially activate innate immune pathways.

The three *Ureaplasma* serovars cultured in both y- and y+ mediums, were used to stimulate mono-mac 6 cells in order to examine the effect the addition of yeast to the culture medium had on TLR expression in MM6 cells. Six independent experiments were carried out; using the three *Ureaplasma* serovars cultured in either y- or y+ growth mediums. TLR2, 4, 6 and 9 expression in MM6 cells was measured before and after stimulations with *Ureaplasma* serovars 2, 3 and 14 cultured in the two different *Ureaplasma* media. TLR2, 4, 6 and 9 were investigated as these TLRs are associated with bacterial PAMP recognition, differences between TLR expression level in y- and y+ cultured *Ureaplasma* serovars would determine which growth culture medium should be used for all future experiments in this study.

Initially the expression levels of TLR1 was investigated before and after stimulation with *Ureaplasma* cultured in y- or y+ growth mediums (Figure 3.2.1.1). Surprisingly, it was shown that the addition of yeast to the *Ureaplasma* selective culture medium had no statistically significant effect on the expression levels of TLR1 when compared to y- culture *Ureaplasma* serovars in MM6 cells.

When the expression levels of TLR2, TLR6 and TLR9 were investigated, it was shown that the addition of yeast could alter the expression levels of the different TLRs in MM6 cells. Interestingly, the effects observed seemed to be *Ureaplasma* serovars- specific. TLR6 was the only TLR that induced significantly different expression levels in all the *Ureaplasma* serovars used (Figure 3.2.1.2: A, B and C). In all *Ureaplasma* serovars examined, TLR6 expression was significantly higher where yeast positive growth culture medium was used compared to serovars grown in the yeast negative growth culture medium.

TLR9 expression levels were significantly increased in *Ureaplasma* SV3 and SV14 after stimulation with yeast positive serovars, compared to yeast negative culturing

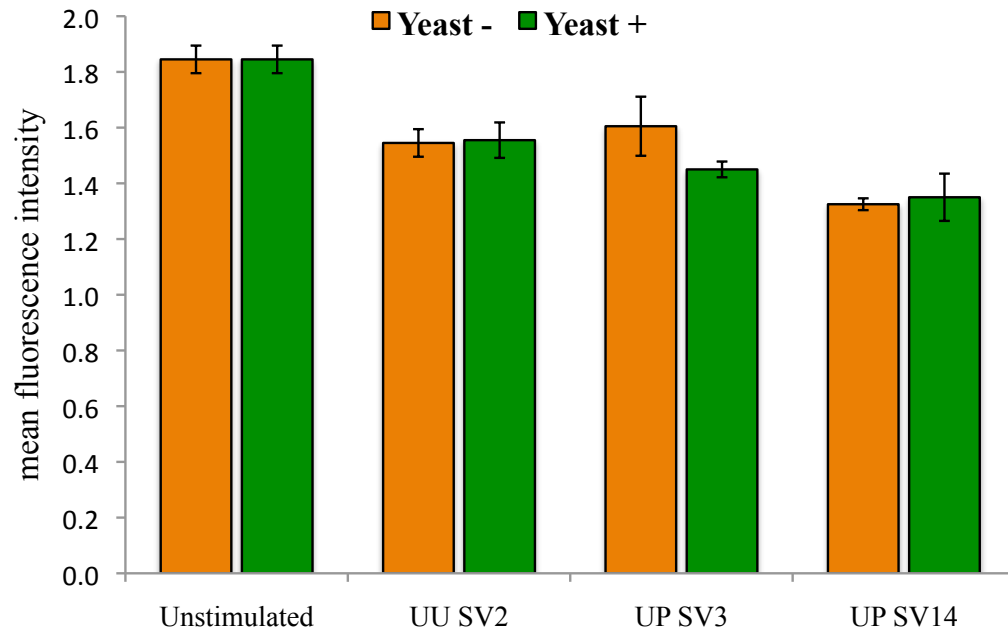
mediums (Figure 3.2.1.2: B and C). The statistical significance measured in TLR9 expression was  $p = <0.05$  and  $<0.01$  after comparing expression levels stimulated with y+ cultured serovars compared to y- cultured serovars, respectively.

TLR2 expression levels were significantly increased when stimulated with *Ureaplasma parvum* 3 cultured in yeast, compared to TLR2 expression levels in MM6 cells incubated with *Ureaplasma* cultured in yeast negative culture medium (Figure 3.2.1.2: B).

TLR expression seemed to be increased in all MM6 samples stimulated with *Ureaplasma* cultured in the presence of yeast. Therefore, the addition of yeast to the *Ureaplasma* selective culture medium augmented the TLR expression levels, therefore its presence could potentially interfere with experiments when deciphering the innate immune mechanisms involved in *Ureaplasma* infections.

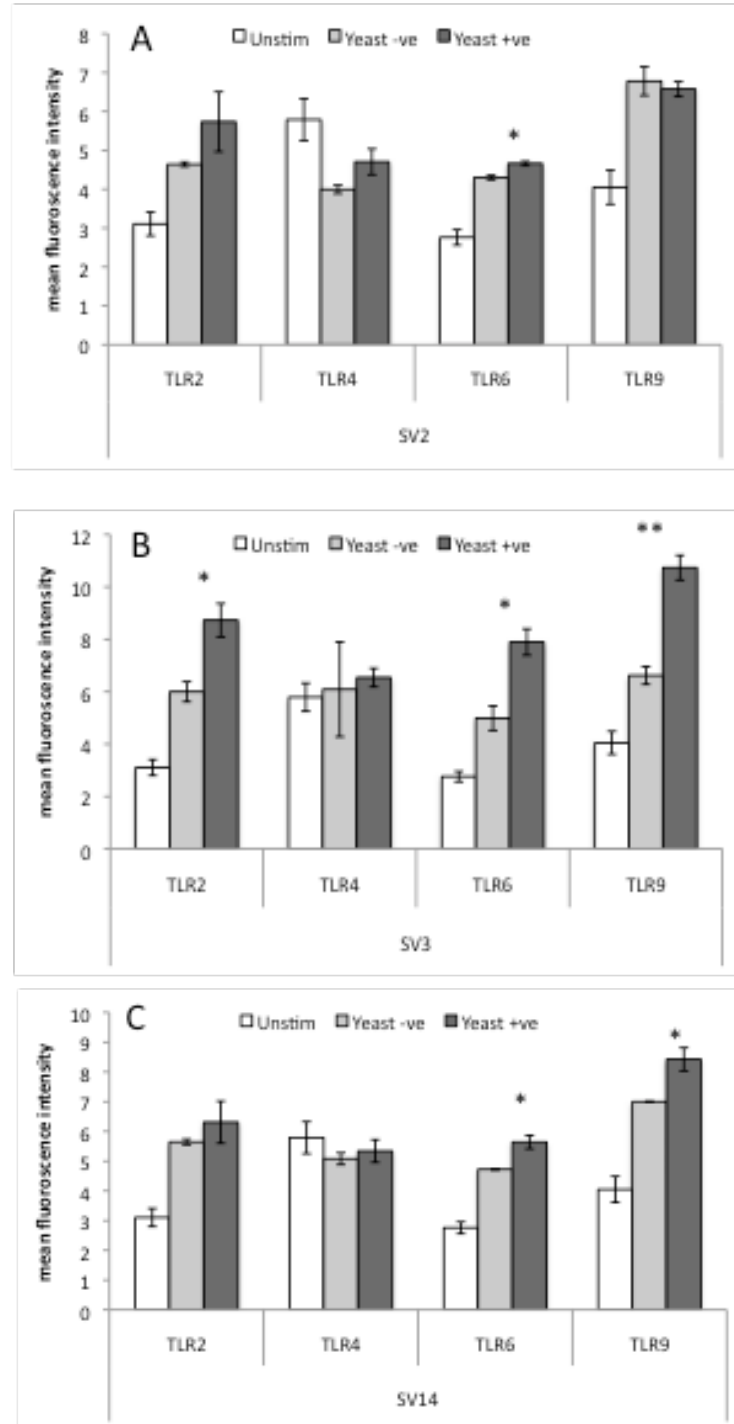
TLR1 expression after stimulation with yeast negative and yeast positive

*Ureaplasma* SV2, SV3 and SV14 culture medium:



**Figure 3.2.1.1:** TLR1 expression in MM6 cells after a 1 hour incubation with *Ureaplasma* SV2, SV3 and SV14, cultured in y- and y+ culture medium. TLR1 expression levels were assessed in MM6 samples after 1-hour stimulation with *U. parvum* 3, 14 and *U. urealyticum* 2, cultured in y- and y+ growth medium. Cells were then fixed (in 4% paraformaldehyde) and permeabilised. The TLR1 expression level was quantitatively measured using indirect immunofluorescence and Flow Cytometry using a FACSCalibur (Becton Dickinson). Each data represents mean  $\pm$  SD of three independent experiments where asterisks indicate statistically significant TLR expression between y- and y+ samples, ( $p$  (\*) = <0.05), however no statistical significance between TLR1 expression levels in y- and y+ culture medium were observed.

TLR expression after stimulation with yeast negative and yeast positive  
*Ureaplasma* SV2, SV3 and SV14 culture medium:



**Figure: 3.2.1.2: TLR expression levels after a 1-hour incubation of MM6 monocyte with *Ureaplasma* SV2 (A), SV3 (B) and SV14 (C).** TLR expression levels in MM6 samples after 1-hour stimulation with *Ureaplasma* serovars, cultured in the two different culture mediums (y-, and y+) and incubated for 60 minutes, and then fixed (in 4% paraformaldehyde) and permeabilised. The TLR expression levels are quantitatively measured using indirect immunofluorescence and Flow Cytometry using a FACSCalibur (Becton Dickinson). Each data represents mean  $\pm$  SD of two independent experiments where asterisks indicate statically significant TLR expression between y- and y+ samples, (p (\*)) = <0.05, (\*\*)) = <0.01).



### *3.2.2: Investigating mono-mac 6 innate immune responses and pathways activated in response to Ureaplasma stimulation*

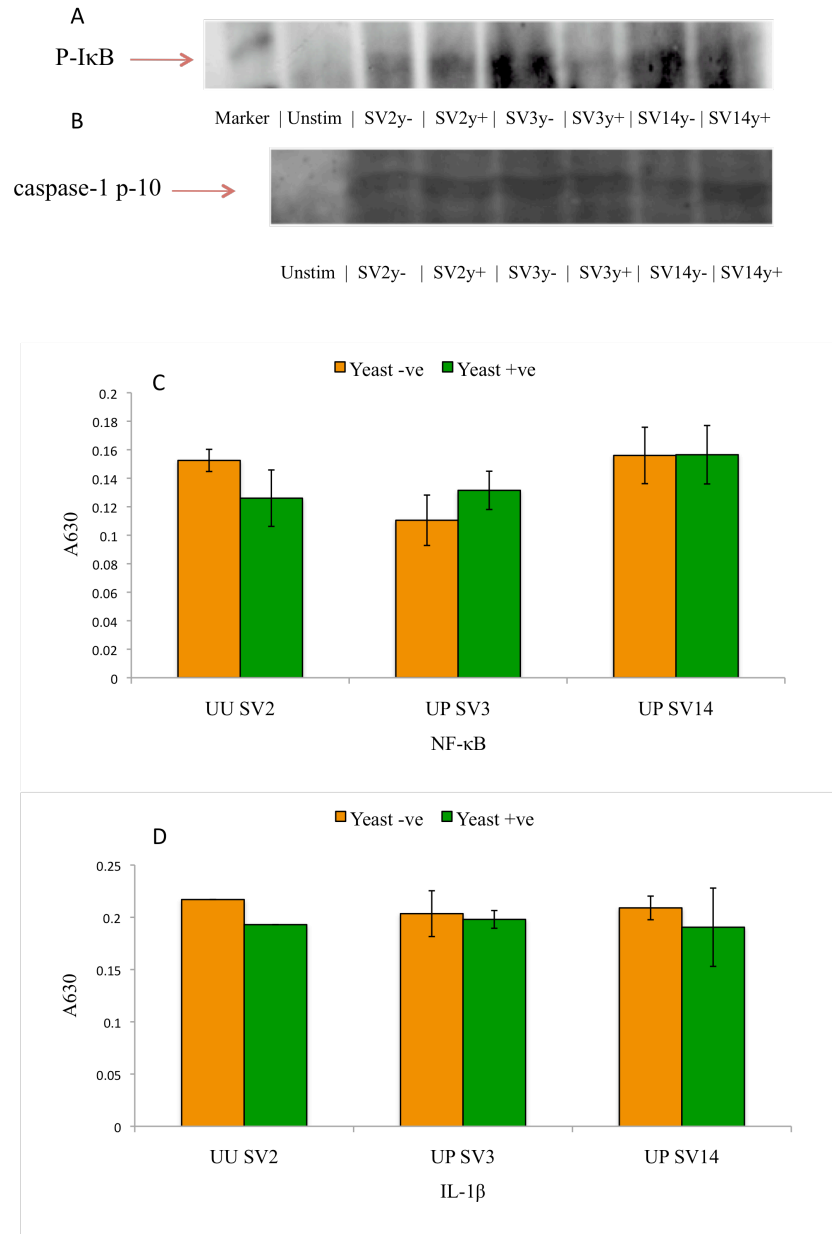
To investigate the *Ureaplasma*-induced innate immune response in MM6 cells, two specific immune signaling pathways were examined NF- $\kappa$ B and the caspase-1 resulting in IL-1 $\beta$  production – both pathways lie downstream of TLR activation. Alternative pathways were not included in this investigation as *Ureaplasma* is not thought to possess any components that would trigger MyD88-independent pathways, thus NF- $\kappa$ B would be the most suitable pathway to study. By determining if these signaling pathways were activated, we could shed light on whether *Ureaplasma* does induce an inflammatory immune response upon recognition by MM6 cells.

The production of NF- $\kappa$ B by *Ureaplasma* stimulation was examined by the protein detection methods of western blotting and HEK-Blue NF- $\kappa$ B reporter cell assays. Phospho-I $\kappa$ B (P-I $\kappa$ B) was detected in lysates of stimulated MM6 samples and comparing the results to unstimulated cell lysates (Figure 3.2.2: A). P-I $\kappa$ B is a constituent protein of the NF- $\kappa$ B inhibitory subunit complex. The presence of P-I $\kappa$ B in sample lysates suggests the NF- $\kappa$ B inhibitory complex has been cleaved from NF- $\kappa$ B, releasing active NF- $\kappa$ B, which in turn upregulates pro-inflammatory cytokine gene transcription and activates other immune responses. NF- $\kappa$ B concentration in sample supernatants was measured using HEK-Blue NF- $\kappa$ B reporter assay, then comparing the measurements recorded to those measured in unstimulated cell samples to give quantitative values of NF- $\kappa$ B (Figure 3.2.2: C). IL-1 $\beta$  concentration in sample supernatants was also measured using HEK-Blue IL-1 $\beta$  reporter assay, which gives quantitative values of IL-1 $\beta$  in sample supernatants that are then compared to IL-1 $\beta$  concentrations in unstimulated cell samples, to show how much IL-1 $\beta$  is produced in response to *Ureaplasma* stimulation (Figure: 3.2.2 D). The

pathway for the production of active IL-1 $\beta$  requires activation of the catalytic protein caspase-1. For caspase-1 to become activated, multiprotein complex inflammasomes must form, to cleave caspase-1's inhibitory subunit from it, converting inactive pro-caspase-1 to active caspase-1. Caspase-1 p-10 fragmentation protein forms part of caspase-1's inhibitory subunit complex, so detection of p-10 protein in cellular lysates indicates inflammasome activation (Figure 3.2.2: B), which is essential for IL-1 $\beta$  production.

The results showed that P-I $\kappa$ B is present in *Ureaplasma* stimulated MM6 cell lysates, suggesting that NF- $\kappa$ B is activated in MM6 cells after stimulation (Figure 3.2.2: A). These results were further supported by the activation of NF- $\kappa$ B as measured by HEK-Blue NF- $\kappa$ B reporter assays (Figure 3.2.2: C), neither P-I $\kappa$ B nor NF- $\kappa$ B was detected in unstimulated MM6 cell in either method (Figure 3.2.2: A and C). Like wise caspase 1 p-10 fragment was shown to be present in stimulated MM6 cell lysates, but not in unstimulated (Figure 3.2.2: B). These results suggest activation of caspase-1 via NLRP inflammasome formation; further support for the formation and activation of inflammasomes is the production of IL-1 $\beta$  by *Ureaplasma*-stimulated MM6 cells (Figure 3.2.2: D). These results support that *Ureaplasma* activates innate immune responses in MM6 monocytes via TLR-dependent signaling pathways, producing NF- $\kappa$ B, and NLR-activated signaling pathways that activate inflammasome formation leading to IL-1 $\beta$  production.

### *Ureaplasma*-induced innate immune responses in mono-mac 6 cells



**Figure 3.2.2:** *Ureaplasma* SV2, SV3 and SV14 induce pro-inflammatory cytokine production and activation of immune responses in MM6 cells. MM6 cells were either not-stimulated or stimulated with *Ureaplasma* SV2, SV3 and SV14 for 1 h, after which cell lysates and supernatants were analysed. Cell lysates were analysed by SDS-PAGE and then transferred to nitrogen cellulose membranes for Western Blotting. Primary P-IkB-specific (A) and caspase-1-specific (B) antibodies were used to probe the membrane, and then incubated with HRP-conjugated secondary antibodies. The bands were visualized using Luminol-based enhanced chemiluminescent (ECL) substrate horseradish peroxidase (HRP). The bands observed are representative images from three independent experiments. Supernatants were incubated in HEK-Blue NF-κB (C) and HEK-Blue IL-1β (D) reporter cells for 24-hours. QUANTI-Blue™ (Invivogen) was then added and quantitative measurements were measured using spectrophotometry at 630nm. Cytokine concentration is proportional to secreted embryonic alkaline phosphates (SEAP) level concentration, which is measured by absorbance using the unstimulated samples as a zero point..

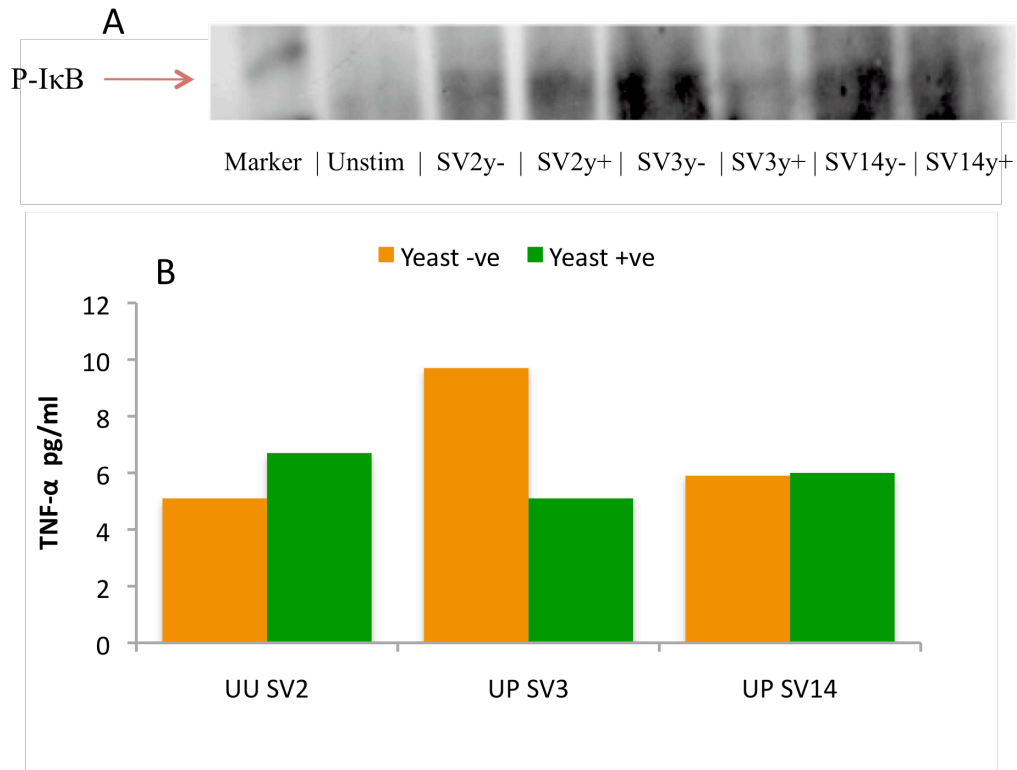
**3.2.3: *Ureaplasma* serovar-induced innate immune responses in MM6 cells using yeast positive and yeast negative *Ureaplasma* culturing medium:**

The increase in TLR2, 6 and 9 expression levels (Figure 3.2.1.2 A, B and C) in response to *Ureaplasma* stimulation and the upregulation of P-IkB shown in the western blot (Figure 3.2.3: A), support that *Ureaplasma* does induce an innate immune response via the MyD88-dependent pathway. To further investigate the immune response in MM6 cells to *Ureaplasma*, cytokine bead assay (CBA) was used to measure the increase in cytokine production between each of the serovars used and the culturing medium *Ureaplasma* was grown in (Figure 3.2.3 B). Comparing the results of TNF- $\alpha$  concentration from unstimulated samples to those that had been stimulated, significant increases were shown in TNF- $\alpha$  in both y- and y+ stimulated samples (Figure 3.2.3: B). The increased production of TNF- $\alpha$  is likely to be directly related to the increase concentration of P-IkB, shown in the western blot (Figure 3.2.3 A), which in turn is likely to be induced by the observed increase in TLR2/6 and TLR9 expression levels, shown in Figure 3.2.1.2: A, B and C.

Increase in TNF- $\alpha$  is strongly associated with the inflammatory immune response to pathogens, which supports the findings that *Ureaplasma* SV2, SV3 and SV14 are all capable of stimulating innate immune responses in MM6 monocytes (Figure 3.2.3: A and B). As monocytes account for the highest proportion of leukocytic cells, and they are able to migrate to virtually any compartment of the body, inflammatory responses produced by these cells, could well be a strong link between *Ureaplasma* infection and adverse reaction, such as pPROM, PTB and BPD.

In addition these results show that the presence of yeast in the culturing medium does produce different levels of immune responses in MM6 cells, which would support the use of y- *Ureaplasma* culture medium in future experiments.

*Ureaplasma*-activated TNF- $\alpha$  production in mono-mac 6 cells after 1-hour stimulation:



**Figure 3.2.3:** *Ureaplasma*-induced TNF- $\alpha$  production in mono-mac 6 monocytes after 1-hour stimulations.

*Ureaplasma*-induced pro-inflammatory cytokine production in mono-mac 6 monocytes, comparing the *Ureaplasma* serovar used for stimulation and the growth medium the serovars were cultured in ( $1 \times 10^8$  bacteria/ml to  $1 \times 10^7$  cells/ml). Lysates were obtained from each sample and using western blotting P-I $\kappa$ B was detected (A). Supernatant from each independent experiment was harvested and assayed for cytokine production using CBA (Becton Dickinson) (B). The concentration of the cytokine in the supernatant was measured by the detection of fluorescence using FACSCalibur (Becton Dickinson). The data represents the mean  $\pm$  SD of two independent experiments. The TNF- $\alpha$  concentrations were compared between *Ureaplasma* serovars used in stimulations and also the growth culture medium was in the culturing each of the serovars, using the unstimulated samples as a zero point.

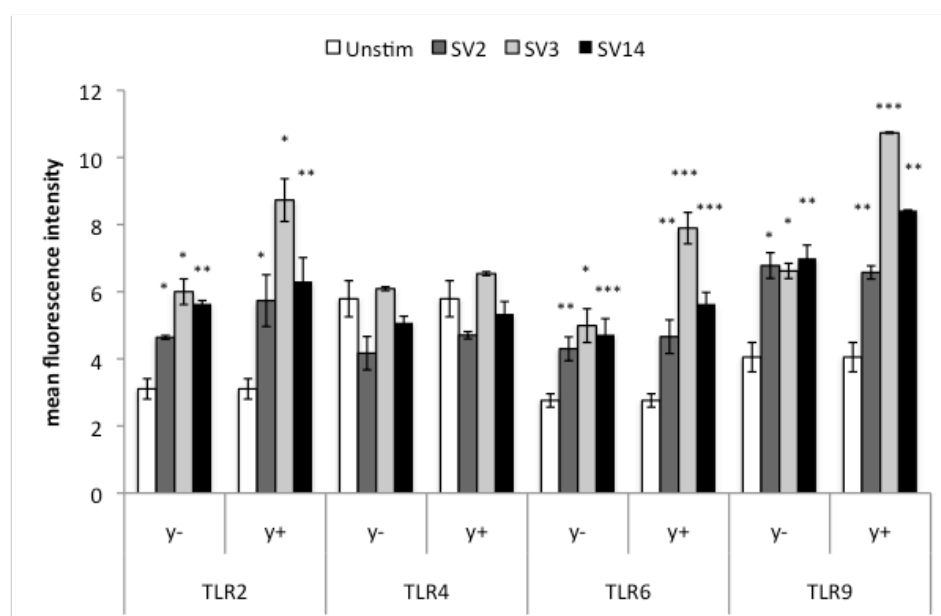
#### 3.2.4: TLR expression in mono-mac 6 in response to stimulation by specific *Ureaplasma* serovars

After investigating the effect the addition of yeast to the *Ureaplasma* culturing medium had on TLR expression levels in MM6 cells, we showed that yeast does effect TLR levels and that it consistently increasing expression in TLR6 and TLR9 in MM6 cells, when compared to y- culturing medium (Figure 3.2.1.2: A, B and C). Interestingly TLR6 was the only TLR to show significant increase across all three serovars examined, but the same pattern was not observed in TLR2 (Figure 3.2.4). As TLR6 requires TLR2 to form an active heterodimer receptor, investigation into TLR expression and regulation in accordance to each individual *Ureaplasma* serovars were examined. Studies have suggested *Ureaplasma spp.* pathogenic potency maybe specific to the different serovars<sup>25,173</sup>. We examined the TLR expression levels in MM6 cells and compared their expression levels before (unstimulated control samples) and after stimulation with *U. parvum* 3, 14 and *U. urealyticum* 2. This set of experiments would show TLR expression level variation according to the *Ureaplasma* serovar used to stimulate each sample. We would then be able to investigate the effect on TLRs resulting from the *Ureaplasma* serovar used and determine the different pathogenic properties of different serovars. The pathogenic properties of different *Ureaplasma* serovars maybe a result why certain serovars are more associated with pPROM, PTB and complications in infants exposed to *Ureaplasma spp.* during gestation.

The results showed statistically significant increase in TLR2, TLR6 and TLR9 expression levels after 1-hour incubation with each *Ureaplasma* serovar (Figure 3.2.4). TLR4 showed no significant difference in expression after stimulation with the different *Ureaplasma* serovars.

SV3 seemed to be able to augment TLR2, TLR6 and TLR9 expression levels the most when compared to the other serovars, whereas SV14 was the least able serovar to affect the TLR expression levels, possibly suggesting that it is the least virulent of the three serovars tested.

#### TLR expression levels in response to *Ureaplasma* serovars in mono-mac 6 cells:



**Figure: 3.2.4:** *TLR expression levels after a 1-hour incubation of MM6 monocyte with Ureaplasma SV2, SV3 and SV14.* TLR expression levels in MM6 samples after 1-hour stimulation with *Ureaplasma* serovars 2, 3 and 14, cultured in the two different culture mediums (y-, and y+) and incubated for 60 minutes, and then fixed (in 4% paraformaldehyde) and permeabilised. Unstimulated control samples (white bar), *U. urealyticum* 2 (dark grey bar), *U. parvum* 3 (light grey bar) and *U. parvum* 14 (black bar) expression levels are quantitatively measured using indirect immunofluorescence, Flow Cytometry using a FACSCalibur (Becton Dickinson) and compared to unstimulated control MM6 samples, treated under the same conditions. Each data represents mean  $\pm$  SD of two independent experiments where asterisks indicate statically significant TLR expression between *Ureaplasma* stimulated and *Ureaplasma* unstimulated samples, (p (\*)) = <0.05, (\*\*) = <0.01, (\*\*\*) = <0.005). The graph shows the expression levels of each TLR, grouped to show the actions of each serovar on the TLRs coupled with the two different culture mediums used.

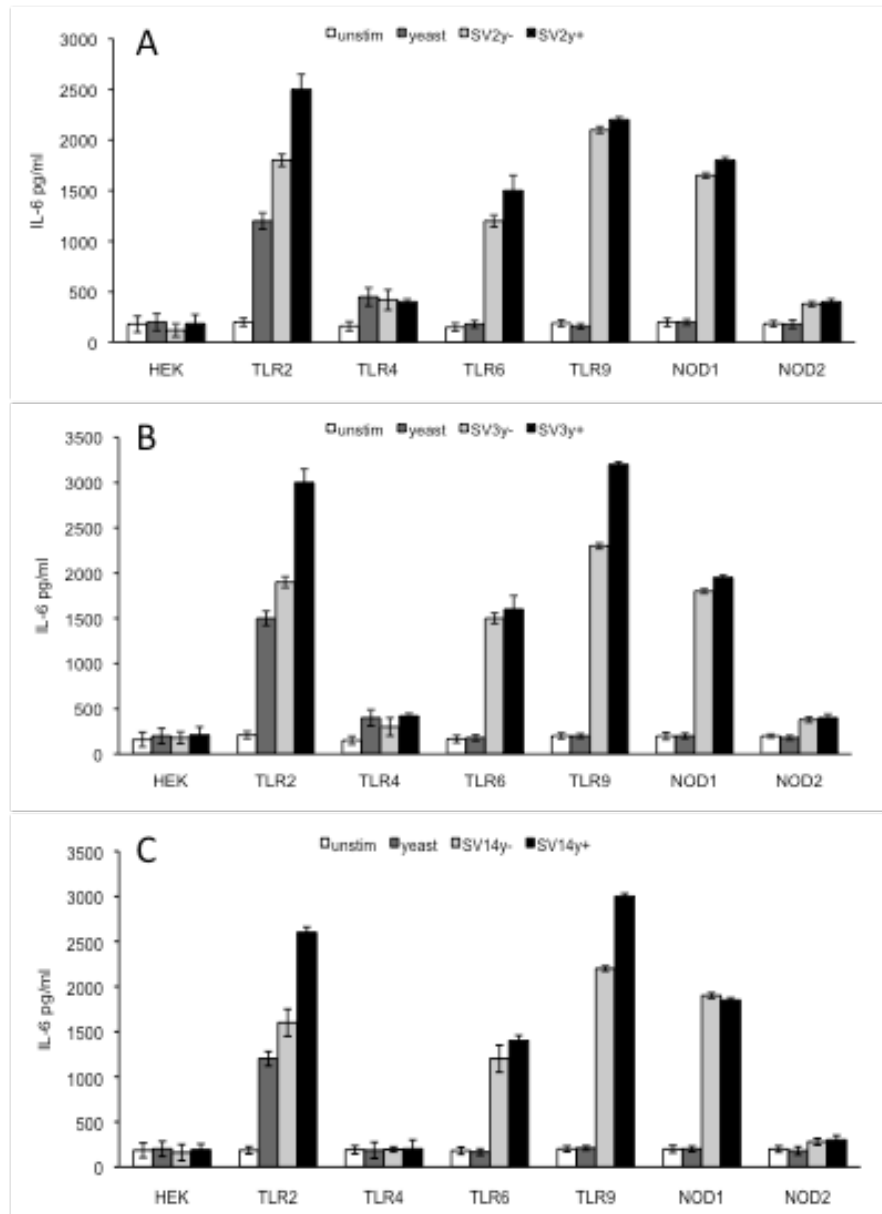
**3.2.5: Determining which PRRs are involved in the innate immune sensing of *Ureaplasma* using HEK-293 transfected cells:**

Clinical studies have shown that elevated levels of inflammatory cytokines or positive amniotic fluid culture for microorganisms such as *Ureaplasma* in the amniotic fluid of symptomatic women at the time of the mid-trimester amniocentesis are associated with increased risk of preterm birth, suggesting that inappropriate innate immune activation in response to these bacteria is the cause of preterm birth and the associated neonatal disorders<sup>174,175</sup>. The question that remains is how does *Ureaplasma* trigger the inflammatory response both in-utero and in the respiratory track and which innate immune receptors are able to sense it? In order to determine which PRRs are involved we investigated which TLR/NLR is being triggered using Human embryonic kidney (HEK) – 293 cells transfected with different TLRs/NLRs. Initially HEK cells transfected with TLR2, TLR4, TLR6, TLR7, TLR9, NOD1 or NOD2 were stimulated with *Ureaplasma* serovars cultured without (SV2 y-) and with yeast (SV2 y+). The presence of yeast in the culture medium seemed to augment the IL-6 response in HEK-TLR2 cells. SV2 with or without yeast seemed to trigger responses from HEK-TLR2, TLR6, TLR9 and NOD1 cells (Figure 3.2.5 A). SV2 did not seem to trigger TLR4 activation. We subsequently proceeded to test the remaining y- and y+ serovars, SV3 and SV14 using the HEK transfectants. Both serovars gave similar results to SV2 by triggering TLR2, TLR6, TLR9 and NOD1 (Figure 3.2.5: B and C). The addition of yeast to the *Ureaplasma* selective culturing medium augmented the responses in all cases (Figure 3.2.5 A, B and C), thus suggesting that using culture medium without yeast is the most appropriate for these studies. Furthermore, HEK cells stimulated with yeast only showed upregulation IL-6 expression in HEK-TLR2 transfected cells, which would be expected as TLR2



forms a heterodimer with TLR1 upon ligand activation by yeast, activating immune cytokine upregulation pathways (Figure 3.2.5: A B and C). No other TLR- or NLR- HEK tranfects showed increased secretion of IL-6 by yeast alone, but the degree of IL-6 upregulation in HEK-TLR2 cells after stimulation with y+ *Ureaplasma* culture was consistently and significantly higher when compared to the IL-6 expression observed in y- cultured *Ureaplasma* serovars. IL-6 secretion was significantly higher in y+ cultured *Ureaplasma* SV3 and SV14, but the same results were not observed in SV2 cultures. This would suggest that immune response is not consistent throughout the *Ureaplasma* serovars; suggesting *Ureaplasma* virulence is serovar dependent. HEK-NOD1 transfected cells showed significant increase in IL-6 production upon stimulation with both y+ and y- *Ureaplasma* cultured serovars, though the addition of yeast showed no difference in IL-6 production compared to y- cultures. NOD1 is most associated with the detection of (DAP)-containing PGN, which is a bacterial cell wall component, as well as other cell wall components. This makes the detection of *Ureaplasma*, which is wall-less, by NOD1, a very interesting finding. The activation of NOD1-immune response was unexpected and suggests that novel NOD1 activation ligands are still to be discovered.

PRR-dependent IL-6 secretion in response to 1-hour *Ureaplasma* SV2, SV3 and SV14 stimulations:



**Figure 3.2.5:** PRR-dependent IL-6 secretion in response to 1-hour *Ureaplasma* SV2 (A), SV3 (B) and SV14 (C) stimulations: HEK-293 cells transfected with TLR2, TLR4, TLR6, TLR7, TLR9, NOD1 or NOD2 were either not incubated (white bar charts) or incubated with with yeast (dark grey barchart) or *Ureaplasma* ( $1 \times 10^8$  bacteria/ml to  $1 \times 10^7$  cells/ml) cultured in yeast asbent culturing medium y- (light grey bar charts) or *Ureaplasma* cultured with the addition of yeast y+ (black barcharts), for 1-hour. The supernatants were harvested and assayed for IL-6 content using the Cytometric Bead Array (CBA) system (Becton Dickinson). Fluorescence was detected using a FACSCalibur (Becton Dickinson). The data represents the mean  $\pm$  SD of three independent experiments.

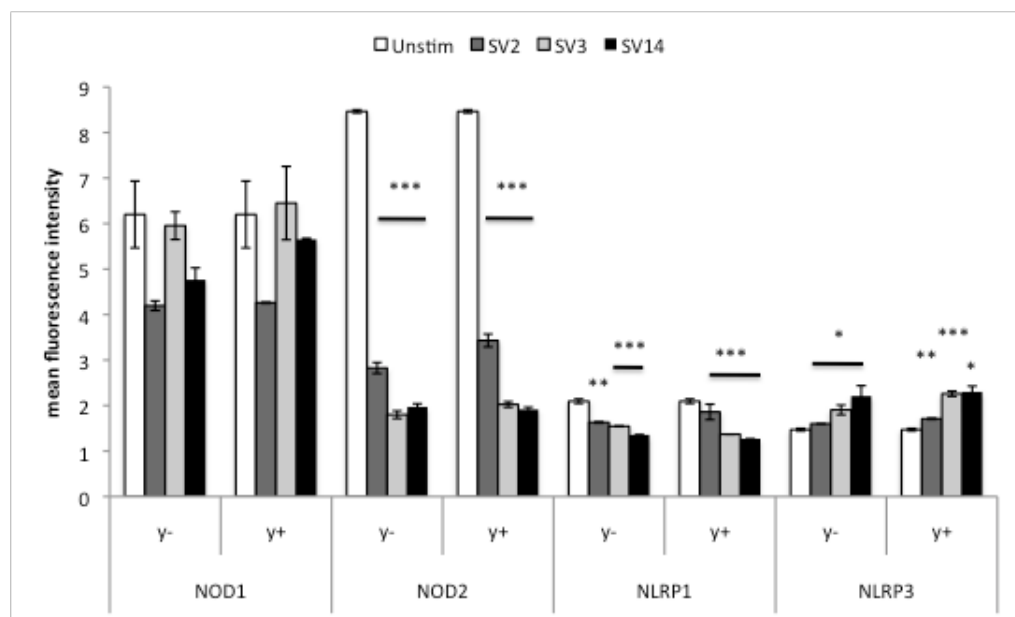
**3.2.6: The expression regulation of NLRs in *Ureaplasma*-activated immune response in mono-mac 6 cells:**

The results from Figure 3.2.3: B and D would suggest that *Ureaplasma* SV2, SV3 and SV14 activate NLR immune response pathways after stimulation in MM6 cells. The presence of caspase-1 p10 as detected by western blotting (Figure 3.2.3 B) from *Ureaplasma* stimulated samples compared to unstimulated control samples supports the activation and formation of inflammasome protein complexes. The activation of inflammasomes causes cleavage of the inhibitory subunit of caspase-1, allowing activation of caspase-1 catalytic activity, after conversion of inactive pro-caspase-1 into mature (active) caspase-1. Mature caspase-1's proteolytic activity, catalyses the maturation of pro-inflammatory cytokines into their mature forms, in a process that is similar to that of the activation of caspase-1 itself. IL-1 $\beta$  and IL-18 are both converted from their immature pro-IL-1 $\beta$  and pro-IL-18 forms into their active forms via caspase-1 activity. Both IL-1 $\beta$  and IL-18 are potent pro-inflammatory cytokines that cause strong inflammation immune responses. The detection of caspase-1 and the elevated concentration of IL-1 $\beta$  (figure 3.2.2: B and D), support the hypothesis that NLRs are activated in response to *Ureaplasma* SV2, SV3 and SV14 stimulation, and that this NLR activation is independent of the addition of yeast, as there is no significant difference in the concentration of caspase-1 p10 or IL-1 $\beta$  in y- and y+ experiments.

We investigated the expression levels of NLRs (NOD1, NOD2, NLRP1 and NLRP3), in MM6 cells after a 1-hour incubation period with *Ureaplasma* serovars 2, 3 and 14, in both y- and y+ culturing medium, using indirect immunofluorescence and measuring fluorescence intensity using FACSCalibur (Becton Dickinson). Interestingly the results observed (figure 3.2.6), show significant decrease in NOD2

and NLRP1 expression levels in MM6 cells after 1-hour stimulation with *U. parvum* 3, 14 and *U. urealyticum* 2 when compared to control unstimulated MM6 cell samples. The expression levels of NLRP3 increased after stimulation with *Ureaplasma* serovars, but to a lesser extent than would be predicted after the robust increase in capsase-1 p-10 and IL-1 $\beta$  that was observed in Figure 3.2.2 B and D, suggesting an additional, but unknown IL-1 $\beta$  activation pathway may be activated. The addition of yeast to the *Ureaplasma* selective growth culture medium was shown have very little effect on the expression levels of NLRs investigated and likewise the *Ureaplasma* serovar used in each stimulation did not appear to cause any significant differences in the NLR expression level measured.

#### NLR expression levels in accordance to the *Ureaplasma* serotypes:



**Figure: 3.2.6:** NLR expression levels after a 1-hour incubation of MM6 monocyte with *Ureaplasma* SV2, SV3 and SV14. NLR expression levels in MM6 samples after 1-hour stimulation with *Ureaplasma* serovars 2, 3 and 14, cultured in the two different culture mediums (y-, and y+) and incubated for 60 minutes, and then fixed (in 4% paraformaldehyde) and permeabilised. Unstimulated control samples (white bar), *U. urealyticum* 2 (dark grey bar), *U. parvum* 3 (light grey bar) and *U. parvum* 14 (black bar) expression levels are quantitatively measured using indirect immunofluorescence, Flow Cytometry and FACSCalibur (Becton Dickinson) and compared to unstimulated control MM6 samples, treated under the same conditions. Each data represents mean  $\pm$  SD of two independent experiments where asterisks indicate statically significant NLR expression between *Ureaplasma* stimulated and *Ureaplasma* unstimulated samples, (p (\*)) = <0.05, (\*\*) = <0.01, (\*\*\*) = <0.005). The graph shows the expression levels of each NLR, grouped to show the actions of each serovar on the NLRs coupled with the two different culture mediums used.

*3.2.7: Ureaplasma serovar-induced innate immune responses in mono-mac 6 monocytes via NLRs:*

Our previous data has suggested that *Ureaplasma* could trigger NLR-induced innate immune responses. In order to determine whether there were any serovar-dependent responses MM6 cells were stimulated with the different serovars and the activation of different signaling cascades was investigated.

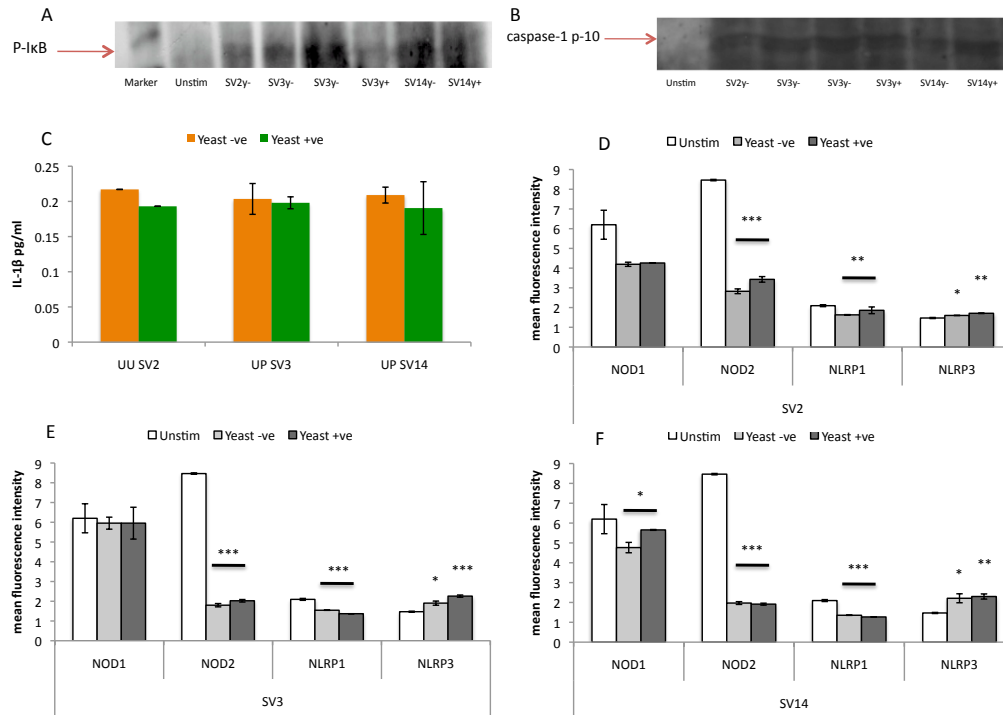
The results shown in figure 3.2.7: A and B, suggest elevated production of P-I $\kappa$ B and caspase-1 p10 (respectively), in MM6 cells stimulated with *Ureaplasma* serovars 2, 3 and 14, when compared to unstimulated control samples.

Similarly, all three serovars were equally capable of triggering caspase-1 activation as well as increased concentration of IL-1 $\beta$  in the stimulated samples compared to unstimulated samples (Figure 3.2.7: B and C).

When the expression levels of different NLRs were assessed, NLRP3 showed a slight increase in expression, NOD1 seemed to remain unaffected in response to stimulation by the different serovars, whereas the expression levels of NOD2 and NLRP1 after *Ureaplasma* stimulation were consistently down regulated (Figure 3.2.7: D, E and F). This was an unexpected finding, as the elevated P-I $\kappa$ B concentration suggests that there is activation of NF- $\kappa$ B immune response signaling in MM6 cell after *Ureaplasma* stimulation, which is the first step of the two-step process of inflammasome complex formation. The production of mature caspase-1 further supports the formation of inflammasome complexes, therefore the decrease in NLR expression in stimulated MM6 cells, compared to unstimulated control MM6 cells is rather perplexing. The elevated production of IL-1 $\beta$  suggests that there must be caspase-1 activation, but taken with the minor increase in NLRP3 expression and down-regulation of the NLRP1, the mechanism by which IL-1 $\beta$  and caspase-1 are

produced must be a novel pathway, and the mechanisms by which this pathway is activated remains unclear.

### *Ureaplasma*-induced innate immune responses in mono-mac 6 monocytes:



**Figure 3.2.7:** *Ureaplasma* SV2, SV3 and SV14 induce pro-inflammatory cytokine production and activation of immune response in MM6 cells. MM6 cells were incubated for 1-hour, being either non-stimulated or stimulated with *Ureaplasma* SV2, SV3 and SV14, after which cell lysates and supernatants were analysed. Cell lysates were analysed by SDS-PAGE and then transferred to nitrogen cellulose membranes using Western Blotting. Primary P-IkB-specific (A) and caspase-1-specific (B) antibodies were used to probe the membrane, and then incubated with HRP-conjugated secondary antibodies. The bands were visualized using Luminol-based enhanced chemiluminescent (ECL) substrate horseradish peroxidase (HRP). The bands observed are images are representatives of the three independent experiments. (C) Supernatants were incubated in HEK-IL-1 $\beta$  reporter cells for 24-hours. QUANTI-Blue™ (Invivogen) was then added and quantitative measurements were measured using spectrophotometry at 630nm. Cytokine concentration is proportional to secreted embryonic alkaline phosphates (SEAP) level concentration, which is measured by absorbance. NLR expression levels in MM6 samples after 1-hour stimulation with *Ureaplasma* serovars, cultured in the two different culture mediums (y-, and y+) and incubated for 1-hour, and then fixed (in 4% paraformaldehyde) and permeabilised. The NLR expression levels are quantitatively measured using indirect immunofluorescence, Flow Cytometry and FACSCalibur (Becton Dickinson). Each data represents mean  $\pm$  SD of two independent experiments where asterisks indicate statically significant NLR expression between y- and y+ samples, (p (\*) = <0.05, (\*\*) = <0.01, (\*\*\*) = <0.005).

### 3.3: Conclusion:

Our investigation showed that the addition of yeast to the *Ureaplasma* culturing medium augmented the immune responses observed in MM6 cells, when compared to *Ureaplasma* that was not cultured in yeast.

*Ureaplasma* SV2, SV3 and SV14 were all shown to significantly upregulate TLR2, TLR6, TLR9 and a very small increase in NLRP3 expression. *Ureaplasma* serovars were shown to be unable to increase TLR1 expression in MM6 cells, whether the *Ureaplasma* was cultured with addition of yeast or not. This was unexpected as the study by Shimizu et al. showed that *Ureaplasma* was able to do so, though in that study *Ureaplasma* serovars were cultured in yeast extract to aid culturing<sup>171</sup>.

There was no consistent or significant upregulation in NOD1, NOD2 or NLRP1 expression. Interestingly HEK-293 cells transfected with NOD1 showed a significant increase in IL-6 production, as did HEK-TLR2, TLR6 and TLR9 transfectants, after stimulation with *Ureaplasma* SV2, SV3 and SV14, compared to unstimulated samples. The increased production of TNF- $\alpha$ , IL-6, and IL-1 $\beta$ , further support TLR/NOD1-mediated activation of MyD88-dependent immune response pathways to *Ureaplasma* infection.

The production of active IL-1 $\beta$  would suggest activation of NLRP inflammasomes, however there was no increase in NLRP1 expression, and only a very small amount upregulation of NLRP3 expression suggests that an NLRP3-independent IL-1 $\beta$  production mechanism may be involved.

The significant increase in pro-inflammatory cytokines and the production of IL-1 $\beta$  shows *Ureaplasma* activation of immune responses in MM6 cells, supporting that *Ureaplasma* does possess pathogenic properties that activate the inflammatory

immune response, strengthening the suggested associations of *Ureaplasma* to adverse health complications.



## **Chapter 4:**

# ***Ureaplasma*-activated immune response in bronchial epithelial cells**

#### 4.1: Introduction:

One of the major implications linked with *Ureaplasma spp.* urogenital tract colonization is its association with lung defects in the newborn infants. BPD and CLD have both been suggested to be directly linked to *Ureaplasma spp.* infection in neonates, whose premature birth has been thought to be initiated by the infection of *Ureaplasma spp.* especially at ~ 22 - 30 weeks gestation period<sup>65</sup>. Fetal lung development occurs during this period of gestation, it is therefore reasonable to suppose that invasion of the fetal respiratory tract by a pathogen that initiates pro-inflammatory cytokine release, could be responsible for bringing about such injuries to the fetal lung tissue associated with BPD and CLD. Pro-inflammatory cytokines have been shown to cause tissue dysregulation and cellular injury in epithelial cells, furthermore histological images taken from neonatal lung tissue with BPD, have shown inhibition of regular tissue formation and interstitial fibrosis, and inadequate alveoli formation<sup>54</sup>. Epithelial cells possess a wide range of PRRs and are able to initiate robust and diverse immune responses, as they are often the first barrier of the immune system, interacting with such a diverse range of pathogens and antigens. This is true of lung epithelial cells, which in addition to the expression of PRRs have a number of other immune defense mechanisms, both cellular and mechanical. Pulmonary surfactant complexes contain a variety of lipoproteins, phospholipids and surfactant-associated proteins and are secreted by type II alveolar cells<sup>176</sup>. These complexes recognise and bind to pathogens that enter the lungs, promoting detection and phagocytosis of pathogens by immune cells present in the pulmonary mucus. Cilia are a mechanical mechanism by which the prevent infection, by 'sweeping' mucus out of the lungs and preventing pooling of mucus that can harbour pathogens. Inhibition of proper lung development in neonates and newborn infants prevents all

of the mentioned immune mechanisms as well as insufficient alveolar surface area for adequate oxygen transfer from the air to the bloodstream.

To investigate the suggested association between *Ureaplasma* with BPD in infected neonates, bronchial epithelial cell-line (BEAS-2B) cells were utilised. This cell line was chosen, as it is the ideal model to determine if *Ureaplasma* is capable of initiating an immune response in the cells that line the lungs. If an immune response is activated, inflammatory cytokines will be produced via the signaling pathways NF- $\kappa$ B and NLR inflammasome complex formation. Examining *Ureaplasma*-induced immune responses in the respiratory tract, we hope to shed light on whether *Ureaplasma* infection alone can be responsible for the tissue damage leading to BPD. If *Ureaplasma* serovars in this study activate pro-inflammatory cytokine production and release in BEAS (BEAS-2B) cells, further association between *Ureaplasma* and neonatal BPD and CLD would be suggested.

We aimed to investigate the role of the NLR inflammasomes in the production of IL-1 $\beta$  in HAECs after stimulation with *Ureaplasma*. IL-1 $\beta$  is therefore the main cytokine being measured, but IL-6 is also observed to assess the role and activation of TLRs, which are responsible for producing the priming signals for NLR inflammasome activation.

From preliminary time course studies using HAECs (data not included), the incubation time was increased from 1 hour (used for MM6 and BEAS-2B cell lines) to 2 hours. Cytokine production after 2 hours incubation was deemed more suitable than after 1 hour, especially when measuring immune response after MBA stimulation.

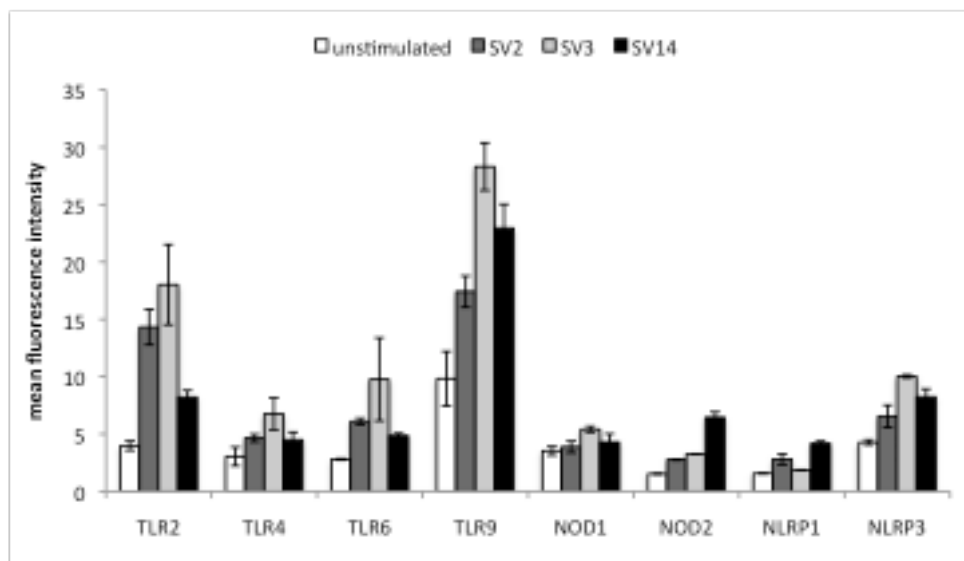
## 4.2: Results:

### 4.2.1: Pathogen recognition receptor expression in response to *Ureaplasma* serovars 2, 3 and 14 in human bronchial epithelial cells:

In order to investigate whether *Ureaplasma* is able to activate an innate immune response in BEAS-2B cells, expression levels of specific PRRs were measured in BEAS-2B cells both before and after stimulation with *Ureaplasma parvum* 3, 14 and *Ureaplasma urealyticum* 2. The results showed minimal PRR expression levels in unstimulated cells, but some showed significant upregulation after *Ureaplasma* stimulation when compared to the unstimulated controls. Similarly to our previous findings, no upregulation of TLR1 expression was observed after stimulation with any of the *Ureaplasma* serovars tested (data not shown). The overall expression levels of the TLRs was shown to be similar to the pattern observed in our previous studies, however the NLR expression levels differ quite greatly. All *Ureaplasma* serovars showed TLR2, TLR6 and TLR9 upregulation after stimulation (Figure 4.2.1). Although *Ureaplasma* SV2 and SV14 both showed upregulation, the pattern of expression was quite different between the two serovars, where SV2 showed significantly greater upregulation in TLR2 but lower TLR9 expression increase compared to SV14 (Figure 4.2.1). *Ureaplasma parvum* 3 was consistently shown to cause the greatest increase in TLR expression, compared to those observed after stimulation with *U. urealyticum* 2 and *U. parvum* 14 (Figure 4.2.1). The results show that TLR4 expression might be slightly upregulated by SV3, however the statistical significance in increase is not that great however TLR4 showed no difference in expression level when stimulated with SV2 or SV14. The expression levels of all of

the NLRs differ from those observed after *Ureaplasma* stimulations in MM6 cells. NOD2 and NLRP3 expression level were increased by all serovars, whilst only SV14 showed upregulation in NLRP1, and showed the most significant increase in NOD2 expression (Figure 4.2.1). SV3 showed the strongest and most significant upregulation in NLRP3 and was the only serovar to show upregulation of NOD1. Comparing the PRR expression levels in the BEAS-2B cell-line and the MM6 cell-line following *Ureaplasma* stimulation, there is a virtually inverse relationship.

*Ureaplasma* SV2, SV3 and SV14 induced PRR expression variation levels in BES cells:



**Figure 4.2.1:** PRR expression level after 1-hour incubation period with *Ureaplasma parvum* 3, 14 and *Ureaplasma urealyticum* 2, compared to non-stimulated BES cells. BES cells were either not stimulated (white bar) or incubated with *Ureaplasma* ( $1 \times 10^8$  bacteria/ml to  $1 \times 10^7$  BES cells/ml) SV2 (dark grey bar), SV3 (light grey bar) or SV14 (black bar). After the 1-hour incubation the cells were fixed and permeabilised, then targeted with primary antibodies specific to each PRR. Incubation with appropriate secondary FITC-conjugated antibodies was carried, and the expression levels were measured by the fluorescence that was detected by FACSCalibur (Becton Dickinson). The data presented is the mean average with the mean  $\pm$  SD of three independent experiments.

**4.2.2: *Ureaplasma*-induced cytokine production in bronchial epithelial cells:**

Our data had demonstrated that *U. parvum* 3 and 14 and *U. urealyticum* 2 could induce upregulation of several different PRRs expressed in bronchial epithelial cells.

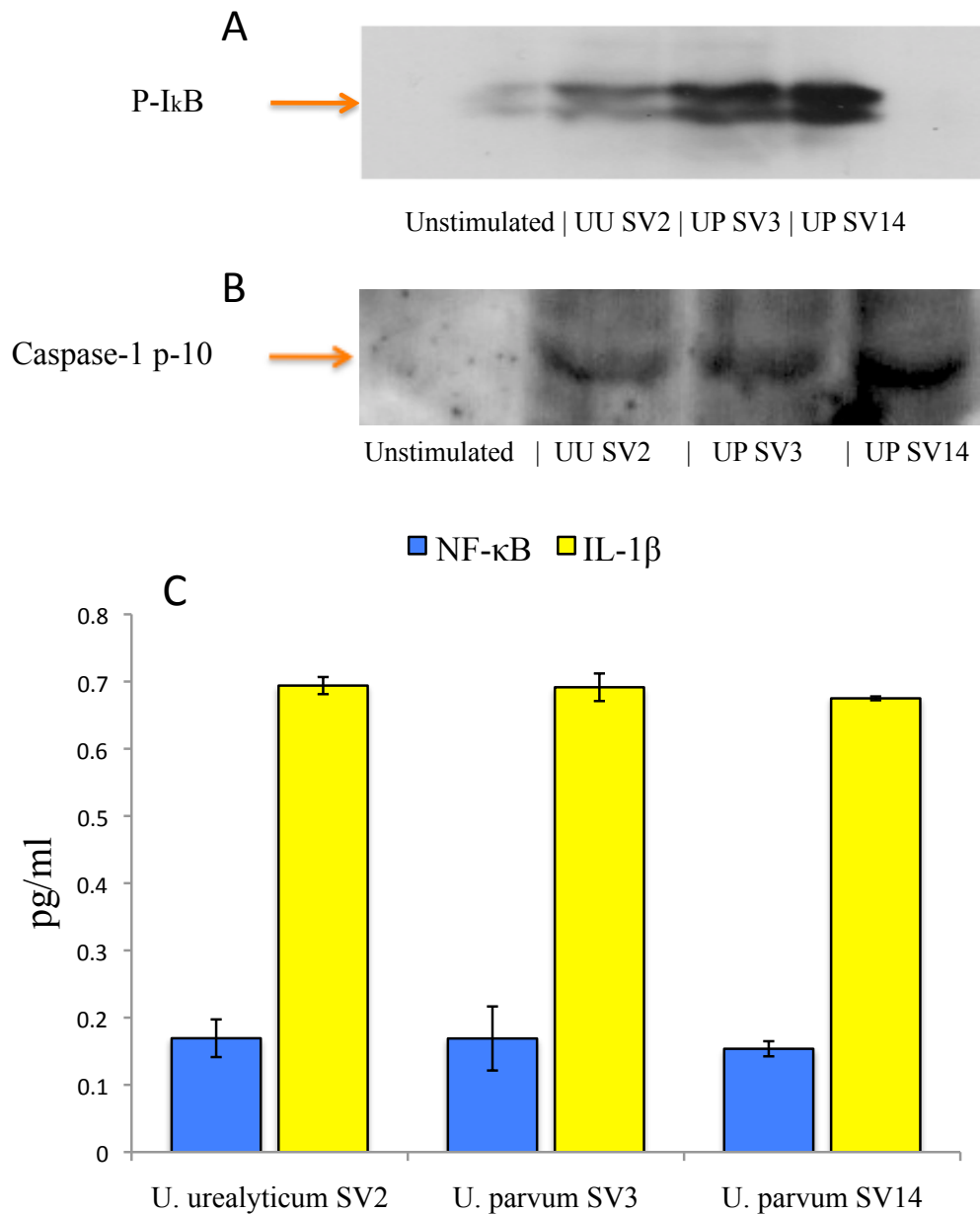
In order to further investigate the innate immune responses of bronchial epithelial cells to *Ureaplasma* SV2, SV3 and SV14 stimulation, we examined the signaling cascades being triggered: the MyD88-dependent NF- $\kappa$ B and caspase-1-mediated immune responses. P-I $\kappa$ B is an essential protein in the signaling pathway for the activation of NF- $\kappa$ B, which is responsible for the upregulation and production of pro-inflammatory cytokine genes and proteins. In addition, NF- $\kappa$ B is essential in the activation of the acquired immune response; therefore it is a protein of great importance to determine the immune response pathways activated by *Ureaplasma* SV2, SV3 and SV14 stimulations in bronchial epithelial cells. P-I $\kappa$ B concentration is directly proportional to the concentration of NF- $\kappa$ B, as it is the inhibitory subunit to NF- $\kappa$ B. Caspase-1 is an inflammasome complex protein that enables activation of IL-1 $\beta$  and IL-18. Caspase-1 is held inactive by its binding to a caspase-1 inhibitory subunit complex. Caspase-1 p-10 forms part of this inhibitory complex, thus by the detection of p-10 from sample lysates, activation of caspase-1 can be established.

In the current study, immune response signaling-associated proteins P-I $\kappa$ B and caspase-1 p-10 were qualitatively examined using western blotting of the lysates from both unstimulated (control) and stimulated bronchial epithelial cells. The results showed that both P-I $\kappa$ B and caspase-1 p-10 were produced in response to all three *Ureaplasma* serovars examined (Figure 4.2.2: A and B). The significant abundance of caspase-1 shown in the western blot (Figure 4.2.2 B) indicates the activation and formation of inflammasome complexes. In addition to western blotting the activation of these pathways was investigated using reporter cell lines for NF- $\kappa$ B and IL-1 $\beta$  (the product of caspase-1 activation) respectively (Figure 4.2.2: C). Both reporter cell lines rely on the secreted embryonic alkaline phosphates (SEAP) secreted by HEK-Blue™ reporter cells, which can be measured using

absorbance colorimetry at a wavelength of 630nm. The SEAP (alkaline) converts the initial pink hue of the (acidic) QUANTI-Blue™ solution to a blue/purple hue, thus allowing quantitative measurement of each protein when comparing the absorbance levels of stimulated samples to unstimulated sample supernatants. The HEK-Blue™ reporter experiments showed that there was significant production of both NF- $\kappa$ B and IL-1 $\beta$  in response to all three *Ureaplasma* serovars samples tested, when compared to the unstimulated samples (Figure 4.2.2: C). No significant difference between the different serovars was observed.

Our results suggest that similar to the monocytes, the bronchial epithelial cells are able to respond to *U. parvum* 3, 14 and *U. urealyticum* 2, by triggering the NF- $\kappa$ B pathway as well as the caspase-1 pathway – resulting in the secretion of pro-inflammatory cytokines, including IL-1 $\beta$ . Detection of P-I $\kappa$ B in all stimulated samples, at significantly higher levels compared to unstimulated samples, shows that NF- $\kappa$ B signaling pathway is activated (figure 4.2.2: A), as too is the activation of inflammasome complex structure formation, via caspase-1 p-10 detection (Figure 4.2.2 B). The results from the HEK-Blue reporter NF- $\kappa$ B and IL-1 $\beta$  experiments (figure 4.2.2: C) show a significant secretion of NF- $\kappa$ B and a very robust increase in IL-1 $\beta$  after stimulation with *Ureaplasma* SV2, SV3 and SV14.

Innate immune activation in BEAS-2B cells in response to *Ureaplasma* SV2, SV3 and SV14:



**Figure 4.2.2:** *Ureaplasma* SV2, SV3 and SV14 induce pro-inflammatory cytokine production and activation of immune response in BEAS-2B cells. BEAS-2B cells were incubated for 1-hour, being either not-stimulated or stimulated with *Ureaplasma* SV2, SV3 and SV14, after which cell lysates and supernatants were analysed. Cell lysates were analysed by SDS-PAGE and then transferred to nitrogen cellulose membranes using Western Blotting. Primary P-IkB-specific (A) and caspase-1-specific (B) antibodies were used to probe the membrane, and then incubated with HRP-conjugated secondary antibodies. The bands were visualized using Luminol-based enhanced chemiluminescent (ECL) substrate horseradish peroxidase (HRP). The bands observed are images are representatives of the three independent experiments. (C) Supernatants were incubated in HEK-NF-κB and HEK-IL-1β reporter cells for 24-hours. QUANTI-Blue™ (Invivogen) was then added and quantitative measurements were measured using spectrophotometry at 630nm. Cytokine concentration is proportional to secreted embryonic alkaline phosphates (SEAP) level concentration, which is measured by absorbance. The unstimulated sample results were used as a zero point.



**4.2.3: IL-1 $\beta$  production in bronchial epithelial cells in response to *Ureaplasma* occurs via NLRP3 and NLRP7 inflammasome activation:**

There are conflicting reports in the literature that suggest that NLRP7 has both activation and an inhibitory effect on active IL-1 $\beta$  production. NLRP7 expression is shown to be upregulated by the secretion of pro-inflammatory cytokines including IL-1 $\beta$ . NLRP7 has been shown to interact with pro-caspase-1, pro-IL-1 $\beta$ , ASC and Fas associated factor-1 (FAF-1), which are a likely link to the multiple mechanisms NLRP7 is associated with<sup>162-164,177</sup>.

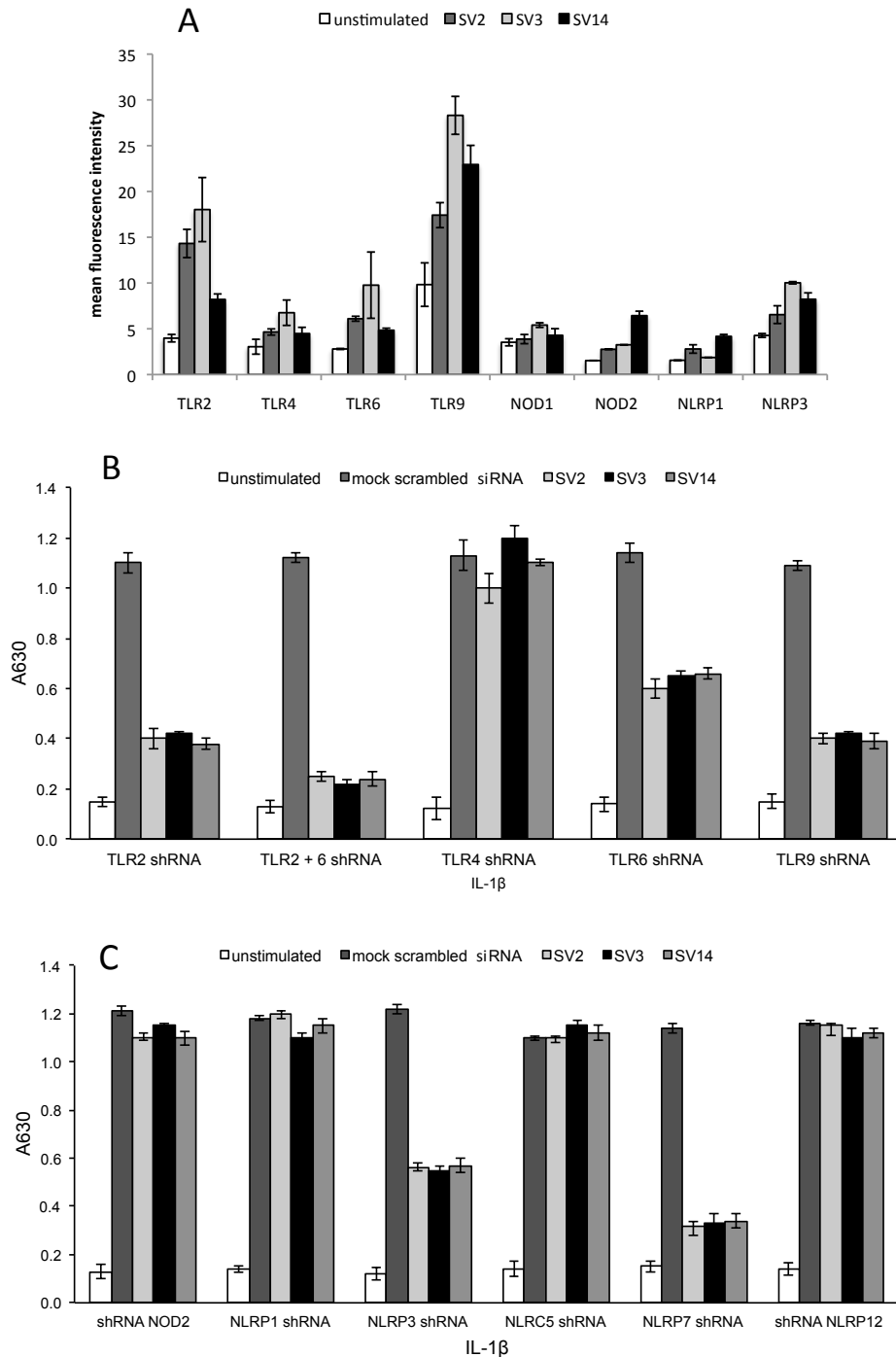
Interestingly, NLRP7 has been observed to also inhibit production of IL-1 $\beta$  and NLRP3 and caspase-1-mediated IL-1 $\beta$ , in addition to the inhibition of pro-caspase-1 and pro-IL-1 $\beta$  activation processing<sup>163</sup>. NLRP7 inflammasome has also been observed to activate caspase-1 and IL-1 $\beta$  by itself. The full regulatory roles of NLRP7 are still little known, but its association with IL-1 $\beta$  production in response to bacterial acylated lipoproteins have prompted us to investigate its role in *Ureaplasma* activation of the immune response<sup>164</sup>.

Other inflammasome associated NLRs will be investigated for their involvement in IL-1 $\beta$  production, as too will the roles of TLR2, TLR6 and TLR9, by using RNA interference to silence specific PRR genes. Bronchial epithelial cells were transfected with shRNA in order to silence (KD) specific PRRs. Once knock-down was achieved, the BEAS-2B-KD cell-lines were stimulated with *U. urealyticum* 2 and *U. parvum* 3 and 14 and incubated for 1-hour. IL-1 $\beta$  production was measured from the supernatants of each sample, using the HEK-Blue IL-1 $\beta$  reporter cell assay. The results showed a significant decrease in IL-1 $\beta$  produced by NLRP3 KD samples in response to all *Ureaplasma* serovars (Figure 4.2.3: C), however a more significant

inhibition of IL-1 $\beta$  was observed after NLRP7 KD (Figure 4.2.3: C), suggesting that NLRP3 and NLRP7 are the main NLRs involved in the innate immune sensing of *Ureaplasma*. There was no decrease in IL-1 $\beta$  after NOD2, NLRP1, NLRP12 or NLRC5 knock-down (Figure 4.2.3: C), suggesting that they do not play a role in *Ureaplasma*-induced IL-1 $\beta$  production.

Interestingly the most profound decrease in IL-1 $\beta$  was observed after TLR KD in BEAS-2B cells. The greatest IL-1 $\beta$  production inhibitor was the combination of TLR2/6 KD, which showed near complete IL-1 $\beta$  inhibition (Figure 4.2.3: B). KD of TLR9 also showed a highly significant decrease in the amount of IL-1 $\beta$  secreted, but to a lesser extent than the inhibition observed after TLR2/6 KD, suggesting that TLR2/6 might be providing the first or priming signal for inflammasome activation. Without the priming signal, the IL-1 $\beta$  production is inhibited.

IL-1 $\beta$  production in BEAS-2B cells in response to *Ureaplasma* occurs via NLRP3 and NLRP7 inflammasome activation:



**Figure 4.2.3:** IL-1 $\beta$  production in BEAS-2B cells in response to *Ureaplasma* occurs via NLRP3 and NLRP7 inflammasome activation. Bronchial epithelial cells were either not stimulated (white bar charts) or stimulated with *Ureaplasma* serovars for 1-hour. Scrambled siRNA was used as a mock transfection. The cells were fixed and permeabilised, followed by antibody staining against the particular PRR molecule, and incubation with the appropriate secondary antibody conjugated to FITC. Fluorescence was detected using a FACSCalibur (Becton Dickinson). The data presented is the mean of two independent experiments (A). PRR expression was knocked down by siRNA and following RNA interference, BEAS cells were not stimulated (white bar charts), or stimulated with *Ureaplasma* ( $1 \times 10^8$  bacteria/ml to  $1 \times 10^7$  cells/ml) *urealyticum* SV2 (dark grey bar chart), *U. parvum* SV3 (light grey bar charts) and *U. parvum* SV14 (black bar charts), for 1-hour (B and C). The supernatants were harvested and assayed for cytokine secretion using HEK-Blue IL-1 $\beta$  reporter cell assays. The data represents the mean  $\pm$  SD of three independent experiments (B and C).

### 4.3: Conclusion:

Bronchial epithelial cells seem to be at the forefront of interaction with *Ureaplasma* during infection. As already mentioned, *Ureaplasma spp.* have been associated with poor lung development in gestating infants, leading to BPD, therefore it is crucial to investigate the molecular mechanisms behind the innate immune recognition of *Ureaplasma* in the lung.

Our data suggests that *Ureaplasma* can trigger significant innate immune responses in bronchial epithelial cells. Following stimulation with *Ureaplasma* species upregulation of PRRs was observed as well as the production of pro-inflammatory cytokines, supporting the hypothesis that infection with *Ureaplasma* is strongly associated with the suggested poor formation of lung tissue during lung development in gestating infants leading to BPD. In particular, we have demonstrated that *Ureaplasma* SV2, SV3 and SV14 can activate the MyD88-dependent NF- $\kappa$ B-pathway, which leads to the secretion of pro-inflammatory cytokines. Furthermore, we have shown that there is *Ureaplasma*-induced caspase-1 activation; leading to secretion of IL-1 $\beta$ . This activation seems to require priming mechanisms via TLRs, most notably TLR2/6, and subsequently activation of NLRP3 and NLRP7 inflammasomes leading to IL-1 $\beta$  secretion. Our results suggest some association between NLRP3 and NLRP7 inflammasomes since the decrease observed in IL-1 $\beta$  after NLRP3 KD is too great to be brought about solely by NLRP3, as NLRP7 KD shows a much more significant role in IL-1 $\beta$  decrease, as it nearly completely inhibits IL-1 $\beta$  production after KD. Surely, the decrease in IL-1 $\beta$  after the KD of NLRP3 would not be so great as NLRP7 is still functioning. Therefore, we propose that there must be some kind of NLRP3-NLRP7 interaction that accounts for this,

maybe NLRP7 requires some NLRP3 function or protein association to function fully, or maybe there is overlap and redundancy for these two NLRs in bronchial epithelial cells.

## **Chapter 5:**

# ***U. parvum* SV3, SV14 and *U. urealyticum* SV2 activation of human amniotic epithelial cells**

## 5.1: Introduction:

Human amniotic epithelial cells (HAECs) are the first immune defense barrier against intrauterine pathogens, such as *Ureaplasma spp.* They are a highly suitable cell-line to investigate the innate immune response to *Ureaplasma spp.*, as their homeostasis is crucial for the welfare of the infant during gestation. Immune responses to pathogens in HAECs can bring about adverse pregnancy outcomes like PTB or spontaneous termination. HAECs possess few MHC antigens, likely due to their embryonic origin, but have been shown to possess TLRs, which could be responsible for the production and release of pro-inflammatory cytokines, such as IL-6, which has been strongly associated with adverse pregnancy outcomes<sup>178</sup>. HAECs were therefore chosen for this investigation and were stimulated with *Ureaplasma parvum* 3, 14 and *Ureaplasma urealyticum* 2 to measure the type and scale of immune response to the pathogens, which will produce information on the whether *Ureaplasma* can initiate immune responses that cause PTB or pPROM.

Carrying on from Chapter 5's preliminary time course studies using HAECs (data not included), the incubation time was increased from 1 hour (used for MM6 and BEAS-2B cell lines) to 2 hours. Cytokine production after 2 hours incubation was deemed more suitable than after 1 hour, especially when measuring immune response after MBA stimulation.

After an initial measurement of IL-12, TNF- $\alpha$ , IL-10, IL-6, IL-1 $\beta$  and IL-8 (all the cytokines included in the inflammatory cytokine bead assay (Becton Dickinson), we decided to investigate the levels of IL-6 in conjunction with pattern recognition receptors. Although levels of TNF- $\alpha$ , IL-1 $\beta$  and IL-8 are measured in some experiments, we concentrate on IL-6 as this is the cytokine most strongly associated with PTB in the literature<sup>193</sup>.

## 5.2: Results:

### 5.2.1: *Ureaplasma*-activation of human amniotic epithelial cells:

Using supernatants taken from HAECs after stimulation with *Ureaplasma parvum* 3, 14 and *Ureaplasma urealyticum* 2, quantitative measurements of pro-inflammatory cytokines (TNF- $\alpha$ , IL-1 $\beta$ , IL-6 and IL-8) produced were measured using CBA and analysed using Flow Cytometry and FACSCalibur. These pro-inflammatory cytokines are then compared to unstimulated HAECs and from the comparison of results, the immune response to *Ureaplasma parvum* 3, 14 and *Ureaplasma urealyticum* 2 by HAECs can be observed. The incubation time of *Ureaplasma parvum* 3, 14 and *Ureaplasma urealyticum* 2 with HAECs was decided to be 2 hours. Figure 5.2 reveals that all *Ureaplasma* servovars tested induced significant increase in TNF- $\alpha$ , IL-6, IFN- $\beta$  and IL-8 production in HAECs.

#### *Ureaplasma*-activation of human amniotic epithelial cells:

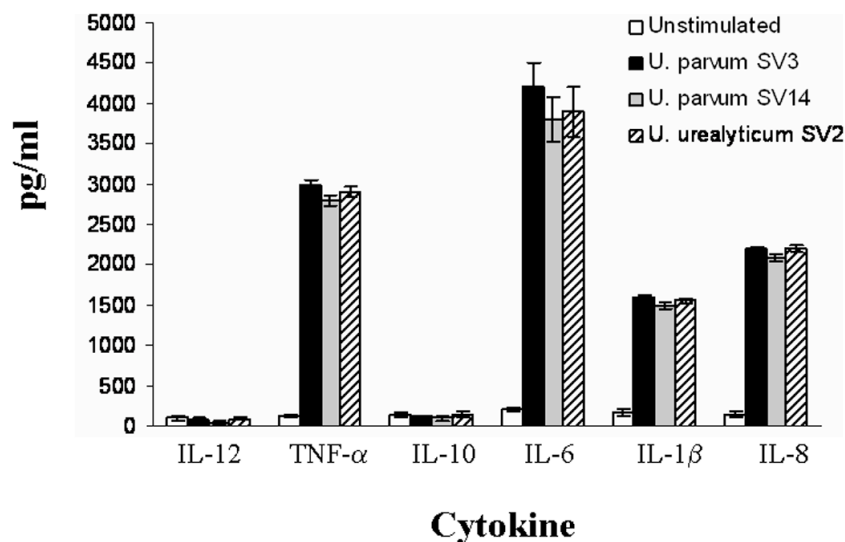


Figure 5.2: *Ureaplasma* activation of human amniotic epithelial cells. Human amniotic epithelial cells were incubated with *Ureaplasma* ( $1 \times 10^8$  bacteria/ml to  $1 \times 10^7$  cells/ml) *parvum* SV3 (black barcharts), *U. parvum* SV14 (white barcharts) or *U. urealyticum* SV2 (striped bar charts) for 2 h. The supernatants were harvested and assayed for cytokine contents using the Cytometric Bead Array (CBA) system (Becton Dickinson). Fluorescence was detected using a FACSCalibur (Becton Dickinson). The data represents the mean  $\pm$  SD of three independent experiments.

doi:10.1371/journal.pone.0061199.g001



### 5.2.2: TLR expression on human amniotic epithelial cells:

Initially we set out to investigate the expression levels of TLRs before and after stimulation with *Ureaplasma*. TLR1, 2, 4, 6, 7 and 9 expression levels in HAECs were measured before and after stimulations with *Ureaplasma parvum* 3, 14, *Ureaplasma urealyticum* 2 and MBA, to investigate which TLRs are upregulated after stimulation. In previous chapters it was shown that TLR1 expression was not upregulated by exposure to *Ureaplasma parvum* 3, 14 and *Ureaplasma urealyticum* 2, however it is included in this study to further investigate its role in *Ureaplasma* infection, as the cell-line is different and as more techniques are being employed in this study, which will further confirm or deny the involvement of TLR1 in stimulations with the *Ureaplasma* serovars chosen.

TLR7 was included in this study as an additional control, as it is a TLR that detects intracellular viral ssRNA and is localized internally bound to endosomes. As TLR7 only recognises ssRNA and *Ureaplasma spp.* do not contain ssRNA, making TLR7 a good control for this experiment.

*Ureaplasma spp.* are known to contain lipoproteins called MBA, which have been widely implicated in the literature as a major virulence factor component that could play a considerable role in initiating immune response during *Ureaplasma* infections<sup>21</sup>. MBA needs to be investigated to gain a better understanding whether MBA does stimulate TLR activation pathways, and if so, which TLRs, and how profound an immune response is initiated. MBA is a potentially extremely interesting PAMP to investigate, as it is a surface exposed lipoprotein that has been shown to be capable of varying its size and undergo phase variation<sup>19,20,179</sup>.

It was shown that after stimulation of HAECs with *Ureaplasma parvum* 3, 14, *Ureaplasma urealyticum* 2 and MBA, a significant increase in TLR2, 6 and 9 expression was observed, with the most significant increase in TLR upregulation being observed in TLR9 (Figure 5.2.3: A). After a 2-hour stimulation period with MBA, significant increase in TLR2 and TLR6 was observed, however upregulation of TLR9 was not observed after MBA stimulation of HAECs, (Figure 5.2.3: B)

### 5.2.3: TLR2/6, TLR4 and TLR9-dependent cytokine secretion in response to *Ureaplasma* serovars:

In order to verify which TLR is responsible for sensing *Ureaplasma*, HEK293 transfectants were used. HEK cells were transfected with TLR2, TLR2 and TLR6, TLR4 and MD-2, TLR7 and TLR9 in order to identify the roles in their immune response to the *Ureaplasma* serovars being investigated. HEK cells do not possess TLRs, and so by transfecting them with specific protein coding gene sequences, cellular models containing only the proteins wanting for investigating can be produced. In this study we produced HEK cell-lines that expressed TLR2, TLR2/6, TLR4/MD-2, TLR7 and TLR9. TLR6 requires TLR2 to form heterodimers to initiate activation, and TLR4 requires the additional transfection of MD-2 gene coding sequence, as TLR4 signaling pathway activation requires the MD-2 to mediate an immune response (Figure 5.2.3: B). HEK cells that were not transfected were used as a control against false positive cytokine production.

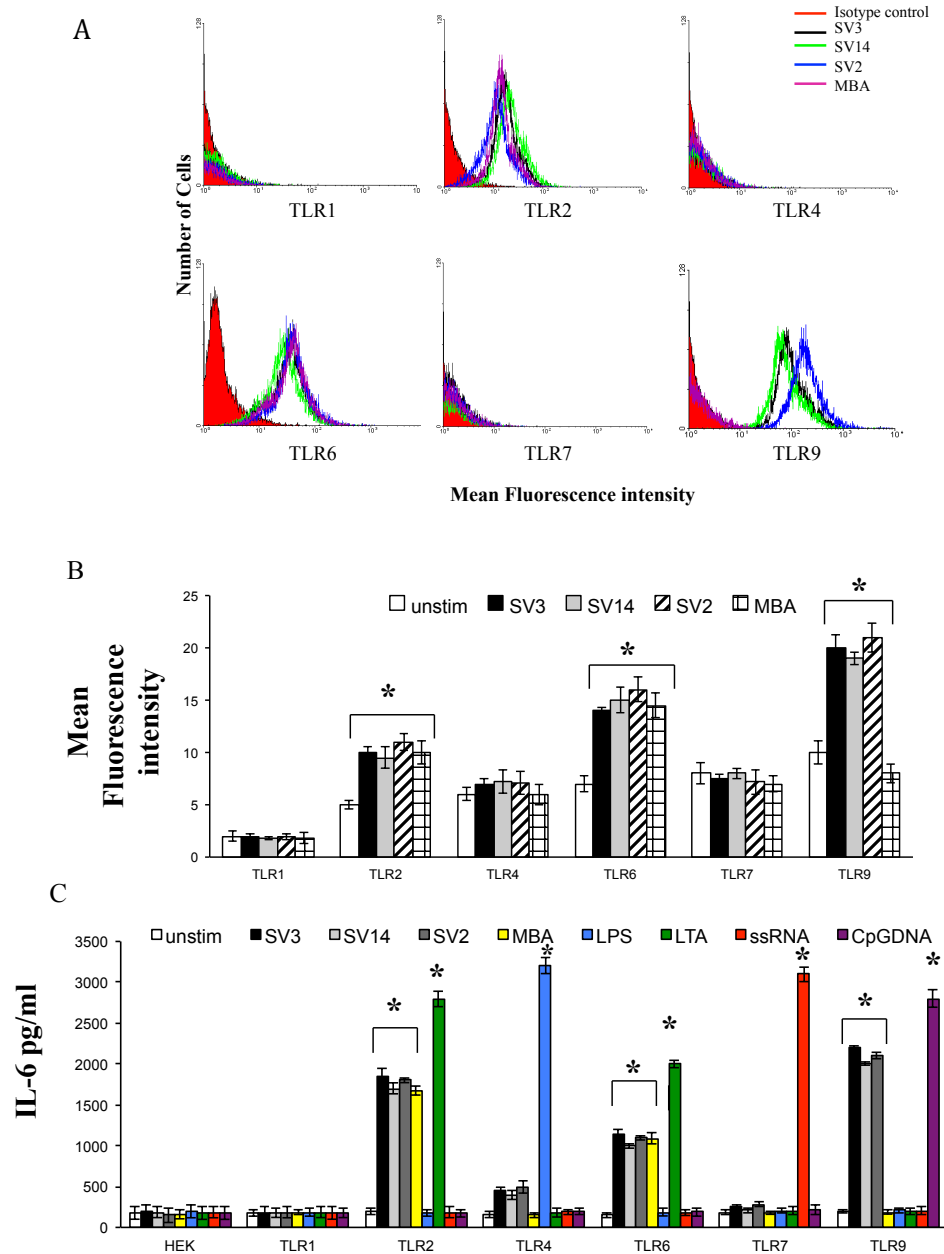
HEK-TLR2, HEK-TLR2/6, and HEK-TLR9 transfected cell-lines produced significantly high levels of IL-6 after stimulation with the *Ureaplasma* serovars, but only HEK-TLR2 and HEK-TLR2/6 transfected cell-lines showed a significant increase in IL-6 production when stimulated with MBA. These data suggest that TLR2/6 and TLR9 are the most effective PRRs at recognizing *Ureaplasma parvum* 3, 14 and *Ureaplasma urealyticum* 2 and TLR2 and TLR2/6 are responsible for recognizing MBA. TLR2 and TLR2/6 detect the PAMPs at the cellular surface, and TLR9 is responsible in detecting the *Ureaplasma* serovars investigated in intracellular compartments (Figure 5.2.3: A, B and C).

Non-transfected HEK cells were shown to produce no IL-6 after stimulation with the *Ureaplasma parvum* 3, 14, *Ureaplasma urealyticum* 2 and MBA; and the same was

found after stimulation of HEK-TLR7 transfected cells, where no IL-6 was produced. Similarly, HEK-TLR4/MD-2 transfected cells produced very low levels of IL-6 when stimulated with the *Ureaplasma* serovars, but did not produce IL-6 after stimulation with MBA (Figure 5.2.3: C).

In this study a number of control PAMPs were used in addition, each PAMP was selected as a positive control for each HEK-TLR transfected cell-line, (apart from HEK-TLR1). LTA is a known ligand of TLR2 and TLR2/6, LPS is a potent TLR4 ligand, ssRNA is a ligand for TLR7 and CpG DNA is a TLR9 ligand. As expected, the control PAMPs produced a more potent IL-6 production increase compared to the *Ureaplasma* serovars and MBA being investigated (Figure 5.2.3: C).

TLR2/6, TLR4 and TLR9-dependent cytokine secretion in response to  
*Ureaplasma* serovars:



**Figure 5.2.3:** TLR2/6 and TLR9-dependent cytokine secretion in response to *Ureaplasma* serovars. Human amniotic epithelial cells (A, B) were either not stimulated (white bar charts) or stimulated with *Ureaplasma* serovars for 2 hours. The cells were fixed and permeabilised, followed by antibody staining against the particular TLR molecule, and incubation with the appropriate secondary antibody conjugated to FITC. Fluorescence was detected using a FACSCalibur (Becton Dickinson). The data presented is the mean of three independent experiments. HEK-293 cells (B) transfected with TLR1, TLR2, TLR2/6, TLR4, TLR7 and TLR9 were either not incubated (white bar charts) or incubated with *Ureaplasma* ( $1 \times 10^8$  bacteria/ml to  $1 \times 10^7$  cells/ml) *parvum* SV3 (black bar charts), *U. parvum* SV14 (grey bar charts), *U. urealyticum* SV2 (stripped bar charts), or MBA (1 mg/ml) for 2 h. Control cultures were stimulated with known TLR2, TLR4, TLR7 or TLR9 ligands. The supernatants were harvested and assayed for IL-6 content using the Cytometric Bead Array (CBA) system (Becton Dickinson). Fluorescence was detected using a FACSCalibur (Becton Dickinson). The data represents the mean  $\pm$  SD of three independent experiments. Asterisks indicate statistically significant ( $p < 0.05$ ) increase in expression (A, B) or IL-6 secretion (C) compared to corresponding unstimulated controls.

**5.2.4: Inhibition of *Ureaplasma*-induced activation of human amniotic epithelial cells by silencing TLR2, TLR6 and TLR9:**

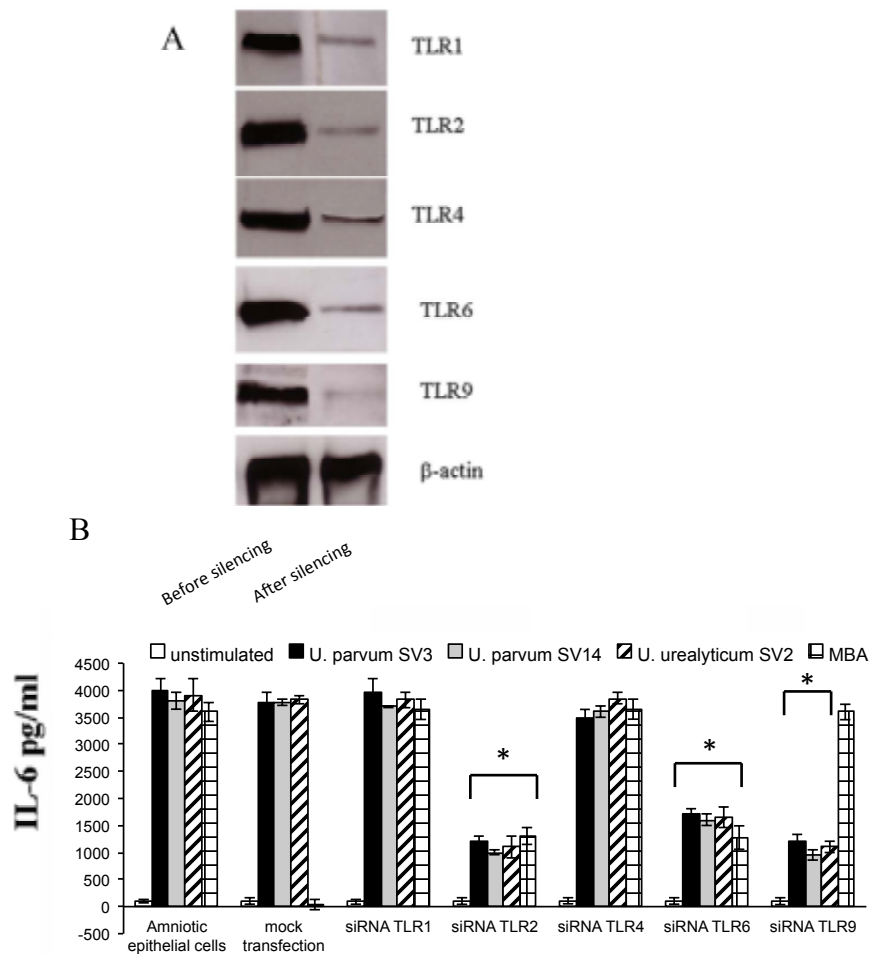
In order to investigate the role of different TLRs in HAEC responses against *Ureaplasma* siRNA was employed. By using RNA interference, specific target TLR expression can be downregulated (knocked down), and in so doing the function of the TLRs in the immune response can be investigated. Transfection with synthetic TLR specific psiRNAs, TLR2, 4, 6 and 9 into HAECs, achieved a TLR knock down (KD) efficiency of approximately 70%, measured by western blot (Figure 5.2.4: A). Control transfections of HAECs with psiRNA vectors had no affect on the expression of TLRs. TLR-KD HAECs were stimulated with *Ureaplasma parvum* 3, 14, *Ureaplasma urealyticum* 2 and MBA for 2 hours, after which, supernatant samples were taken for cytokine assaying and analysis using FACSCalibur.

TLR2 KD caused a significant decrease in the production of IL-6 by HAECs after the stimulation with *Ureaplasma parvum* 3, 14, *Ureaplasma urealyticum* 2 and MBA (Figure 5.2.4: B). A similar pattern of IL-6 production was found with TLR6 KD HAECs, however the extent of decrease in IL-6 production was slightly less than that of TLR2-KD. TLR9-KD again produced significant decreases in IL-6 when stimulated with *Ureaplasma parvum* 3, 14 and *Ureaplasma urealyticum* 2, however IL-6 production was unaffected by MBA stimulation in TLR9-KD (Figure 5.2.4: B).

Taking together these, results support that TLR2 homodimers and TLR2/6 heterodimers are the main cell surface detection receptors for these *Ureaplasma* serovars and MBA, and are responsible for *Ureaplasma*- and MBA-mediated immune response in HAECs. The importance of TLR9 in *Ureaplasma*-mediated immune activation is highlighted. TLR9 is the main intracellular receptor for

detecting *Ureaplasma parvum* 3, 14 and *Ureaplasma urealyticum* 2, but TLR9 does not detect MBA.

Inhibition of *Ureaplasma*-induced activation of human amniotic epithelial cells by silencing TLR2, TLR6 and TLR9:



**Figure 5.2.4:** Inhibition of *Ureaplasma* activation of human amniotic epithelial cells by silencing TLR2 and TLR9. TLR expression was knocked down by siRNA and confirmed by western blotting (A). Following RNA interference, human amniotic epithelial cells were not stimulated (white bar charts), or stimulated with *Ureaplasma* ( $1 \times 10^8$  bacteria/ml to  $1 \times 10^7$  cells/ml) *parvum* SV3 (black bar charts), *U. parvum* SV14 (grey bar charts), *U. urealyticum* SV2 (striped bar charts) or MBA (1 mg/ml) for 2 h (B). The supernatants were harvested and assayed for cytokine secretion using the Cytometric Bead Array (CBA) system (Becton Dickinson). Fluorescence was detected using a FACSCalibur (Becton Dickinson). The data represents the mean  $\pm$  SD of three independent experiments. Scrambled siRNA was used as a mock transfection. Asterisks indicate statistically significant (p,0.05) decrease in IL-6 secretion compared to corresponding unsilenced controls.

#### 5.2.5: TLR2 heterotypic association in response to *Ureaplasma*:

To investigate if *Ureaplasma parvum* 3, 14 and *Ureaplasma urealyticum* 2 were able to induce the formation of receptor activation clusters on the cellular surface of HAECs, FRET measurements were taken of selected TLR molecules, to establish their proximal interactions. Complete photobleaching of acceptor fluorophore enabled measurements of dequenching of donor fluorophores by confocal microscopy. A positive control was setup to establish the energy transfer efficiency in the system, which would allow for a relative maximum energy transfer efficiency (E%) value. To do this mAbs bound to different epitopes on TLR4 molecules were used, producing an E% of  $37 \pm 1.2$ .

The receptor we investigated was TLR2 and its interactions with the TLRs that had been implicated in forming receptor clusters (dimerizing) in response to *Ureaplasma*-induced activation, TLR1, 4 and 6. FRET measurements between TLR2 and the other receptor molecules were made after stimulation of HAECs with *Ureaplasma parvum* 3, 14, *Ureaplasma urealyticum* 2 and MBA. Prior to stimulations, no association between TLR2 and the other receptor molecules was detected. TLR2 was bound by Cy3-conjugated mAbs, whilst Cy5-conjugated mAbs were used to label the PRR molecule being investigated. The energy transfer between TLR2-Cy3 and PRR-Cy5 was measured in order to determine the level of association between the two molecules.

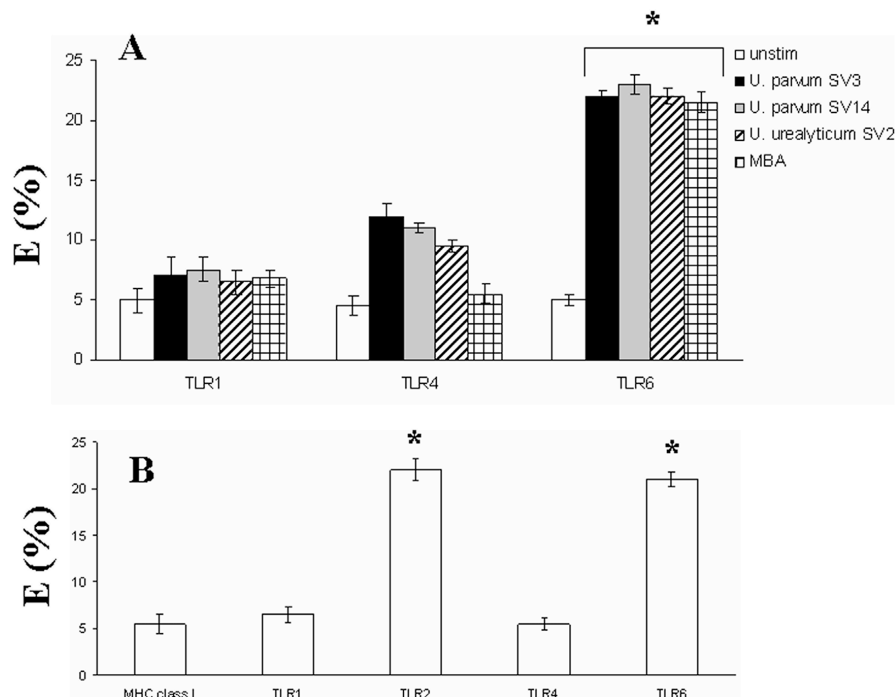
Association between TLR2 and TLR1 was not observed, a low level of association was observed between TLR2 and TLR4, but TLR2 and TLR6 were shown to associate very strongly after stimulation with the all *Ureaplasma* serovars (Figure 5.2.5: A). After stimulation with MBA, TLR2 was found to associate with TLR6, suggesting that MBA may induce TLR2/6 heterodimerization (Figure 5.2.5: A). To



investigate if MBA interacts directly with TLR2/6, FRET measurements between MBA-Cy3 and PRR-Cy5 were used. MBA was shown to interact directly with TLR2 and TLR6 ((Figure 5.2.5: B), supporting the hypothesis that MBA binds to TLR2/6 to initiate activation of the TLR2/6 immune response pathway.

To rule out the possibility that the FRET measurement could be due to randomly disturbed molecules control experiments were carried out in accordance with the methods described by Kenworthy et al, (data not shown).

#### TLR2 heterotypic association in response to *Ureaplasma*:



**Figure 5.2.5:** TLR2 heterotypic associations in response to *Ureaplasma*. (A) Human amniotic epithelial cells were stimulated with no stimulus (white bar charts), or incubated with *Ureaplasma* ( $1 \times 10^8$  bacteria/ml to  $1 \times 10^7$  cells/ml) *parvum* SV3 (black bar charts), *U. parvum* SV14 (grey bar charts), *U. urealyticum* SV2 (striped bar charts) or MBA (1 mg/ml) for 1 h. Energy transfer between TLR2 (Cy3) and the different receptors was measured from the increase in donor (Cy3) fluorescence after acceptor (Cy5) photobleaching. (B) Energy transfer between MBA (Cy3) and the different receptors was measured from the increase in donor (Cy3) fluorescence after acceptor (Cy5) photobleaching. The percentage of energy transfer and standard deviation was calculated from three independent experiments. Asterisks indicate statistically significant ( $p,0.05$ ) increase in energy transfer compared to corresponding unstimulated controls.  
doi:10.1371/journal.pone.0061199.g004

**5.2.6: TLR and GM-1 ganglioside FRET measurements before and after *Ureaplasma* stimulation:**

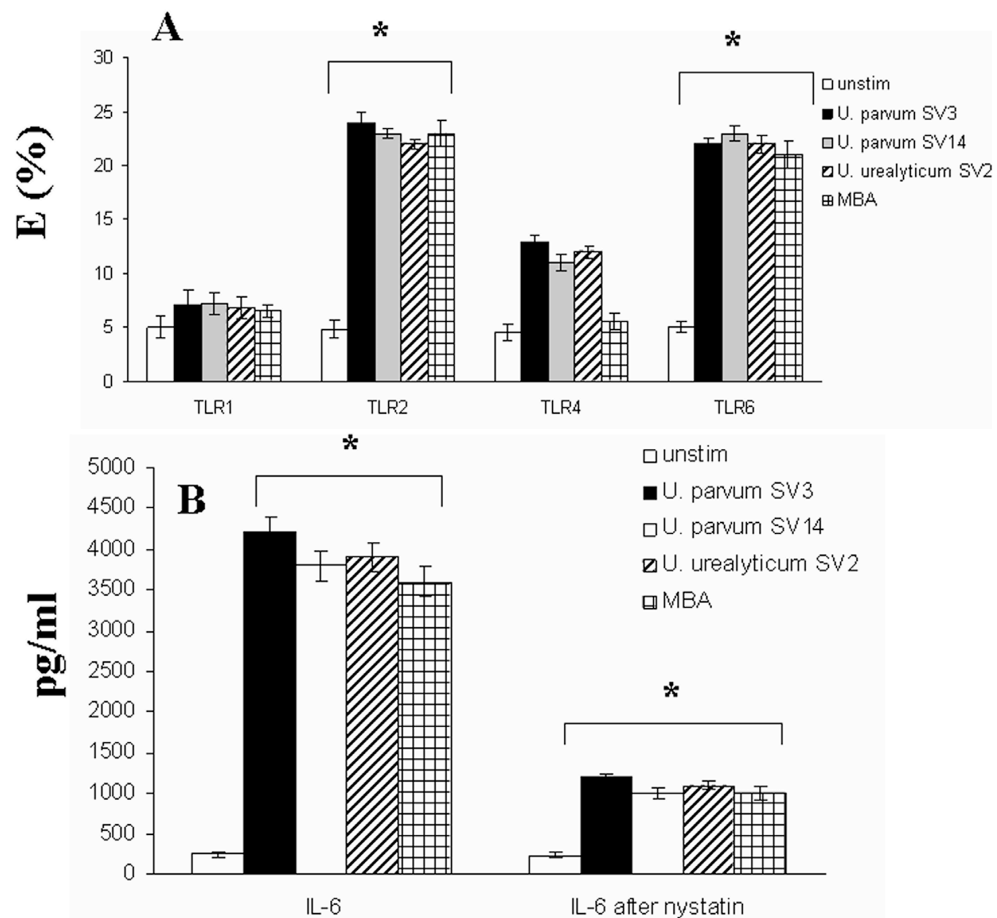
Recruitment of TLR4 to lipid rafts after stimulation with LPS has been shown to be crucial for TLR4 LPS-mediated activation and pro-inflammatory cytokine response<sup>180,181</sup>. TLR2 recruitment to lipid raft domains has also been shown to occur upon stimulation of TLR2 ligands<sup>182</sup>, and as we have observed that TLR2 is the main cellular surface receptor in detecting *Ureaplasma parvum* 3, 14 and *Ureaplasma urealyticum* 2, recruitment of TLR2 to lipid rafts was investigated. We measured FRET between TLR2 and GM-1 ganglioside, a raft associated lipid molecule to determine if TLR2-lipid raft association occurs after *Ureaplasma* and MBA stimulation in HAECs. TLR2 was labeled with Cy3-cojugated mAbs and GM-1 ganglioside was labeled with Cy5-cholera toxin and imaged using confocal microscopy. FRET experiments between TLR2 and GM-1 ganglioside were performed before and after stimulation the *Ureaplasma* serovars being investigated and MBA.

The results showed that TLR2 and TLR6 recruitment to lipid rafts does occur after stimulation with both *Ureaplasma parvum* 3, 14 and *Ureaplasma urealyticum* 2 and MBA (Figure 5.2.6: A). TLR1-GM-1 ganglioside association was not observed, further supporting that none of the *Ureaplasma* serovars, nor MBA are ligands for TLR1 and therefore TLR1 plays no role in the immune response of HAECs against the *Ureaplasma* serovars used in this investigation. Likewise TLR4-GM-1 ganglioside association was minimal when compared to TLR2-GM-1 ganglioside association after stimulation with the *Ureaplasma* serovars used and MBA (Figure 5.2.6: A). These findings lead us to believe that TLR2/6 heterodimer needs to form for the recognition of *Ureaplasma* serovars.

To test the significance of the TLR-lipid raft recruitment FRET measurements observed, nystatin, a lipid raft-disrupting molecule was used. By disrupting the lipid raft formation, we could determine if the TLR2-lipid raft recruitment is necessary for *Ureaplasma*-induced TLR2 activation. After comparing IL-6 levels produced by HAECs treated with or without nystatin, following stimulation with *Ureaplasma parvum* 3, 14 and *Ureaplasma urealyticum* 2, it was shown that HAECs pretreated with nystatin produced significantly less IL-6 compared to non-treated HAECs (Figure 5.2.6: B). These data support the hypothesis that the accumulation and recruitment of TLR2 and TLR6 within lipid rafts is crucial for the immune signaling and pro-inflammatory cytokine production in response to the *Ureaplasma* serovars investigated.

## TLR and GM-1 ganglioside FRET measurements before and after

### Ureaplasma stimulation:

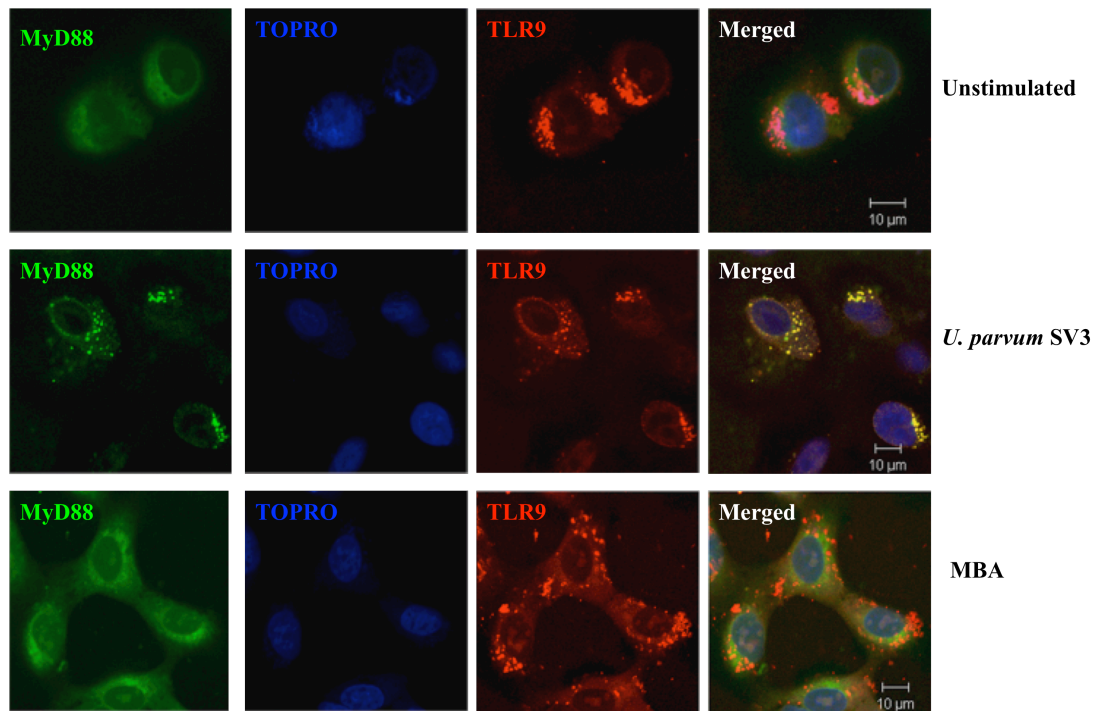


**Figure 5.2.6:** TLR and GM-1 ganglioside FRET measurements before and after Ureaplasma stimulation. TLR and GM-1 ganglioside FRET measurements before and after Ureaplasma stimulation of human amniotic epithelial cells (A). Energy transfer between Cy3-labelled TLR1, TLR2, TLR4 or TLR6 and GM-1 ganglioside (Cy5-cholera-toxin) before (white bar charts) and after stimulation with Ureaplasma ( $1 \times 10^8$  bacteria/ml to  $1 \times 10^7$  cells/ml) parvum SV3 (black bar charts), U. parvum SV14 (grey bar charts), U. urealyticum SV2 (striped bar charts) or MBA (1 mg/ml). Energy transfer between GM1 (Cy5) and the different receptors was measured from the increase in donor (Cy3) fluorescence after acceptor (Cy5) photobleaching. The percentage of energy transfer and standard deviation was calculated from three independent experiments. Asterisks indicate statistically significant ( $p, 0.05$ ) increase in energy transfer compared to corresponding unstimulated controls. (B) Inhibition of IL-6 production after lipid raft disruption. Human amniotic epithelial cells were either not treated (white bar charts) or pre-treated with nystatin and subsequently stimulated with the different Ureaplasma serovars or MBA. The supernatants were harvested and assayed for cytokine content using the Cytometric Bead Array (CBA) system (Becton Dickinson). Fluorescence was detected using a FACSCalibur (Becton Dickinson). The data represents the mean  $\pm$  SD of three independent experiments. Asterisks indicate statistical significance ( $p, 0.05$ ).  
doi:10.1371/journal.pone.0061199.g005

#### 5.2.7: *Ureaplasma* internalization recruits MyD88 in endosomes:

Using confocal microscopy, we investigated the intracellular recognition mechanism in response to *Ureaplasma* stimulation. Since our data has suggested that TLR9 is the main intracellular receptor, confocal microscopy was employed to further elucidate the intracellular interactions between TLR9, *Ureaplasma parvum* 3 and MBA. Anti-MyD88-FITC was used to fluorescently tag MyD88 molecules, which is an obligatory adaptor molecule for the TLR9 MyD88-dependent signaling pathway. TLR9 molecules were fluorescently tagged using anti-TLR9-TRITC and TORRO was used to fluorescently tag the nucleus of HAECs. HAECs stimulated with *Ureaplasma parvum* 3 or MBA were compared to unstimulated HAECs. By imaging the intracellular trafficking of TLR9 and MyD88, in addition to imaging the cellular nucleus, we could determine whether signal transduction occurs through TLR9 that is a receptor associated to the endosome. The results showed MyD88 recruits to endosomes, where it associates with TLR9 after stimulation with *Ureaplasma urealyticum* 3 (Figure 5.2.7: middle row). MBA stimulation did not cause recruitment of MyD88 to the endosome, as we were expecting from the previous experiments (Figure 5.2.7: bottom row).

### *Ureaplasma* internalization recruits MyD88 in endosomes:



**Figure 5.2.7: *Ureaplasma* internalization recruits MyD88 in endosomes.** Human amniotic epithelial cells were either not stimulated (top panels) or stimulated with either *Ureaplasma* SV3 (middle panels) or MBA (bottom panels) and imaged using a Zeiss 510 META confocal microscope. Intracellular MyD88 was stained using a polyclonal antibody directly labelled with FITC. TLR9 were labelled using anti-TLR9-TRITC. TOPRO was used to label the nucleus of the cells. Merged images showing extensive overlay of areas positive for MyD88 and TLR9 are seen as yellow (Scale Bar, 10  $\mu$ m).  
doi:10.1371/journal.pone.0061199.g006

### **5.3: Conclusion:**

The results showed that *Ureaplasma* SV2, SV3 and SV14 stimulation significantly increased levels of the pro-inflammatory cytokines TNF- $\alpha$ , IL-6, IL-8 and IL-1 $\beta$  in HAECs compared to unstimulated HAECs. Expression levels of TLR2, TLR26 and TLR9 were significantly increased in response to *Ureaplasma* stimulation, which supports that TLR-mediated MyD88-dependent immune signaling pathways are activated in response to the serovars examined. After stimulating HAECs with the *Ureaplasma* cell surface exposed lipoprotein MBA, only TLR2 and TLR6 showed

upregulated expression of the cell surface TLRs, TLR2 and TLR6, but not TLR9. These results suggest that *Ureaplasma* is first detected at the HAEC cell surface via TLR2 and TLR6 and then by TLR9 after *Ureaplasma* internalization.

The transfection of HEK-293 cells with TLR2, TLR6 and TLR9 all showed increased IL-6 cytokine production in response to *Ureaplasma* serovar stimulations, but did not show an increase in IL-6 production in HEK-TLR9 transfects after stimulation with MBA, which further supports the hypothesis that TLR2 and TLR6 detect *Ureaplasma* MBA at the HAEC surface, and that TLR9 only detects internalised *Ureaplasma* material. FRET measurements confirmed that TLR2 and TLR6 co-localise after *Ureaplasma* and MBA stimulation. FRET measurements also confirmed that TLR2/6 localise in cellular lipid rafts after both *Ureaplasma* and MBA stimulation, supported by the lack of association of TLR2/6 to lipid rafts after incubating the cells in nystatin, a lipid raft disruptor, which also resulted in inhibition of IL-6 production. In addition, using FRET the co-localisation of TLR9 and MyD88 at the endosomal membrane was shown, but that this co-localisation did not occur after MBA stimulation, supporting the hypothesis that TLR9 does detect *Ureaplasma* but not MBA. The activation of inflammatory immune responses in HAECs by *Ureaplasma* and its lipoproteins, support the studies linking *Ureaplasma* upper genital tract infection with PTB and pPROM.

## **Chapter 6:**

# **Investigation into NLRs in *Ureaplasma*-activated immune response in human amniotic epithelial cells**



## 6.1: Introduction:

NLRs are a family of intracellular PRRs that detect cytoplasmic PAMPs and DAMPs<sup>146</sup>. Different member of receptors within the NLR family have been shown to perform different roles in the innate immune response, for example NOD1 and NOD2 activate NF- $\kappa$ B signaling cascades upon recognition of PAMPs and initiate upregulation of pro-inflammatory cytokines, where as NLRP1 and NLRP3 have been shown to form multiprotein complexes called inflammasomes that trigger activation of IL-1 $\beta$  and IL-18 via caspase-1 activation. Furthermore recent studies have shown that NLRPs can have both a stimulatory effect on the innate immune response as well as an inhibitory role<sup>162,163</sup>. NLRs, such as NLRP7 have recently been shown to not only regulate immune responses, but also play a crucial role in development of the fetus during gestation, like the initial Toll receptor first identified in *Drosophila*. NLRP7 has been associated with recurrent miscarriages, as well as playing a role in the inflammasome regulation and immune response to acylated bacterial lipoproteins FSL-1 and triacylated Pam<sub>3</sub>CSK<sub>4</sub><sup>164,183</sup>. The association between recurrent miscarriage and immune response to lipoproteins peaked our interest into the possible involvement of this NLRP and *Ureaplasma*-activated immune response, though the mechanisms surrounding NLRP7 activation and functions still remain far from clear.

Inflammasome activation is thought to require a two-step signaling process, step-one ‘priming’ signals that activate transcription of specific cytokine genes, in their inactive pro-forms, such as pro-IL-1 $\beta$  and pro-IL-18. This upregulation in transcription is thought to be achieved via PRRs such as TLRs and NOD1 and

NOD2 NLRs<sup>156</sup>. The second step requires signaling of inflammasome multiprotein complex formation and activation, via an as yet unknown mechanism. There are four suggested mechanisms for the formation of NLRP3 inflammasomes, 1) K<sup>+</sup> efflux, 2) ROS reaction, 3) lysosomal disruption and 4) cellular Ca<sup>2+</sup> influx<sup>146-149 150 151 152</sup>.

NLRP7 activation mechanisms are even less well understood than those of NLRP3, however Khare's study implicated the possible involvement of K<sup>+</sup> and cathepsin B, after the use of inhibitors to both these mechanisms and finding that they reduced IL-1 $\beta$  production in response to FSL-1 via NLRP7<sup>164</sup>. In this chapter, we investigate the actions of cell wall-less bacterial (*Ureaplasma*) lipoproteins to determine NLRP7s involvement in the detection of *Ureaplasma*, as our previous data have shown that neither NLRP1 nor NLRP3 inflammasomes have shown to form upon stimulation with *Ureaplasma*-activation.

In this chapter, we demonstrate that NLRP7 is responsible for the detection of lipoproteins found in *Ureaplasma* and furthermore that it is this mechanism that is responsible for the production of active IL-1 $\beta$  and caspase-1 observed in response to *Ureaplasma*.

Serovars 1,2,4 and 6 were chosen in this chapter so we could observe the effect of two *U. urealyticum* serovars (SV 2 and 4) and two *U. parvum* serovars (SV 1 and 6), which would enable us to determine if the immune response was directly related to serovar or if other factors contributed to the immune response. Procurement of serovars 3 and 14 was difficult, but there was no significant difference in urease activity or immune response in HAECs (when tested in preliminary experiments, not included), between serovars 3 and 14, and serovars 1, 3 and 6. For these reasons serovars 1, 3 and 14 were used in the investigation in this chapter.

## 6.2: Results:

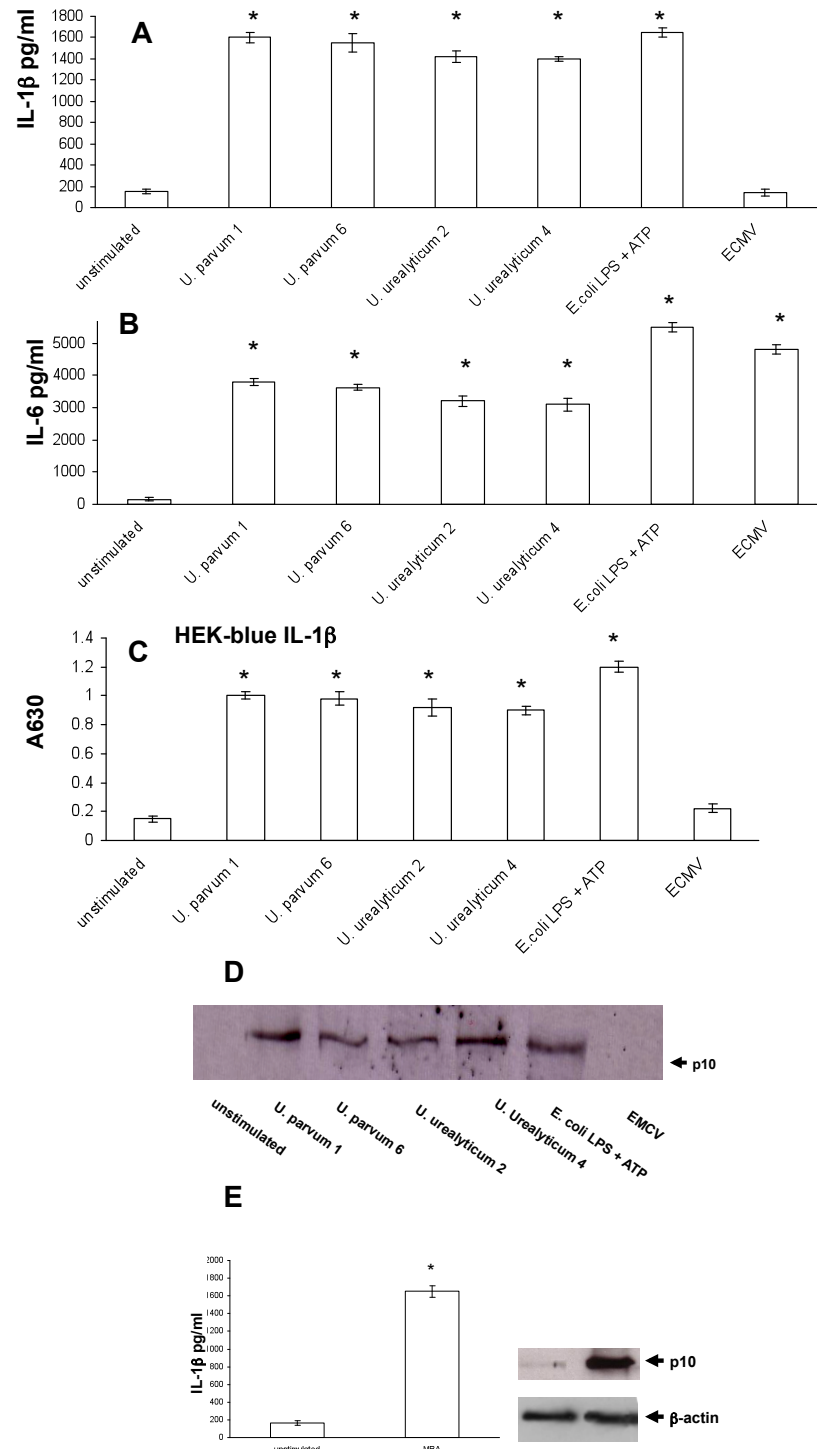
### 6.2.1: *Ureaplasma* infection induces inflammasome activation:

Using HAECs we investigated whether *Ureaplasma* initiated inflammasome activation by measuring IL-1 $\beta$  production after *Ureaplasma parvum* 1 and 6, and *Ureaplasma urealyticum* 2 and 4 stimulation. Positive controls were set up for each experiment, using *E.coli* LPS+ATP, which in combination are well-established IL-1 $\beta$  and NLRP 1 and NLRP3 inflammasome activators. For negative controls, encephalomyocarditis virus (EMCV) was used, as it is unable to activate inflammasome complex formation without initial priming by a PAMP such as LPS. Inflammasome complex activation was measured by the production of IL-1 $\beta$  and caspase p10 activation/fragmentation (Figure 6.2.1: A, B and D, respectively). IL-1 $\beta$  concentrations were measured from sample supernatant using CBA cytokine assaying and FACSCalibur (Becton Dickinson) (Figure 6.2.1: A), HEK-Blue IL-1 $\beta$  reporter cells (Figure 6.2.1: C), whilst the presence of caspase-1 p10 was detected from lysates using western blotting (Figure 6.2.1: D). Caspase 1 p10 is part of the inhibitory subunit that keeps caspase-1 in an inactive pro-form until inflammasome complexes cleave the inhibitory subunit, releasing active (mature) caspase-1. The results show production of IL-1 $\beta$  and caspase-1 p10 after stimulation with all of the *Ureaplasma* serovars investigated, the positive control, LPS+ATP, but not by EMCV (as expected).

To investigate whether the observed results were a result of whole cell *Ureaplasma* detection or whether HAECs initiated immune response to the surface exposed *Ureaplasma* lipoprotein MBA, MBA-induced IL-1 $\beta$  and caspase-1 p10 production

was measured, (Figure 6.2.1: E). Like in chapter 5, MBA was shown to be detected by HAECs and also activate production of active IL-1 $\beta$  and capsase-1, which further support the potential pathogenic properties of MBA as well as the ability for MBA to activate inflammasome-mediated immune responses<sup>22</sup>. All *Ureaplasma* serovars samples, positive and negative controls stimulated significant increases in the production of IL-6 compared to unstimulated cell samples, which was to be expected, since it is independent of NLRP inflammasome activity (Figure 6.2.1: B).

### *Ureaplasma* infection induces inflammasome activation:



**Figure 6.2.1:** *Ureaplasma* infection induces inflammasome activation. Amniotic epithelial cells were infected with *Ureaplasma* species ( $1 \times 10^8$  bacteria/ml to  $1 \times 10^7$  cells/ml) or 5 MOI ECMV, or 100 ng/ml *E. Coli* LPS+ 5 mM ATP. Supernatant was collected at 12 hr post infection and analysed for IL-1 $\beta$  (A) and IL-6 (B) using the CBA bead array system on a FACSCalibur (Becton Dickinson). Activation of the inflammasome was confirmed using the HEK-blue IL-1 $\beta$  reporter cell line (C). Cell supernatants were analysed for the presence of caspase 1 p10 and cell extracts for the presence of pro-IL1 $\beta$  by western blotting (D). Amniotic epithelial cells were also stimulated with 1  $\mu$ g/ml MBA and inflammasome activation was confirmed by IL-1 $\beta$  secretion as well as by the presence of caspase 1 p10 by western blotting (E). The data represent the mean of three independent experiments. Asterisks indicate statistically significant ( $p < 0.05$ ) increase in cytokine secretion compared to corresponding unstimulated controls.

**6.2.2:** *The NLRP7 and NLRP3 inflammasome are triggered in response to Ureaplasma infection:*

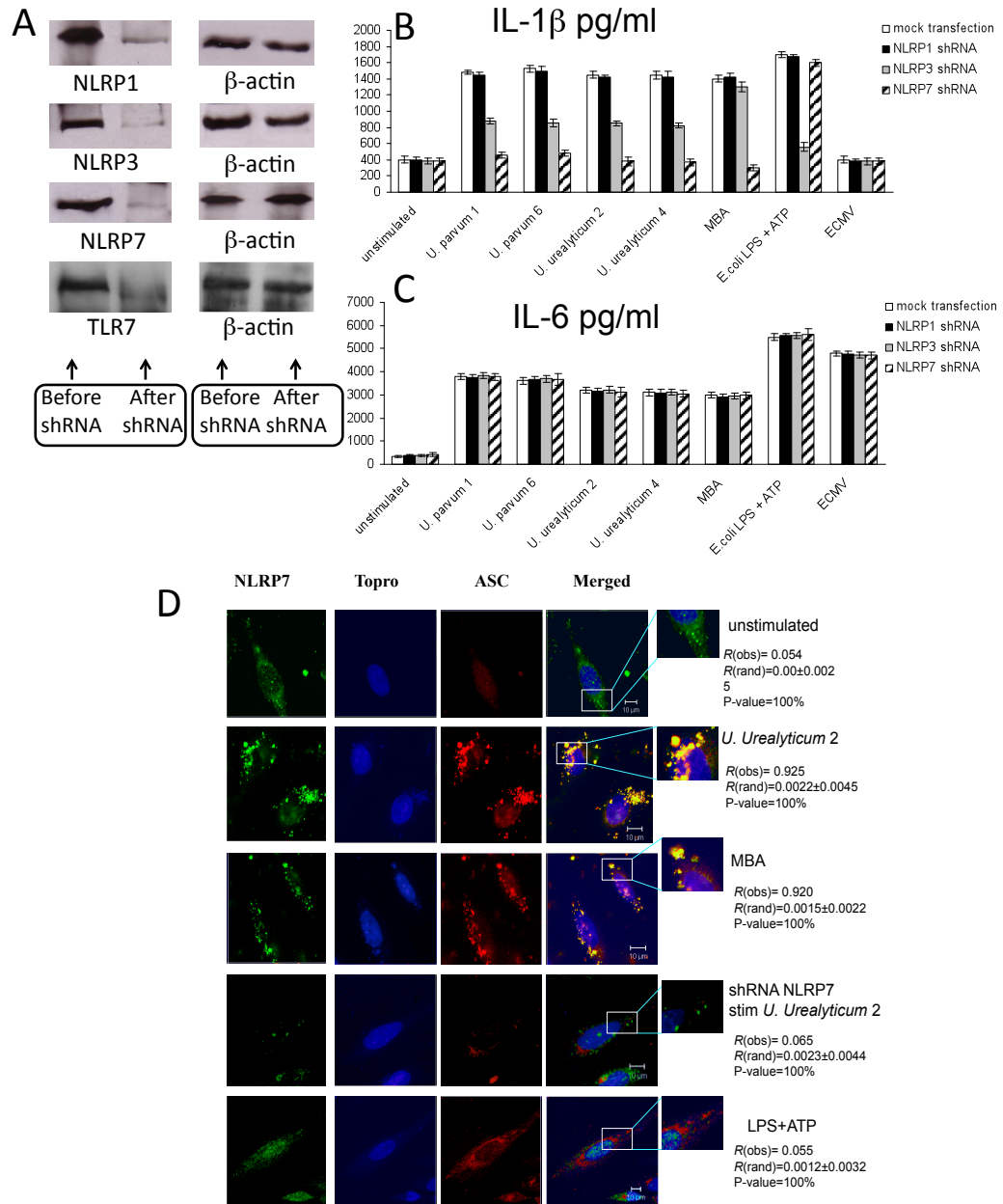
To identify the NLR inflammasomes activated by stimulation with *Ureaplasma* and MBA, RNA interference of NLRP1, NLRP3 and NLRP7 genes was performed using shRNA to knock down (KD) the expression of each of these proteins. Western blots taken from lysates of KD HAECs were compared to wild-type HAECs to assess if KD of these NLRs was achieved (Figure 6.2.2 A) TLR7 shRNA was also examined as a negative control. IL-1 $\beta$  and IL-6 (Figure 6.2.2 B and C) concentrations were measured in KD HAECs and compared to concentrations measured in wild-type HAECs using CBA (Becton Dickinson), in order to examine the effect of each NLR KD on the *Ureaplasma* and MBA stimulated cell samples. There was a significant reduction in IL-1 $\beta$  production in NLRP7 KD cell-lines after stimulation with both *Ureaplasma* serovars and with MBA. NLRP3 KD HAECs showed a reduction in IL-1 $\beta$  production after stimulation with *Ureaplasma* serovars, but the extent of reduction in IL-1 $\beta$  was far smaller than that observed in NLRP7 KD samples. Interestingly no reduction in IL-1 $\beta$  production was observed in NLRP3 KD samples after stimulation with MBA, and furthermore no reduction was observed after stimulation with either MBA or any of the *Ureaplasma* serovars in NLRP1 KD HAECs. As predicted ECMV was unable to produce IL-1 $\beta$  production in any of the KD cell-lines, and IL-6 production was unaffected by the NLR KDs (Figure 6.2.2: B and C). Taken together these data suggest that NLRP7 is the major sensory mechanism in the detection of *Ureaplasma* and through its lipoprotein MBA.

To verify NLRP7 activation in response to *Ureaplasma* and MBA, confocal microscopy was used to measure association and interaction of inflammasome associated protein ASC with NLRP7 after stimulation with *Ureaplasma* and MBA.

In unstimulated samples NLRP7 and ASC did not co-localise, suggesting that there was no NLRP7 inflammasome activation (Figure 6.2.2: D top row). In samples stimulated with *Ureaplasma* SV2 (Figure 6.2.2: D second row) and MBA (Figure 6.2.2: D third row) co-localisation between NLRP7 and ASC was observed supporting NLRP7 inflammasome activation after stimulation with *Ureaplasma* and MBA. Further support for these findings were shown, when no co-localisation was observed in NLRP7 KD cell-lines after the same stimulations were performed (Figure 6.2.2: D forth row). LPS+ATP (NLRP3 activators) stimulation showed to induce co-localisation between NLRP7 and ASC, supporting the conclusion that no inflammasome activation was established (Figure 6.2.2: D bottom row).

Costes' approach was used to quantify the degree of co-localisation, which uses Pearson's correlation coefficient to remove random pixel distribution from the observed images. This technique returned statistically significant measurements of 0.925 and 0.920 after *Ureaplasma* SV2 and MBA stimulation, respectively. These results are about as close to the theoretical maximal values achievable, where +1.0 indicates total positive significance, 0.0 indicates total randomness and -1.0 indicates total negative significance. These findings strongly support that NLRP7 directly interacts and associates with ASC after stimulation with *Ureaplasma* SV2 and MBA, and NLRP7 inflammasome formation results. In contrast NLRP7 KD and LPS+ATP results returned values of 0.065 and 0.055 (respectively), indicating no significant co-localisation.

The NLRP7 and NLRP3 inflammasome are triggered in response to *Ureaplasma* infection:



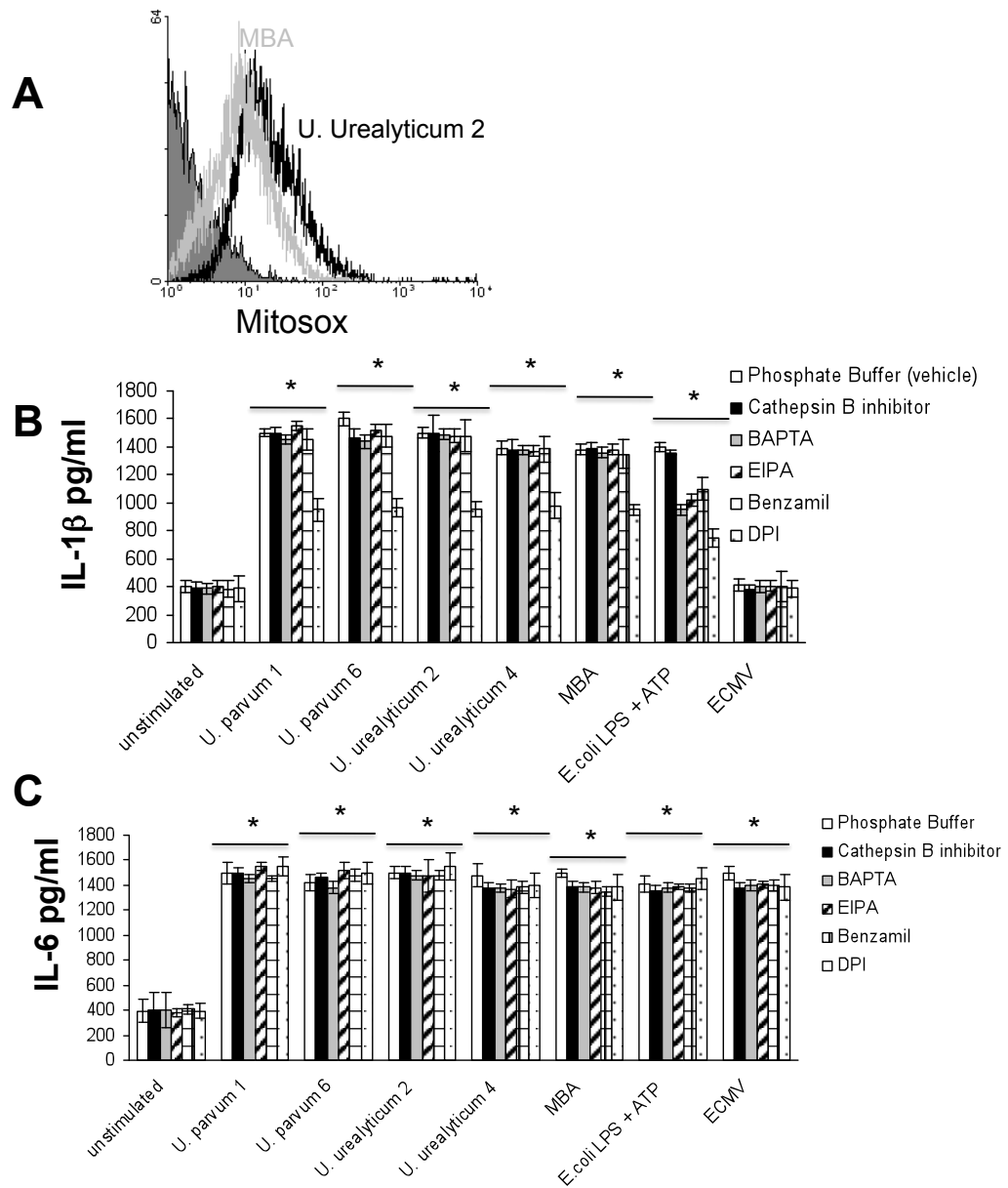
**Figure 6.2.2:** The NLRP7 and NLRP3 inflammasome are triggered in response to *Ureaplasma* infection. NLRP1, NLRP3 and NLRP7 expression was knocked down by shRNA (A). The levels of non-targeted NLRs were also determined by western blotting in order to confirm specificity of the knockdown. shRNA TLR7 is also used as an irrelevant control and the expression levels of NLRs are investigated (A). The knocked down cells were infected with *Ureaplasma* species ( $1 \times 10^8$  bacteria/ml to  $1 \times 10^7$  cells/ml) or ECMV (5 moi) or stimulated with 1  $\mu\text{g/ml}$  MBA, or 100 ng/ml *E. coli* LPS + 5 mM ATP. Supernatant was collected after 12hr and analysed for IL-1 $\beta$  (B) and IL6 (C) using the CBA system. The data represent the mean of three independent experiments. Asterisks indicate statistically significant ( $p < 0.05$ ) increase in cytokine secretion compared to corresponding unstimulated controls. The localisation of NLRP7 and ASC was investigated when cells were either not stimulated (D, top row) or stimulated with *U. urealyticum* 2 (D, second row), with MBA (D, third row), or with 100 ng/ml LPS + 5 mM ATP (D, fifth row). Cells expressing NLRP7 shRNA were also challenged with *U. urealyticum* 2 (D, fourth row). Cells were stimulated with the different stimuli for 1 h and subsequently fixed. NLRP7 was stained using a rabbit anti NLRP7 Fab conjugated to Alexa 488, ASC was stained using a goat anti ASC Fab conjugated to Alexa 546. Cells were imaged using a Zeiss 510 confocal microscope. Bars represent 10  $\mu\text{m}$ . Co-localization coefficients [ $R(\text{obs})$ ] between NLRP7 and ASC were calculated using Costes' approach.



### 6.2.3: Effects of inhibitors on *Ureaplasma*-induced inflammasome activation:

As mentioned above, initial priming signal is thought to be required to upregulate transcription of pro-IL-1 $\beta$  and pro-IL-18 genes<sup>156</sup>, which has been associated with *Ureaplasma*-activated TLR responses<sup>22</sup>. From the pre-mentioned four suggested mechanisms for signal-two activation, we set out to determine which could be associated with NLRP7 inflammasome activation by *Ureaplasma* and MBA. To do this we used ROS inhibitor Mitosox (Figure 6.2.3: A), cathepsin B inhibitor treated HAECs, BAPTA (a Ca<sup>2+</sup> chelator), ethyl-isopropyl amiloride (EIPA), (ion channel inhibitor), Benzamil (Na<sup>+</sup>/H<sup>+</sup> inhibitor) and Diphenyleneiodonium (DPI), (ROS inhibitor), and carried out stimulations with *Ureaplasma* serovars, MBA and controls LPS+ATP and ECMV (figure 6.2.3: B). MBA-induced production of IL-1 $\beta$  was reduced by DPI as well as in *Ureaplasma* stimulated samples, however the reduction in IL-1 $\beta$  was not fully inhibited, suggesting *Ureaplasma* must trigger some IL-1 $\beta$  production via ROS. None of the other inhibitors showed the same levels of IL-1 $\beta$  reduction in response to *Ureaplasma* and MBA stimulation. As expected, IL-6 levels, which are inflammasome independent, remained unaffected (Figure 6.2.3: C).

### Effects of inhibitors on *Ureaplasma*-induced inflammasome activation:



**Figure 6.2.3:** Effects of inhibitors on *Ureaplasma*-induced inflammasome activation.

Amniotic epithelial cells were either infected with *Ureaplasma* species ( $1 \times 10^8$  bacteria/ml to  $1 \times 10^7$  cells/ml) or stimulated with  $1 \mu\text{g/ml}$  MBA and ROS production was detected by flow cytometry using Mitosox (A). Amniotic epithelial cells were infected with 5 MOI of *Ureaplasma* species or ECMV (5 moi) or stimulated with  $1 \mu\text{g/ml}$  MBA, or  $100 \text{ ng/ml}$  *E. coli* LPS+5 mM ATP in the presence of cathepsin B inhibitor, BAPTA (a  $\text{Ca}^{2+}$  inhibitor), EIPA (ethyl-isopropyl amiloride, an ion channel inhibitor), Benzamil (inhibitor of  $\text{Na}^+/\text{H}^+$ ) and Diphenyleneiodonium or DPI (a ROS inhibitor). Phosphate buffer (20mM) was used as the vehicle control. Supernatant was collected after 12hr and analysed for IL-1 $\beta$  (B) and IL6 (C) using the CBA system. The data represent the mean of three independent experiments. Asterisks indicate statistically significant ( $p < 0.05$ ) increase in cytokine secretion compared to corresponding unstimulated controls.

#### 6.2.4: $\text{NH}_3$ triggers NLRP7 inflammasome activation:

The generation of  $\text{NH}_3$  (ammonia) by urease in *Ureaplasma* was a suitable second-step signal pathway initiator to investigate. Initial investigations into the speed at which  $\text{NH}_3$  accumulates in cultured HAECs infected with *Ureaplasma* were examined. The results showed rapid production of  $\text{NH}_3$  in cellular supernatants, which continued to increase with increased incubation time (Figure 6.2.4: A). No  $\text{NH}_3$  production was detected in any of the controls sample, of LPS+ATP, ECMV or in MBA stimulated cultures.

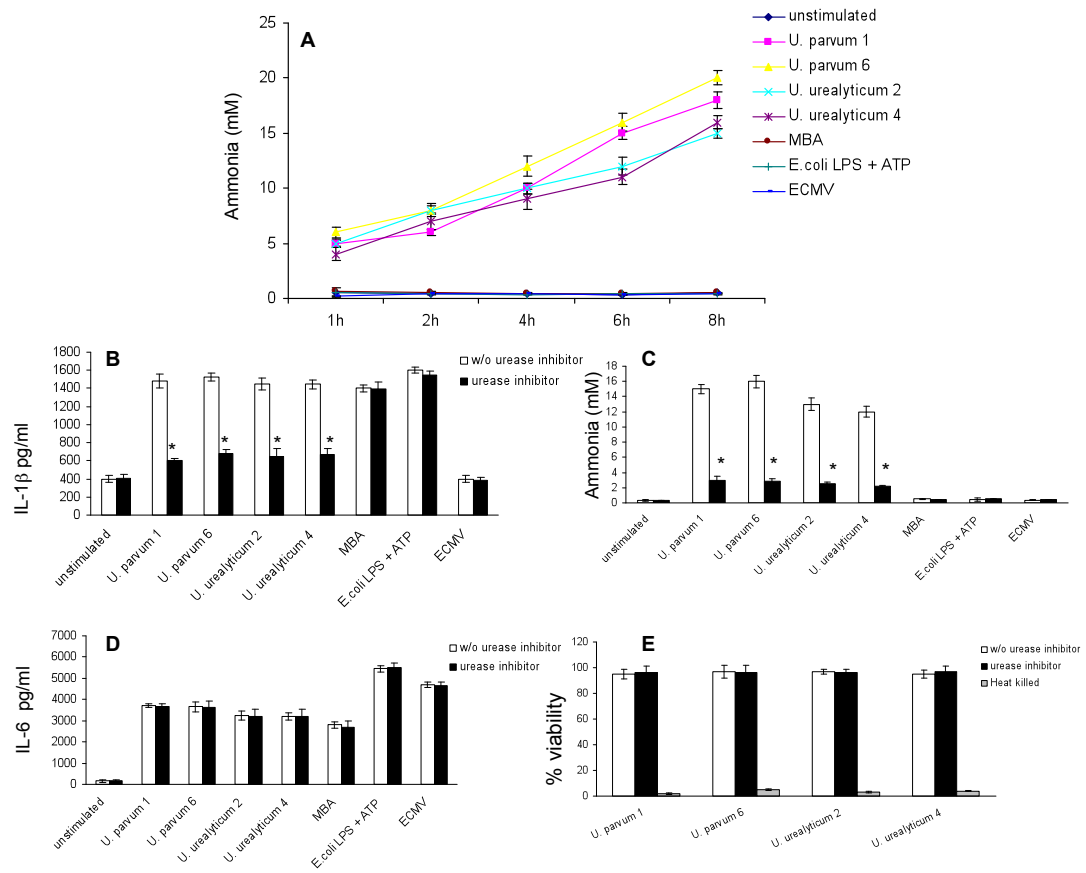
A possible mechanism for the activation of IL-1 $\beta$  by  $\text{NH}_3$  is that  $\text{NH}_3$  is recognised as a damage-associated molecular pattern (DAMP) by an NLR, causing that activation of an inflammasome complex. The inflammasome would then activate IL-1 $\beta$  from its pro-form and activate an inflammatory response.

In order to verify that the  $\text{NH}_3$  produced by *Ureaplasma* urease was responsible for the *Ureaplasma*-induced IL-1 $\beta$  production, acetohydroxamic acid (urease inhibitor) was added to *Ureaplasma* cultures during incubation periods, after which  $\text{NH}_3$  concentration in culture supernatants was measured. The results showed inhibition of  $\text{NH}_3$  produced in *Ureaplasma* cultures with urease inhibitors (Figure: 6.2.4: B). IL-1 $\beta$  production was measured in HAECs, stimulated with *Ureaplasma* cultures containing urease inhibitor and compared to IL-1 $\beta$  production by stimulation with *Ureaplasma* cultures without urease inhibitors (Figure 6.2.4: C). The urease inhibitor showed to inhibit the production of IL-1 $\beta$  in HAECs samples examined, further supporting that  $\text{NH}_3$  is directly associated with inflammasome activation. IL-6 levels remained unchanged as was expected (Figure 6.2.4: D).

We had to rule out the possibility that the observed results were due to diminished *Ureaplasma* viability, so the bacterial viability was measured both in the presence

and absence of urease inhibitors after the same incubation times. Using propidium iodide (PI) and thiazole orange staining and flow cytometry, discrimination and quantification of live/dead bacteria was analysed, showing that urease inhibitor did not alter the viability of *Ureaplasma* (Figure 6.2.4: E), confirming the observed results were a result of urease inhibition and not due to bacterial diminished burden.

### NH<sub>3</sub> triggers NLRP7 inflammasome activation:



**Figure 6.2.4:** NH<sub>3</sub> triggers NLRP7 inflammasome activation.

Human amniotic epithelial cells were infected with *Ureaplasma* species ( $1 \times 10^8$  bacteria/ml to  $1 \times 10^7$  cells/ml) or ECMV (5 moi) or stimulated with 1  $\mu$ g/ml MBA, or 100 ng/ml *E. coli* LPS + 5 mM ATP. Supernatant was collected after 12hr and analysed for ammonia using the indophenols reaction (A). Ammonia production (B) as well as IL-1 $\beta$  (C) and IL-6 (D) secretion was also assessed in the presence (black bar charts) and absence (white bar charts) of urease inhibitor, acetohydroxamic acid. The data represent the mean of three independent experiments. Asterisks indicate statistically significant ( $p < 0.05$ ) decrease in ammonia (B) or cytokine secretion (C, D) in the presence of urease inhibitor compared to the absence of urease inhibitor. Asterisks indicate statistically significant ( $p < 0.05$ ) increase in viability (E) compared to heat-killed bacteria.

#### 6.2.5: pH alkalization in response to *Ureaplasma* infection is sensed by NLRP7:

To investigate the role of pH in the activation of NLRP7, a study of the rate of pH change in HAECs stimulated with *Ureaplasma*, MBA and control cultures at different time points was investigated (Figure 6.2.5: A). These results showed that the pH (like  $\text{NH}_3$ ) increased rapidly and continued to increase as time went on in cultures stimulated with *Ureaplasma*, but no increase in pH was shown in MBA and/or control cultures. To determine whether the results observed in increased IL-1 $\beta$  production are associated with a general increase in pH or whether it is due to an increase  $\text{NH}_3$  concentration, a set of experiments were arranged to assess whether pH or  $\text{NH}_3$  concentration increases IL-1 $\beta$  production. 8mM of NaOH,  $\text{NH}_3$  and  $\text{NH}_4\text{Cl}$  were added to HAECs cultures and incubated for 6 hours, after which IL-1 $\beta$  concentrations were measured (Figure 6.2.5 B). NaOH was used to determine whether an immune response was initiated by a simple change in pH, or if it was due to  $\text{NH}_3$  specifically. Like wise,  $\text{NH}_4\text{Cl}$  was used to determine if the immune response was activated by an ammonium ion, or specifically to  $\text{NH}_3$ .

From the results NaOH is shown to increase the pH of the HAEC cultures after incubation, however it showed no increase in IL-1 $\beta$  production.  $\text{NH}_3$  on the other hand, showed an increase in pH and an increase in IL-1 $\beta$  production. The non-ionised ammonium compound ( $\text{NH}_4\text{Cl}$ ) is more permeable to cells than  $\text{NH}_4^+$  ammonium ions and as a result was used in this experiment, and showed a slight increase IL-1 $\beta$  by HAEC cultures. These results further strengthen the theory that it is  $\text{NH}_3$  that is responsible for the activation of inflammasome activated IL-1 $\beta$  production in HAECs.

In order to conclusively determine whether NLRP7 inflammasome is responsible for the detection of *Ureaplasma* and the production of IL-1 $\beta$  and caspase-1 in

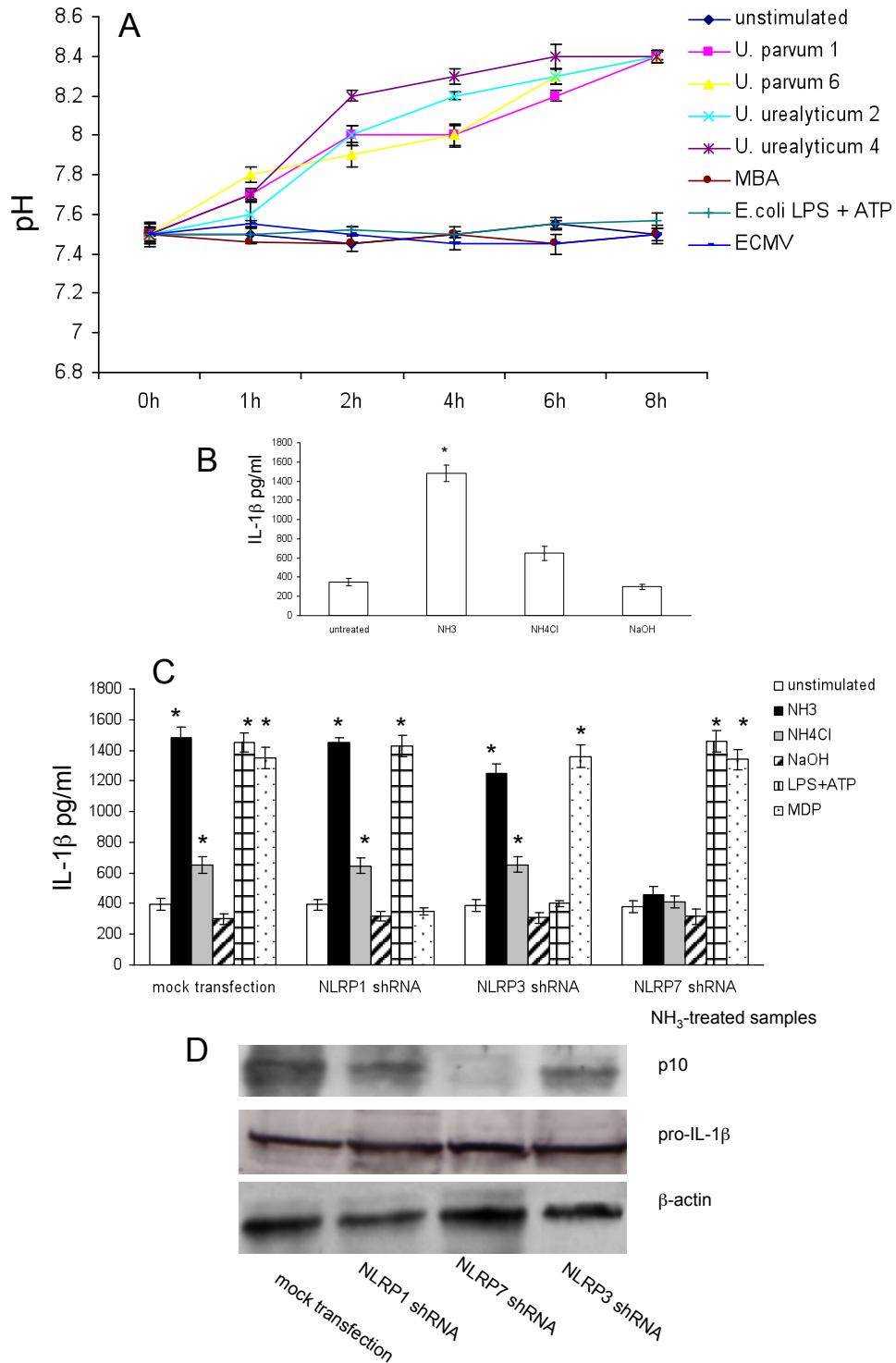
HAECs after stimulation with *Ureaplasma*, NLR KD HAECs sample were examined, using shRNA to KD specific NLRs. 8mM NH<sub>3</sub>, NH<sub>4</sub>Cl and NaOH were added to NLRP1, NLRP3 and NLRP7 KD HAEC cultures for 6 hours, after which IL-1 $\beta$  (Figure 6.2.5: C and D) and caspase-1 (Figure 6.2.5: D) concentrations in each cultured sample was measured. Muramyl dipeptide (MDP) and LPS in the presence of ATP are known ligands for NLRP1 and NLRP3 respectively. Figure 6.2.5 C shows that silencing NLRP1 reduces IL-1 $\beta$  production when compared to mock transfects after incubation with MDP. There is no reduction in IL-1 $\beta$  after stimulation with LPS and ATP, NH<sub>3</sub>, NaOH or NH<sub>4</sub>Cl, suggesting that as predicted, NLRP1 is responsible for the detection as immune response initiation for MDP.

A slight decrease in IL-1 $\beta$  was observed in NLRP3 KD HAECs, however NLRP7 KD HAECs showed almost complete inhibition of IL-1 $\beta$  production after a 6-hour *Ureaplasma* incubation time. Again NLRP7 KD HAECs showed an almost complete inhibition of caspase-1 p-10 fragmentation, meaning NLRP7 KD prevents the formation of inflammasomes and therefore activated caspase-1.

Taking all these results together, we can conclude that NLRP7 is the NLR responsible for *Ureaplasma* detection and *Ureaplasma*-activated inflammasome immune response in HAECs.

The results from Figure 6.2.5 show that pH increases in HAECs when they are incubated with *Ureaplasma*, strongly suggesting that alkalization is occurring, which is in turn likely to be due to the production of NH<sub>3</sub>. As MBA cannot hydrolyse urea, it does not cause alkalysation when incubated with HAECs.

pH alkalization in response to *Ureaplasma* infection is sensed by NLRP7:



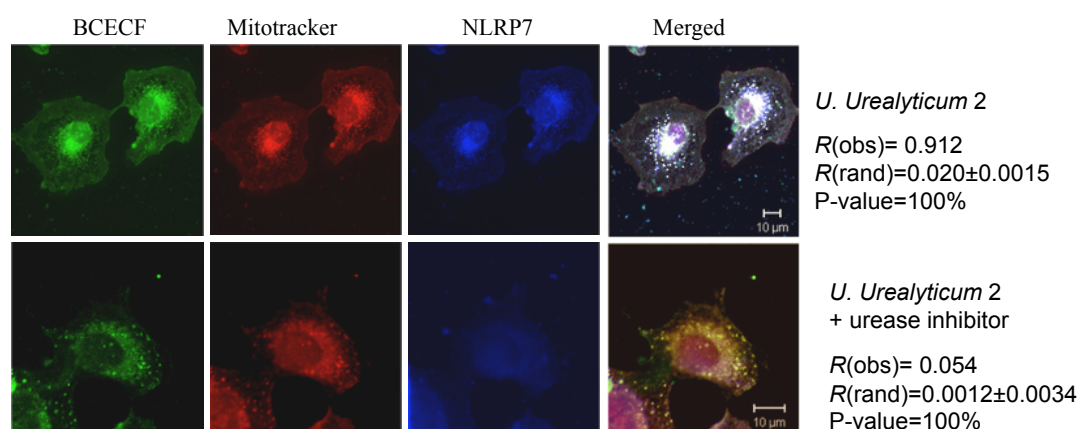
**Figure 6.2.5:** pH alkalization in response to *Ureaplasma* infection is sensed by NLRP7: Human amniotic epithelial cells were infected with *Ureaplasma* species ( $1 \times 10^8$  bacteria/ml to  $1 \times 10^7$  cells/ml) or ECMV (5 moi) or stimulated with 1  $\mu$ g/ml MBA, or 100 ng/ml *E. coli* LPS + 5 mM ATP. Supernatant was collected over an 8 hr period and pH of the supernatant was determined (A). Human amniotic cells were treated with either not treated or treated with 8 mM of NH<sub>3</sub>, NH<sub>4</sub><sup>+</sup> or NaOH solution for 6 hours. The supernatant was collected and the level of IL-1β was determined using CBA (B). NLRP1, NLRP3 and NLRP7 expression was knocked down by shRNA and the cells were stimulated with 8 mM of NH<sub>3</sub>, NH<sub>4</sub><sup>+</sup>, NaOH, 100 ng/ml LPS + 5 mM ATP, or 10 mg/ml MDP + 5 mM ATP for 6 hours. Supernatant was collected after 12hr and analysed for IL-1β (C) using the CBA system as well as caspase-1 activation (p10) and pro-IL1b (D). The data represent the mean of three independent experiments. Asterisks indicate statistically significant ( $p < 0.05$ ) increase in cytokine secretion compared to corresponding unstimulated controls.

**6.2.6: Localisation of NLRP7 in alkalized mitochondria in response to *Ureaplasma* infection:**

Tsujii et al. reported that  $\text{NH}_3$  inhibits mitochondrial respiration in gastric mucosal cells, and a possible association with apoptosis in these alkalised cells<sup>184</sup>. We investigated if the same could be true of the HAECs we were using in these experiments, which could implicate the *Ureaplasma* produced  $\text{NH}_3$  in apoptosis of HAECs and therefore a possible link to pPROM. This was investigated by performing confocal microscopy, using pH-sensitive, fluorescent, cytoplasmic dye, BCECF (2,7-bis(carboxyethyl)-5-(6)-carboxyfluorescein) (Life Technologies, UK), to measure intracellular pH (Paradiso et al., 1986), and if *Ureaplasma*-induced  $\text{NH}_3$  concentration increase could be attributed to HAEC apoptosis via NLRP7 immune response<sup>185</sup>. We have previously shown that NLRP7 co-localises with mitochondria after stimulation with *Ureaplasma* SV2 (Figure 6.2.2: D second row), and intent to investigate any association between  $\text{NH}_3$  depolarisation of the mitochondria and other organelles that may lead to apoptosis. *Ureaplasma* stimulated, BCECF HAECs showed strong fluorescence in the mitochondria, suggesting an increase in  $\text{NH}_3$  concentration in the mitochondrial matrix (Figure 6.2.6: top row). The experiment was repeated only this time with the addition of urease inhibitor after which, no co-localisation was observed between NLRP7 with BCECF or the mitochondria (bottom row). The Costes' approach returned significance values of 0.914 and 0.056, respectively, supporting that  $\text{NH}_3$  production increases inside the mitochondrial matrix, increasing its pH, which in turn triggers NLRP7 inflammasome immune response by mitochondrial membrane potential disruption and possible apoptosis.



### Localisation of NLRP7 in alkalized mitochondria in response to *Ureaplasma* infection:



**Figure 6.2.6:** Localisation of NLRP7 in alkalized mitochondria in response to *Ureaplasma* infection.

(A) Human amniotic epithelial cells were loaded with BCECF and stimulated with *Ureaplasma* SV2 for 6hr in the presence (bottom row) and absence (top row) of the urease inhibitor, acetohydroxamic acid. NLRP7 was stained using a rabbit anti NLRP7 Fab conjugated to Cy5, mitochondria were stained using mitotracker. Cells were imaged using a Zeiss 510 confocal microscope. Bars 10 mm. Co-localization coefficients [ $R(\text{obs})$ ] were calculated using Costes' approach. (B) Effects of  $\text{NH}_3$  on intracellular pH (pHi) in control and *Ureaplasma* treated cells. BCECF-loaded amniotic epithelial cells were perfused with 20 mM  $\text{NH}_4\text{Cl}$  (Trace A), *Ureaplasma* (Trace B) or *Ureaplasma* plus urease inhibitor (Trace C). The data are means from three experiments (50 cells/experiment).

### **6.3: Conclusion:**

*Ureaplasma* serovars SV2, SV3, SV 4 and SV6 in addition to *Ureaplasma* MBA stimulation of HAECs showed a significant increase in IL-1 $\beta$  compared to negative controls and unstimulated samples. Using RNA interference with shRNA, specific inflammasome NLRs were silenced. NLRP1, NLRP3 and NLRP7 KD was showed and the amount of IL-1 $\beta$  produced in response to *Ureaplasma* was measured. No inhibition of IL-1 $\beta$  was shown in NLRP1 KD HAECs, but a significant reduction was observed in NLRP3 KD, whilst NLRP7 KD HAECs greatly inhibited IL-1 $\beta$  production after stimulation with *Ureaplasma* serovars and MBA. Confocal microscopy of the co-localization between NLRP7 and the inflammasome associated protein ASC was shown to be highly significant after stimulation with both

*Ureaplasma* and MBA, but the co-localisations were inhibited when the NLRP7 was knocked down.

In order to determine how the second signal of inflammasome activation occurs, different inhibitors were utilized. From the inhibitors tested, the ROS inhibitor DPI was shown to have a moderate decrease in IL-1 $\beta$  production when HAECs were stimulated with *Ureaplasma* serovars and MBA. The role of *Ureaplasma* produced NH<sub>3</sub> was then investigated and it was shown that NH<sub>3</sub> triggered NLRP7 inflammasome activation. This was supported by the use of urease inhibitor acetohydroxamic acid, which inhibits NH<sub>3</sub> production and was shown to also inhibit IL-1 $\beta$  production. Activation of NLRP7 as a result of NH<sub>3</sub>, as opposed to pH changes was investigated, and the results showed that indeed it was the NH<sub>3</sub> that triggered NLRP7 inflammasome activation, and not just a change in pH. Finally the NH<sub>3</sub> alkalization of the mitochondrial matrix was shown using confocal microscopy and confirmed, in addition to the co-localisation of NLRP7 to the mitochondrial surface. These findings suggest that NH<sub>3</sub> alkalisation of the mitochondria may lead to apoptosis of amniotic cells and therefore leads to PTB and pPROM.

Future investigations into the apoptotic effect of NH<sub>3</sub> on HAECs via NLRP7 would be useful in supporting the findings of this chapter. Apoptosis of HAECs would be a likely mechanism for causing pPROM and PTB, as these cells form the amniotic membrane. Cytochrome C activates cell apoptosis mechanisms; therefore by investigating cytochrome C production by HAECs after stimulation with *Ureaplasma* derived NH<sub>3</sub> further light would be shed on *Ureaplasma* involvement in pPROM and PTB. By knocking down NLRP7 using siRNA in HAECs, a comparison of cytochrome C production could be made between unstimulated and *Ureaplasma* stimulated samples. If there was a decrease in cytochrome C production

and HAEC apoptosis in NLRP7 KDs, the role of NLRP7 in HAEC apoptosis after stimulation with *Ureaplasma* would be supported.

## **Chapter 7:**

# **Discussions**

### **7.1: *Ureaplasma* activated immune response in mono-mac 6 monocytes:**

*Ureaplasma* has long been suggested to have pathogenic properties that have been associated with a wide range of implications, such as adverse pregnancy outcomes, PTB, pPROM, still birth, recurrent miscarriage, infertility in both men and women and complications in infants exposed to the bacteria during gestation, such as BPD and CLD<sup>1,18,47,186</sup>. The prevalence of *Ureaplasma* spp. is extremely high, with some studies suggesting up to 80% of the population harbour at least one serovar of the bacteria. *Ureaplasma* spp. is considered common bacteria of the urogenital tract flora. There is controversy as to whether *Ureaplasma* is able to activate inflammatory immune responses, and if so, why the adverse effects are experienced by a relatively small number of people that harbour the bacteria. The association of *Ureaplasma* with the activation of the innate immune response and adverse health reactions is growing stronger, but the debate still remains.

Initially in this study, we used mono-mac 6 monocytes, which constitute a significant proportion of the human innate immune cell population and are able to accessing nearly all compartments and tissue within the body, only excluding immunoprivileged sites. This makes them the ideal front line immune cell to investigate possible pathogenic responses to *Ureaplasma*.

We investigated the *Ureaplasma*-induced PRR expression response as well as the immune response pathways activated in MM6 monocytes. MyD88-mediated NF- $\kappa$ B pathways leading to pro-inflammatory cytokines as well as NLR inflammasome-activated pathway leading to IL-1 $\beta$  production in response to *Ureaplasma* stimulation were examined.

In addition to *Ureaplasma*-induced immune response in MM6 monocytes, we investigated what, if any, effect the addition of yeast to *Ureaplasma* selective growth

culture medium has. Our results showed that contrary to a previous study, *Ureaplasma* had no effect on the expression levels of TLR1, whether the *Ureaplasma* had been cultured in yeast or not<sup>171</sup>.

TLR2, TLR6 and TLR9 expression was upregulated by *Ureaplasma* stimulation, whilst *Ureaplasma* cultured in yeast was shown to augment the upregulation in PRR expression when compared to yeast negative *Ureaplasma* cultures. *Ureaplasma* was also shown to activate the MyD88-mediated NF- $\kappa$ B pathway, with the production of TNF- $\alpha$  and IL-6. In addition there was *Ureaplasma*-induced activation of NLR inflammasome leading to the production of IL-1 $\beta$ . Interestingly no upregulation of NLRP1 or NLRP3 was observed, posing the question, which immune mechanism/pathway is responsible for the production of active caspase-1 and IL-1 $\beta$ . Different *Ureaplasma* serovars were shown to trigger immune responses in both TLR expression levels and quantities of cytokines produced by MM6 cells, supporting the hypothesis that *Ureaplasma* virulence is associated with the serovar. TLR2/6 appears to be the initial pathogen detector on the cellular membrane, and then TLR9 detects intracellular PAMPs of *Ureaplasma* once they become internalised<sup>51,179</sup>. The activation of immune response in MM6 supports the association between *Ureaplasma* infection and PTB, pPROM and BPD in neonates<sup>1,18,47,186</sup>. Addition of yeast to *Ureaplasma* selective culturing medium produced different levels of immune responses to *Ureaplasma* not cultured in yeast, therefore it was decided that yeast will not be added to *Ureaplasma* culture medium in any future experiments as its presence may invalidate future findings. Further investigation was needed to be carried out to investigate the activation mechanism of IL-1 $\beta$  and inflammasome formation.

## **7.2: *Ureaplasma*-activated immune response in bronchial epithelial cells:**

In order for IL-1 $\beta$  to be produced, IL-1 $\beta$ s inhibitory subunit must be cleaved, converting pro-IL-1 $\beta$  into active IL-1 $\beta$ . This conversion of inactive IL-1 $\beta$  to its active form requires the proteolytic activity of caspase-1, so the presence of active caspase-1 (Figure: 4.2.2 B) and the high levels of protein concentration measured (Figure 4.2.2: C), strongly support the formation of inflammasome complexes by stimulation with the *Ureaplasma* serovars studied.

*Ureaplasma* infection has been suggested to cause neonatal pulmonary complications, such as BPD and CLD, however this is only theorized as of yet as no *in vitro* or *in vivo* studies have investigated whether *Ureaplasma* colonization of the fetal pulmonary system can cause the damage and injury to lung tissue that has been suggested. The proposed mechanisms for BPD and CLD by *Ureaplasma* are suggested to be due to dysregulation of the inflammatory immune response and over production of pro-inflammatory cytokines that prevent proper development and result in damage to pulmonary epithelial cells during gestation<sup>54,186</sup>. For these reasons bronchial epithelial cells (BEAS-2B) were chosen as a relevant cell-line to study the immune response resulting from *Ureaplasma* stimulation. The PRR expression levels of these cells were measured both before and after a 1-hour stimulation period, as well as cytokine production and immune signaling pathways activated.

HEK-Blue IL-1 $\beta$  assays from *Ureaplasma*-infected BEAS-2B cells showed a very strong increase in IL-1 $\beta$  secretion in all of the *Ureaplasma* serovars that were examined. Inflammasome activation requires a two-step model of activation, where there is a “priming step” when a PRR is triggered leading to pro-IL-1 $\beta$  production and a “second signal” leading to inflammasome assembly and activation of caspase-

1<sup>111</sup>. In this case, the theoretical priming signals suggested for inflammasome activation are present, since NF- $\kappa$ B is produced (Figure 4.2.2: A and C), significantly increased after *Ureaplasma* stimulation. Regulation of PRR expression in response to the different *Ureaplasma* serovars is shown in Figure 4.2.1. The most significantly upregulated TLRs were shown to be TLR2 and TLR9 and to a lesser extent, TLR6. The degree of these TLR's upregulation differed between the *Ureaplasma* serovars, however there was a consistently significant increase in NF- $\kappa$ B and IL-1 $\beta$  in all of the serovars tested (Figure 4.2.2: C).

Western blotting confirmed the activation of MyD88-dependent immune signaling cascade, demonstrated by the significant increase in P-I $\kappa$ B in the lysates of the BEAS-2B cells stimulated with each of the *Ureaplasma* serovars, compared to the P-I $\kappa$ B detected in the unstimulated samples (Figure 4.2.2: A). Western blotting also showed strong production of caspase-1 p-10 fragmentation protein in the lysates, supporting the formation of multiprotein inflammasome complexes, thus activating caspase-1, which is classically required for the maturation of IL-1 $\beta$  (Figure: 4.2.2 B). Taken together, these results suggest that TLRs, such as TLR2, TLR6 and TLR9 must act as the PRRs that trigger the inflammasome “priming signal”. Therefore, we set out to determine which NLRPs were responsible for the subsequent inflammasome assembly and how this second signal was being triggered.

The expression levels of NLRP1 after stimulation were not shown to be significantly upregulated for NLRP1 IL-1 $\beta$  activation, and though NLRP3 expression levels were upregulated, still would seem to be inadequate for the high levels of IL-1 $\beta$  produced. For this reason, possible alternative mechanisms for IL-1 $\beta$  production were investigated, using RNA interference and gene silencing. From the literature, we chose to investigate NLRP7, NLRP12 and NLRC5 in addition to NLRP1 and



NLRP3, for their role in IL-1 $\beta$  activation. shRNA was used to silence specific PRRs: TLR2, TLR2/6, TLR4, TLR6, TLR9, NOD2, NLRP1, NLRP3, NLRP7, NLRP12 and NLRC5. NOD2, NLRP1, NLRP12 and NLRC5 KD BEAS-2B cells showed no significant decrease in IL-1 $\beta$  production, however significant decrease in IL-1 $\beta$  was observed in NLRP3 KD cell-lines, and a greater inhibition of IL-1 $\beta$  was observed in NLRP7 KD cell-lines. These results suggest that NLRP7 inflammasome activation is the main mechanism by which IL-1 $\beta$  is activated in bronchial epithelial cells after *Ureaplasma* stimulation, and that NLRP3 inflammasome is also involved in IL-1 $\beta$  production after *Ureaplasma* stimulation.

Interestingly the most significant reduction in IL-1 $\beta$  production was not through silencing of NLRs, but through the silencing of TLRs, most notably in TLR2/6 KD cell-lines, where almost complete inhibition of IL-1 $\beta$  was observed, suggesting that the inflammasome priming signals produced these TLRs are of very high significance in IL-1 $\beta$  production after *Ureaplasma* stimulation.

### **7.3: *Ureaplasma*-induced immune response via TLR- activated immune response in human amniotic epithelial cells:**

The association between intrauterine infection and PTB and pPROM is high, with over 60% of PTB presenting with chorioamniotitis and/or inflammation for the fetal membrane<sup>41,186,187</sup>. *Ureaplasma spp.* is present in the upper genital tract and amniotic fluid in a significant percentage of PTBs. Another significant factor associated with PTB and pPROM is the presence of pro-inflammatory cytokines, especially IL-6, where increased load has been associated with increase chance of PTB<sup>46,188,189</sup>. *Ureaplasma parvum* 3, 14 and *Ureaplasma urealyticum* 2 have all been shown to

initiate pro-inflammatory production in both MM6 and BEAS-2B cell-lines, therefore we investigated if this was the same in HAECs. Due to the high significance of IL-6 levels in rates of PTB, IL-6 would be the pro-inflammatory cytokine of interest in this part of the study.

We initially investigated whether *Ureaplasma parvum* 3, 14 and *Ureaplasma urealyticum* 2 were capable of initiating pro-inflammatory cytokine production in HAECs, and found that all were capable of initiating production of TNF- $\alpha$ , IL-8, IFN- $\alpha$  and importantly IL-6, within 2 hours of stimulation. Furthermore there was no significant difference in the level of each cytokine produced in response to the *Ureaplasma* serovar used.

We then set out to investigate the mechanisms responsible for the cytokine production in HAECs, therefore the expression levels of TLRs were examined, and using HEK-293 cells, the role of each TLR involved in the immune response to the *Ureaplasma* serovars could be examined. In addition to the *Ureaplasma* serovars being used, the *Ureaplasma* surface exposed lipoprotein MBA was investigated to determine its possible involvement in the immune response in HAECs. TLR expression levels in HAECs cells were measured using indirect immunofluorescence, and flow cytometry. The results showed the upregulation in expression of TLR2, TLR6 and TLR9 after stimulation with all of the *Ureaplasma* serovars used, but there was only TLR2 and TLR6 upregulation after stimulation with MBA.

HEK-293 cells were transfected with specific TLR and TLR associated gene coding sequences, to produce cell-line models that would express only specific TLRs, by which they will enable examination of the function of each of the TLRs involved in the response to the PAMPs being used. The results showed that all of the

*Ureaplasma* serovars tested activated immune responses and pro-inflammatory cytokine IL-6 production in HEK-TLR2, -TLR2/6 and -TLR9 cell-lines, but only low levels of immune response were observed in HEK-TLR4 transfected cells. Interestingly, when the same cell-lines were stimulated with MBA, only HEK-TLR2 and HEK-TLR2/6 cells were shown to activate immune responses. Taken together, these results support that TLR2 and TLR2/6 are the first TLRs to detect *Ureaplasma parvum* 3, 14 and *Ureaplasma urealyticum* 2 at the HAEC surface, and that the immune responses observed are as a result of interaction of the surface exposed lipoprotein MBA with these TLRs. From these results we can also conclude that the *Ureaplasma* serovars tested then infiltrate and replicate within the HAECs, as TLR9 is activated upon stimulation with these *Ureaplasma* serovars, but not with MBA. TLR9 is an intracellular, endosomally located PRR.

Investigation into receptor clustering could be initiated on the HAEC surface by the *Ureaplasma* serovars and MBA, showed that TLR2/6 clustering does indeed occur after stimulation, but that TLR4 clustering does not. The TLR2/6 clusters form within lipid rafts at the cell surface, and could potentially recruit the TLR2/6 cluster associated molecule CD36 to the complex, which could exacerbate the inflammatory immune response, as CD36 has been shown to do so in other studies<sup>96</sup>.

*Ureaplasma parvum* 3, 14 and *Ureaplasma urealyticum* 2 were shown to trigger TLR9 signaling from HAECs endosomes, where it was observed to co-localize with the signaling adaptor molecule MyD88. The *Ureaplasma* CpG-DNA is targeted to endosomal compartments, which is where TLR9 is expressed, thus making TLR9 ideally positioned for detecting *Ureaplasma* endocytosed material, thus activating TLR9-mediated immune response.

The overall findings of this chapter suggests and supports that HAEC inflammatory

response is triggered by *Ureaplasma parvum* 3, 14 and *Ureaplasma urealyticum* 2 via synergic activation of specific TLRs, namely TLR2, TLR2/6 and TLR9. In addition, MBA was shown to activate immune responses in HAECs via TLR2 and TLR2/6. TLR2 and TLR6 are both cell surface expressed receptors, suggesting that the initial immune response is activated by TLR2 and TLR2/6-mediated immune signaling pathways, and this activation is caused by direct interaction of the *Ureaplasma* serovars tested and MBA in HAECs. It is possible that MBA is the major virulence PAMP in response to *Ureaplasma parvum* 3, 14 and *Ureaplasma urealyticum* 2. Previous studies have suggested that TLR1-activation is initiated by *Ureaplasma spp.*; however as discussed in chapter 3, 4 and 5 the *Ureaplasma* serovars we showed no such TLR1-activation<sup>171</sup>.

The finding that *Ureaplasma parvum* 3, 14 and *Ureaplasma urealyticum* 2 activate TLR2 but not TLR4, could be a reason why *Ureaplasma* does not activate a large and acute immune response, it rather triggers a chronic low level inflammatory immune response that could cause irreversible damage to the fetal membrane. This chronic inflammation and damage to HAECs could be directly responsible for pPROM.

Additionally the ability of size and phase variation of MBA could be responsible for the virulence variability, not only between different *Ureaplasma* serovars, but also within different isolates of the same serovar<sup>10,11,23</sup>. This could be a reason as to why *Ureaplasma spp.* prevalence is so high, but the risk of adverse pregnancy outcomes is so varied.

#### **7.4: NLRP7 inflammasome role in the immune activation of human amniotic epithelial cells after stimulation with *Ureaplasma*:**

NLRs have been strongly associated as cytoplasmic sensors of PAMPs and DAMPs, and also in their fundamental role in the activation of caspase-1 to enable maturation of IL-1 $\beta$  and IL-18 into their active forms. Some NLRs have recently been shown to be essential for successful embryonic development, such as NLRP7. In addition to having two separate roles, NLRP7 has been shown to both positively and negatively regulate innate immune responses.

We set out to determine if NLRP7 could detect the cell wall-less bacteria, *Ureaplasma*, which is reported to be present in 40-80% of sexually active adults. *Ureaplasma* is considered to a commensal bacterium in the lower genital tract flora, but it has also been strongly associated with many adverse health complications. It has been associated with a wide range of obstetric complications, such as infertility (in both males and females), histological chorioamnionitis, and neonatal morbidity, such as PTB, pPROM, BPD, CLD, meningitis and intraventricular hemorrhage<sup>1,8,13,28,30,32,54</sup>. *Ureaplasma* infection also associated with neonatal mortality by spontaneous miscarriage, stillbirths and perinatal mortality, resulting from complications listed above, such as BPD. *Ureaplasma* is the most commonly isolated organism found in infected placentas and amniotic fluid<sup>1,28,30,54,187</sup>.

The cause of these health complications is likely to be attributed to inappropriate activation of the immune response, especially after intrauterine invasion during pregnancy.

Intrauterine infection could produce increased secretion of pro-inflammatory cytokines, such as TNF- $\alpha$ , IL-6, IL-8 and IL-1 $\beta$ , which could be directly associated

to PTB, pPROM and the presence of *Ureaplasma* in bronchial lavage fluid could account for BPD in neonates<sup>37</sup>.

TLR2, TLR2/6 and TLR9 have been shown to be the likely priming signals for inflammasome activation in response to *Ureaplasma*. The TLR priming signal increases the transcription and expression of pro-IL-1 $\beta$  and other pro-inflammatory cytokines. Since NLRP1 inflammasome activation and formation has been shown not to be initiated in response to *Ureaplasma*, and only minor activation of NLRP3 (discussion chapters 6), we investigated the possible role of NLRP7 inflammasome activation as a mechanism for caspase-1 and IL-1 $\beta$  activation that has been observed in previous studies.

Our results showed that NLRP7 inflammasome formation was activated by *Ureaplasma* stimulation, which activates caspase-1 and in turn the production of IL-1 $\beta$ . Furthermore our investigations showed that the *Ureaplasma* cell surface exposed lipoprotein MBA was responsible for the triggering of NLRP7 inflammasome activation but was not shown to produce increased IL-1 $\beta$  secretion.

In order to determine the second signal required for NLRP7 inflammasome activation, the four previously proposed NLRP3 activation signals were investigated to see if they could activate NLRP7. K<sup>+</sup> efflux, ROS production, lysosomal disruption and Ca<sup>2+</sup> cellular influx, have been proposed as the second signal of activation, therefore inhibitors against these were used to determine if any of these were responsible for NLRP7 inflammasome activation<sup>146-149 150 151 152</sup>. Out of all the inhibitors used, only the ROS inhibitor DPI was shown to reduce IL-1 $\beta$  production, but that the level of IL-1 $\beta$  production inhibition was not great enough for ROS to be the main second signal for NLRP7 activation in response to *Ureaplasma* and MBA. DPI was shown to have less of a IL-1 $\beta$  reduction to *Ureaplasma* than MBA,

suggesting whole *Ureaplasma* bacteria and MBA have different mechanisms of immune response activation. These finding also support the study by Potts et al. that associate *Ureaplasma* infection with abnormal ROS levels<sup>190</sup>.

To determine the second inflammasome activation signal for NLRP7 we investigated possible pathogenic molecules that are unique to *Ureaplasma*. *Ureaplasma* urease is entirely unique to *Ureaplasma* bacteria and its main metabolic mechanism of producing ATP, from urea<sup>1,8</sup>. A product of the hydrolysis reaction of urea is  $\text{NH}_3$ , which was decided to be a suitable DAMP to investigate for its ability to activate NLRP7 inflammasome.

Our studies showed that indeed  $\text{NH}_3$  was able to trigger NLRP7 inflammasome activation. To verify that  $\text{NH}_3$  is the trigger, specific urease inhibitors were used which were shown to inhibit IL-1 $\beta$  production in HAECs, further supporting the hypothesis that  $\text{NH}_3$  is associated with NLRP7 inflammasome and caspase-1 activation.

Under normal metabolic homeostasis,  $\text{NH}_3$  is present in the body via the deamination of protein in to urea.  $\text{NH}_3$  levels are kept to pH equilibrium with  $\text{NH}_4^+$  (ammonium ions). In physiological pH levels,  $\text{NH}_3$  accounts for approximately 1% of the  $\text{NH}_3/\text{NH}_4^+$  concentration.  $\text{NH}_3$  is more cellular permeable than  $\text{NH}_4^+$  and at this  $\text{NH}_3/\text{NH}_4^+$  concentration level,  $\text{NH}_3$  remains unharmed<sup>191</sup>. *Ureaplasma* infection increases cytoplasmic  $\text{NH}_3$  concentration, which increases the intracellular pH. To verify that it was  $\text{NH}_3$  that triggers NLRP7 activation and not just increased pH, a comparison of the affects of  $\text{NH}_3$  to NaOH, in addition to  $\text{NH}_4\text{Cl}$  was employed.  $\text{NH}_4\text{Cl}$  and  $\text{NH}_3$  showed increase in IL-1 $\beta$  in HAECs, where NaOH showed no IL-1 $\beta$  production, suggesting that it is not the increase in pH that triggers the response but rather  $\text{NH}_3$  itself. To test that pH increase did not kill HAECs, thus

preventing IL-1 $\beta$  production, viability tests were set up that showed that the pH did not affect the bacterial viability. A proposed mechanism of HAEC apoptosis due to *Ureaplasma*-induced cytoplasmic NH<sub>3</sub> increase and permeation into the inner membrane of the mitochondria, causes mitochondrial dysfunction ROS (Figure 7.5.1). This could trigger release of cytochrome C, which together with IL-1 $\beta$  increase could well lead to HAEC apoptosis<sup>192</sup>.

Taken together, these results support the hypothesis that *Ureaplasma* infection causes increase in NH<sub>3</sub>, which activates NLRP7 inflammasome formation, activating caspase-1 that activates IL-1 $\beta$ .

### **7.5: Overall conclusions:**

*Ureaplasma* was shown to initiate inflammatory immune responses in the three cell-lines we examined, causing secretion of pro-inflammatory cytokines. The presence of the pro-inflammatory cytokine IL-6 and IL-1 $\beta$  in amniotic fluid has been strongly associated with adverse pregnancy outcomes, especially, preterm birth and preterm premature rupture of the membrane<sup>189,193</sup>. TNF- $\alpha$ , IL-6 and IL-1 $\beta$  are capable of causing localised tissue damage, as well as damage to surrounding tissues due to the innate inflammatory response. From the viewpoint of the fetus, these pro-inflammatory cytokines could be directly responsible for inducing lung tissue damage during gestational development. Pro-inflammatory cytokines could impair correct development of tissue development in fetal respiratory tract, preventing adequate alveoli development and fibrosis of the lungs, leading to bronchopulmonary dysplasia and chronic lung disease. Innate immune response activation in monocytes by *Ureaplasma* stimulation would induce pro-inflammatory cytokine secretion wherever *Ureaplasma* is present, as monocytes can migrate to



nearly all compartments of the body, thus producing inflammatory responses wherever *Ureaplasma* is detected by monocytes.

From the maternal side, *Ureaplasma* is initially detected at the cell surface of human amniotic epithelial cells by TLR2/6 in response to recognition of the *Ureaplasma* surface exposed lipoprotein, and is detected intracellularly by TLR9 in response to internalised *Ureaplasma* PAMPs. These TLRs activate TLR-mediated MyD88-dependent immune responses, which produce pro-inflammatory cytokine release and upregulation of pro-IL-1 $\beta$  (signal 1 of inflammasome activation). Inflammasome activation of caspase-1, cleaves IL-1 $\beta$ s inhibitory subunit, releasing active IL-1 $\beta$ . The mechanism by which caspase-1 was activated and therefore IL-1 $\beta$  becomes activated, was shown to be mainly attributed to NLRP7 inflammasome activation, and to a lesser extent NLRP3 inflammasome activation. Signal two of inflammasome activation was shown to be the NH<sub>3</sub> produced by *Ureaplasma* urease which causes alkalinisation of the mitochondrial matrix, augmenting the innate immune response, and may lead to innate immune response apoptosis, which again could lead to pregnancy complications.

This study would strongly support that *Ureaplasma* is capable of initiating preterm birth and respiratory disorders in neonates, associations that have long been suggested in the literature. In light of this, *Ureaplasma* colonisation and infection should be regarded as a significant health risk to pregnant women and gestating infants, and detection and treatment of *Ureaplasma* infections should be greatly improved.

Screening for *Ureaplasma* should be implemented in pregnant women at the start of the second and third trimester, which, if treated, would reduce the risk of

bronchopulmonary dysplasia and preterm birth, (respectively). Due to the inaccuracy of culture screening methods, qPCR should be used, to reduce the risk of false negative results.

Treatment for *Ureaplasma* infection also requires improvement, as the current antibiotic of choice, erythromycin, has been shown to be ineffective in eradicating the bacterial colonisation. Azithromycin and clindamycin have been shown to be effective in clearing *Ureaplasma* infections, though the safety of their use in infants has yet to be fully established.

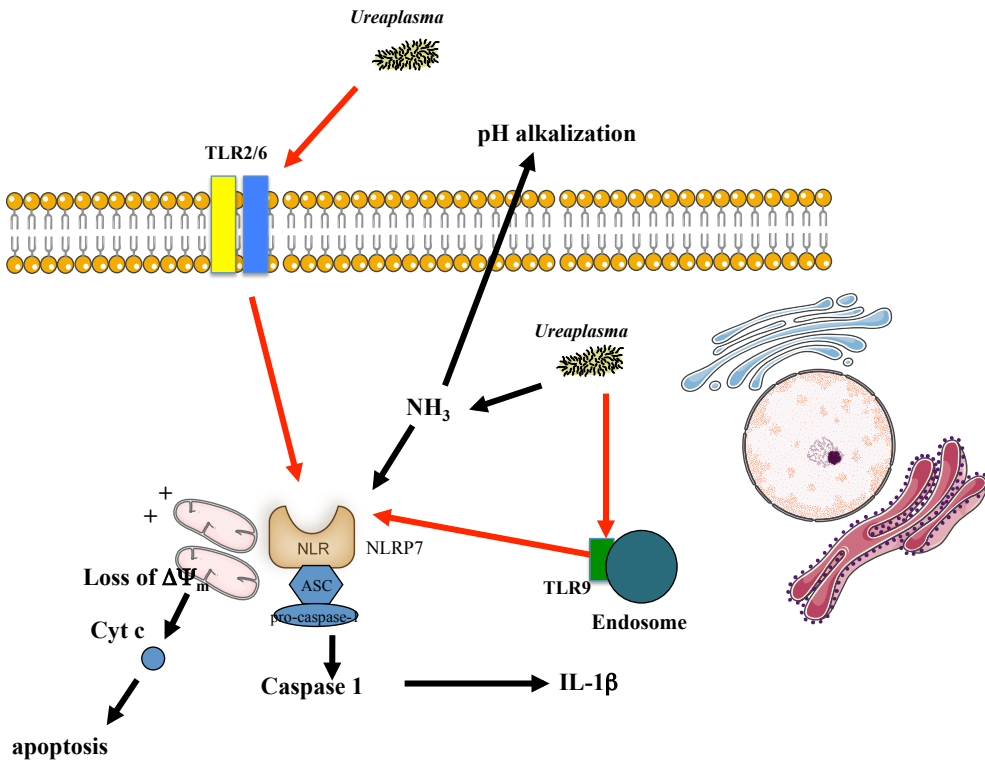
Possible alternative treatments for *Ureaplasma* could utilise TLR suppressors, monoclonal antibodies and urease inhibitors, though these suggestions are purely theoretical at this point.

Specific TLR suppressors would be able to reduce the immune response to *Ureaplasma* and therefore, reduce the damage to tissue caused by inflammatory cytokines. The suppression of TLRs would also lead to the reduction in IL-1 $\beta$ , by removing the priming signal that is required for the activation of the inflammasome complex. The suppression of TLRs would leave the patient vulnerable to infection, as TLRs play a constant and significant role in the detection and response to pathogens that are endlessly coming into contact with the body. TLR2, TLR6 and TLR9 have been shown to be the TLRs that are responsible for recognizing *Ureaplasma* and for initiating an immune response. Suppression of TLR2 and TLR9 may leave the patient too susceptible to infection and therefore, TLR6 could be a better target for suppression. The suppression of TLR6 was shown to significantly reduce IL-1 $\beta$  production after *Ureaplasma* stimulation, so could reduce tissue damage caused by *Ureaplasma* infection, whilst still enabling TLR2 and TLR9 to protect against pathogens.

Monoclonal antibodies could be used to target and bind to TLRs, which would inhibit ligand binding and enable their suppression.

The use of urease inhibitor should be investigated as a treatment for *Ureaplasma* infection. As humans do not use or possess urease, its inhibition in the body would not harm a person. Urease enables hydrolysis of urea to produce ATP, which is the primary energy source for *Ureaplasma*. Firstly, the inhibition of urease would reduce *Ureaplasma* growth and potentially, it would actively kill *Ureaplasma*. Secondly, the inhibition of  $\text{NH}_3$  production would prevent the activation of NLRP3 and NLRP7 inflammasome complexes. This would prevent production of IL-1 $\beta$  and therefore, reduce the tissue damage it is known to create.

Proposed model of NH<sub>3</sub>-induced-NLRP7 inflammasome activation:

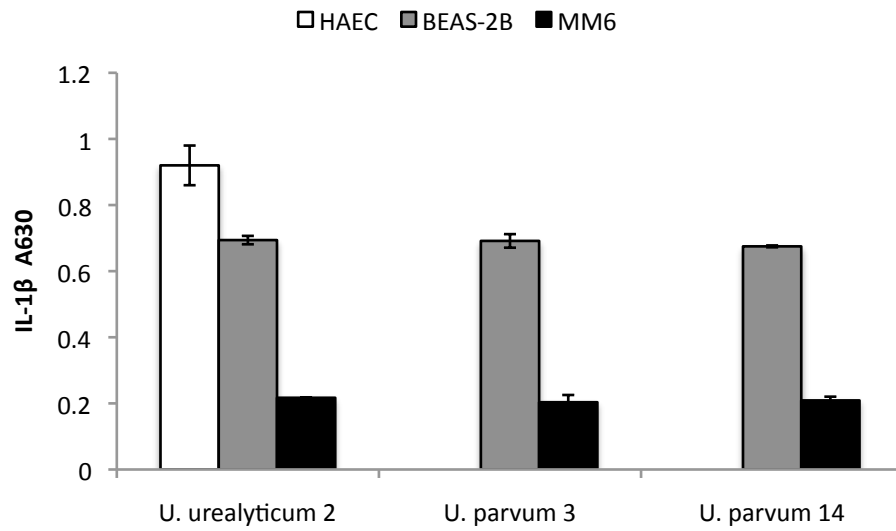


**Figure 7.5.1:** Proposed model of NH<sub>3</sub>-induced-NLRP7 inflammasome activation:

*Ureaplasma* infection results in the production of NH<sub>3</sub> by hydrolysis of urea by urease. These in turn causes alkalization of the cytoplasm and NH<sub>3</sub> uptake in the inner mitochondrial membrane, leading to loss of mitochondrial transmembrane potential. NLRP7 senses the increase in NH<sub>3</sub> and pH as well as the mitochondrial dysfunction, triggering caspase-1 activation and IL-1β secretion. A release of cytochrome C in addition to IL-1β increase and alkalization could trigger activation of the apoptosome, leading to apoptosis of the infected cell.

The production of IL-1β was shown to vary between cell-lines and tissue types in response to *Ureaplasma* infection. The level of IL-1β produced in mono-mac 6 monocytes was significantly less than that produced in human amniotic and bronchial cell-lines (Figure: 7.5.2), after stimulation with *Ureaplasma* at the same incubation times (1-hour). This could suggest a reason for the observed localized inflammatory response-associated cellular damage and health complication in the amniotic and bronchial epithelial cells in *Ureaplasma* infected pregnant women, and account for an absence in an observed systemic immune response.

IL-1 $\beta$  production after stimulation of different cell-lines with *Ureaplasma*:



**Figure 7.5.2:** IL-1 $\beta$  production after stimulation of different cell-lines with *Ureaplasma*:

IL-1 $\beta$  levels were measured after a 1-hour incubation period with *Ureaplasma* ( $1 \times 10^8$  bacteria/ml to  $1 \times 10^7$  cells/ml) *urealyticum* SV2, *U. parvum* SV3 and *U. parvum*, using HEK-Blue IL-1 $\beta$  reporter cell assays. The data represents the mean  $\pm$  SD of three independent experiments in HAECs (white barcharts), and  $\pm$ SD of two independent experiments in BEAS-2B (grey barcharts) and MM6 cells (black barcharts).

## References:

1. Capoccia R, Greub G, Baud D. *Ureaplasma urealyticum*, *Mycoplasma hominis* and adverse pregnancy outcomes. *Current Opinion in Infectious Diseases*. 2013;26(3):231–240. doi:10.1097/QCO.0b013e328360db58.
2. Stamm WE, Wagner KF, Amsel R, et al. Causes of the acute urethral syndrome in women. *N Engl J Med*. 1980;303(8):409–415.
3. Viscardi RM. *Ureaplasma* Species: Role in Diseases of Prematurity. *Clinics in Perinatology*. 2010;37(2):393–409. doi:10.1016/j.clp.2009.12.003.
4. Glass JI, Lefkowitz EJ, Glass JS, Heiner CR, Chen EY, Cassell GH. The complete sequence of the mucosal pathogen *Ureaplasma urealyticum*. *Nature*. 2000;407(6805):757–762. doi:10.1038/35037619.
5. Sung T-J. *Ureaplasma urealyticum* or *Ureaplasma parvum*: what's the difference? *Korean J Pediatr*. 2013;56(11):474. doi:10.3345/kjp.2013.56.11.474.
6. Viscardi RM. *Ureaplasma* species: role in neonatal morbidities and outcomes. *Archives of Disease in Childhood - Fetal and Neonatal Edition*. 2013. doi:10.1136/archdischild-2012-303351.
7. Fanrong K, James G, Zhenfang M, Gordon S, Wang B, Gilbert GL. Phylogenetic analysis of *Ureaplasma urealyticum*—support for the establishment of a new species, *Ureaplasma parvum*. *International Journal of Systematic and Evolutionary Microbiology*. 1999;49(4):1879–1889.
8. Gwee A, Curtis N. *Ureaplasma* – Are you sitting comfortably? *Journal of Infection*. 2014;68:S19–S23. doi:10.1016/j.jinf.2013.09.027.
9. Waites KB, Katz B, Schelonka RL. *Mycoplasmas* and *ureaplasmas* as neonatal pathogens. *Clinical Microbiology Reviews*. 2005;18(4):757–789. doi:10.1128/CMR.18.4.757-789.2005.
10. Paralanov V, Lu J, Duffy LB, et al. Comparative genome analysis of 19 *Ureaplasma urealyticum* and *Ureaplasma parvum* strains. *BMC Microbiology*. 2012;12(1):1–1. doi:10.1186/1471-2180-12-88.
11. Monecke S, Helbig JH, Jacobs E. Phase variation of the multiple banded protein in *Ureaplasma urealyticum* and *Ureaplasma parvum*. *International Journal of Medical Microbiology*. 2003;293(2-3):203–211. doi:10.1078/1438-4221-00239.
12. Van Waarde WM, Brus F, Okken A, Kimpen JL. *Ureaplasma urealyticum* colonization, prematurity and bronchopulmonary dysplasia. *European Respiratory Journal*. 1997;10(4):886–890. doi:10.1183/09031936.97.10040886.
13. Romero R, Oyarzun E, Mazor M, Sirtori M, Hobbins JC, Bracken M. Meta-

- analysis of the relationship between asymptomatic bacteriuria and preterm delivery/low birth weight. *Obstet Gynecol.* 1989;73(4):576–582.
14. Iwasaka T, Wada T, Kidera Y, Sugimori H. Hormonal status and mycoplasma colonization in the female genital tract. *Obstet Gynecol.* 1986;68(2):263–266.
  15. Gupta A, Gupta A, Gupta S, Mittal A, Chandra P, Gill AK. Correlation of mycoplasma with unexplained infertility. *Arch Gynecol Obstet.* 2009;280(6):981–985. doi:10.1007/s00404-009-1042-z.
  16. De Silva NS, Quinn PA. Localization of endogenous activity of phospholipases A and C in *Ureaplasma urealyticum*. *J Clin Microbiol.* 1991;29(7):1498–1503.
  17. Kallapur SG, Kramer BW, Jobe AH. *Ureaplasma* and BPD. *Semin Perinatol.* 2013;37(2):94–101. doi:10.1053/j.semperi.2013.01.005.
  18. Viscardi RM, Hasday JD. Role of *Ureaplasma* Species in Neonatal Chronic Lung Disease: Epidemiologic and Experimental Evidence. *Pediatr Res.* 2009;65(5 Part 2):84R–90R. doi:10.1203/PDR.0b013e31819dc2f9.
  19. Zimmerman C-UR, Stiedl T, Rosengarten R, Spargser J. Alternate phase variation in expression of two major surface membrane proteins (MBA and UU376) of *Ureaplasma parvum* serovar 3. *FEMS Microbiol Lett.* 2009;292(2):187–193. doi:10.1111/j.1574-6968.2009.01505.x.
  20. Zheng X, Teng LJ, Glass JI, et al. Size variation of a major serotype-specific antigen of *Ureaplasma urealyticum*. *Ann N Y Acad Sci.* 1994;730:299–301.
  21. Watson HL, Blalock DK, Cassell GH. Variable antigens of *Ureaplasma urealyticum* containing both serovar-specific and serovar-cross-reactive epitopes. *Infect Immun.* 1990;58(11):3679–3688.
  22. Triantafilou M, de Glanville B, Aboklaish AF, Spiller OB, Kotecha S, Triantafilou K. Synergic activation of toll-like receptor (TLR) 2/6 and 9 in response to *Ureaplasma parvum* & *urealyticum* in human amniotic epithelial cells. *PLoS ONE.* 2013;8(4):e61199.
  23. Dando SJ, Nitsos I, Kallapur SG, et al. The Role of the Multiple Banded Antigen of *Ureaplasma parvum* in Intra-Amniotic Infection: Major Virulence Factor or Decoy? *PLoS ONE.* 2012;7(1):e29856. doi:10.1371/journal.pone.0029856.t004.
  24. Jacobsson B, Aaltonen R, Rantakokko-Jalava K, Morken N-H, Alanen A. Quantification of *Ureaplasma urealyticum* DNA in the amniotic fluid from patients in PTL and pPROM and its relation to inflammatory cytokine levels. *Acta Obstet Gynecol Scand.* 2009;88(1):63–70. doi:10.1080/00016340802572646.
  25. Ligon JV, Kenny GE. Virulence of ureaplasma urease for mice. *Infect Immun.* 1991;59(3):1170–1171.

26. Keck C, Gerber-Schafer C, Clad A, Wilhelm C, Breckwoldt M. Seminal tract infections: impact on male fertility and treatment options. *Hum Reprod Update*. 1998;4(6):891–903.
27. Friberg J, Gnärpe H. Mycoplasmas in semen from fertile and infertile men. *Andrologia*. 1974;6(1):45–52.
28. O'Leary WM. Ureaplasmas and human disease. *Crit Rev Microbiol*. 1990;17(3):161–168. doi:10.3109/10408419009105723.
29. Takebe S, Numata A, Kobashi K. Stone formation by *Ureaplasma urealyticum* in human urine and its prevention by urease inhibitors. *J Clin Microbiol*. 1984;20(5):869–873.
30. Gomez R, Romero R, Ghezzi F, Yoon BH, Mazor M, Berry SM. The fetal inflammatory response syndrome. *American Journal of Obstetrics and Gynecology*. 1998;179(1):194–202.
31. Marlow N, Wolke D, Bracewell MA, Samara M. Neurologic and Developmental Disability at Six Years of Age after Extremely Preterm Birth. *N Engl J Med*. 2005;352(1):9–19. doi:10.1056/NEJMoa041367.
32. Walkty A, Lo E, Manickam K, Alfa M, Xiao L, Waites K. *Ureaplasma parvum* as a Cause of Sternal Wound Infection. *J Clin Microbiol*. 2009;47(6):1976–1978. doi:10.1128/JCM.01849-08.
33. Perni SC, Vardhana S, Korneeva I, et al. *Mycoplasma hominis* and *Ureaplasma urealyticum* in midtrimester amniotic fluid: association with amniotic fluid cytokine levels and pregnancy outcome. *American Journal of Obstetrics and Gynecology*. 2004;191(4):1382–1386. doi:10.1016/j.ajog.2004.05.070.
34. Cassell GH, Waites KB, Watson HL, Crouse DT, Harasawa R. *Ureaplasma urealyticum* intrauterine infection: role in prematurity and disease in newborns. *Clinical Microbiology Reviews*. 1993;6(1):69–87. doi:10.1128/CMR.6.1.69.
35. Dammann O, Allred EN, Genest DR, Kundsinn RB, Leviton A. Antenatal mycoplasma infection, the fetal inflammatory response and cerebral white matter damage in very-low-birthweight infants. *Paediatr Perinat Epidemiol*. 2003;17(1):49–57.
36. Daskalakis G, Thomakos N, Papapanagiotou A, Papantoniou N, Mesogitis S, Antsaklis A. Amniotic fluid interleukin-18 at mid-trimester genetic amniocentesis: relationship to intraamniotic microbial invasion and preterm delivery. *BJOG: An International Journal of Obstetrics & Gynaecology*. 2009;116(13):1743–1748. doi:10.1111/j.1471-0528.2009.02364.x.
37. Veleminsky M, Tosner J. Relationship of vaginal microflora to PROM, pPROM and the risk of early-onset neonatal sepsis. *Neuro Endocrinol Lett*. 2008;29(2):205–221.



38. Goldenberg RL, Culhane JF, Iams JD, Romero R. Epidemiology and causes of preterm birth. *The Lancet*. 2008;371(9606):75–84.
39. Slattery MM, Morrison JJ. Preterm delivery. *The Lancet*. 2002;360(9344):1489–1497. doi:10.1016/S0140-6736(02)11476-0.
40. Levene MI, Wild J, Steer P. Higher multiple births and the modern management of infertility in Britain. The British Association of Perinatal Medicine. *Br J Obstet Gynaecol*. 1992;99(7):607–613.
41. Steer P. The epidemiology of preterm labour. *BJOG: An International Journal of Obstetrics & Gynaecology*. 2005;112(s1):1–3.
42. Balchin I, Whittaker JC, Steer PJ, Lamont RF. Are reported preterm birth rates reliable? An analysis of interhospital differences in the calculation of the weeks of gestation at delivery and preterm birth rate. *BJOG: An International Journal of Obstetrics & Gynaecology*. 2004;111(2):160–163. doi:10.1046/j.1471-0528.2003.00026.x.
43. McCormick MC. The contribution of low birth weight to infant mortality and childhood morbidity. *N Engl J Med*. 1985;312(2):82–90. doi:10.1056/NEJM198501103120204.
44. Smith LK, Draper ES, Manktelow BN, Dorling JS, Field DJ. Socioeconomic inequalities in very preterm birth rates. *Archives of Disease in Childhood - Fetal and Neonatal Edition*. 2007;92(1):F11–F14. doi:10.1136/adc.2005.090308.
45. Tucker JM, Goldenberg RL, Davis RO, Copper RL, Winkler CL, Hauth JC. Etiologies of preterm birth in an indigent population: is prevention a logical expectation? *Obstet Gynecol*. 1991;77(3):343–347.
46. Kasper DC, Mechtler TP, Reischer GH, et al. The bacterial load of *Ureaplasma parvum* in amniotic fluid is correlated with an increased intrauterine inflammatory response. *Diagn Microbiol Infect Dis*. 2010;67(2):117–121. doi:10.1016/j.diagmicrobio.2009.12.023.
47. Lee SE, Park I-S, Romero R, Yoon BH. Amniotic fluid prostaglandin F2 increases even in sterile amniotic fluid and is an independent predictor of impending delivery in preterm premature rupture of membranes. *J Matern Fetal Neonatal Med*. 2009;22(10):880–886. doi:10.1080/14767050902994648.
48. Kapatais-Zoumbos K, Chandler DK, Barile MF. Survey of immunoglobulin A protease activity among selected species of *Ureaplasma* and *Mycoplasma*: specificity for host immunoglobulin A. *Infect Immun*. 1985;47(3):704–709.
49. Larsen B, Hwang J. *Mycoplasma*, *Ureaplasma*, and adverse pregnancy outcomes: a fresh look. *Infect Dis Obstet Gynecol*. 2010;2010. doi:10.1155/2010/521921.
50. Francesco MA, Negrini R, Pinsi G, Peroni L, Manca N. Detection of

Ureaplasma biovars and polymerase chain reaction-based subtyping of Ureaplasma parvum in women with or without symptoms of genital infections. *Eur J Clin Microbiol Infect Dis*. 2009;28(6):641–646. doi:10.1007/s10096-008-0687-z.

51. Kong F, Ma Z, James G, Gordon S, Gilbert GL. Species identification and subtyping of Ureaplasma parvum and Ureaplasma urealyticum using PCR-based assays. *J Clin Microbiol*. 2000;38(3):1175–1179.
52. Hilton J, Azariah S, Reid M. A case-control study of men with non-gonococcal urethritis at Auckland Sexual Health Service: rates of detection of Mycoplasma genitalium. *Sex Heal*. 2010;7(1):77–81. doi:10.1071/SH09092.
53. Jobe AH, Ikegami M. Antenatal infection/inflammation and postnatal lung maturation and injury. *Respir Res*. 2001;2(1):27–32.
54. Viscardi RM, Manimtim WM, Sun C-CJ, Duffy L, Cassell GH. Lung pathology in premature infants with Ureaplasma urealyticum infection. *Pediatr Dev Pathol*. 2002;5(2):141–150. doi:10.1007/s10024-001-0134-y.
55. Brunner H. Models of mycoplasma respiratory and genital tract infections. *Wien Klin Wochenschr*. 1997;109(14-15):569–573.
56. Baier RJ, Loggins J, Kruger TE. Failure of erythromycin to eliminate airway colonization with ureaplasma urealyticum in very low birth weight infants. *BMC Pediatr*. 2003;3:10.
57. Bowman ED, Dharmalingam A, Fan WQ, Brown F, Garland SM. Impact of erythromycin on respiratory colonization of Ureaplasma urealyticum and the development of chronic lung disease in extremely low birth weight infants. *The Pediatric Infectious Disease Journal*. 1998;17(7):615–620.
58. Renaudin H, Bebear C. Comparative in vitro activity of azithromycin, clarithromycin, erythromycin and lomefloxacin against Mycoplasma pneumoniae, Mycoplasma hominis and Ureaplasma urealyticum. *Eur J Clin Microbiol Infect Dis*. 1990;9(11):838–841.
59. Waites KB, Sims PJ, Crouse DT, et al. Serum concentrations of erythromycin after intravenous infusion in preterm neonates treated for Ureaplasma urealyticum infection. *The Pediatric Infectious Disease Journal*. 1994;13(4):287–293.
60. Ozdemir R, Erdevi O, Dizdar EA, et al. Clarithromycin in preventing bronchopulmonary dysplasia in Ureaplasma urealyticum-positive preterm infants. *Pediatrics*. 2011;128(6):e1496–501. doi:10.1542/peds.2011-1350.
61. Hassan HE, Othman AA, Eddington ND, et al. Pharmacokinetics, safety, and biologic effects of azithromycin in extremely preterm infants at risk for ureaplasma colonization and bronchopulmonary dysplasia. *J Clin Pharmacol*. 2011;51(9):1264–1275. doi:10.1177/0091270010382021.

62. Viscardi RM, Othman AA, Hassan HE, et al. Azithromycin to prevent bronchopulmonary dysplasia in ureaplasma-infected preterm infants: pharmacokinetics, safety, microbial response, and clinical outcomes with a 20-milligram-per-kilogram single intravenous dose. *Antimicrob Agents Chemother*. 2013;57(5):2127–2133. doi:10.1128/AAC.02183-12.
63. Ray WA, Murray KT, Hall K, Arbogast PG, Stein CM. Azithromycin and the risk of cardiovascular death. *N Engl J Med*. 2012;366(20):1881–1890. doi:10.1056/NEJMoa1003833.
64. Vouga M, Greub G, Prod'homme G, et al. Treatment of genital mycoplasma in colonized pregnant women in late pregnancy is associated with a lower rate of premature labour and neonatal complications. Paul M, ed. *Clin Microbiol Infect*. 2014:n/a–n/a. doi:10.1111/1469-0691.12686.
65. Burri PH. Structural Aspects of Postnatal Lung Development & Alveolar Formation and Growth. *Biol Neonate*. 2006;89(4):313–322. doi:10.1159/000092868.
66. Anderson KV, Bokla L, Nüsslein-Volhard C. Establishment of dorsal-ventral polarity in the drosophila embryo: The induction of polarity by the Toll gene product. *Cell*. 1985;42(3):791–798.
67. Anderson KV, Jürgens G, Nüsslein-Volhard C. Establishment of dorsal-ventral polarity in the Drosophila embryo: Genetic studies on the role of the Toll gene product. *Cell*. 1985;42(3):779–789.
68. Janeway CAJ. Approaching the asymptote? Evolution and revolution in immunology. *Cold Spring Harb Symp Quant Biol*. 1989;54 Pt 1:1–13.
69. Lemaitre B, Nicolas E, Michaut L, Reichhart J-M, Hoffmann JA. The Dorsoventral Regulatory Gene Cassette *spätzle*/Toll/cactus Controls the Potent Antifungal Response in Drosophila Adults. *Cell*. 1996;86(6):973–983.
70. Medzhitov R, Preston-Hurlburt P, Janeway CA. A human homologue of the Drosophila Toll protein signals activation of adaptive immunity. *Nature*. 1997;388(6640):394–397.
71. Rock FL, Hardiman G, Timans JC, Kastelein RA, Bazan JF. A family of human receptors structurally related to Drosophila Toll. *Proc Natl Acad Sci U S A*. 1998;95(2):588–593.
72. Jin MS, Lee J-O. Structures of TLR-ligand complexes. *Current Opinion in Immunology*. 2008;20(4):414–419. doi:10.1016/j.coi.2008.06.002.
73. Jin MS, Kim SE, Heo JY, et al. Crystal structure of the TLR1-TLR2 heterodimer induced by binding of a tri-acylated lipopeptide. *Cell*. 2007;130(6):1071–1082. doi:10.1016/j.cell.2007.09.008.
74. Kawai T, Akira S. Toll-like receptors and their crosstalk with other innate receptors in infection and immunity. *Immunity*. 2011;34(5):637–650.

doi:10.1016/j.immuni.2011.05.006.

75. Akira S, Takeda K. Toll-like receptor signalling. *Nat Rev Immunol*. 2004;4(7):499–511. doi:10.1038/nri1391.
76. Kawai T, Akira S. The roles of TLRs, RLRs and NLRs in pathogen recognition. *International Immunology*. 2009;21(4):317–337. doi:10.1093/intimm/dxp017.
77. Nilsen NJ, Deininger S, Nonstad U, et al. Cellular trafficking of lipoteichoic acid and Toll-like receptor 2 in relation to signaling: role of CD14 and CD36. *J Leukoc Biol*. 2008;84(1):280–291. doi:10.1189/jlb.0907656.
78. Bagheri V, Askari A, Arababadi MK, Kennedy D. Can Toll-Like Receptor (TLR) 2 be considered as a new target for immunotherapy against hepatitis B infection? *Human Immunology*. 2014;75(6):549–554. doi:10.1016/j.humimm.2014.02.018.
79. Abe T, Fukuhara T, Wen X, et al. CD44 participates in IP-10 induction in cells in which hepatitis C virus RNA is replicating, through an interaction with Toll-like receptor 2 and hyaluronan. *J Virol*. 2012;86(11):6159–6170. doi:10.1128/JVI.06872-11.
80. Cooper A, Tal G, Lider O, Shaul Y. Cytokine induction by the hepatitis B virus capsid in macrophages is facilitated by membrane heparan sulfate and involves TLR2. *J Immunol*. 2005;175(5):3165–3176.
81. Takeuchi O, Kawai T, Mühlradt PF, et al. Discrimination of bacterial lipoproteins by Toll-like receptor 6. *International Immunology*. 2001;13(7):933–940.
82. Takeuchi O, Sato S, Horiuchi T, et al. Cutting edge: role of Toll-like receptor 1 in mediating immune response to microbial lipoproteins. *The Journal of Immunology*. 2002;169(1):10–14. doi:10.4049/jimmunol.169.1.10.
83. Triantafilou M, Gamper FGJ, Haston RM, et al. Membrane sorting of toll-like receptor (TLR)-2/6 and TLR2/1 heterodimers at the cell surface determines heterotypic associations with CD36 and intracellular targeting. *Journal of Biological Chemistry*. 2006;281(41):31002–31011. doi:10.1074/jbc.M602794200.
84. Fan H, Cook JA. Molecular mechanisms of endotoxin tolerance. *J Endotoxin Res*. 2004;10(2):71–84. doi:10.1179/096805104225003997.
85. Liao Y, Tang L. The critical roles of HSC70 in physiological and pathological processes. *Curr Pharm Des*. 2014;20(1):101–107.
86. Lee CC, Avalos AM, Ploegh HL. Accessory molecules for Toll-like receptors and their function. *Nature Publishing Group*. 2012;12(3):168–179. doi:10.1038/nri3151.

87. Kim HM, Park BS, Kim J-I, et al. Crystal structure of the TLR4-MD-2 complex with bound endotoxin antagonist Eritoran. *Cell*. 2007;130(5):906–917. doi:10.1016/j.cell.2007.08.002.
88. Verstrepen L, Bekaert T, Chau T-L, Tavernier J, Chariot A, Beyaert R. TLR-4, IL-1R and TNF-R signaling to NF-kappaB: variations on a common theme. *Cell Mol Life Sci*. 2008;65(19):2964–2978. doi:10.1007/s00018-008-8064-8.
89. McGettrick AF, Neill LAO. Localisation and trafficking of Toll-like receptors: an important mode of regulation. *Current Opinion in Immunology*. 2010;22(1):20–27. doi:10.1016/j.coi.2009.12.002.
90. Dalpke A, Zimmermann S, Heeg K. CpG DNA in the prevention and treatment of infections. *BioDrugs*. 2002;16(6):419–431.
91. Hemmi H, Takeuchi O, Kawai T, et al. A Toll-like receptor recognizes bacterial DNA. *Nature*. 2000;408(6813):740–745. doi:10.1038/35047123.
92. Lund JM, Alexopoulou L, Sato A, et al. Recognition of single-stranded RNA viruses by Toll-like receptor 7. *Proc Natl Acad Sci U S A*. 2004;101(15):5598–5603.
93. Windheim M, Stafford M, Pegg M, Cohen P. Interleukin-1 (IL-1) induces the Lys63-linked polyubiquitination of IL-1 receptor-associated kinase 1 to facilitate NEMO binding and the activation of IkappaBalpha kinase. *Molecular and Cellular Biology*. 2008;28(5):1783–1791. doi:10.1128/MCB.02380-06.
94. Seki E. NALPs: a novel protein family involved in inflammation. *Nat Rev Mol Cell Biol*. 2003;4(2):95–104. doi:10.1038/nrm1019.
95. Calvo D, Dopazo J, Vega MA. The CD36, CLA-1 (CD36L1), and LIMPII (CD36L2) gene family: cellular distribution, chromosomal location, and genetic evolution. *Genomics*. 1995;25(1):100–106.
96. Hoebe K, Georgel P, Rutschmann S, et al. CD36 is a sensor of diacylglycerides. *Nature*. 2005;433(7025):523–527. doi:10.1038/nature03253.
97. Dziarski R, Tapping RI, Tobias PS. Binding of bacterial peptidoglycan to CD14. *J Biol Chem*. 1998;273(15):8680–8690.
98. Baumann CL, Aspalter IM, Sharif O, et al. CD14 is a coreceptor of Toll-like receptors 7 and 9. *J Exp Med*. 2010;207(12):2689–2701. doi:10.1084/jem.20101111.
99. Hailman E, Lichenstein HS, Wurfel MM, et al. Lipopolysaccharide (LPS)-binding protein accelerates the binding of LPS to CD14. *J Exp Med*. 1994;179(1):269–277.
100. Lee H-K, Dunzendorfer S, Soldau K, Tobias PS. Double-stranded RNA-

- mediated TLR3 activation is enhanced by CD14. *Immunity*. 2006;24(2):153–163. doi:10.1016/j.immuni.2005.12.012.
101. Zanoni I, Ostuni R, Marek LR, et al. CD14 controls the LPS-induced endocytosis of Toll-like receptor 4. *Cell*. 2011;147(4):868–880. doi:10.1016/j.cell.2011.09.051.
  102. Akashi-Takamura S, Miyake K. TLR accessory molecules. *Current Opinion in Immunology*. 2008;20(4):420–425. doi:10.1016/j.coi.2008.07.001.
  103. da Silva Correia J, Soldau K, Christen U, Tobias PS, Ulevitch RJ. Lipopolysaccharide is in close proximity to each of the proteins in its membrane receptor complex. transfer from CD14 to TLR4 and MD-2. *J Biol Chem*. 2001;276(24):21129–21135.
  104. Gioannini TL, Teghanemt A, Zhang D, et al. Isolation of an endotoxin-MD-2 complex that produces Toll-like receptor 4-dependent cell activation at picomolar concentrations. *Proc Natl Acad Sci U S A*. 2004;101(12):4186–4191.
  105. Jiang Z, Georgel P, Du X, et al. CD14 is required for MyD88-independent LPS signaling. *Nat Immunol*. 2005;6(6):565–570. doi:10.1038/ni1207.
  106. Compton T, Kurt-Jones EA, Boehme KW, et al. Human cytomegalovirus activates inflammatory cytokine responses via CD14 and Toll-like receptor 2. *J Virol*. 2003;77(8):4588–4596.
  107. Ronco C. Endotoxin removal: history of a mission. *Blood Purif*. 2014;37 Suppl 1:5–8. doi:10.1159/000356831.
  108. Kotsaki A, Giamarellos-Bourboulis EJ. Emerging drugs for the treatment of sepsis. *Expert Opin Emerg Drugs*. 2012;17(3):379–391. doi:10.1517/14728214.2012.697151.
  109. Elinav E, Strowig T, Henao-Mejia J, Flavell RA. Regulation of the Antimicrobial Response by NLR Proteins. *Immunity*. 2011;34(5):665–679. doi:10.1016/j.immuni.2011.05.007.
  110. Ferrand J, Ferrero RL. Recognition of extracellular bacteria by NLRs and its role in the development of adaptive immunity. *Front Immunol*. 2013;4. doi:10.3389/fimmu.2013.00344/abstract.
  111. Schroder K, Tschopp J. The inflammasomes. *Cell*. 2010;140(6):821–832. doi:10.1016/j.cell.2010.01.040.
  112. Stutz A, Golenbock DT, Latz E. Inflammasomes: too big to miss. *J Clin Invest*. 2009;119(12):3502–3511. doi:10.1172/JCI40599.
  113. Lupfer C, Kanneganti T-D. Unsolved mysteries in NLR biology. *Front Immunol*. 2013;4. doi:10.3389/fimmu.2013.00285/abstract.
  114. Nickerson K, Sisk TJ, Inohara N, et al. Dendritic cell-specific MHC class II

- transactivator contains a caspase recruitment domain that confers potent transactivation activity. *J Biol Chem*. 2001;276(22):19089–19093.
115. Davis BK, Wen H, Ting JPY. The Inflammasome NLRs in Immunity, Inflammation, and Associated Diseases. *Annu Rev Immunol*. 2011;29(1):707–735. doi:10.1146/annurev-immunol-031210-101405.
  116. Bourhis L, Benko S, GIRARDIN S. Nod1 and Nod2 in innate immunity and human inflammatory disorders. *Biochemical Society Transactions*. 2007;35:1479–1484.
  117. Neerincx A, Castro W, Guarda G, Kufer TA. NLRC5, at the Heart of Antigen Presentation. *Front Immunol*. 2013;4. doi:10.3389/fimmu.2013.00397/abstract.
  118. Kobayashi KS, van den Elsen PJ. NLRC5: a key regulator of MHC class I-dependent immune responses. *Nat Rev Immunol*. 2012;12(12):813–820. doi:10.1038/nri3339.
  119. Pavot V, Rochereau N, Primard C, et al. Encapsulation of Nod1 and Nod2 receptor ligands into poly(lactic acid) nanoparticles potentiates their immune properties. *J Control Release*. 2013;167(1):60–67. doi:10.1016/j.jconrel.2013.01.015.
  120. Kim Y-G, Park J-H, Shaw MH, Franchi L, Inohara N, Núñez G. The Cytosolic Sensors Nod1 and Nod2 Are Critical for Bacterial Recognition and Host Defense after Exposure to Toll-like Receptor Ligands. *Immunity*. 2008;28(2):246–257. doi:10.1016/j.immuni.2007.12.012.
  121. Sutterwala FS, Mijares LA, Li L, Ogura Y, Kazmierczak BI, Flavell RA. Immune recognition of *Pseudomonas aeruginosa* mediated by the IPAF/NLRC4 inflammasome. *Journal of Experimental Medicine*. 2007;204(13):3235–3245. doi:10.1016/S0378-1119(98)00130-9.
  122. Dharancy S, Malapel MB, Louvet A, et al. Neutrophil Migration During Liver Injury Is Under Nucleotide-Binding Oligomerization Domain 1 Control. *YGASt*. 2010;138(4):1546–1556.e5. doi:10.1053/j.gastro.2009.12.008.
  123. Deshmukh HS, Hamburger JB, Ahn SH, McCafferty DG, Yang SR, Fowler VG. Critical role of NOD2 in regulating the immune response to *Staphylococcus aureus*. *Infect Immun*. 2009;77(4):1376–1382. doi:10.1128/IAI.00940-08.
  124. Girardin SE, Travassos LH, Herve M, et al. Peptidoglycan molecular requirements allowing detection by Nod1 and Nod2. *J Biol Chem*. 2003;278(43):41702–41708.
  125. Chamaillard M, Hashimoto M, Horie Y, et al. An essential role for NOD1 in host recognition of bacterial peptidoglycan containing diaminopimelic acid. *Nat Immunol*. 2003;4(7):702–707.

126. Girardin SE, Boneca IG, Carneiro LAM, et al. Nod1 detects a unique muropeptide from gram-negative bacterial peptidoglycan. *Science*. 2003;300(5625):1584–1587.
127. Girardin SE, Boneca IG, Viala J, et al. Nod2 is a general sensor of peptidoglycan through muramyl dipeptide (MDP) detection. *J Biol Chem*. 2003;278(11):8869–8872.
128. Franchi L, Park J-H, Shaw MH, et al. Intracellular NOD-like receptors in innate immunity, infection and disease. *Cell Microbiol*. 2007;0(0):071018055442002–??? doi:10.1111/j.1462-5822.2007.01059.x.
129. Strober W, Murray PJ, Kitani A, Watanabe T. Signalling pathways and molecular interactions of NOD1 and NOD2. *Nat Rev Immunol*. 2005;6(1):9–20. doi:10.1038/nri1747.
130. Franchi L, Warner N, Viani K, Núñez G. Function of Nod-like receptors in microbial recognition and host defense. *Immunological Reviews*. 2009;227(1):106–128. doi:10.1111/j.1600-065X.2008.00734.x.
131. Cui J, Zhu L, Xia X, et al. NLRC5 Negatively Regulates the NF-κB and Type I Interferon Signaling Pathways. *Cell*. 2010;141(3):483–496. doi:10.1016/j.cell.2010.03.040.
132. Davis BK, Roberts RA, Huang MT, et al. Cutting edge: NLRC5-dependent activation of the inflammasome. *J Immunol*. 2011;186(3):1333–1337. doi:10.4049/jimmunol.1003111.
133. Henao-Mejia J, Elinav E, Strowig T, Flavell RA. Inflammasomes: far beyond inflammation. *Nat Immunol*. 2012;13(4):321–324. doi:10.1038/ni.2257.
134. Bonardi V, Cherkis K, Nishimura MT, Dangl JL. A new eye on NLR proteins: focused on clarity or diffused by complexity? *Current Opinion in Immunology*. 2012;24(1):41–50. doi:10.1016/j.coi.2011.12.006.
135. McIlwain DR, Berger T, Mak TW. Caspase Functions in Cell Death and Disease. *Cold Spring Harbor Perspectives in Biology*. 2013;5(4):a008656–a008656. doi:10.1101/cshperspect.a008656.
136. Taylor RC, Cullen SP, Martin SJ. Apoptosis: controlled demolition at the cellular level. *Nat Rev Mol Cell Biol*. 2008;9(3):231–241. doi:10.1038/nrm2312.
137. Garlanda C, Dinarello CA, Mantovani A. The Interleukin-1 Family: Back to the Future. *Immunity*. 2013;39(6):1003–1018. doi:10.1016/j.immuni.2013.11.010.
138. Fantuzzi G, Ku G, Harding MW, et al. Response to local inflammation of IL-1 beta-converting enzyme- deficient mice. *J Immunol*. 1997;158(4):1818–1824.



139. Coeshott C, Ohnemus C, Pilyavskaya A, et al. Converting enzyme-independent release of tumor necrosis factor alpha and IL-1beta from a stimulated human monocytic cell line in the presence of activated neutrophils or purified proteinase 3. *Proc Natl Acad Sci U S A*. 1999;96(11):6261–6266.
140. Sahoo M, Ceballos-Olvera I, del Barrio L, Re F. Role of the inflammasome, IL-1beta, and IL-18 in bacterial infections. *ScientificWorldJournal*. 2011;11:2037–2050. doi:10.1100/2011/212680.
141. Martinon F, Burns K, Tschopp J. The inflammasome: a molecular platform triggering activation of inflammatory caspases and processing of proIL- $\beta$ . *Molecular Cell*. 2002;10(2):417–426.
142. Faustin B, Lartigue L, Bruey J-M, et al. Reconstituted NALP1 Inflammasome Reveals Two-Step Mechanism of Caspase-1 Activation. *Molecular Cell*. 2007;25(5):713–724. doi:10.1016/j.molcel.2007.01.032.
143. Bruey J-M, Bruey-Sedano N, Luciano F, et al. Bcl-2 and Bcl-XL Regulate Proinflammatory Caspase-1 Activation by Interaction with NALP1. *Cell*. 2007;129(1):45–56. doi:10.1016/j.cell.2007.01.045.
144. Hsu L-C, Ali SR, McGillivray S, et al. A NOD2–NALP1 complex mediates caspase-1-dependent IL-1 $\beta$  secretion in response to *Bacillus anthracis* infection and muramyl dipeptide. *Proc Natl Acad Sci U S A*. 2008;105(22):7803–7808.
145. Mariathasan S, Weiss DS, Newton K, et al. Cryopyrin activates the inflammasome in response to toxins and ATP. *Nature*. 2006;440(7081):228–232. doi:10.1038/nature04515.
146. Kanneganti T-D, Lamkanfi M, Kim Y-G, et al. Pannexin-1-mediated recognition of bacterial molecules activates the cryopyrin inflammasome independent of Toll-like receptor signaling. *Immunity*. 2007;26(4):433–443. doi:10.1016/j.immuni.2007.03.008.
147. Dostert C, Pétrilli V, Van Bruggen R, Steele C, Mossman BT, Tschopp J. Innate immune activation through Nalp3 inflammasome sensing of asbestos and silica. *Science*. 2008;320(5876):674–677. doi:10.1126/science.1156995.
148. Halle A, Hornung V, Petzold GC, et al. The NALP3 inflammasome is involved in the innate immune response to amyloid- $\beta$ . *Nat Immunol*. 2008;9(8):857–865. doi:10.1038/ni.1636.
149. Hornung V, Bauernfeind F, Halle A, et al. Silica crystals and aluminum salts activate the NALP3 inflammasome through phagosomal destabilization. *Nat Immunol*. 2008;9(8):847–856. doi:10.1038/ni.1631.
150. Feldmeyer L, Keller M, Niklaus G, Hohl D, Werner S, Beer H-D. The inflammasome mediates UVB-induced activation and secretion of interleukin-1beta by keratinocytes. *Curr Biol*. 2007;17(13):1140–1145. doi:10.1016/j.cub.2007.05.074.

151. Murakami T, Ockinger J, Yu J, et al. Critical role for calcium mobilization in activation of the NLRP3 inflammasome. *Proc Natl Acad Sci U S A*. 2012;109(28):11282–11287. doi:10.1073/pnas.1117765109.
152. Lee G-S, Subramanian N, Kim AI, et al. The calcium-sensing receptor regulates the NLRP3 inflammasome through Ca<sup>2+</sup> and cAMP. *Nature*. 2012;492(7427):123–127. doi:10.1038/nature11588.
153. Yamasaki K, Muto J, Taylor KR, et al. NLRP3/cryopyrin is necessary for interleukin-1beta (IL-1beta) release in response to hyaluronan, an endogenous trigger of inflammation in response to injury. *Journal of Biological Chemistry*. 2009;284(19):12762–12771. doi:10.1074/jbc.M806084200.
154. Meissner F, Seger RA, Moshous D, Fischer A, Reichenbach J, Zychlinsky A. Inflammasome activation in NADPH oxidase defective mononuclear phagocytes from patients with chronic granulomatous disease. *Blood*. 2010;116(9):1570–1573. doi:10.1182/blood-2010-01-264218.
155. Pétrilli V, Papin S, Dostert C, Mayor A, MARTINON F, TSCHOPP J. Activation of the NALP3 inflammasome is triggered by low intracellular potassium concentration. *Cell Death Differ*. 2007;14(9):1583–1589. doi:10.1038/sj.cdd.4402195.
156. Bauernfeind FG, Horvath G, Stutz A, et al. Cutting Edge: NF- B Activating Pattern Recognition and Cytokine Receptors License NLRP3 Inflammasome Activation by Regulating NLRP3 Expression. *The Journal of Immunology*. 2009;183(2):787–791. doi:10.4049/jimmunol.0901363.
157. Franchi L, Kanneganti T-D, Dubyak GR, Núñez G. Differential requirement of P2X7 receptor and intracellular K<sup>+</sup> for caspase-1 activation induced by intracellular and extracellular bacteria. *Journal of Biological Chemistry*. 2007;282(26):18810–18818. doi:10.1074/jbc.M610762200.
158. Pelegrin P, Surprenant A. Pannexin-1 couples to maitotoxin- and nigericin-induced interleukin-1beta release through a dye uptake-independent pathway. *J Biol Chem*. 2007;282(4):2386–2394. doi:10.1074/jbc.M610351200.
159. Pelegrin P, Surprenant A. Pannexin-1 mediates large pore formation and interleukin-1beta release by the ATP-gated P2X7 receptor. *EMBO J*. 2006;25(21):5071–5082. doi:10.1038/sj.emboj.7601378.
160. Dobo J, Swanson R, Salvesen GS, Olson ST, Gettins PGW. Cytokine Response Modifier A Inhibition of Initiator Caspases Results in Covalent Complex Formation and Dissociation of the Caspase Tetramer. *Journal of Biological Chemistry*. 2006;281(50):38781–38790. doi:10.1074/jbc.M605151200.
161. Mayor A, Martinon F, De Smedt T, Pétrilli V, Tschopp J. A crucial function of SGT1 and HSP90 in inflammasome activity links mammalian and plant innate immune responses. *Nat Immunol*. 2007;8(5):497–503.

doi:10.1038/ni1459.

162. Radian AD, de Almeida L, Dorfleutner A, Stehlik C. NLRP7 and related inflammasome activating pattern recognition receptors and their function in host defense and disease. *Microbes and Infection*. 2013;15(8-9):630–639. doi:10.1016/j.micinf.2013.04.001.
163. Kinoshita T, Wang Y, Hasegawa M, Imamura R, Suda T. PYPAF3, a PYRIN-containing APAF-1-like protein, is a feedback regulator of caspase-1-dependent interleukin-1 $\beta$  secretion. *Journal of Biological Chemistry*. 2005;280(23):21720–21725. doi:10.1074/jbc.M410057200.
164. Khare S, Dorfleutner A, Bryan NB, et al. An NLRP7-Containing Inflammasome Mediates Recognition of Microbial Lipopeptides in Human Macrophages. *Immunity*. 2012;36(3):464–476. doi:10.1016/j.immuni.2012.02.001.
165. Murdoch S, Djuric U, Mazhar B, et al. Mutations in NALP7 cause recurrent hydatidiform moles and reproductive wastage in humans. *Nat Genet*. 2006;38(3):300–302. doi:10.1038/ng1740.
166. Arthur JC, Lich JD, Ye Z, et al. Cutting Edge: NLRP12 Controls Dendritic and Myeloid Cell Migration To Affect Contact Hypersensitivity. *The Journal of Immunology*. 2010;185(8):4515–4519. doi:10.4049/jimmunol.1002227.
167. Zaki MH, Vogel P, Malireddi RKS, et al. The NOD-like receptor NLRP12 attenuates colon inflammation and tumorigenesis. *Cancer Cell*. 2011;20(5):649–660. doi:10.1016/j.ccr.2011.10.022.
168. Ye Z, Lich JD, Moore CB, Duncan JA, Williams KL, Ting JPY. ATP Binding by Monarch-1/NLRP12 Is Critical for Its Inhibitory Function. *Molecular and Cellular Biology*. 2008;28(5):1841–1850. doi:10.1128/MCB.01468-07.
169. Allen IC. Non-inflammasome forming NLRs in inflammation and tumorigenesis. *Front Immunol*. 2014;5. doi:10.3389/fimmu.2014.00169/abstract.
170. Wenstrom KD, Andrews WW, Tamura T, DuBard MB, Johnston KE, Hemstreet GP. Elevated amniotic fluid interleukin-6 levels at genetic amniocentesis predict subsequent pregnancy loss. *American Journal of Obstetrics and Gynecology*. 1996;175(4 Pt 1):830–833.
171. Shimizu T, Kida Y, Kuwano K. Ureaplasma parvum lipoproteins, including MB antigen, activate NF- $\kappa$ B through TLR1, TLR2 and TLR6. *Microbiology*. 2008;154(Pt 5):1318–1325. doi:10.1099/mic.0.2007/016212-0.
172. Okuda H, Fujii S, Kawashima Y. A direct colorimetric determination of blood ammonia. *Tokushima J Exp Med*. 1965;12(1):11–23.

173. Uchida K, Nakahira K, Mimura K, et al. Effects of *Ureaplasma parvum* lipoprotein multiple-banded antigen on pregnancy outcome in mice. *Journal of Reproductive Immunology*. 2013;100(2):118–127. doi:10.1016/j.jri.2013.10.001.
174. Horowitz S, Mazor M, Romero R, Horowitz J, Glezerman M. Infection of the amniotic cavity with *Ureaplasma urealyticum* in the midtrimester of pregnancy. *J Reprod Med*. 1995;40(5):375–379.
175. Gray DJ, Robinson HB, Malone J, Thomson RBJ. Adverse outcome in pregnancy following amniotic fluid isolation of *Ureaplasma urealyticum*. *Prenat Diagn*. 1992;12(2):111–117.
176. Yee M, Buczynski BW, O'Reilly MA. Neonatal hyperoxia stimulates the expansion of alveolar epithelial type II cells. *Am J Respir Cell Mol Biol*. 2014;50(4):757–766. doi:10.1165/rcomb.2013-0207OC.
177. Messaed C, Akoury E, Djuric U, et al. NLRP7, a nucleotide oligomerization domain-like receptor protein, is required for normal cytokine secretion and co-localizes with Golgi and the microtubule-organizing center. *J Biol Chem*. 2011;286(50):43313–43323. doi:10.1074/jbc.M111.306191.
178. Gillaux C, Mehats C, Vaiman D, Cabrol D, Breuiller-Fouche M. Functional screening of TLRs in human amniotic epithelial cells. *J Immunol*. 2011;187(5):2766–2774. doi:10.4049/jimmunol.1100217.
179. Zheng X, Watson HL, Waites KB, Cassell GH. Serotype diversity and antigen variation among invasive isolates of *Ureaplasma urealyticum* from neonates. *Infect Immun*. 1992;60(8):3472–3474.
180. Triantafilou M, Miyake K, Golenbock DT, Triantafilou K. Mediators of innate immune recognition of bacteria concentrate in lipid rafts and facilitate lipopolysaccharide-induced cell activation. *J Cell Sci*. 2002;115(Pt 12):2603–2611.
181. Wang PY, Kitchens RL, Munford RS. Bacterial lipopolysaccharide binds to CD14 in low-density domains of the monocyte-macrophage plasma membrane. *J Inflamm*. 1995;47(3):126–137.
182. Triantafilou M, Morath S, Mackie A, Hartung T, Triantafilou K. Lateral diffusion of Toll-like receptors reveals that they are transiently confined within lipid rafts on the plasma membrane. *J Cell Sci*. 2004;117(Pt 17):4007–4014.
183. Murdoch S, Djuric U, Mazhar B, et al. Activation of the NALP3 inflammasome is triggered by low intracellular potassium concentration. *Cell Death Differ*. 2007;14(9):1583–1589. doi:10.1038/sj.cdd.4402195.
184. Tsujii M, Kawano S, Tsuji S, Fusamoto H, Kamada T, Sato N. Mechanism of gastric mucosal damage induced by ammonia. *YGA*. 1992;102(6):1881–1888.

185. Paradiso AM, Negulescu PA, Machen TE. Na<sup>+</sup>-H<sup>+</sup> and Cl<sup>-</sup>-OH-(HCO<sub>3</sub><sup>-</sup>) exchange in gastric glands. *Am J Physiol*. 1986;250(4 Pt 1):G524–34.
186. Waites KB, Schelonka RL, Xiao L, Grigsby PL, Novy MJ. Congenital and opportunistic infections: Ureaplasma species and Mycoplasma hominis. *Seminars in Fetal and Neonatal Medicine*. 2009;14(4):190–199. doi:10.1016/j.siny.2008.11.009.
187. Kirchner L, Helmer H, Heinze G, et al. Amnionitis with Ureaplasma urealyticum or other microbes leads to increased morbidity and prolonged hospitalization in very low birth weight infants. *Eur J Obstet Gynecol Reprod Biol*. 2007;134(1):44–50. doi:10.1016/j.ejogrb.2006.09.013.
188. HEE L. Likelihood ratios for the prediction of preterm delivery with biomarkers. *Acta Obstet Gynecol Scand*. 2011;90(11):1189–1199. doi:10.1111/j.1600-0412.2011.01187.x.
189. Bashiri A, Horowitz S, Huleihel M, Hackmon R, Dukler D, Mazor M. Elevated concentrations of interleukin-6 in intra-amniotic infection with Ureaplasma urealyticum in asymptomatic women during genetic amniocentesis. *Acta Obstet Gynecol Scand*. 1999;78(5):379–382.
190. Potts JM, Sharma R, Pasqualotto F, Nelson D, Hall G, Agarwal A. Association of ureaplasma urealyticum with abnormal reactive oxygen species levels and absence of leukocytospermia. *J Urol*. 2000;163(6):1775–1778.
191. Boron WF. Intracellular pH transients in giant barnacle muscle fibers. *Am J Physiol*. 1977;233(3):C61–73.
192. Huttemann M, Helling S, Sanderson TH, et al. Regulation of mitochondrial respiration and apoptosis through cell signaling: cytochrome c oxidase and cytochrome c in ischemia/reperfusion injury and inflammation. *Biochim Biophys Acta*. 2012;1817(4):598–609. doi:10.1016/j.bbabbio.2011.07.001.
193. Marconi C, de Andrade Ramos BR, Peraçoli JC, Donders GGG, da Silva MG. Amniotic fluid interleukin-1 beta and interleukin-6, but not interleukin-8 correlate with microbial invasion of the amniotic cavity in preterm labor. *Am J Reprod Immunol*. 2011;65(6):549–556. doi:10.1111/j.1600-0897.2010.00940.x.

## Appendix: